Mathematical models for ecoepidemiological interactions, with applications to herd behaviour and bovine tuberculosis, and evolutionary interactions of alarm calls

(Article begins on next page)

03 May 2024

University of Torino

Department of Mathematics "Giuseppe Peano"

Doctoral School in Life and Health Sciences

PhD Programme in Complex Systems for the Life Sciences
cycle XXXI

University of São Paulo

Faculty of Medicine, University of São Paulo

PhD Programme in Experimental Physiopathology

Mathematical models for ecoepidemiological interactions, with applications to herd behaviour and bovine tuberculosis, and evolutionary interactions of alarm calls

Luciana Mafalda Elias de Assis

Supervisors:
Prof. Ezio Venturino
Prof. Eduardo Massad

PhD programme Coordinator:
Prof. Michele De Bortoli

Academic years: 2015-2016, 2016-2017, 2017-2018

Code of scientific discipline MAT/08

Luciana Mafalda Elias de Assis

Mathematical models for ecoepidemiological interactions, with applications to herd behaviour and bovine tuberculosis, and evolutionary interactions of alarm calls

PhD Thesis presented to PhD Programme of Complex Systems for the Life Sciences of the Doctoral School in Life and Health Sciences of the University of Torino (UNITO) in Italy to obtain the degree of Doctor in Complex Systems for the Life Sciences from University of Torino (UNITO) and Doctor in Sciences from Faculty of Medicine of the University of São Paulo (FMUSP).

Torino
2019

II

ABSTRACT

This thesis presents several nonlinear mathematical models applied to ecoepidemiology and evolution. A detailed study involving predator-prey type models considering an alternative resource for the predator was carried out, investigating the situation of infection in the prey and in the predator on separate models. Such study served as a theoretical contribution to the investigation of problems such as bovine tuberculosis in wild animal species presented in a specific model. We also developed models to explain the evolution of alarm calls in species of birds and mammals. The theoretical framework adopted for those evolution models is that of Population Ecology. The models were developed using Ordinary Differential Equations (ODEs) to describe the population dynamics. The biological assumptions of the systems that we wanted to analyse were enumerated and explained.

Keywords: predator-prey models; bovine turberculosis; evolution models; alarm call behaviour.

RESUMO

Esta tese apresenta vários modelos matemáticos não-lineares aplicados à ecopidemiologia e à evolução. Foi realizado um estudo detalhado envolvendo modelos do tipo predador-presa considerando um recurso alternativo para o predador, investigando situações de infecção na presa e no predador em modelos separados. Tal estudo, serviu de aporte teórico para a investigação de problemas como a tuberculose bovina em espécies de animais selvagens apresentado em um modelo específico. Também desenvolvemos modelos para explicar a evolução dos chamados de alarme em espécies de aves e mamíferos. O quadro teórico adotado para esses modelos de evolução é o da Ecologia de População. Nos modelos desenvolvidos usamos as Equações Diferenciais Ordinárias (EDOs) para descrever a dinâmica populacional. Consideramos pressupostos biológicos dos sistemas biológicos analisados.

Palavras-chave: modelos predador-presa; tuberculose bovina; modelos de evolução; comportamento de chamado de alarme.

ACKNOWLEDGEMENTS

CONTENTS

INTRODUCTION

In this thesis we introduced several nonlinear mathematical models applied to ecoepidemiology (fieldwork that investigates how transmissible diseases affect interacting populations) and evolution (change in the heritable characteristics of biological populations over successive generations).

A detailed study involving predator-prey type models considering an alternative resource for the predator was carried out, investigating the situation of infection in the prey and in the predator on separate models. Such study served as a theoretical contribution to the investigation of problems such as bovine tuberculosis in wild animal species presented in a specific model. We also developed models to explain the evolution of alarm calls in species of birds and mammals. The theoretical framework adopted for those evolution models was that of Population Ecology. The models were developed using Ordinary Differential Equations (ODEs) to describe the population dynamics. In every model we considered the underlying suitable biological assumptions in order to formulate it.

The methodological approach used to analyse the dynamical systems that we developed was similar for all the models introduced in this thesis. It consisted in finding the equilibrium points and analysing their local stability and when its possible, to analyse the global stability too. To make the analysis of local stability we generally evaluated the Jacobian matrix at each equilibrium point and analysed the signs of its eigenvalues. For the most complicated situations for which the theoretical analysis was not enough, numerical simulations have been used to gather information on equilibria existence and stability, and more generally, on the system behaviour. Furthermore, for the equilibria for which the analysis was possible, the numerical simulations were used as a tool to reinforce the theoretical results.

This thesis is divided into two main parts: the first one addresses the problem of the epidemic spread in wild animal species, where some mathematical models are introduced and analysed, Chapters 1-2-3-4-5. In the second part of the thesis some mathematical models of evolution are presented and describe the interaction of two types of individuals in the same species, Chapter 6.

In the first Chapter two mathematical models are proposed and analyzed

to elucidate the influence on a generalist predator of its hidden and explicit resources. Boundedness of the system's trajectories, feasibility, local and global stabilities of the equilibria for both models are established, as well as possible local bifurcations. The findings indicate that the relevant behaviour of the system, including switching of stability, extinction and persistence of the involved populations, depends mainly on the reproduction rate of the favorite prey. To achieve full ecosystem survival some balance between the respective grazing pressures exerted by the predator on the prey populations needs to be maintained, while higher grazing pressure just on one species always leads to its extinction.

Chapter 2 investigates mathematical models of predator-prey systems where a transmissible disease spreads only among the prey species. Two mathematical models are proposed, analysed and compared in order to assess the influence of hidden or explicit resources for the predator. The predator is assumed to be a generalist in the first model and a specialist on two prey species in the second one. Existence and boundedness of the solutions of the models are established, as well as local and global stability and bifurcations. The equilibria of two systems possessing the same biological meaning are compared. The study shows that the relevant ecosystem behaviour, including stability switching, extinction and persistence for any species depends on four important parameters, viz., the reproduction rate and the infection rate of the main prey, the mortality rate of infected prey and the reproduction rate of the alternative prey.

Chapter 3 deals with two mathematical models of predator-prey type where a transmissible disease spreads among the predator species only. in the same way as it was done in the Chapter 2 we analysed and compared the models in order to assess the influence of hidden and explicit alternative resource for predator. The analyse show boundedness as well as local stability and transcritical bifurcations for equilibria of systems. Numerical simulations support our theoretical analysis.

In Chapter 4 we presented and analysed a model for the spread of Bovine Tuberculosis (BT) between buffaloes and lions. The most important system parameters are identified: vertical and horizontal disease transmission among the buffaloes and the influence of intraspecific competition between healthy and diseased buffaloes on the infected buffaloes population. Removal of diseased prey appears to be the most effective strategy to render the ecosystem disease-free.

In order to investigate in more detail the herd behaviour, the prey group defense presented in Chapter 4 we proposed and analysed in Chapter 5 a modified model where different response functions have been formulated to model predator-prey interactions. In particular, Lotka-Volterra models work with the Mass Action Law, resulting in a Holling type I response function. More recently, authors have proposed a term proportional to the square root of the prey population, in order to model herd behaviour and group defense. We

present a model in which the response function is defined piecewisely: below a certain threshold (populations too small to display group defense) we have a Lotka-Volterra type interaction and above it we have herd behaviour type response. The model is analysed using standard techniques and also complementary techniques designed specifically for piecewise systems. Both stability of equilibria and bifurcations are investigated. In particular, we were able to prove that both supercritical and subcritical Hopf bifurcations occur, one of those leading to the existence of two limit cycles (one stable and the other unstable). We concluded that the proposed model displays novel behaviour in comparison to previous models and serves as a coherent tool to model predator-prey interactions. It is important to highlight that the model described in 5 is a generalization of herd behaviour that has other possible developments.

Finally, in Chapter 6 the evolution of alarm call behaviour under individual selection is studied. Four mathematical models of increasing complexity are proposed and analysed. Theoretical conditions for the evolution of "selfish", "mutualistic", "altruistic" or "spiteful" alarm calls are established. The models indicate that the hypotheses of benefits of retaining group members or avoiding group detection are not sufficient to explain the evolution of alarm call behaviour, but serve as a complementary factor to facilitate its evolution in most cases. It is hypothesized that the evolution of alarm calls between non-kin should evolve probably when calls are mutualistic, mildly altruistic and there are beneficial group size effects against predation.

General conclusions will finally be presented.

Most of the research presented in this thesis has previously been either published or submitted for publication. The papers are in order of chapters:

- de Assis, L. M. E., Banerjee, M., Venturino, E. Comparing Predator-Prey Models with Hidden and Explicit Resources. Annali dell'Universitá di Ferrara, 64(2), 259-283, 2018. Presented in this thesis as Chapter 1.

- de Assis, L. M. E., Banerjee, M., Venturino, E. Comparison of Hidden and Explicit Resources in Ecoepidemic Models of Predator-Prey Type. *Preprint accepted on Journal Computational and Applieds Mathematics*, 2019. Presented in this thesis as Chapter 2.

- de Assis, L. M. E., Banerjee, M., Cecconello, M., Venturino, E. Lotka-Volterra Type Predator-prey Models: Comparison of hidden and explicit resources with a transmissible disease in the predator species. Journal Applications of Mathematics, 63(5), 569-600, 2018. Presented in this thesis as Chapter 3.

- de Assis, L. M. E., Massad, E., Assis, R. A., Martorano, S. R., Venturino, E. A Mathematical Model for the Propagation of Bovine Tuberculosis in

Wild Animals. *17th CMMSE Conference Proceedings,* ISBN: 978-84-617-8694-7, 1323–1355, 2017. Presented in this thesis as Chapter 4.

- Assis, L. M. E., Massad, E., Assis, R. A., Martorano, S. R., Venturino, E. A mathematical model for bovine tuberculosis among buffaloes and lions in the Kruger National Park. Mathematical Methods in the Applied Sciences, 41(2), 525-543, 2018. Presented in this thesis as Chapter 4.

- Assis, L. M. E., Carnevarollo Jr, M. R. P., Assis, R. A., Venturino, E. On periodic regimes triggered by herd behaviour in population systems. *Preprint submitted,* 2019. Presented in this thesis as Chapter 5.

- de Assis, L. M. E., de Assis, R. A., Cecconello, M., Venturino, E. Models for alarm call behaviour. Theoretical Ecology, 11(1), 1-18, 2018. Presented in this thesis as Chapter 6.

Part I

Ecological interacting population models

CHAPTER 1

COMPARING PREDATOR-PREY MODELS WITH HIDDEN AND EXPLICIT RESOURCES

The mathematical study of predator-prey interactions is an important research component in mathematical ecology. Various types of interactions and population models with two or more trophic levels have been formulated and received significant attention from several researchers in the past and the more recent literature. The basic building block for a wide range of study are the two populations predator-prey models, in which mathematical models describe the interactions of a hunter species that feeds on a prey, thereby being beneficial for the former and detrimental for the latter. In real life situations this may occur when possibly also other resources are available for the predator. The latter can be subdivided into two broad sets, the specialist predators, that feed only on one species, see for instance the case of the weasel *Mustela nivalis* exploiting the field vole *Microtus agrestis*, [11], and the generalist predators with several options for their diet, e.g. the spiders, that hunt every possible insects, [58, 73]. In this latter situation, mainly with more than two resources available, predators focus generally on the most abundant one, changing to exploiting the substitute prey, the second most abundant population, when the primary becomes scarce, [13].

It is a matter of fact that the literature on predator-prey models with generalist predator appears to be smaller compared to that with specialist predator. Primarily, this is due to the fact that the models with a generalist predator are a little bit tougher to handle mathematically. Indeed in most of the cases the components of the coexisting equilibrium point cannot be obtained explicity when the functional responses are represented by highly nonlinear functions of both populations involved, prey and predators.

3

In case of a two species predator-prey model with a specialist predator, the latter cannot survive in the absence of prey as its reproduction and growth rates are functions of the prey density and in its absence these functions vanish. On the other hand, the growth rate of the generalist predator is different from zero even if the explicit prey disappears, because they can feed on other resources. The mathematical models of two-species generalist predator-prey models can be divided into two types: (*i*) those in which the predators growth rate follows a logistic law, to which the prey density contributes enhancing it with an additional growth; (*ii*) those whose predators growth rate follows logistic growth, where the carrying capacity is a function of prey population density. The second type of systems is known as Leslie-Gower [48] or Holling-Tanner [6, 43] model, depending upon the type of the functional response [81, 42, 41] term involved to describe the grazing pattern of the prey by their predator.

Predator-prey models with two-prey and one predator are investigated in particular because this leads to the question of prey switching, [50, 51]. This occurs when the primary resource by overexploitation becomes more difficult to find. The alternative, less palatable prey at that moment is seen as a new potential diet for their survival by the hungry predators. They thus switch their attention to it, instead of wasting time in a difficult search for the primary hard-to-find resource. As a result, in these cases the absence of either primary or substitute prey does not necessarily drive the predator towards extinction. The main objective of the present work is to elucidate the existing relationship between two predator-prey models with a generalist predator, distinguishing the model with implicit secondary prey and the one in which the latter population is explicitly modeled as an additional ecosystem's variable.

The chapter is organized as follows. In the next Section the two types of models are formulated and their basic properties are analyzed. Global stability of the coexistence equilibria in both models is assessed in Section 1.2 and next the possible bifurcations are analytically investigated, Section 1.3, and numerically, Section 1.4, investigated.

Section 1.5 performs the system's comparative study, the subsequent section contains further numerical simulations on bifurcations. A final discussion concludes the chapter.

1.1   The predator-prey models

The predator population is denoted by Z, thriving in the presence respectively of one and two of its only resources, the prey are represented by X and Y. Considering the two possible demographic situations, the following two different predator-prey models can be formulated. The first one with two-populations, i.e. the primary food source for the predators, whose equilibria are denoted by [p_hp], the first "p" referring to predators, the second one to prey, "h" standing

for the "hidden" substitute resource not explicitly modeled in the equations, is classical, see Chapter 3 of [65]:

$$
\begin{aligned}
\frac{dX}{dt} &= rX\left(1 - \frac{X}{K}\right) - aXZ, \\
\frac{dZ}{dt} &= uZ\left(1 - \frac{Z}{L}\right) + aeXZ.
\end{aligned}
\tag{1.1}
$$

The first equation models the logistic prey growth and its additional mortality due to encounters between prey individuals with the predators. The last term in the second one accounts for the benefits the latter gain from this successful hunting, while the first term indicates that the predators have an alternative food sources.

Its three dimensional counterpart, with the additional resource explicitly modeled, has equilibria denoted by [p_ep], "e" standing for "explicit".

As a one-predator-two prey system, it is also present in the literature, but here a correction on the mortality rate discussed below is made:

$$
\begin{aligned}
\frac{dX}{dt} &= rX\left(1 - \frac{X}{K}\right) - aZX, \\
\frac{dY}{dt} &= sY\left(1 - \frac{Y}{H}\right) - bZY, \\
\frac{dZ}{dt} &= -mZ^2 + e(aZX + bZY).
\end{aligned}
\tag{1.2}
$$

The first and second equations are replicae of the first equation in (1.1) for the prey, in this case there being explicitly two food resources in the ecosystem.

Note that here the alternative prey Y is the unnamed resource in model (1.1).

The predators' equation is the same of the former model, with the exception that now they feed only on these two types of prey, and therefore the predator individuals are no more generalist as in (1.1), but two-population specialists on X and Y. This entails that they will not survive in the absence of both prey.

The parameters are non-negative in both models. In (1.2) we take mortality in the quadratic form $-mZ^2$ since this term is related to the intraspecific competition term $-uL^{-1}Z^2$ of the system (1.1). Indeed, comparing the second equation of (1.1) with the third one of (1.2), the last term in the former is identical with the second one of the latter. The first (reproductive) term in the generalist model (1.1) is now replaced by the hunting on the Y prey, last term of (1.2). To make the comparison fair, then the mortality due to intraspecific competition in (1.1) must correspond to the first term in (1.2). This entails that in the specialist system the predators essentially die by intraspecific competition for the needed resources.

Mathematically, the connection between (1.1) and (1.2) is given by

$$u = ebY, \quad L = eb\frac{Y}{m}, \quad \text{i.e.} \quad u = Lm. \tag{1.3}$$

Here we should understand the value of the population Y at steady state, namely $Y = Y^*$, otherwise (1.3) would be "unbalanced", i.e. it would have only one time-dependent side.

The Jacobians for models (1.1) and (1.2) are respectively

$$J^{[p\_hp]} = \begin{pmatrix} r - 2\frac{r}{K}X - aZ & -aX \\ aeZ & u - 2\frac{u}{L}Z + aeX \end{pmatrix} \tag{1.4}$$

and

$$J^{[p\_ep]} = \begin{pmatrix} r - 2\frac{r}{K}X - aZ & 0 & -aX \\ 0 & s - 2\frac{s}{H}Y - bZ & -bY \\ aeZ & ebZ & -2mZ + e(aX + bY) \end{pmatrix}. \tag{1.5}$$

1.1.1 Boundedness

In order to obtain a well-posed model, we need to show that the systems trajectories remain confined within a compact set. Since $0 \leq X, Z \leq \varphi$ and $0 \leq X, Y, Z \leq \psi$, the boundedness of the original ecosystem populations is immediate. Trajectories in systems (1.1) and (1.2) remain non-negative follows directly from the facts that $\dot{X} = 0$ if $X = 0$, $\dot{Y} = 0$ if $Y = 0$, $\dot{Z} = 0$ if $Z = 0$ and that initial conditions for the model should always be non-negative to make biological sense.

Consider the total environment population $\varphi(t) = X(t) + Z(t)$. Let $\varphi(t)$ be a differentiable function, then taking an arbitrary $0 < \mu$, summing the equations in model (1.1), and observing that $e \leq 1$ we find the estimate:

$$\frac{d\varphi(t)}{dt} + \mu\varphi(t) \leq rX\left(1 - \frac{X}{K} + \frac{\mu}{r}\right) + uZ\left(1 - \frac{Z}{L} + \frac{\mu}{u}\right) = p_1(X) + p_2(Z).$$

The functions $p_1(X)$ and $p_2(Z)$ are concave parabolae, with maxima located at $X^\star$, $Z^\star$, and corresponding maximum values

$$M_1 = p_1(X^\star) = \frac{rK}{4}\left(1 + \frac{\mu}{r}\right)^2, \quad M_2 = p_2(Z^\star) = \frac{uL}{4}\left(1 + \frac{\mu}{u}\right)^2,$$

Thus,

$$\frac{d\varphi(t)}{dt} + \mu\varphi(t) \leq M_1 + M_2 = M.$$

Integrating the differential inequality, we find

$$\varphi(t) \leq \left(\varphi(0) - \frac{M}{\mu}\right)e^{-\mu t} + \frac{M}{\mu} \leq \max\left\{\varphi(0), \frac{M}{\mu}\right\}.$$

From this the boundedness of the original ecosystem populations is immediate. The proof for system (1.2) follows a similar patter, after remarking that setting $\psi(t) = X(t) + Y(t) + Z(t)$ and summing the equations in model (1.2), we find again for an arbitrary $0 < \mu$ and observing that $e \leq 1$ we find:

$$
\begin{aligned}
\frac{d\psi(t)}{dt} + \mu\psi(t) \;&\leq\; rX\left(1 - \frac{X}{K} + \frac{\mu}{r}\right) + sY\left(1 - \frac{Y}{H} + \frac{\mu}{s}\right) + Z(\mu - mZ) \\
&=\; q_1(X) + q_2(Y) + q_3(Z).
\end{aligned}
$$

The functions $q_1(X)$, $q_2(Y)$ and $q_3(Z)$ are concave parabolae, with maxima located at $X^\star$, $Y^\star$, $Z^\star$, and corresponding maximum values

$$
M_1 = q_1(X^\star) = \frac{rK}{4}(1 + \mu/r)^2, \quad M_2 = q_2(Y^\star) = \frac{sH}{4}(1 + \mu/s)^2,
$$

and

$$
M_3 = q_3(Z^\star) = \frac{\mu^2}{4m}.
$$

Thus,

$$
\frac{d\psi(t)}{dt} + \mu\psi(t) \leq M_1 + M_2 + M_3 = M.
$$

Integrating the differential inequality, we find

$$
\psi(t) \leq \left(\psi(t)(0) - \frac{M}{\mu}\right)e^{-\mu t} + \frac{M}{\mu} \leq \max\left\{\psi(t)(0), \frac{M}{\mu}\right\}
$$

Thus for both models, the solutions are always non-negative and remain bounded.

1.1.2 Equilibria of model (1.1)

The model (1.1) is standard in mathematical biology, see for instance Chapter 3 of [65] where also more complex models of such type are described.

Proposition 1. *The trivial equilibria $P_1^{[p\_hp]} = (0,0)$ and the point $P_2^{[p\_hp]} = (K,0)$ exist, are always feasible and unstable.*

Proof. For $X = Z = 0$ we obtain that the equilibrium $P_1^{[p\_hp]}$ exists and is feasible. The Jacobian matrix (1.4) evaluated at $P_1^{[p\_hp]}$ is given by

$$
J_{P_1}^{[p\_hp]} = \begin{pmatrix} r & 0 \\ 0 & u \end{pmatrix}
$$

which provides the eigenvalues r, u. As both eigenvalues are positive, the equilibrium $P_1^{[p\_hp]}$ is unstable.

For $Z = 0$, we obtain the system (1.1) becomes,

$$rX \left(1 - \frac{X}{K}\right) = 0.$$

Solving the equation with respect to X we find $X = K$ and then, we obtain that the equilibrium point $P_2^{[p\_hp]}$ exists and it is feasible. The Jacobian matrix (1.4) evaluated at the $P_2^{[p\_hp]}$ is given by

$$J_{P_2}^{[p\_hp]} = \begin{pmatrix} -r & -aK \\ 0 & u + aeK \end{pmatrix}$$

which provides the eigenvalues $-r, u + aeK$. As one eigenvalue is positive, the equilibrium $P_2^{[p\_hp]}$ is unstable. $\qquad\square$

Proposition 2. *The equilibrium point $P_3^{[p\_hp]} = (0, L)$ exists and it is always feasible. Furthermore, it is conditionally stable if the following condition holds*

$$r < aL. \tag{1.6}$$

Proof. For $X = 0$ in the system we get that $P_3^{[p\_hp]}$ always exists. The Jacobian matrix evaluated at $P_3^{[p\_hp]}$ is

$$J_{P_3}^{[p\_hp]} = \begin{pmatrix} r - aL & 0 \\ aeL & -u \end{pmatrix}$$

for which the eigenvalues are given by $r - aL$ and $-u$. Thus, $P_3^{[p\_hp]}$ is stable if $r < aL$. $\qquad\square$

Proposition 3. *The equilibrium point $P_4^{[p\_hp]} = \left(uK\frac{r-aL}{ur+a^2eKL}, \frac{r}{a}\left(1 - u\frac{r-aL}{ur+a^2eKL}\right)\right)$, exists and it is feasible if $K \geq X_4^{[p\_hp]} \geq 0$, i.e., $r \geq aL$. $P_4^{[p\_hp]}$, whenever feasible, is stable, because the Routh-Hurwitz conditions are satisfied:*

$$-tr(J_{P_4}^{[p\_hp]}) > 0, \quad \det(J_{P_4}^{[p\_hp]}) > 0.$$

Proof. To show that the coexistence exists, we consider $X \neq 0$, and $Z \neq 0$ the system (1.1) becomes,

$$rX \left(1 - \frac{X}{K}\right) - aXZ = 0$$

$$uZ \left(1 - \frac{Z}{L}\right) + aeXZ = 0$$

Solving this system with respect to X and Z we find

$$X_4^{[p\_hp]} = uK\frac{r - aL}{ur + a^2eKL}, \quad Z_4^{[p\_hp]} = \frac{r}{a}\left(1 - u\frac{r - aL}{ur + a^2eKL}\right).$$

For the feasibility of $P_4^{[p\_hp]}$ we need to ask the positivity of $X_4^{[p\_hp]}$ and $Z_4^{[p\_hp]}$. Thus the condition

$$r \geq aL \tag{1.7}$$

must hold. The Jacobian matrix evaluated at $P_4^{[p\_hp]}$ is

$$J_{P_4}^{[p\_hp]} = \begin{pmatrix} \frac{aruL - ur^2}{a^2 eKL + ur} & \frac{a^2 uKL - aurK}{a^2 eKL + ur} \\ \frac{a^2 e^2 rKL + aeruL}{a^2 eKL + ur} & \frac{-u^2 r - aeruK}{a^2 eKL + ur} \end{pmatrix}$$

Thus, $X_4^{[p\_hp]}$ whenever feasible, is unconditionally stable, because the Routh-Hurwitz conditions are satisfied:

$$-\mathrm{tr}(J_{P_4}^{[p\_hp]}) = rK^{-1}X_4^{[p\_hp]} + uL^{-1}Z_4^{[p\_hp]} > 0,$$

$$\det(J_{P_4}^{[p\_hp]}) = (rK^{-1}uL^{-1} + a^2 e)X_4^{[p\_hp]}Z_4^{[p\_hp]} > 0.$$

$\square$

Remark 1.1.1. In particular, note that the condition on the trace being strictly positive prevents the occurrence of Hopf bifurcations at this equilibrium. They cannot also occur at $P_3^{[p\_hp]}$ since the corresponding eigenvalues are both real.

1.1.3 Equilibria of model (1.2)

To find the equilibrium points of the model (1.2), we need to solve the equilibrium equations:

$$rX\left(1 - \frac{X}{K}\right) - aZX = 0,$$

$$sY\left(1 - \frac{Y}{H}\right) - bZY = 0, \tag{1.8}$$

$$-mZ^2 + e(aZX + bZY) = 0.$$

Proposition 4. *The trivial equilibrium point* $P_1^{[p\text{-}ep]} = (0,0,0)$, $P_2^{[p\text{-}ep]} = (0, H, 0)$, $P_3^{[p\text{-}ep]} = (K, 0, 0)$ *and* $P_4^{[p\text{-}ep]} = (K, H, 0)$ *are always feasible and unstable.*

Proof. In the same way that we made before, we can solve the system (1.8) for $X = Y = Z = 0$, $X = Z = 0$ and $Y \neq 0$, $X \neq 0$ and $Y = Z = 0$, $Z = 0$ and $X \neq 0$, $Y \neq 0$ to obtain the coordinates of equilibria $P_1^{[p\text{-}ep]} = (0,0,0)$, $P_2^{[p\text{-}ep]} = (0, H, 0)$, $P_3^{[p\text{-}ep]} = (K, 0, 0)$ and $P_4^{[p\text{-}ep]} = (K, H, 0)$, respectively. The Jacobian matrix of these equilibria are

$$J_{P_1}^{[p\text{-}ep]} = \begin{pmatrix} r & 0 & 0 \\ 0 & s & 0 \\ 0 & 0 & 0 \end{pmatrix}, \quad J_{P_2}^{[p\text{-}ep]} = \begin{pmatrix} r & 0 & 0 \\ 0 & -s & -bH \\ 0 & 0 & ebH \end{pmatrix},$$

$$J_{P_3}^{[p\_ep]} = \begin{pmatrix} -r & 0 & -aK \\ 0 & s & 0 \\ 0 & 0 & aeK \end{pmatrix}, \quad J_{P_4}^{[p\_ep]} = \begin{pmatrix} -r & 0 & aK \\ 0 & -s & -bH \\ 0 & 0 & e(aK+bH) \end{pmatrix},$$

and their eigenvalues are r, s, 0 for $P_1^{[p\_ep]}$, r, $-s$, ebH for $P_2^{[p\_ep]}$, $-r$, s, eaK for $P_3^{[p\_ep]}$ and $-r$, $-s$, $aeK + beH$ for $P_4^{[p\_ep]}$. Finally, these equilibria are always feasible and unstable because at least one eigenvalue of each one is positive. $\qquad\square$

Proposition 5. *The equilibrium point $P_5^{[p\_ep]} = (0, Y_5^{[p\_ep]}, Z_5^{[p\_ep]})$ where $Y_5^{[p\_ep]} = \frac{msH}{b^2eH+ms}$, $Z_5^{[p\_ep]} = \frac{ebsH}{b^2eH+ms}$ exists and it is always feasible. Furthermore, it is stable if the condition*

$$aZ_5^{[p\_ep]} = \frac{abesH}{b^2eH + ms} > r \tag{1.9}$$

holds and if the Routh-Hurwitz conditions are satisfied:

$$-tr(\overline{J}_{P_5}^{[p\_ep]}) > 0, \quad \det(\overline{J}_{P_5}^{[p\_ep]}) > 0.$$

Proof. The coordinates of $P_5^{[p\_ep]}$ are obtained solving the system (1.8) for $X = 0$, $Y \neq 0$ and $Z \neq 0$ and the equilibrium is always feasible. The Jacobian matrix (1.5) evaluated at $P_5^{[p\_ep]}$ is given by

$$J_{P_5}^{[p\_ep]} = \begin{pmatrix} r - aZ_5^{[p\_ep]} & 0 & 0 \\ 0 & -\frac{s}{H}Y_5^{[p\_ep]} & -bY_5^{[p\_ep]} \\ aeZ_5^{[p\_ep]} & ebZ_5^{[p\_ep]} & -mZ_5^{[p\_ep]} \end{pmatrix}.$$

that provides one explicity eigenvalue $r - aZ_5^{[p\_ep]}$. The equilibrium $P_5^{[p\_ep]}$ is stable if

$$aZ_5^{[p\_ep]} = \frac{abesH}{b^2eH + ms} > r \tag{1.10}$$

holds and if the Routh-Hurwitz conditions for the remaining minor are always satisfied, i.e.

$$\frac{s}{H}Y_5^{[p\_ep]} + mZ_5^{[p\_ep]} > 0, \quad \left(\frac{ms}{H} + b^2e\right) Y_5^{[p\_ep]} Z_5^{[p\_ep]} > 0,$$

with

$$\overline{J}_{P_5}^{[p\_ep]} = \begin{pmatrix} -\frac{s}{H}Y_5^{[p\_ep]} & -bY_5^{[p\_ep]} \\ beZ_5^{[p\_ep]} & -mZ_5^{[p\_ep]} \end{pmatrix}.$$

$\qquad\square$

Proposition 6. *The equilibrium point* $P_6^{[p\_ep]} = (X_6^{[p\_ep]}, 0, Z_6^{[p\_ep]})$ *where* $X_6^{[p\_ep]} = \frac{mrK}{a^2eK+mr}$, $Z_6^{[p\_ep]} = \frac{aerK}{a^2eK+mr}$. *exists and it is always feasible. Furthermore, it is stable if the condition*

$$bZ_6^{[p\_ep]} = \frac{aberK}{a^2eK+mr} > s, \tag{1.11}$$

holds and if the Routh-Hurwitz conditions are satisfied:

$$-tr(\overline{J}_{P_6}^{[p\_ep]}) > 0, \quad \det(\overline{J}_{P_6}^{[p\_ep]}) > 0.$$

Proof. The coordinates of $P_6^{[p\_ep]}$ are obtained solving the system (1.8) for $X \neq 0$, $Y = 0$ and $Z \neq 0$ and the equilibrium is always feasible. The Jacobian matrix (1.5) evaluated at $P_6^{[p\_ep]}$ is given by

$$J_{P_6}^{[p\_ep]} = \begin{pmatrix} -\frac{r}{K}X_6^{[p\_ep]} & 0 & -aX_6^{[p\_ep]} \\ 0 & s-bZ_6^{[p\_ep]} & 0 \\ aeZ_6^{[p\_ep]} & ebZ_6^{[p\_ep]} & -mZ_6^{[p\_ep]} \end{pmatrix}.$$

that provides one explicity eigenvalue $s - bZ_6^{[p\_ep]}$. The equilibrium $P_6^{[p\_ep]}$ is stable if

$$bZ_6^{[p\_ep]} = \frac{aberK}{a^2eK+mr} > s, \tag{1.12}$$

holds and if the Routh-Hurwitz conditions for the remaining minors are always satisfied, i.e. $\frac{r}{K}X_6^{[p\_ep]} + mZ_6^{[p\_ep]} > 0$, $\left(\frac{mr}{K} + a^2e\right)X_6^{[p\_ep]}Z_6^{[p\_ep]} > 0$, with

$$\overline{J}_{P_6}^{[p\_ep]} = \begin{pmatrix} -\frac{r}{K}X_6^{[p\_ep]} & -aX_6^{[p\_ep]} \\ aeZ_6^{[p\_ep]} & -mZ_6^{[p\_ep]} \end{pmatrix}.$$

$\square$

Proposition 7. *The coexistence* $P_7^{[p\_ep]} = (X_7^{[p\_ep]}, Y_7^{[p\_ep]}, Z_7^{[p\_ep]})$, *with* $X_7^{[p\_ep]} = K - aKr^{-1}Z_7^{[p\_ep]}$, $Y_7^{[p\_ep]} = H - bHs^{-1}Z_7^{[p\_ep]}$, $Z_7^{[p\_ep]} = \frac{ers(bH+aK)}{s(a^2eK+mr)+b^2erH} > 0$ *is feasible if* $X_7^{[p\_ep]} \geq 0$ *and* $Z_7^{[p\_ep]} \geq 0$. *Furthermore, it is stable if the Routh-Hurwitz conditions are satisfied.*

Proof. The coordinates of $P_7^{[p\_ep]}$ are obtained solving the system (1.8) for $X \neq 0$, $Y \neq 0$ and $Z \neq 0$ and the feasibility requirements for $X_7^{[p\_ep]} \geq 0$ and for $Y_7^{[p\_ep]} \geq 0$ are given, respectively, by

$$r \geq aZ_7^{[p\_ep]} = \frac{abesH}{b^2eH+ms}, \quad s \geq bZ_7^{[p\_ep]} = \frac{aberK}{a^2eK+mr}. \tag{1.13}$$

For stability of the latter, the Jacobian evaluated at $P_7^{[p\_ep]}$ is

$$J_{P7}^{[p\_ep]} = \begin{pmatrix} -rK^{-1}X_7^{[p\_ep]} & 0 & -aX_7^{[p\_ep]} \\ 0 & -sH^{-1}Y_7^{[p\_ep]}, & -bY_7^{[p\_ep]} \\ aeZ_7^{[p\_ep]} & ebZ_7^{[p\_ep]} & -mZ_7^{[p\_ep]} \end{pmatrix}$$

and we have that

$$-\text{tr}(J_{P_7}^{[p\_ep]}) = \frac{r}{K}X_7^{[p\_ep]} + \frac{s}{H}Y_7^{[p\_ep]} + mZ_7^{[p\_ep]} > 0,$$

$$-\det(J_{P_7}^{[p\_ep]}) = \frac{X_7^{[p\_ep]}Y_7^{[p\_ep]}Z_7^{[p\_ep]}}{HK}(a^2esK + b^2erH + mrs) > 0.$$

Finally, the remaining Routh-Hurwitz conditions are satisfied, i.e.

$$\frac{r^2s}{K^2H}(X_7^{[p\_ep]})^2Y_7^{[p\_ep]} + \left(\frac{ra^2e}{K} + r^2m\right)(X_7^{[p\_ep]})^2Z_7^{[p\_ep]}$$

$$+ \left(\frac{3rms}{KH} + \frac{rb^2e}{K} + \frac{sa^2e}{H}\right)X_7^{[p\_ep]}Y_7^{[p\_ep]}Z_7^{[p\_ep]} + \left(\frac{sm^2}{H} + mb^2e\right)(Y_7^{[p\_ep]})^2Z_7^{[p\_ep]}$$

$$+ \left(\frac{s^2m}{H^2} + \frac{sb^2e}{H}\right)(Y_7^{[p\_ep]})^2Z_7^{[p\_ep]} + \left(\frac{m^2r}{K} + ea^2m\right)X_7^{[p\_ep]}(Z_7^{[p\_ep]})^2$$

$$+ \frac{s^2r}{KH^2}X_7^{[p\_ep]}(Y_7^{[p\_ep]})^2 + \left(\frac{b^2erH + a^2esK + rms}{KH}\right)X_7^{[p\_ep]}Y_7^{[p\_ep]}Z_7^{[p\_ep]} > 0,$$

is clearly satisfied as well. Thus the coexistence equilibrium $P_7^{[p\_ep]}$ of (1.2) is unconditionally stable, when feasible. $\square$

From (1.10) and the first condition of (1.13) there is a transcritical bifurcation linking $P_7^{[p\_ep]}$ with $P_5^{[p\_ep]}$ and, from (1.12) and the second condition of (1.13) there is a transcritical bifurcation linking $P_7^{[p\_ep]}$ with $P_6^{[p\_ep]}$.

1.2 Global stability for the equilibria of models (1.1) and (1.2)

The coexisting equilibrium point $P_4^{[p\_hp]}$ of the model (1.1) cannot undergo any Hopf-bifurcation, recall Remark (1.1.1) in Section 1.1.2. Here we prove that the feasibility of $P_4^{[p\_hp]}$ implies that it is globally asymptotically stable. For this purpose we consider the following Lyapunov function,

$$V_4^{[p\_hp]}(X(t), Z(t)) = \left(X - X_4^{[p\_hp]} - X_4^{[p\_hp]}\ln\frac{X}{X_4^{[p\_hp]}}\right)$$

$$+ \alpha_1\left(Z - Z_4^{[p\_hp]} - Z_4^{[p\_hp]}\ln\frac{Z}{Z_4^{[p\_hp]}}\right),$$

where α_1 is a positive constant, yet to be determined. Differentiating the above function with respect to t along the solution trajectories of system (1.1), we find

$$\frac{dV_4^{[p\_hp]}}{dt} = -\frac{r}{K}\left(X - X_4^{[p\_hp]}\right)^2 - \alpha_1 \frac{u}{L}\left(Z - Z_4^{[p\_hp]}\right)^2$$
$$+ \; a(\alpha_1 e - 1)(X - X_4^{[p\_hp]})(Z - Z_4^{[p\_hp]}).$$

If we choose $\alpha_1 = \frac{1}{e} > 0$, then the above derivative is negative definite except at the equilibrium point $P_4^{[p\_hp]}$. Hence $P_4^{[p\_hp]}$ is a globally stable equilibrium point whenever it is feasible.

For the equilibrium $P_3^{[p\_hp]}$ we instead choose

$$V_3^{[p\_hp]}(X(t),\, Z(t)) = \alpha_2 X + \alpha_1 \left(Z - Z_3^{[p\_hp]} - Z_3^{[p\_hp]} \ln \frac{Z}{Z_3^{[p\_hp]}}\right),$$

and differentiation along the system trajectories leads to

$$\frac{dV_3^{[p\_hp]}}{dt} = -\alpha_2 \frac{r}{K} X^2 - \alpha_1 \frac{u}{L}\left(Z - Z_3^{[p\_hp]}\right)^2 + [aZ(\alpha_2 e - \alpha_1) + \alpha_1 r - \alpha_2 eaL]X$$

so that choosing $\alpha_2 e = \alpha_1$ and using the feasibility condition (1.6), the derivative of $V_3^{[p\_hp]}$ becomes negative definite. Hence, when feasible, also $P_3^{[p\_hp]}$ is globally asymptotically stable.

Similarly, by choosing the following Lyapunov function,

$$W_7^{[p\_ep]}(X(t),\, Y(t),\, Z(t)) = \left(X - X_7^{[p\_ep]} - X_7^{[p\_ep]} \ln \frac{X}{X_7^{[p\_ep]}}\right)$$
$$+ \; \left(Y - Y_7^{[p\_ep]} - Y_7^{[p\_ep]} \ln \frac{Y}{Y_7^{[p\_ep]}}\right)$$
$$+ \; \beta_1 \left(Z - Z_7^{[p\_ep]} - Z_7^{[p\_ep]} \ln \frac{Z}{Z_7^{[p\_ep]}}\right),$$

β_1 is a positive constant required to be determined. Differentiating the function $W_7^{[p\_ep]}$ along the solution trajectories of the system (1.2) we find, after some algebraic manipulation,

$$\frac{dW_7^{[p\_ep]}}{dt} = -\frac{r}{K}\left(X - X_7^{[p\_ep]}\right)^2 - \frac{s}{H}\left(Y - Y_7^{[p\_ep]}\right)^2 - m\beta_1 \left(Z - Z_7^{[p\_ep]}\right)^2$$
$$+ \; [a(1 - e\beta_1)(X - X_7^{[p\_ep]}) + b(1 - e\beta_1)(Y - Y_7^{[p\_ep]})](Z - Z_7^{[p\_ep]}).$$

Choosing $\beta_1 = \frac{1}{e}$ we find that the derivative of $W_7^{[p\_ep]}$ is negative definite except at $P_7^{[p\_ep]}$. Hence $P_7^{[p\_ep]}$ is a global attractor whenever it is feasible.

For the other equilibria, again when locally asymptotically stable, they are also globally asymptotically stable. Indeed we consider instead, e.g. for $P_5^{[p\_ep]}$, the function

$$W_5^{[p\_ep]}(X(t), Y(t), Z(t)) = \alpha_2 X + \alpha_3 \left(Y - Y_5^{[p\_ep]} - Y_5^{[p\_ep]} \ln \frac{Y}{Y_5^{[p\_ep]}} \right)$$

$$+ \alpha_1 \left(Z - Z_5^{[p\_ep]} - Z_5^{[p\_ep]} \ln \frac{Z}{Z_5^{[p\_ep]}} \right).$$

Once more, differentiation along the trajectories gives

$$\frac{dW_5^{[p\_ep]}}{dt} = -\alpha_2 \frac{r}{K} \left(X - X_5^{[p\_ep]} \right)^2 - \alpha_3 \frac{s}{H} \left(Y - Y_5^{[p\_ep]} \right)^2 - \alpha_1 m \left(Z - Z_5^{[p\_ep]} \right)^2$$

$$+ [a(1 - e\alpha_1)(X - X_5^{[p\_ep]}) + X[\alpha_2 r - \alpha_3 a Z_5^{[p\_ep]} - aZ(\alpha_3 - \alpha_2)]$$

and choosing $\alpha_2 = \alpha_3 = e\alpha_1$ and using the local stability condition (1.10) the above derivative of $W_5^{[p\_ep]}$ is negative definite. Hence the global stability for $P_5^{[p\_ep]}$. For $P_6^{[p\_ep]}$ the result is obtained in the same way, using (1.12).

1.3 Transcritical bifurcation of model (1.1)

Here we verify the analytical transversality conditions required for the transcritical bifurcation between the equilibrium points $P_3^{[p\_hp]}$ and $P_4^{[p\_hp]}$. For convenience we consider r as the bifurcation parameter. The axial equilibrium point $P_3^{[p\_hp]}$ coincides with the coexistence equilibrium $P_4^{[p\_hp]}$ at the parametric threshold $r_{TC} = aL$.

The Jacobian matrix of the system (1.1) evaluated at $P_3^{[p\_hp]}$ and at the parametric threshold $r = aL$, we find

$$J_{P_3}^{[p\_hp]}(r_{TC}) = \begin{pmatrix} 0 & 0 \\ eaL & -u \end{pmatrix},$$

and its right and left eigenvectors, corresponding to the zero eigenvalue, are given by $V_1 = \varphi_1(1, \frac{er}{u})^T$ and $Q_1 = \omega_1(1, 0)^T$, where φ_1 and ω_1 are arbitrary nonzero real numbers. Differentiating partially the right hand sides of the equation (1.1) with respect to r and calculating its Jacobian matrix, we respectively find

$$f_r = \begin{pmatrix} X_3^{[p\_hp]}(1 - \frac{X_3^{[p\_hp]}}{K}) \\ 0 \end{pmatrix}, \quad Df_r = \begin{pmatrix} 1 - \frac{2X_3^{[p\_hp]}}{K} & 0 \\ 0 & 0 \end{pmatrix}.$$

Here we use the same notations of [70] to verify the Sotomayor's conditions for the existence of a transcritical bifurcation. Let $D^2 f((X, Z); r)(V_1, V_1)$ be

14

defined by

$$
\begin{pmatrix}
\frac{\partial^2 f_1}{\partial X^2}\xi_1^2 + 2\frac{\partial^2 f_1}{\partial X \partial Z}\xi_1\xi_2 + \frac{\partial^2 f_1}{\partial Z^2}\xi_2^2 \\
\frac{\partial^2 f_2}{\partial X^2}\xi_1^2 + 2\frac{\partial^2 f_2}{\partial X \partial Z}\xi_1\xi_2 + \frac{\partial^2 f_2}{\partial Z^2}\xi_2^2
\end{pmatrix},
$$

where $f_1 = rX\left(1 - XK^{-1}\right) - aZX$, $f_2 = uZ\left(1 - ZL^{-1}\right) + aeZX$ are the right hand sides of (1.1) and ξ_1, ξ_2 are the components of the eigenvector V_1.

After calculating D^2f we can easily verify the following three conditions

$$
Q_1^T f_r((0,L); r_{TC}) = 0, \quad Q_1^T Df_r((0,L); r_{TC})V_1 = 1 \neq 0,
$$

$$
Q_1^T D^2 f((0,L); r_{TC})(V_1, V_1) = -2aL\left(\frac{1}{K} + \frac{ae}{u}\right) \neq 0.
$$

Hence all the conditions for transcritical bifurcation are satisfied. In the above expression, $Df_r((0,L); r_{TC})$ denotes the Jacobian of the matrix f_r evaluated at $(0,L)$ for $r = r_{TC}$.

Figure 1.1 illustrates the simulation explicitly showing the transcritical bifurcation between $P_3^{[p\_hp]}$ and $P_4^{[p\_hp]}$ for the chosen parameters values (see the caption of Fig. 1.1) when the parameter r crosses a critical value r_{TC}

$$
r_{TC} = aL = 1 \tag{1.14}
$$
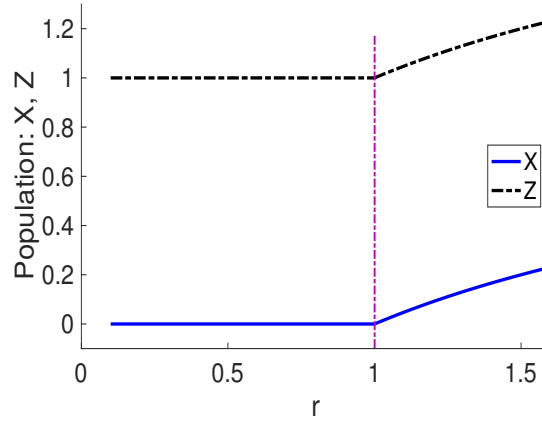
Figure 1.1: Transcritical bifurcation between $P_3^{[p\_hp]}$ and $P_4^{[p\_hp]}$ for the parameter values: $K = a = u = L = e = 1$. Initial conditions $X_0 = Z_0 = 0.01$. The equilibrium $P_3^{[p\_hp]}$ is stable from 0.1 to 1 and $P_4^{[p\_hp]}$ is stable past 1; the vertical line corresponds at the transcritical bifurcation threshold between the equilibria.

1.4 Numerical simulation results of model (1.2)

Similar to what was done in Section 1.3 we also verify the transversality conditions required for the transcritical bifurcations between the coexistence equilibrium $P_7^{[p\_ep]}$ and first the equilibrium point $P_5^{[p\_ep]}$, and secondly with the equilibrium point $P_6^{[p\_ep]}$. Considering a and b for convenience as the bifurcation parameters in the two cases, these bifurcations occur respectively at the parametric thresholds

$$a_{TC} = \frac{mrs + b^2 erH}{besH}, \quad b_{TC} = \frac{mrs + a^2 esK}{aerK}.$$

The Jacobian matrix of the system (1.2) evaluated at $P_7^{[p\_ep]}$ and at the parametric threshold a_{TC} becomes

$$J_{P_7}^{[p\_ep]}(a_{TC}) = \begin{pmatrix} 0 & 0 & 0 \\ 0 & -\frac{ms^2}{b^2eH+ms} & -\frac{bmsH}{b^2eH+ms} \\ er & \frac{b^2e^2sH}{b^2eH+ms} & -\frac{bemsH}{b^2eH+ms} \end{pmatrix},$$

and its right and left eigenvectors, corresponding to the zero eigenvalue, are given by

$$V_2 = \varphi_2(1, -\frac{r}{s}, \frac{r}{bH})^T, \quad Q_2 = \omega_2(1, 0, 0)^T,$$

where φ_2 and ω_2 represent arbitrary nonzero real numbers. Differentiating partially the right hand sides of (1.2) with respect to a, we find

$$f_a = \begin{pmatrix} -X_7^{[p\_ep]} Z_7^{[p\_ep]} \\ 0 \\ eX_7^{[p\_ep]} Z_7^{[p\_ep]} \end{pmatrix},$$

and calculating its Jacobian matrix, we get

$$Df_a = \begin{pmatrix} -Z_7^{[p\_ep]} & 0 & -X_7^{[p\_ep]} \\ 0 & 0 & 0 \\ eZ_7^{[p\_ep]} & 0 & eX_7^{[p\_ep]} \end{pmatrix}.$$

After calculating $D^2 f$ we can then verify the following three conditions

$$Q_2^T f_a(P_7^{[p\_ep]}; a_{TC}) = 0, \tag{1.15}$$

$$Q_2^T Df_a(P_7^{[p\_ep]}; a_{TC})V_2 = -\varphi_2\omega_2 \frac{besH}{b^2eH+ms} \neq 0 \tag{1.16}$$

and

$$Q_2^T D^2 f(P_7^{[p\_ep]}; a_{TC})(V_2, V_2) = -\varphi_2^2\omega_2(\frac{2r}{K} + \frac{2r^2}{sH} + \frac{2mr^2}{b^2eH^2}) \neq 0. \tag{1.17}$$

16

Now, considering the parametric threshold, b_{TC}, the Jacobian matrix of the system (1.2) evaluated at $P_7^{[p\text{-}ep]}$ and at b_{TC} is

$$J_{P_7}^{[p\text{-}ep]}(b_{TC}) = \begin{pmatrix} -\frac{mr^2}{a^2eK+mr} & 0 & -\frac{amrK}{a^2eK+mr} \\ 0 & 0 & 0 \\ \frac{a^2e^2rK}{a^2eK+mr} & es & -\frac{aemrK}{a^2eK+mr} \end{pmatrix},$$

and its right and left eigenvectors, corresponding to the zero eigenvalue, are given by

$$V_3 = \varphi_3(1, -\frac{r}{s}, \frac{r}{aK})^T, \quad Q_3 = \omega_3(0, 1, 0)^T,$$

where φ_3 and ω_3 are any nonzero real numbers. Differentiating partially the right hand sides of the equation (1.2) with respect to b, we find

$$f_b = \begin{pmatrix} 0 \\ -Y_7^{[p\text{-}ep]} Z_7^{[p\text{-}ep]} \\ eY_7^{[p\text{-}ep]} Z_7^{[p\text{-}ep]} \end{pmatrix},$$

and calculating its Jacobian matrix, we get

$$Df_b = \begin{pmatrix} 0 & 0 & 0 \\ 0 & -Z_7^{[p\text{-}ep]} & -Y_7^{[p\text{-}ep]} \\ 0 & eZ_7^{[p\text{-}ep]} & Y_7^{[p\text{-}ep]} \end{pmatrix}.$$

After calculating D^2f we can once more easily verify the following three conditions

$$Q_3^T f_b(P_7^{[p\text{-}ep]}; b_{TC}) = 0, \tag{1.18}$$

$$\begin{aligned} Q_3^T Df_b(P_7^{[p\text{-}ep]}; b_{TC})V_3 &= -\varphi_3\omega_3 \frac{a^2er^2K^2 + a^2ersHK + mr^2sH}{a^3esK^2 + ab^2erHK + amrsK} \\ &\neq 0 \end{aligned} \tag{1.19}$$

and

$$Q_3^T D^2 f(P_7^{[p\text{-}ep]}; b_{TC})(V_3, V_3) = -\varphi_3{}^2\omega_3(\frac{2r}{K} + \frac{2r^2}{sH} + \frac{2mr^2}{b^2eH^2}) \neq 0. \tag{1.20}$$

Hence all the conditions for transcritical bifurcation are satisfied. Note that $Df_a(P_7^{[p\text{-}ep]}; a_{TC})$ and $Df_b(P_7^{[p\text{-}ep]}; b_{TC})$ in the above expressions (1.16) and (1.19) denote the Jacobian of the matrix f_a and f_b evaluated at $P_7^{[p\text{-}ep]}$ for

17

$a = a_{TC}$ and $b = b_{TC}$, respectively. Finally, (1.17) and (1.20) are obtained from

$$D^2 f((X, Y, Z); \psi)(V, V) \tag{1.21}$$
$$= \begin{pmatrix} \frac{\partial^2 f_1}{\partial X^2}\xi_1^2 + 2\frac{\partial^2 f_1}{\partial X \partial Y}\xi_1\xi_2 + 2\frac{\partial^2 f_1}{\partial X \partial Z}\xi_1\xi_3 + 2\frac{\partial^2 f_1}{\partial Y \partial Z}\xi_2\xi_3 + \frac{\partial^2 f_1}{\partial Y^2}\xi_2^2 + \frac{\partial^2 f_1}{\partial Z^2}\xi_3^2 \\ \frac{\partial^2 f_2}{\partial X^2}\xi_1^2 + 2\frac{\partial^2 f_2}{\partial X \partial Y}\xi_1\xi_2 + 2\frac{\partial^2 f_2}{\partial X \partial Z}\xi_1\xi_3 + 2\frac{\partial^2 f_2}{\partial Y \partial Z}\xi_2\xi_3 + \frac{\partial^2 f_2}{\partial Y^2}\xi_2^2 + \frac{\partial^2 f_2}{\partial Z^2}\xi_3^2 \\ \frac{\partial^2 f_3}{\partial X^2}\xi_1^2 + 2\frac{\partial^2 f_3}{\partial X \partial Y}\xi_1\xi_2 + 2\frac{\partial^2 f_3}{\partial X \partial Z}\xi_1\xi_3 + 2\frac{\partial^2 f_3}{\partial Y \partial Z}\xi_2\xi_3 + \frac{\partial^2 f_3}{\partial Y^2}\xi_2^2 + \frac{\partial^2 f_3}{\partial Z^2}\xi_3^2 \end{pmatrix},$$

where

$$f_1 = rX\left(1 - \frac{X}{K}\right) - aZX, \quad f_2 = sY\left(1 - \frac{Y}{H}\right) - bZY,$$

$$f_3 = -mZ^2 + e(aZX + bZY)$$

are the right hand sides of (1.2), ψ is the bifurcation parameter and ξ_1, ξ_2, ξ_3 are the components of the eigenvector V.

We now consider a numerical example to understand the dynamics of the model (1.2). We fix the parameter values $r = 3$, $K = 100$, $s = 4$, $H = 120$, $m = 0.2$ and $e = 0.5$. The other two parameters, a and b are considered as bifurcation parameters. We verify that the trivial equilibrium $P_1^{[p\text{-}ep]}$, two axial equilibria $P_2^{[p\text{-}ep]}$ and $P_3^{[p\text{-}ep]}$ and boundary equilibrium $P_4^{[p\text{-}ep]}$ are always unstable irrespective of the parameter values for a and b. $P_5^{[p\text{-}ep]}$ is stable for $300b > 3(250b^2 + 1)$ and is unstable otherwise. Similary $P_6^{[p\text{-}ep]}$ is stable for $250a > 4(250a^2 + 1)$. The coexistence equilibrium point $P_7^{[p\text{-}ep]}$ is feasible when the parametric restrictions $300b < 3(250b^2 + 1)$ and $250a < 4(250a^2 + 1)$ are satisfied simultaneously. The coexisting equilibrium point is stable whenever it is feasible.

Analytically we have discovered that the coexisting equilibrium point for the model (1.1) is stable whenever it is feasible. Now we can demonstrate how the stability of this coexisting equilibrium point is altered by explicitly considering the alternative prey population in the system. We fix the parameter values $r = 3$, $K = 100$ and $e = 0.5$. The existence and hence the stability of the coexistence equilibrium is determined by the grazing rate a and the carrying capacity L of the generalist predator. For $a = 0.1$, $P_4^{[p\_hp]}$ is feasible and stable for $L < 30$ but for $a = 0.3$ we find $P_4^{[p\_hp]}$ is feasible and stable only for $L < 10$. Here, the intrinsic growth rate of the generalist predator has no role in determining the stability of $P_4^{[p\_hp]}$; rather, stable coexistence depends just on L. Now we consider the model (1.2) with two fixed parameter values of a, that is $a = 0.1$ and $a = 0.3$, respectively.

The components of $P_1^{[p\text{-}ep]}$, $P_2^{[p\text{-}ep]} = (0, H, 0)$, $P_3^{[p\text{-}ep]} = (K, 0, 0)$, $P_4^{[p\text{-}ep]} = (K, H, 0)$ and $P_6^{[p\text{-}ep]} = (54.54545455, 0, 13.63636364)$ are independent of b
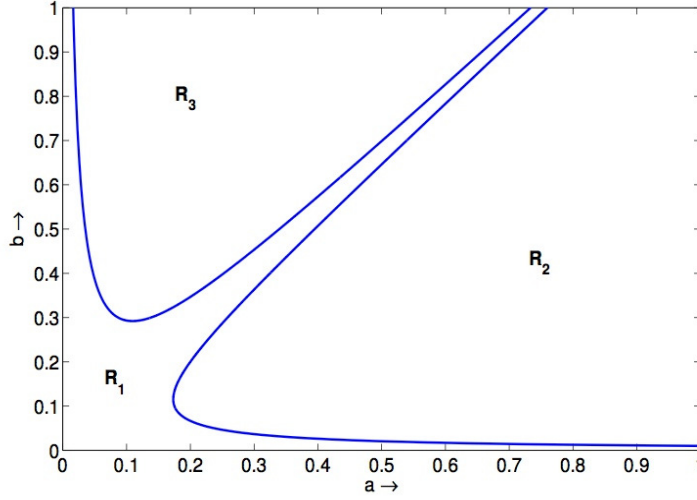
Figure 1.2: Bifurcation diagram in the $a - b$ parameter space. The two trans-critical bifurcation curves divide the parameter space into the three regions. In R_1 the coexistence equilibrium $P_7^{[p\text{-}ep]}$ is stable; in R_2 instead the primary-prey-free $(X_5^{[p\text{-}ep]} = 0)$ equilibrium $P_5^{[p\text{-}ep]}$ is stable; in R_3 we find the substitute-prey-free $(Y_6^{[p\text{-}ep]} = 0)$ equilibrium $P_6^{[p\text{-}ep]}$ to be stable.

however $P_6^{[p\text{-}ep]} = (54.54545455, 0, 13.63636364)$ and

$$P_5^{[p\text{-}ep]} = \left(0, \frac{12}{1 + 75b^2}, \frac{300b}{1 + 75b^2}\right),$$

$$P_7^{[p\text{-}ep]} = \left(\frac{45000b^2 - 6000b + 600}{11 + 450b^2}, \frac{1320 - 4500b}{11 + 450b^2}, \frac{1800b + 150}{11 + 450b^2}\right).$$

depend on b.

The coexistence equilibrium is feasible and stable for $b < 0.29333333$. For $b > 0.29333333$, instead the coexistence point does not exists, the substitute prey species goes to extinction and $P_6^{[p\text{-}ep]}$ is stable.

Next, we consider $a = 0.3$. In this case we discover an interesting situation: coexistence is feasible and stable for $b < 0.03670068382$ and $0.3632993162 < b < 0.4533333333$, while the primary prey resource becomes extinct and $P_5^{[p\text{-}ep]}$ is stable for $0.03670068382 < b < 0.3632993162$ and finally, the substitute prey population vanishes and $P_6^{[p\text{-}ep]}$ is stable for $b > 0.4533333333$. Increasing grazing pressure on substitute prey leads to its extinction when the predation on the primary resource does not vary. On the other hand, extinction of the main prey is observed if the hunting on it increases while the grazing pressure on the second population remains fixed. These numerical results, obtained by our own MATLAB code, are in agreement with the bifurcation diagram shown in Figure 1.2.

19

1.5 Comparing analytical findings for the models (1.1) and (1.2)

Both models are capable to represent the extinction of prey $X(t)$ and the survival of the predators $Z(t)$. In model (1.1) this situation corresponds to the equilibrium point $P_3^{[p\_hp]} = (0, L)$ while the analogue situation in model (1.2) is represented by point $P_5^{[p\_ep]} = (0, Y_5^{[p\_ep]}, Z_5^{[p\_ep]})$. Note that in model (1.1) predator survival is due to the existence of a hidden resource, i.e., there is one population able to sustain the predator. This situation is represented by the equilibrium point $P_5^{[p\_ep]}$ in model (1.2), where here the resource is explicitly exhibited at the non-vanishing level $Z_5^{[p\_ep]}$. If we now use these correspondences between the points and compare the coordinates X and Z of models (1.1) and (1.2) we obtain

$$L = Z_5^{[p\_ep]} = \frac{eb}{m} Y_5^{[p\_ep]}, \tag{1.22}$$

which is consistent with the result obtained earlier, compare indeed the second condition in (1.3). In view of the first above equality, (1.22), stability of the two equilibria is completely analogous, compare indeed (1.6) and (1.10), while both are unconditionally feasible. Note also that the results on global stability of these corresponding equilibria is again analogous, whenever viable, they are also globally asymptotically stable. In summary, $P_3^{[p\_hp]}$ and $P_5^{[p\_ep]}$ are completely equivalent.

Using a similar reasoning for the coexistence situation in both models we obtain the correspondence between the equilibrium points $P_4^{[p\_hp]}$ and $P_7^{[p\_ep]}$. Indeed in both these equilibria, the main prey and the predators coexist. In this case, both are unconditionally locally and globally asymptotically stable. Note that substituting $X_4^{[p\_hp]}$ into $Z_4^{[p\_hp]}$ we find $X_4^{[p\_hp]} = K(1 - ar^{-1} Z_4^{[p\_hp]})$, which corresponds to the formula for $X_7^{[p\_ep]}$. For feasibility we find a correspondence between the conditions (1.7) and the first one of (1.13), but in the latter case another additional condition is needed. Therefore acting on this second feasibility condition, essentially on the parameter s, $P_7^{[p\_ep]}$ could be made unfeasible while $P_4^{[p\_hp]}$ in principle retains its feasibility.

Note also that equilibrium $P_6^{[p\_ep]} = (X_6^{[p\_ep]}, 0, Z_6^{[p\_ep]})$ does not have any correspondent point in the model (1.1), since this system assumes that the alternative prey is always available, because we cannot set $L = 0$ in it.

1.6 An application

In this section we provide a numerical example based on a realistic ecosystem. We consider as predator the pine marten Z, *Martes martes L.*, that feeds possibly on the grey squirrel X, *Sciurus carolinensis*, taken here as the

primary prey, and on the European hare Y, *Lepus Europaeus*, considered as the alternative resource. This example has practical relevance since both the European hare and the grey squirrel are nowadays established invasive species in Piemonte, NW Italy, [35, 64]. Some indications on the parameter values are given in the available literature, first line of (1.23); for the parameters for which an estimate does not exist instead, we choose hypothetical values, second line of (1.23), and numerically explore the possible ecosystem behaviour as they are varied. From [79], the pine marten net reproductive rate ranges in the interval 0.9-1.2; also, for the Swiss and Italian Alps, its density is about 0.1-0.8 individual per square Km, [59]. For the hare, the net reproductive rate is about 1.96, while the density in the Alps ranges between 2-5 individuals to a maximum value of 10 individuals per square Km, [64]. The grey squirrel has a net reproductive rate of 1.28 and density of 20 individuals per square Km, [10]. The time unit is taken as the year.

Based on the above information, the parameter reference values that we use for the simulations are:

$$r = 1.28, \quad K = 20, \quad s = 1.96, \quad H = 5, \quad u = 1.2, \quad L = 0.1;$$
$$e = 0.8, \quad a = 1, \quad m = 12, \quad b = 1.$$

We have assumed that in the absence of food a pine marten dies in about a month, thereby setting the value for m. Note that with this choice the last condition in (1.3) is satisfied.

In Fig. 1.3 we plot the equilibrium values of the three population densities as functions of the hunting parameters a and b. In agreement with the findings of the previous section, the squirrels, the main prey X, vanishes in the left portion of the parameter space, while the alternative prey thrives there and vanishes in the opposite portion of the space. The predator Z thrives instead in the whole parameter space by feeding on each surviving prey in the two different portions of the space. Both prey densities are depressed for larger values of both hunting rates. Somewhat counterintuitively, the predator density in such conditions drops also. This can be explained by the fact that in such case both prey are removed faster and therefore there are less resources for the pine marten, so that a large predator population cannot be sustained.

We investigate then the behaviour of the model (1.2) in the $a - m$ parameter space for the subsequent comparison with the system with the generalist predator, i.e. with model (1.1), Fig. 1.4. Note that in the left part of the parameter space, the main prey X vanishes, while in the remaining part of the plane the ecosystem attains coexistence. Here again the predator population density drops as both its mortality and the hunting rate increase independently of each other. The prey experience a gain from higher predator mortalities. The main prey is also depressed by a higher hunting rate, while the alternative prey has a relief: indeed in this case the predation rate a concerns only the primary resource, so that if it is exploited more, the secondary prey suffers
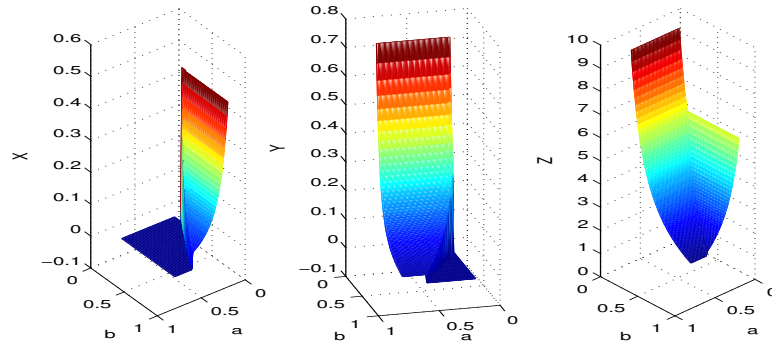
Figure 1.3: The coexistence equilibrium value in the $a - b$ parameter space for the model (1.2). Left to right the squirrels X, hares Y and pine marten Z population densities. The remaining fixed parameters values are given in (1.23).

less.

Finally in Fig. 1.5 we consider model (1.1). In the $a - u$ parameter space, we let u vary in a domain that is comparable with the range used for m in Fig. 1.4. Clearly, here the squirrels density behaviour mimicks the one found in Fig. (1.2). Instead, the predators behave in the same way as for the mortality rate m in Fig. 1.4, when the reproduction rate u is concerned, but their density drops with increasing hunting rate, at least for low values of u, while in Fig. 1.4 it remains essentially constant.
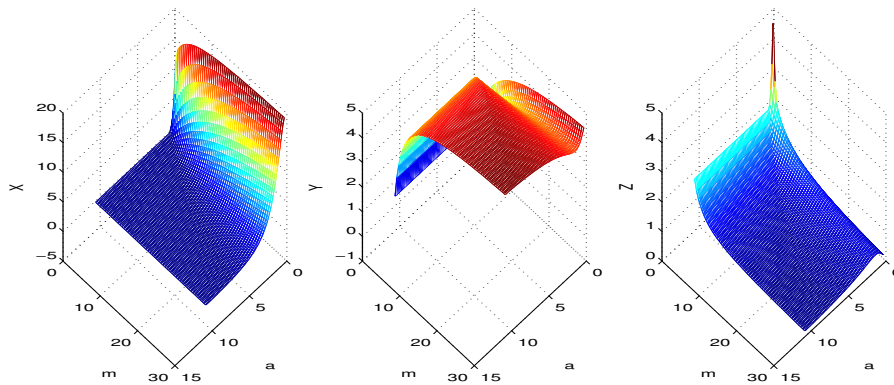
Figure 1.4: The coexistence equilibrium value in the $a - m$ parameter space for the model (1.2). Left to right the squirrels X, hares Y and pine marten Z population densities. The remaining fixed parameters values are given in (1.23).

22
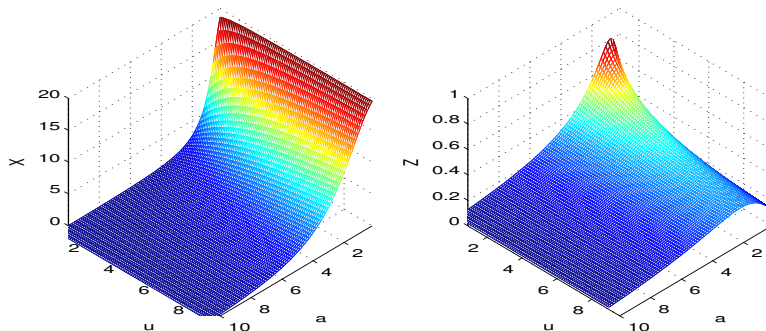
Figure 1.5: The coexistence equilibrium value in the $a - u$ parameter space for the model (1.1). Left to right the squirrels X, hares Y and pine marten Z population densities. The remaining fixed parameters values are given in (1.23).

1.7 Discussion

This chapter is devoted to investigate the differences in the dynamics between two predator-prey models with a generalist predator in the first model and a specialist predator on two prey in the second on. The alternative food source for the predator is implicit in the first model, but in the second model we have considered it explicitly. The most significant difference between the two models lies in the fact that the grazing pressure on the preferred prey and carrying capacity of the predator determine the stable coexistence of prey and predator when the alternative resource is implicit. It is interesting to note that for predator-prey models with specialist predator and logistic growth for the prey population, we cannot find any prey species extinction scenario due to overexploitation. However, if the predators have an alternative resource other than their favorite prey, higher rate of consumption of one prey species can drive them towards extinction. Due to the presence of the alternative food source for the generalist predator, no predators' extinction scenario can be observed as the prey-only equilibrium point $(K, 0)$ is always unstable. Although the predators have an alternative food source, they still survive on their most favorite food. As a result the ecosystem extinction and the predator-free equilibrium point $(K, 0)$ are always non-achievable by the system trajectories, as they are unstable. The generalist predator grazing rate on the primary prey a determines which one of the equilibria is stable, the favorite prey-free point $P_3^{[p\_hp]}$ or the coexistence $P_4^{[p\_hp]}$.

To ensure the coexistence of both the prey populations and the generalist predator some balance between the respective grazing pressures exerted on them needs to be maintained. Higher grazing pressure only on one species always leads to its extinction, but we never find total system collapse, where

23

extinction of both the prey populations is responsible for the extinction of the predator as well. For both types of models, the feasibility and local asymptotic stability of the equilibria imply also their global asymptotic stability.

Note finally that when we consider the ecosystem with both prey populations explicitly modeled, there is no equilibrium point of the form $(0, 0, Z)$. In such case thus the survival of the predator population alone is not possible. This result is quite reasonable, because then the predator is left with no food available and thus starves to death. The model with implicit prey however cannot show the same behaviour, as the alternative food source is constant and thus remains unaltered and therefore predicts something different.

The numerical simulations performed on a concrete ecosystem show that there could be a difference in the model behaviour whether or not the alternative resource is explicitly built into the system. The predator density drops with decreasing hunting rate for low values of the reproduction rate when the secondary prey is hidden and the predators are treated as generalist, while if they are specialist on both species their steady state level remains about constant. So at least in this case, apparently the hiding of the secondary prey as a generic alternative resource plays a significant role, in that it changes a bit the behaviour of the predators steady state outcomes.

CHAPTER 2

COMPARING PREDATOR-PREY MODELS WITH HIDDEN AND EXPLICIT RESOURCES WITH A TRANSMISSIBLE DISEASE IN THE PREY SPECIES

Currently, mathematical models in ecoepidemiology play an important tools in the analysis of the spread and control of infectious diseases among interacting animal communities [4, 37, 82]. Most models dealing with the transmission of infectious diseases descend from the classic SIR model [43, 49, 84]. However, in this chapter we consider models only of type SI, [83], to keep the presentation simple without obscuring the main goals with unnecessary mathematical complications.

The main focus of this investigation concerns the fact that in modeling some selected features in nature are chosen as being part of the general picture one wants to set in the mathematical framework, while necessarily some others are neglected. The situation is similar to the well-know story that cartographers were asked to produce a very accurate map of the terrain, and to obtain that any scale smaller than the 1:1 would be insufficient. But the result was that such a map would cover completely the ground and therefore be absolutely useless. When looking at ecological situations, apart from including or excluding particular features of the ecosystem at hand, it is important to decide which dependent variables are essential for the effective description of the picture. In that respect, including too many may lead to a full illustration of the system dynamics, which can be simulated via numerical devices but excludes any sort of mathematical qualitative analysis, in view of its complexity. Needless to

say, the simulations must be repeated over and over again giving each time different values to the relevant parameters, in order to obtain qualitative information on the future system behaviour. On the contrary the mathematical analysis, if it can be carried out, would answer these evolution questions in a relatively easy fashion. When it comes to quantitative predictions, the roles reverse, and it is the numerical simulations that could provide more or less reliable answers, but those would depend on the accurate measurements of the parameters of the model, which may not all be known or available.

Setting our perspective from the qualitative viewpoint, sometimes of the many actors on the scene, i.e. the several species interacting in a natural scenery, some should be excluded in order to render the mathematical description analytically tractable. It may thus happen that some populations are judged to play a less relevant role and are not therefore modeled as system's variables. For instance, a (generalist) predator may sussist on several prey, but to reduce the number of interacting populations in the dynamical system formulation, only the main one is explicitly taken into account. But in so doing something is lost and it is not clear if this entails relevant consequences for the ensuing analysis. Here we would like to consider exactly this issue, and exploring namely what are the implications of omitting one explicit (prey) population from the dynamical formulation of a predator-prey interaction. We thus compare two models, one in which the omission is compensated by some "generic" alternative resources available for the predator, and a second one in which the previously omitted population is instead explicitly accounted for as a system variable. In nature there are very many such instances, we mention for instance the pine marten *Martes martes L.*, that can feed possibly on grey squirrel *Sciurus carolinensis* and the European hare *Lepus Europaeus*, both now invasive species in Northern Italy, [35, 64]. Either one could be forgotten, if the focus of the model is for instance finding eradication measures for the other one.

The main objective of this Chapter is therefore the comparative study of two predator-prey ecoepidemic models, an example of which is discussed in [13, 42], although food webs can also be considered, see for instance [48]. We assume that the disease spreads among the prey population. The difference between the models is represented by the predator having an alternative food source, which is implicit in the first formulation and explicit in the second one. Thus the predator is assumed to be generalist in the first model, while in the second model, because of this explicitly accounted for alternative food resource, the predator is regarded as specialist on both prey species. This Chapter extends to ecoepidemic situations the analysis already performed on the purely demographic ecosystems, [5, 51, 81].

The presentation is organized as follows: In Section 2.1, we present the model for the generalist predator and in Section 2.2, the corresponding model with two prey and the specialist predator. In both situations, we show that

the systems trajectories remain confined within a compact set, we study local and global stability, and determine existing bifurcations between the equilibria of the model. The outcomes of the two models are compared in Section 2.3 and a final discussion concludes the Chapter.

2.1 The model with hidden resources

Let the prey population be denoted by X, the infected prey population U, which is assumed to be weakened by the disease so as not to be able to reproduce nor to interfere with the susceptibles, and the predator population Z. The predator population has an alternative food supply, indicated by a suitable logistic growth term. The model, in which all the parameters are nonnegative, reads:

$$
\begin{aligned}
\frac{dX}{dt} &= rX\left(1 - \frac{X}{K}\right) - aZX - \lambda XU, \\
\frac{dU}{dt} &= \lambda XU - cZU - \mu U, \\
\frac{dZ}{dt} &= uZ\left(1 - \frac{Z}{L}\right) + eZ(aX + cU).
\end{aligned}
\tag{2.1}
$$

The first equation of model (2.1) describes the healthy prey propulation dynamics. The first term on the right hand side expresses logistic growth with r being the per capita net reproduction rate and K the carrying capacity of the environment. The second term models the hunting process of predators on healthy individuals at rate a and the third term describes the infection process by "successful" contacts with an infected individual via a simple mass action law, with contact rate λ. The second equation describes the infected prey evolution, recruited by the infection process at rate c, hunted via a classical mass action term and subject to natural plus disease-related mortality μ. The third equation contains the dynamics of the predators, who in the absence of both healthy and infected prey have an alternative resource, that is hidden in the model and originating a logistic growth, with per capita net reproduction rate u and the carrying capacity of the environment L. The term $eZ(aX + cU)$ instead accounts for the reward obtained by hunting healthy and infected prey, respectively, e denoting the conversion factor. The equilibria of this model are denoted by the superscript $[p\_ehp]$, the first "p" referring to predators and the second one to prey, "e" standing for "epidemics" and "h" for "hidden".

In shorthand notation, the model (2.1) can be rewritten in a vector form

$$
\frac{dP}{dt} = f(P), \quad P = (X, U, Z)^T, \quad f = (f_1, f_2, f_3)^T,
\tag{2.2}
$$

with the components of f given by the right hand side of model (2.1).

2.1.1 Boundedness

In order to obtain a well-posed model, we need to show that the trajectories of
system remain confined within a compact set. Consider the total environment
population $\varphi(t) = X(t) + U(t) + Z(t)$. Taking an arbitrary $0 < \eta < \mu$, summing
the equations in model (2.1), we obtain:

$$\frac{d\varphi(t)}{dt} = rX\left(1 - \frac{X}{K}\right) + uZ\left(1 - \frac{Z}{L}\right) - \mu U + (e - 1)(aXZ + cUZ). \quad (2.3)$$

Since $e \leq 1$, from (2.3) we can obtain:

$$
\begin{aligned}
\frac{d\varphi(t)}{dt} &= rX\left(1 - \frac{X}{K}\right) + uZ\left(1 - \frac{Z}{L}\right) - \mu U + (e - 1)(aXZ + cUZ) \\
&\leq rX\left(1 - \frac{X}{K}\right) + uZ\left(1 - \frac{Z}{L}\right) - \mu U. \quad (2.4)
\end{aligned}
$$

Adding $\eta\varphi(t)$ on both sides of inequality (2.4) we find the estimate:

$$\frac{d\varphi(t)}{dt} + \eta\varphi(t) \leq rX\left(1 - \frac{X}{K} + \frac{\eta}{r}\right) + uZ\left(1 - \frac{Z}{L} + \frac{\eta}{u}\right)$$
$$+(\eta - \mu)U \leq p_1(X) + p_2(Z),$$
$$p_1(X) = rX\left(1 - \frac{X}{K} + \frac{\eta}{r}\right), \quad p_2(Z) = \left(1 - \frac{Z}{L} + \frac{\eta}{u}\right).$$

The functions $p_1(X)$ and $p_2(Z)$ are concave parabolae, with maxima located
at X^*, Z^*, and corresponding maximum values

$$M_1 = p_1(X^*) = \frac{rK}{4}\left(1 + \frac{\eta}{r}\right)^2, \quad M_2 = p_2(Z^*) = \frac{uL}{4}\left(1 + \frac{\eta}{u}\right)^2.$$

Thus,

$$\frac{d\varphi(t)}{dt} + \eta\varphi(t) \leq M; \quad M_1 + M_2 = M.$$

Integrating the differential inequality, we find

$$\varphi(t) \leq \left(\varphi(0) - \frac{M}{\eta}\right)e^{-\eta t} + \frac{M}{\eta} \leq \max\left\{\varphi(0), \frac{M}{\eta}\right\}. \quad (2.5)$$

From this result, since $0 \leq X, U, Z \leq \varphi$, the boundedness of the original
ecosystem populations is immediate. The coordinate subspace are solution
trajectories in system (2.1) and, by the uniqueness theorem [70], they cannot
be crossed by other trajectories. Indeed, $\dot{X} = 0$ if $X = 0$, $\dot{U} = 0$ if $U = 0$,
$\dot{Z} = 0$ if $Z = 0$ and when nonvanishing, the initial conditions for the model
should always be positive to make biological sense.

2.1.2 Local stability analysis

The Jacobian matrix of the system (2.1), is given by

$$J^{[p\_ehp]} = \begin{pmatrix} J_{11}^{[p\_ehp]} & -\lambda X & -aX \\ \lambda U & -cZ + \lambda X - \mu & -cU \\ aeZ & ceZ & J_{33}^{[p\_ehp]} \end{pmatrix} \tag{2.6}$$

with

$$J_{11}^{[p\_ehp]} = -\lambda U - aZ + r\left(1 - \frac{2X}{K}\right), \quad J_{33}^{[p\_ehp]} = u - 2u\frac{Z}{L} + eaX + ecU,$$

There are 7 equilibria for model (2.1), but four must be rejected. At first, the two always feasible but unstable points: the origin $P_1^{[p\_ehp]} = (0,0,0)$, with eigenvalues $r, -\mu, u$, and $P_2^{[p\_ehp]} = (K,0,0)$, with eigenvalues $-r, K\lambda - \mu, u + aeK$. In addition, for the equilibrium point $P_3^{[p\_ehp]} = (\mu\lambda^{-1}, r\lambda^{-1}(1 - \mu\lambda^{-1}K^{-1}), 0)$ the feasibility condition requires $U_3^{[p\_ehp]} \geq 0$ which explicitly is given by $1 \geq \mu\lambda^{-1}K^{-1}$.

Furthermore, the Jacobian matrix (2.6) evaluated at $P_3^{[p\_ehp]}$ gives one explicit eigenvalue which should be negative to ensure stability, i.e. $u + ae\mu\lambda^{-1} + cer\lambda^{-1}(1 - \mu\lambda^{-1}K^{-1}) < 0$ must be satisfied. Clearly, if the condition for feasibility of $P_3^{[p\_ehp]}$ holds, this eigenvalue is positive and thus $P_3^{[p\_ehp]}$ is unstable whenever feasible. Finally, the point $P_4^{[p\_ehp]} = (0, -(u\mu + ucL)e^{-1}c^{-2}L^{-1}, -\mu c^{-1})$ is not feasible.

The equilibrium point $P_5^{[p\_ehp]} = (0,0,L)$ is always feasible and stable if

$$\frac{r}{a} < L. \tag{2.7}$$

The point $P_6^{[p\_ehp]} = (X_6^{[p\_ehp]}, 0, Z_6^{[p\_ehp]})$, with explicit populations levels:

$$X_6^{[p\_ehp]} = \frac{urK - auKL}{a^2eKL + ur}, \quad Z_6^{[p\_ehp]} = \frac{L(aerK + ur)}{a^2eKL + ur},$$

is feasible if

$$\frac{r}{a} \geq L. \tag{2.8}$$

The characteristic equation of the Jacobian matrix (2.6) evaluated at $P_6^{[p\_ehp]}$ can be factorized into the product of one linear equation and one quadratic equation providing one explicit eigenvalue producing the following condition, written both in implicit and explicit forms:

$$\lambda X_6^{[p\_ehp]} < cZ_6^{[p\_ehp]} + \mu, \quad \lambda < \frac{acerKL + ucrL + u\mu r + a^2e\mu KL}{uK(r - aL)}, \tag{2.9}$$

while the Routh-Hurwitz conditions for the remaining minor

$$\overline{J}_{P_6}^{[p\_ehp]} = \begin{pmatrix} -\dfrac{ru(r-aL)}{ur+a^2eKL} & -\dfrac{auK(r-aL)}{ur+a^2eKL} \\[3mm] \dfrac{aerL(aeK+u)}{ur+a^2eKL} & -\dfrac{ru(aeK+u)}{ur+a^2eKL} \end{pmatrix}$$

are always satisfied, if the feasibility condition (2.8) holds sharply, namely

$$\text{tr}(\overline{J}_{P_6}^{[p\_ehp]}) = \frac{-ru(r-aL)-ruaeK-ru^2}{ur+a^2eKL} < 0 \qquad (2.10)$$

and

$$\det(\overline{J}_{P_6}^{[p\_ehp]}) = \frac{(r-aL)(aeK+u)(a^2uerKL+r^2u^2)}{(a^2eKL+ru)^2} > 0. \qquad (2.11)$$

Thus, if the condition (2.9) is satisfied, equilibrium $P_6^{[p\_ehp]}$ is stable.

For the coexistence $P_7^{[p\_ehp]} = (X_7^{[p\_ehp]}, U_7^{[p\_ehp]}, Z_7^{[p\_ehp]})$, we find

$$X_7^{[p\_ehp]} = \frac{cZ_7^{[p\_ehp]}+\mu}{\lambda}, \quad U_7^{[p\_ehp]} = \frac{r}{\lambda}\left(1-\frac{\mu}{\lambda K}\right) - \frac{Z_7^{[p\_ehp]}}{\lambda}\left(a+\frac{rc}{\lambda K}\right)$$

and

$$Z_7^{[p\_ehp]} = \frac{L}{K\lambda^2 u + c^2 erL}(ae\mu\lambda K + u\lambda^2 K + cer\lambda K - cer\mu).$$

Feasibility requirements for $U_7^{[p\_ehp]} \geq 0$ and $Z_7^{[p\_ehp]} \geq 0$ are given, respectively, by

$$\lambda \geq \frac{au\lambda KL + rcuL + acerKL + a^2 e\mu KL + \mu ru}{urK},$$

$$\mu \leq \frac{ae\mu\lambda K + u\lambda^2 K + cer\lambda K}{cer}.$$

which in turn reduce to

$$uk(r-aL)\lambda \geq rcuL + acerKL + a^2 e\mu KL + \mu ru, \qquad (2.12)$$

which is satisfied for

$$\lambda \geq \lambda_*, \quad \lambda_* = \frac{rcuL + acerKL + a^2 e\mu KL + \mu ru}{uk(r-aL)}, \qquad (2.13)$$

where λ_* is the root of the equality associated to (2.12) when (2.8) holds, while in the opposite case no solution exists and $P_7^{[p\_ehp]}$ in unfeasible, and

$$\Psi(\lambda) = u\lambda^2 K + e(aK\mu + crK)\lambda - cer\mu \geq 0$$

for which, denoting by $\lambda_\pm$ the roots of $\Psi(\lambda)$, the quadratic inequality is satisfied for

$$0 \le \lambda \le \lambda_\pm. \tag{2.14}$$

For stability, the diagonal entries in the generic Jacobian(2.6) simplify to

$$J_{11}^{[p\_ehp]} = -\frac{r}{K}X_7^{[p\_ehp]}, \quad J_{22}^{[p\_ehp]} = 0, \quad J_{33}^{[p\_ehp]} = -\frac{u}{L}Z_7^{[p\_ehp]}.$$

Evaluating all the principal minors of the opposite of the Jacobian at coexistence, $-J(P_7^{[p\_ehp]})$, we find that it is positive definite.

Thus, whenever feasible, $P_7^{[p\_ehp]}$ is stable:

$$\frac{r}{K}X_7^{[p\_ehp]} > 0, \quad \lambda^2 U_7^{[p\_ehp]} X_7^{[p\_ehp]} > 0,$$
$$\left(\frac{c^2 er}{K} + \frac{u\lambda^2}{L}\right) X_7^{[p\_ehp]} U_7^{[p\_ehp]} Z_7^{[p\_ehp]} > 0.$$

In Table 4.1 we summarize the behaviour of the equilibrium points of model (2.1).

Table 2.1: Behaviour and feasibility and stability conditions of the equilibria of model (2.1).

Equilibria	Feasibility	Stability
$P_1^{[p\_ehp]}$	always	unstable
$P_2^{[p\_ehp]}$	always	unstable
$P_3^{[p\_ehp]}$	$\mu \le \lambda K$	unstable if feasible
$P_4^{[p\_ehp]}$	unfeasible	
$P_5^{[p\_ehp]}$	always	$r < aL$
$P_6^{[p\_ehp]}$	$r \ge aL$	(2.9)
$P_7^{[p\_ehp]}$	(2.12), (2.13), (2.14)	stable if feasible

2.1.3 Global stability analysis

Table 4.1 shows that of the seven equilibria in model (2.1), only three may be stable. In this section we prove that their local stability, as proved through the analysis of the eigenvalues, also implies their global stability as well. To accomplish this task, suitable Lyapunov functions are constructed.

We now prove that feasibility of $P_7^{[p\_ehp]}$ implies its global asymptotic stability. Consider the following function,

$$V_7^{[p\_ehp]}(X(t), U(t), Z(t)) = \alpha_2 \left(X - X_7^{[p\_ehp]} - X_7^{[p\_ehp]} \ln \frac{X}{X_7^{[p\_ehp]}} \right)$$

$$+ \alpha_1 \left(U - U_7^{[p\_ehp]} - U_7^{[p\_ehp]} \ln \frac{U}{U_7^{[p\_ehp]}} \right) + \alpha_0 \left(Z - Z_7^{[p\_ehp]} - Z_7^{[p\_ehp]} \ln \frac{Z}{Z_7^{[p\_ehp]}} \right),$$

where α_2, α_1 and α_0 are arbitrary positive constants. Differentiating along the solution trajectories of (2.1), we find

$$
\begin{aligned}
\frac{dV_7^{[p\_ehp]}}{dt} &= -\alpha_2 \frac{r}{K} \left(X - X_7^{[p\_ehp]} \right)^2 - \alpha_0 \frac{u}{L} \left(Z - Z_7^{[p\_ehp]} \right)^2 \\
&+ \lambda(\alpha_1 - \alpha_2) \left(X - X_7^{[p\_ehp]} \right) \left(U - U_7^{[p\_ehp]} \right) \\
&+ a(\alpha_0 e - \alpha_2) \left(X - X_7^{[p\_ehp]} \right) \left(Z - Z_7^{[p\_ehp]} \right) \\
&+ c(\alpha_0 e - \alpha_1) \left(U - U_7^{[p\_ehp]} \right) \left(Z - Z_7^{[p\_ehp]} \right).
\end{aligned}
$$

If we choose $\alpha_2 = \alpha_1 = \alpha_0 e$, then the above derivative is negative definite except at the equilibrium point $P_7^{[p\_ehp]}$, so it is a Lyapunov function. Hence $P_7^{[p\_ehp]}$ is a globally stable equilibrium point whenever it is feasible.

Analogous results can be shown for the remaining two equilibria, $P_5^{[p\_ehp]}$ and $P_6^{[p\_ehp]}$.

For $P_5^{[p\_ehp]}$ we need to choose

$$V_5^{[p\_ehp]}(X(t), U(t), Z(t)) = \beta_2 X + \beta_1 U + \beta_0 \left(Z - Z_5^{[p\_ehp]} - Z_5^{[p\_ehp]} \ln \frac{Z}{Z_5^{[p\_ehp]}} \right),$$

with β_2, β_1 and β_0 positive constants to be determined. Differentiation along the system trajectories leads to

$$
\begin{aligned}
\frac{dV_5^{[p\_ehp]}}{dt} &= -\beta_2 \frac{r}{K} X^2 - \beta_0 \frac{u}{L} \left(Z - Z_5^{[p\_ehp]} \right)^2 + a(\beta_0 e - \beta_2) XZ \\
&+ \lambda(\beta_1 - \beta_2) XU + c(\beta_2 e - \beta_1) UZ + (\beta_2 r - \beta_0 eaL) X \\
&+ (-\beta_1 \mu - \beta_0 ecL) U
\end{aligned}
$$

so that choosing $\beta_2 = \beta_1 = \beta_0 e$ and using the local stability condition (2.7) the above derivative of $V_5^{[p\_ehp]}$ is negative definite and the equilibrium point $P_5^{[p\_ehp]}$ is globally asymptotically stable.

Similarly, for the equilibrium point $P_6^{[p\_ehp]}$ consider the following candidate

Lyapunov function:

$$
\begin{aligned}
V_6^{[p\_ehp]}(X(t), U(t), Z(t)) &= \gamma_2 \left(X - X_6^{[p\_ehp]} - X_6^{[p\_ehp]} \ln \frac{X}{X_6^{[p\_ehp]}} \right) \\
&+ \gamma_1 U + \gamma_0 \left(Z - Z_6^{[p\_ehp]} - Z_6^{[p\_ehp]} \ln \frac{Z}{Z_6^{[p\_ehp]}} \right),
\end{aligned}
$$

γ_2, γ_1 and γ_0 being positive constants to be determined. Once more, differentiating $V_6^{[p\_ehp]}$ along the trajectories of (2.1) we find, after some algebraic manipulations,

$$
\begin{aligned}
\frac{dV_6^{[p\_ehp]}}{dt} &= -\gamma_2 \frac{r}{K} \left(X - X_6^{[p\_ehp]} \right)^2 - \gamma_0 \frac{u}{L} \left(Z - Z_6^{[p\_ehp]} \right)^2 \\
&+ a(\gamma_0 e - \gamma_2) \left(X - X_6^{[p\_ehp]} \right) \left(Z - Z_6^{[p\_ehp]} \right) + \lambda(\gamma_1 - \gamma_2) X U \\
&+ c(\gamma_0 e - \gamma_1) U Z + \left(\gamma_2 \lambda X_6^{[p\_ehp]} - \gamma_0 e c Z_6^{[p\_ehp]} - \gamma_1 \mu \right) U.
\end{aligned}
$$

Choosing $\gamma_1 = \gamma_2 = \gamma_0 e$ and using the local stability condition (2.9) we find that the derivative of $V_6^{[p\_ehp]}$ is negative definite except at $P_6^{[p\_ehp]}$. Thus, the equilibrium point $P_6^{[p\_ehp]}$ is globally asymptotically stable.

Remark 1. These results indicate that if feasible, the equilibria $P_5^{[p\_ehp]}$, $P_6^{[p\_ehp]}$ and $P_7^{[p\_ehp]}$ of the system (2.1) are globally asymptotically stable. Indeed these three equilibria are mutually exclusive. This statement for $P_5^{[p\_ehp]}$ and $P_6^{[p\_ehp]}$ follows by comparing their respective feasibility and stability conditions in Table 1. Further, for $r < aL$, $P_5^{[p\_ehp]}$ is stable and $P_7^{[p\_ehp]}$ is unfeasible, because (2.12) does not hold. Conversely, for $r \geq aL$, $P_6^{[p\_ehp]}$ is feasible but then (2.9) and (2.12), (2.13) contradict each other, so that $P_6^{[p\_ehp]}$ and $P_7^{[p\_ehp]}$ are also excluding each other. These remarks suggest the existence of transcritical bifurcations linking these equilibria, a question that will be investigated analytically in the next section.

2.1.4 Transcritical bifurcations

To study the local bifurcations of the equilibrium points of model (2.1), we use Sotomayor's theorem [70]. The general second order term of the Taylor expansion of f in (2.2) is given by

$$
D^2 f(P, \psi)(V, V) \tag{2.15}
$$

$$
= \begin{pmatrix}
\frac{\partial^2 f_1}{\partial X^2}\xi_1^2 + \frac{\partial^2 f_1}{\partial U^2}\xi_2^2 + \frac{\partial^2 f_1}{\partial Z^2}\xi_3^2 + 2\frac{\partial^2 f_1}{\partial X \partial U}\xi_1\xi_2 + 2\frac{\partial^2 f_1}{\partial X \partial Z}\xi_1\xi_3 + 2\frac{\partial^2 f_1}{\partial U \partial Z}\xi_2\xi_3 \\
\frac{\partial^2 f_2}{\partial X^2}\xi_1^2 + \frac{\partial^2 f_2}{\partial U^2}\xi_2^2 + \frac{\partial^2 f_2}{\partial Z^2}\xi_3^2 + 2\frac{\partial^2 f_2}{\partial X \partial U}\xi_1\xi_2 + 2\frac{\partial^2 f_2}{\partial X \partial Z}\xi_1\xi_3 + 2\frac{\partial^2 f_2}{\partial U \partial Z}\xi_2\xi_3 \\
\frac{\partial^2 f_3}{\partial X^2}\xi_1^2 + \frac{\partial^2 f_3}{\partial U^2}\xi_2^2 + \frac{\partial^2 f_3}{\partial Z^2}\xi_3^2 + 2\frac{\partial^2 f_3}{\partial X \partial U}\xi_1\xi_2 + 2\frac{\partial^2 f_3}{\partial X \partial Z}\xi_1\xi_3 + 2\frac{\partial^2 f_3}{\partial U \partial Z}\xi_2\xi_3
\end{pmatrix},
$$

where ψ represents the parametric threshold and ξ_1, ξ_2, ξ_3 are the components of the eigenvector $V = (\xi_1, \xi_2, \xi_3)^T$ of the variations in X, U and Z.

Bifurcation of the equilibrium point $P_6^{[p\_ehp]}$

The axial equilibrium point $P_6^{[p\_ehp]}$ coincides with the equilibrium $P_5^{[p\_ehp]}$ at the parametric threshold $r^\dagger$ and with equilibrium $P_7^{[p\_ehp]}$ at the parametric threshold $\lambda^\dagger$, where

$$r^\dagger = aL, \quad \lambda^\dagger = \frac{aeKL(cr + a\mu) + ur(\mu + cL)}{uK(r - aL)} \tag{2.16}$$

when we compare the feasibility condition (2.8) of $P_6^{[p\_ehp]}$ together with the stability condition (2.7) of $P_5^{[p\_ehp]}$ as well as, respectively, the stability condition (2.9) of $P_6^{[p\_ehp]}$ and the feasibility condition (2.12) of the equilibrium $P_7^{[p\_ehp]}$.

The Jacobian matrix of the system (2.1) evaluated at $P_6^{[p\_ehp]}$ and at $r^\dagger$ is

$$J_{P_6}^{[p\_ehp]}(r^\dagger) = \begin{pmatrix} 0 & 0 & 0 \\ 0 & -cL - \mu & 0 \\ aeL & ceL & -u \end{pmatrix}.$$

Its right and left eigenvectors, corresponding to the zero eigenvalue, are given by $V_1 = \varphi_1(1, 0, aeL/u)^T$ and $Q_1 = \omega_1(1, 0, 0)^T$, where φ_1 and ω_1 are any nonzero real numbers. Differentiating partially the right hand sides of the equation (2.1) with respect to r and calculating its Jacobian matrix, we find, respectively:

$$f_r = \begin{pmatrix} X_6^{[p\_ehp]}(1 - X_6^{[p\_ehp]}/K) \\ 0 \\ 0 \end{pmatrix}, \quad Df_r = \begin{pmatrix} 1 - \frac{1}{K}X_6^{[p\_ehp]} & 0 & 0 \\ 0 & 0 & 0 \\ 0 & 0 & 0 \end{pmatrix}.$$

After calculating $D^2 f$ in (2.15) evaluated at $P_6^{[p\_ehp]}$, the parametric threshold $r^\dagger$ and the eigenvector V_1 we can verify the following three conditions

$$Q_1{}^T f_r(P_6^{[p\_ehp]}, aL) = 0,$$
$$Q_1{}^T [Df_r(P_6^{[p\_ehp]}, aL)V_1] = \varphi_1\omega_1 \neq 0,$$
$$Q_1^T [D^2 f_r(P_6^{[p\_ehp]}, aL)(V_1, V_1)] = -\omega_1\varphi_1{}^2 \left(\frac{aL}{K} + \frac{2a^2eL}{u} \right) \neq 0.$$

When $P_6^{[p\_ehp]}$ coincides with the equilibrium $P_7^{[p\_ehp]}$ at the threshold $\lambda^\dagger$,

the Jacobian matrix of the system (2.1) is

$$J_{P_6}^{[p\_ehp]}(\lambda^\dagger) \tag{2.17}$$

$$= \begin{pmatrix} -\dfrac{ru(r-aL)}{ur+a^2eKL} & -\dfrac{L(acerK+a^2e\mu K+cru)+ru\mu}{ur+a^2eKL} & \dfrac{a^2uKL-aruK}{ur+a^2eKL} \\[2ex] 0 & 0 & 0 \\[2ex] \dfrac{L(a^2e^2rK+aeru)}{ur+a^2eKL} & \dfrac{L(ace^2rK+ceru)}{ur+a^2eKL} & -\dfrac{aeruK+ru^2}{ur+a^2eKL} \end{pmatrix}.$$

For the zero eigenvalue in (2.17), the corresponding eigenvector is $V_2 = \varphi_2(1, v_1, v_2)^T$, where φ_2 is any nonzero real number and v_1 and v_2 are

$$v_1 = \frac{-a^3eKL^2 - L(aru - a^2erK) + r^2u)}{a^2ceKL^2 + L(-2acerK - a^2e\mu K - cru) - \mu ru}$$

and

$$v_2 = \frac{L^2(a^2ce^2rK + a^3e^2\mu K + 2aceru) + uL(ae\mu r - cer^2)}{a^2ceuKL^2 + L(-2aceruK - a^2e\mu uK - cru^2) - \mu ru^2}. \tag{2.18}$$

Besides that, $Q_2 = \omega_2(0, 1, 0)^T$ represents the eigenvector corresponding to the zero eigenvalue of $(J_{P_6}^{[p\_ehp]}(r^\dagger))^T$, where ω_2 is any nonzero real number. Differentiating partially the right hand sides of (2.1) with respect to λ and calculating its Jacobian matrix, we respectively find

$$f_\lambda = \begin{pmatrix} -X_6^{[p\_ehp]}U_6^{[p\_ehp]} \\ X_6^{[p\_ehp]}U_6^{[p\_ehp]} \\ 0 \end{pmatrix}, \quad Df_\lambda = \begin{pmatrix} 0 & -X_6^{[p\_ehp]} & 0 \\ 0 & X_6^{[p\_ehp]} & 0 \\ 0 & 0 & 0 \end{pmatrix}.$$

After calculating D^2f in (2.15) evaluated at $P_6^{[p\_ehp]}$, the parametric threshold $\lambda^\dagger$ and the eigenvector V_2 we can verify the following three conditions, the latter being satisfied in view of (2.18) and (2.16):

$$Q_2{}^T f_\lambda(P_6^{[p\_ehp]}, \lambda^\dagger) = 0, \quad Q_2{}^T[Df_\lambda(P_6^{[p\_ehp]}, \lambda^\dagger)V_2] = \varphi_2\omega_2 v_1 X_6^{[p\_ehp]} \neq 0,$$
$$Q_2^T[D^2f_\lambda(P_6^{[p\_ehp]}, \lambda^\dagger)(V_2, V_2)] = 2v_1\omega_2\varphi_2{}^2\left(\lambda^\dagger - cv_2\right) \neq 0.$$

Thus, all the conditions for transcritical bifurcation are satisfied. Figure 4.1 illustrates the simulation explicitly showing the transcritical bifurcation between $P_6^{[p\_ehp]}$ and $P_5^{[p\_ehp]}$ for the chosen parameter values (see the caption of Fig. 4.1 (a)) when the parameter r crosses a critical value $r^\dagger = aL = 1$ given by (2.16) and the transcritical bifurcation between $P_6^{[p\_ehp]}$ and $P_7^{[p\_ehp]}$ for the chosen parameters values (see the caption of Fig. 4.1 (b)) when the parameter λ crosses a critical value $\lambda^\dagger \approx 1.072$ given by (2.16).
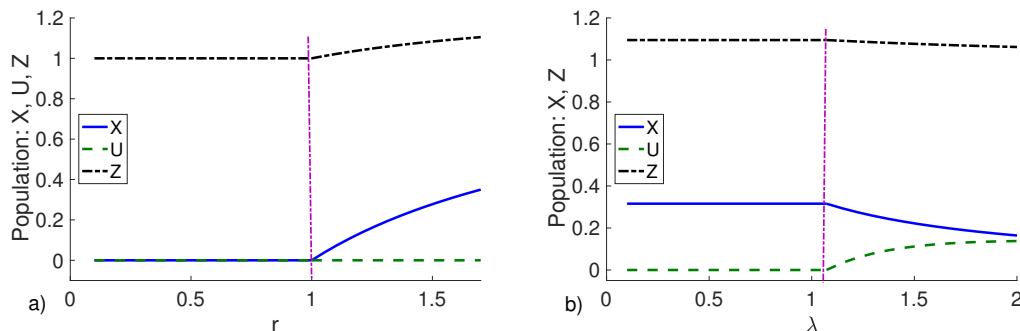
Figure 2.1: a) Transcritical bifurcation between $P_6^{[p\_ehp]}$ and $P_5^{[p\_ehp]}$ for the parameter values: $\mu = 0.01$, $K = L = a = u = 1$, $e = c = 0.3$ and $\lambda = 1.01$. Initial conditions $X_0 = U_0 = Z_0 = 0.01$. The equilibrium $P_5^{[p\_ehp]}$ is stable for $\lambda \in [0.1, 1.01]$ and $P_6^{[p\_ehp]}$ is stable past $\lambda = 1.01$. The vertical line shows the transcritical bifurcation threshold. b) Transcritical bifurcation between $P_6^{[p\_ehp]}$ and $P_7^{[p\_ehp]}$ for the parameter values: $\mu = 0.01$, $K = L = a = u = 1$, $e = c = 0.3$ and $r = 1.6$ and the same initial conditions. The equilibrium $P_6^{[p\_ehp]}$ is stable for $\lambda \in [0.1, 1.072]$ and $P_7^{[p\_ehp]}$ is stable past $\lambda = 1.072$. The vertical line has the same meaning as in (a).

2.2 The model with explicit resources

Now, we render the hidden resource for the predator explicit, naming it Y. The model is denoted with the superscript $[p\_eep]$, where the first "p" refers to predators and the last one to prey, the first "e" stands for "epidemics" (in the prey) and the second one stands for explicit resource for the predator. The model, in which all the parameters are nonnegative, reads:

$$
\begin{aligned}
\frac{dX}{dt} &= rX\left(1 - \frac{X}{K}\right) - aZX - \lambda XU, \\
\frac{dU}{dt} &= \lambda XU - cZU - \mu U, \\
\frac{dY}{dt} &= sY\left(1 - \frac{Y}{H}\right) - bYZ, \\
\frac{dZ}{dt} &= -mZ^2 + e(aXZ + bYZ + cUZ).
\end{aligned}
\tag{2.19}
$$

The first and second equations of model (2.19), respectively representing the healthy and infected prey, have the same meaning as described for model (2.1). The third equation describes the alternative prey population dynamics. The first term on the right hand side expresses logistic growth with s being the per capita net reproduction rate and H the environment carrying capacity. The second term models hunting of Y by the predator at rate b. The fourth equation describes the predator propulation dynamics and is essentially the

same as described for (2.1), with an additional gain due to the hunting of the alternative prey.

2.2.1 Boundedness

The proof for system (2.19) follows a similar pattern as in Section 2.1.1 and is therefore omitted. Setting $\psi(t) = X(t) + U(t) + Y(t) + Z(t)$, for an arbitrary $0 < \eta < \mu$, we find an estimate similar to the one in equation (3.6), where only the definition of M slightly changes, again ensuring boundedness of all the ecosystem populations.

2.2.2 Local stability analysis

The Jacobian matrix of system (2.19) is given by

$$
J^{[p\_eep]} = \begin{pmatrix}
J_{11}^{[p\_eep]} & -\lambda X & 0 & -aX \\
\lambda U & -cZ + \lambda X - \mu & 0 & -cU \\
0 & 0 & s - \frac{2s}{H}Y - bZ & -bY \\
aeZ & ceZ & beZ & J_{44}^{[p\_eep]}
\end{pmatrix} \tag{2.20}
$$

with

$$
J_{11}^{[p\_eep]} = r - \frac{2r}{K}X - aZ - \lambda U, \quad J_{44}^{[p\_eep]} = eaX + ebY + ecU - 2mZ.
$$

There are 13 possible equilibria for model (2.19). The four always unstable points: the origin $P_1^{[p\_eep]} = (0,0,0,0)$, with eigenvalues $r, \mu, s, 0$, $P_2^{[p\_eep]} = (K,0,0,0)$, with eigenvalues $-r, -\mu, s, eaK$, $P_3^{[p\_eep]} = (0,0,H,0)$, with eigenvalues $r, -\mu, -s, ebH$ and $P_4^{[p\_eep]} = (K,0,H,0)$, with eigenvalues $-r, -s, -\mu + \lambda K, aeK + ebH$.

Further, the point $P_5^{[p\_eep]} = (X_5^{[p\_eep]}, U_5^{[p\_eep]}, 0, 0)$, where $X_5^{[p\_eep]} = \mu\lambda^{-1}$ and $U_5^{[p\_eep]} = r\lambda^{-1} - r\mu\lambda^{-2}K^{-1}$, which is feasible if $\mu \leq \lambda K$, is unconditionally unstable because the Jacobian (2.20) evaluated at the $P_5^{[p\_eep]}$, has two explicit eigenvalues, $ea\mu\lambda^{-1} + ecr\lambda^{-1} - ecr\mu\lambda^{-2}K^{-1}$ and $s > 0$. Similarly, the equilibrium $P_8^{[p\_eep]} = (\mu\lambda^{-1}, -r\lambda^{-1} + r\mu\lambda^{-2}K^{-1}, H, 0)$, is feasible if

$$
\mu \geq \lambda K, \tag{2.21}
$$

but unconditionally unstable when feasible, since one of the two explicit eigenvalues of the Jacobian at $P_8^{[p\_eep]}$ is positive in view of (2.21):

$$
-s < 0, \quad ebH + \frac{ea\mu}{\lambda} - \frac{ecr}{\lambda}\left(1 - \frac{\mu}{\lambda K}\right) > 0.
$$

There are also two unconditionally unfeasible points:

$$
P_6^{[p\_eep]} = (0, -\frac{m\mu}{ec^2}, 0, -\frac{\mu}{c}), \quad P_7^{[p\_eep]} = (0, U_7^{[p\_eep]}, Y_7^{[p\_eep]}, Z_7^{[p\_eep]}),
$$

with

$$U_7^{[p\_eep]} = \frac{ecsbH - e\mu b^2 H - ms\mu}{c^2 es}, \quad Y_7^{[p\_eep]} = \frac{\mu bH + csH}{cs}, \quad Z_7^{[p\_eep]} = -\frac{\mu}{c}.$$

The equilibrium $P_9^{[p\_eep]} = (X_9^{[p\_eep]}, 0, 0, Z_9^{[p\_eep]})$, where

$$X_9^{[p\_eep]} = \frac{mrK}{a^2 eK + mr}, \quad Z_9^{[p\_eep]} = \frac{aerK}{a^2 eK + mr}$$

is always feasible and conditionally stable, because two explicit eigenvalues of the Jacobian at $P_9^{[p\_eep]}$ give the stability conditions

$$s < \frac{aberK}{a^2 eK + mr}, \quad \lambda < \frac{aeK(a\mu + cr) + mr\mu}{mrK}. \tag{2.22}$$

while the Routh-Hurwitz conditions for the remaining minor $\overline{J}_{P_9}^{[p\_eep]}$ hold:

$$-\mathrm{tr}(\overline{J}_{P_9}^{[p\_eep]}) = \frac{r}{K} X_9^{[p\_eep]} + m Z_9^{[p\_eep]} > 0,$$

$$\det(\overline{J}_{P_9}^{[p\_eep]}) = \frac{mr}{K} X_9^{[p\_eep]} Z_9^{[p\_eep]} + a^2 e X_9^{[p\_eep]} Z_9^{[p\_eep]} > 0.$$

The point $P_{10}^{[p\_eep]} = (0, 0, Y_{10}^{[p\_eep]}, Z_{10}^{[p\_eep]})$, with

$$Y_{10}^{[p\_eep]} = \frac{msH}{b^2 eH + ms}, \quad Z_{10}^{[p\_eep]} = \frac{ebsH}{b^2 eH + ms}$$

is similarly always feasible and conditionally stable. From the Jacobian at $P_{10}^{[p\_eep]}$ one explicit eigenvalue is $-c Z_{10}^{[p\_eep]} - \mu < 0$ while another explicit eigenvalue provides the stability condition

$$Z_{10}^{[p\_eep]} = \frac{abesH}{b^2 eH + ms} > \frac{r}{a}. \tag{2.23}$$

The Routh-Hurwitz criterion on the remaining minor $\overline{J}_{P10}^{[p\_eep]}$ holds:

$$-\mathrm{tr}(\overline{J}_{P_{10}}^{[p\_eep]}) = \frac{s}{H} Y_{10}^{[p\_eep]} + m Z_{10}^{[p\_eep]} > 0,$$

$$\det(\overline{J}_{P_{10}}^{[p\_eep]}) = \frac{ms}{H} Y_{10}^{[p\_eep]} Z_{10}^{[p\_eep]} + b^2 e Y_{10}^{[p\_eep]} Z_{10}^{[p\_eep]} > 0.$$

The equilibrium $P_{11}^{[p\_eep]} = (X_{11}^{[p\_eep]}, 0, Y_{11}^{[p\_eep]}, Z_{11}^{[p\_eep]})$, with

$$X_{11}^{[p\_eep]} = K - \frac{aK}{r} Z_{11}^{[p\_eep]}, \quad Y_{11}^{[p\_eep]} = H - \frac{bH}{s} Z_{11}^{[p\_eep]},$$

$$Z_{11}^{[p\_eep]} = \frac{rs(beH + aeK)}{a^2 esK + b^2 erH + mrs}$$

is feasible if

$$r \geq aZ_{11}^{[p\_eep]} = \frac{abesH}{b^2eH + ms}, \quad s \geq bZ_{11}^{[p\_eep]} = \frac{aberK}{a^2eK + mr}. \tag{2.24}$$

The second condition can be rewritten giving either an upper bound on r or no bound at all, respectively if $abeK > ms$ holds or not. In the former case the condition is

$$r \leq \frac{a^2eKs}{abeK - ms}, \quad abeK > ms. \tag{2.25}$$

Its Jacobian has one explicit eigenvalue, providing the stability condition

$$\lambda X_{11}^{[p\_eep]} < \mu + cZ_{11}^{[p\_eep]}, \tag{2.26}$$

which explicitly becomes

$$r[ces(aK + bH) + (\mu - \lambda K)(b^2eH + ms)] > -aesK(bH\lambda + a\mu), \tag{2.27}$$

so that if $ces(aK + bH) + (\mu - \lambda K)(b^2eH + ms) > 0$ no costraint on r arises, while conversely we must have

$$r < \frac{aesK(bH\lambda + a\mu)}{(\lambda K - \mu)(b^2eH + ms) - ces(aK + bH)}, \tag{2.28}$$
$$ces(aK + bH) + \mu(b^2eH + ms) < \lambda K(b^2eH + ms).$$

Besides that, the remaining submatrix of the Jacobian, $-\overline{J}_{P_{11}}^{[p\_eep]}$, is positive definite, since its principal minors are all positive, so no further stability conditions arise:

$$\frac{r}{K}X_{11}^{[p\_eep]} > 0, \quad \frac{rs}{HK}X_{11}^{[p\_eep]}Y_{11}^{[p\_eep]} > 0,$$
$$\left(\frac{mrs}{HK} + \frac{a^2es}{H} + \frac{b^2er}{K}\right)X_{11}^{[p\_eep]}Y_{11}^{[p\_eep]}Z_{11}^{[p\_eep]} > 0.$$

Thus, $\overline{J}_{P_{11}}^{[p\_eep]}$ is negative definite and $P_{11}^{[p\_eep]}$ is stable.

The equilibrium $P_{12}^{[p\_eep]} = (X_{12}^{[p\_eep]}, U_{12}^{[p\_eep]}, 0, Z_{12}^{[p\_eep]})$, with

$$X_{12}^{[p\_eep]} = \frac{c^2erK + ace\mu K + m\mu\lambda K}{c^2er + m\lambda^2 K}, \quad Z_{12}^{[p\_eep]} = -\frac{\mu}{c} + \frac{\lambda}{c}X_{12}^{[p\_eep]},$$

$$U_{12}^{[p\_eep]} = \frac{a\mu}{c\lambda} + \frac{r}{\lambda} - \frac{r}{\lambda K}X_{12}^{[p\_eep]} - \frac{a}{c}X_{12}^{[p\_eep]}$$

is feasible if

$$\lambda \geq \frac{a^2e\mu K + mr\mu + acerK}{mrK} \tag{2.29}$$

39

and $\mu \leq \lambda K(rc + a\mu)(rc)^{-1}$. The latter can be rewritten as

$$\mu \leq \frac{cr\lambda K}{cr - a\lambda K}, \quad cr > a\lambda K, \tag{2.30}$$

while in the case for which the second inequality in (2.30) does not hold, no
solution exists for μ and the equilibrium $P_{12}^{[p\_eep]}$ is therefore unfeasible.

Again, one eigenvalue is explicit, to give the stability condition

$$\lambda > \frac{cer(cs + b\mu) + ms\lambda^2 K}{beK(cr + a\mu)}. \tag{2.31}$$

The explicit condition (2.31) in terms of λ hinges on the roots $\lambda_\pm$ of the
quadratic

$$\Phi(\lambda) = msK\lambda^2 - beK(cr + a\mu)\lambda + cer(cs + b\mu) < 0. \tag{2.32}$$

If the discriminant of $\Phi(\lambda)$ is negative, no solution of (2.32) exists, while in
the opposite case we find the stability conditions become

$$\lambda_- \leq \lambda \leq \lambda_+, \quad b^2 eK(cr + a\mu)^2 \geq 4cmrs(cs + b\mu). \tag{2.33}$$

Also, no further stability conditions arise, as the submatrix

$$-\overline{J}_{P_{12}}^{[p\_eep]} = \begin{pmatrix} \frac{r}{K}X_{12}^{[p\_eep]} & \lambda X_{12}^{[p\_eep]} & aX_{12}^{[p\_eep]} \\ -\lambda U_{12}^{[p\_eep]} & 0 & cU_{12}^{[p\_eep]} \\ -aeZ_{12}^{[p\_eep]} & -ceZ_{12}^{[p\_eep]} & mZ_{12}^{[p\_eep]} \end{pmatrix}$$

is positive definite:

$$\frac{r}{K}X_{12}^{[p\_eep]} > 0, \quad \lambda^2 X_{12}^{[p\_eep]}U_{12}^{[p\_eep]} > 0,$$

$$\left(m\lambda^2 + \frac{c^2 er}{K}\right)X_{12}^{[p\_eep]}U_{12}^{[p\_eep]}Z_{12}^{[p\_eep]} > 0.$$

The coexistence equilibrium $P_{13}^{[p\_eep]} = (X_{13}^{[p\_eep]}, U_{13}^{[p\_eep]}, Y_{13}^{[p\_eep]}, Z_{13}^{[p\_eep]})$ can also
be explicitly evaluated,

$$X_{13}^{[p\_eep]} = \frac{\lambda K(bcesH + b^2 e\mu H + ms\mu) + c^2 ersK + aces\mu K}{\lambda^2 K(b^2 eH + ms) + ersc^2},$$

$$U_{13}^{[p\_eep]} = \left[\lambda^2 K(b^2 eH + ms) + ersc^2\right]^{-1}\left[\lambda K(b^2 erH + mrs - abesH)\right.$$
$$\left. - aesK(rc + a\mu) - berH(sc + b\mu) - mrs\mu\right],$$

$$Y_{13}^{[p\_eep]} = \frac{\lambda HK(-bcer - abe\mu) + c^2 ersH + bcer\mu H + ms\lambda^2 HK}{\lambda^2 K(b^2 eH + ms) + ersc^2},$$

$$Z_{13}^{[p\_eep]} = \frac{aes\mu\lambda K + cers\lambda K + bes\lambda^2 HK - cers\mu}{\lambda^2 K(b^2 eH + ms) + ersc^2}.$$

The feasibility requirements are:

$$r \geq \frac{aesK(bH\lambda + a\mu)}{(\lambda K - \mu)(b^2eH + ms) - ces(aK + bH)}, \tag{2.34}$$

$$ces(aK + bH) + \mu(b^2eH + ms) < \lambda K(b^2eH + ms);$$

$$\lambda \leq \frac{cer(cs + b\mu) + ms\lambda^2 K}{beK(cr + a\mu)}; \tag{2.35}$$

$$\mu \leq \frac{\lambda K(b\lambda H + cr + a\mu)}{rc}. \tag{2.36}$$

These conditions can be made explicit in terms of λ by considering $\Phi_1(\lambda) \geq 0$

$$\Phi_1(\lambda) = [rK(b^2eH+ms)-aesKbH]\lambda-a^2esK\mu-r[\mu(b^2eH+ms)+ces(aK+bH)]$$

whose root λ_0 is positive if

$$r(b^2eH + ms) \geq aesbH \tag{2.37}$$

in which case the inequality is satisfied for $\lambda > \lambda_0$, while in the opposite case, for which (2.37) does not hold, no solution exists, and we have to consider the following inequalities:

$$\Phi_2(\lambda) = mKs\lambda^2 - \lambda beK(cr + a\mu) + cer(cs + b\mu) \geq 0,$$
$$\Phi_3(\lambda) = bKH\lambda^2 + \lambda K(cr + a\mu) - cr\mu \geq 0.$$

If the respective roots of the associated equalities are denoted by $\lambda_\pm^{(k)}$, $k = 2, 3$, feasibility is ensured for $\lambda \geq \lambda_0$, $\lambda_-^{(2)} \geq \lambda \geq 0$ or $\lambda \geq \lambda_+^{(2)}$, $0 \leq \lambda \leq \lambda_+^{(3)}$, i.e. in the interval

$$\min\left\{\lambda_+^{(3)}, \lambda_-^{(2)}\right\} \geq \lambda \geq \max\left\{\lambda_0, \lambda_+^{(2)}\right\}. \tag{2.38}$$

The diagonal of the Jacobian at $P_{13}^{[p\_eep]}$ simplifies using the equilibrium equations:

$$J_{11} = -\frac{r}{K}X_{13}^{[p\_eep]}, \quad J_{33} = -\frac{s}{H}Y_{13}^{[p\_eep]}, \quad J_{44} = -mZ_{13}^{[p\_eep]}.$$

Now, $-J_{P_{13}}^{[p\_eep]}$ is positive definite because its principal minors are

$$\frac{r}{K}X_{13}^{[p\_eep]} > 0, \quad \lambda^2 U_{13}^{[p\_eep]}X_{13}^{[p\_eep]} > 0, \quad \frac{\lambda^2 s}{H}X_{13}^{[p\_eep]}U_{13}^{[p\_eep]}Y_{13}^{[p\_eep]} > 0,$$

$$\left(\frac{s}{H}\left(\lambda^2 m + \frac{rec^2}{K}\right) + b^2 m\lambda^2\right)X_{13}^{[p\_eep]}U_{13}^{[p\_eep]}Y_{13}^{[p\_eep]}Z_{13}^{[p\_eep]} > 0.$$

Thus whenever feasible, coexistence is unconditionally stable. In Table 4.2 we summarize the behaviour of the equilibrium points of model (2.19).

Table 2.2: Behaviour and feasibility and stability conditions of the equilibria of model (2.19).

Equilibria	Feasibility	Stability
$P_1^{[p\_eep]}$	always	unstable
$P_2^{[p\_eep]}$	always	unstable
$P_3^{[p\_eep]}$	always	unstable
$P_4^{[p\_eep]}$	always	unstable
$P_5^{[p\_eep]}$	$\mu \geq \lambda K$	unstable
$P_6^{[p\_eep]}$	unfeasible	
$P_7^{[p\_eep]}$	unfeasible	
$P_8^{[p\_eep]}$	$\mu \leq \lambda K$	unstable if feasible
$P_9^{[p\_eep]}$	always	$s < \frac{aberK}{a^2eK+mr}$,
		$\lambda < \frac{aeK(cr+a\mu)+mr\mu}{mrK}$
$P_{10}^{[p\_eep]}$	always	$r < \frac{abesH}{b^2eH+ms}$
$P_{11}^{[p\_eep]}$	$r \geq \frac{abesH}{b^2eH+ms}$,	(2.27), (2.28)
	$s \geq \frac{aberK}{a^2eK+mr}$	
$P_{12}^{[p\_eep]}$	(2.29), (2.30)	(2.33)
$P_{13}^{[p\_eep]}$	(2.34), (2.37), (2.38)	stable if feasible

2.2.3 Global stability analysis

We prove the global stability for the equilibria of (2.19) following the pattern of Section 2.1.3. For this reason, we just summarize the results.

For each equilibrium, se select the following Lyapunov functions candidates, using always the same positive coefficients δ_3, δ_2, δ_1 and δ_0, whose specific choice will possibly be different for each equilibrium, though:

$$W_{13}^{[p\_eep]}(X(t), U(t), Y(t), Z(t)) = \delta_3 \left(X - X_{13}^{[p\_eep]} - X_{13}^{[p\_eep]} \ln \frac{X}{X_{13}^{[p\_eep]}} \right)$$

$$+\delta_2 \left(U - U_{13}^{[p\_eep]} - U_{13}^{[p\_eep]} \ln \frac{U}{U_{13}^{[p\_eep]}} \right) + \delta_1 \left(Y - Y_{13}^{[p\_eep]} - Y_{13}^{[p\_eep]} \ln \frac{Y}{Y_{13}^{[p\_eep]}} \right)$$

$$+\delta_0 \left(Z - Z_{13}^{[p\_eep]} - Z_{13}^{[p\_eep]} \ln \frac{Z}{Z_{13}^{[p\_eep]}} \right),$$

Differentiating along the trajectories we find

$$
\begin{aligned}
\frac{dW_{13}^{[p\_eep]}}{dt} &= -\delta_3 \frac{r}{K} \left(X - X_{13}^{[p\_eep]} \right)^2 - \delta_1 \frac{s}{H} \left(Y - Y_{13}^{[p\_eep]} \right)^2 \\
&- m\delta_0 \left(Z - Z_{13}^{[p\_eep]} \right)^2 + \lambda(\delta_2 - \delta_3) \left(X - X_{13}^{[p\_eep]} \right) \left(U - U_{13}^{[p\_eep]} \right) \\
&+ a(\delta_0 e - \delta_3) \left(X - X_{13}^{[p\_eep]} \right) \left(Z - Z_{13}^{[p\_eep]} \right) \\
&+ b(\delta_0 e - \delta_1) \left(Y - Y_{13}^{[p\_eep]} \right) \left(Z - Z_{13}^{[p\_eep]} \right) \\
&+ c(\delta_0 e - \delta_2) \left(U - U_{13}^{[p\_eep]} \right) \left(Z - Z_{13}^{[p\_eep]} \right).
\end{aligned}
$$

which is negative definite, giving global stability, if we choose

$$\delta_3 = \delta_2 = \delta_1 = \delta_0 e. \tag{2.39}$$

The Lyapunov function candidates for the remaining equilibria are:

$$W_9^{[p\_eep]}(X(t), U(t), Y(t), Z(t)) = \delta_3 \left(X - X_9^{[p\_eep]} - X_9^{[p\_eep]} \ln \frac{X}{X_9^{[p\_eep]}} \right)$$

$$+ \delta_2 U + \delta_1 Y + \delta_0 \left(Z - Z_9^{[p\_eep]} - Z_9^{[p\_eep]} \ln \frac{Z}{Z_9^{[p\_eep]}} \right),$$

$$W_{10}^{[p\_eep]}(X(t), U(t), Y(t), Z(t)) = \delta_1 \left(Y - Y_{10}^{[p\_eep]} - Y_{10}^{[p\_eep]} \ln \frac{Y}{Y_{10}^{[p\_eep]}} \right)$$

$$+ \delta_3 X + \delta_2 U + \delta_0 \left(Z - Z_{10}^{[p\_eep]} - Z_{10}^{[p\_eep]} \ln \frac{Z}{Z_{10}^{[p\_eep]}} \right),$$

$$W_{11}^{[p\_eep]}(X(t), U(t), Y(t), Z(t)) = \delta_3 \left(X - X_{11}^{[p\_eep]} - X_{11}^{[p\_eep]} \ln \frac{X}{X_{11}^{[p\_eep]}} \right) + \delta_2 U$$

$$+ \delta_1 \left(Y - Y_{11}^{[p\_eep]} - Y_{11}^{[p\_eep]} \ln \frac{Y}{Y_{11}^{[p\_eep]}} \right) + \delta_0 \left(Z - Z_{11}^{[p\_eep]} - Z_{11}^{[p\_eep]} \ln \frac{Z}{Z_{11}^{[p\_eep]}} \right),$$

$$W_{12}^{[p\_eep]}(X(t), U(t), Y(t), Z(t)) = \delta_3 \left(X - X_{12}^{[p\_eep]} - X_{12}^{[p\_eep]} \ln \frac{X}{X_{12}^{[p\_eep]}} \right) + \delta_1 Y$$

$$+ \delta_2 \left(U - U_{12}^{[p\_eep]} - U_{12}^{[p\_eep]} \ln \frac{U}{U_{12}^{[p\_eep]}} \right) + \delta_0 \left(Z - Z_{12}^{[p\_eep]} - Z_{12}^{[p\_eep]} \ln \frac{Z}{Z_{12}^{[p\_eep]}} \right)$$

and upon differentiation, they are all seen to produce negative definite derivatives using always the choice (2.39).

Remark 2. These results indicate that there is no possibility of Hopf bifurcations at all the equilibria also of the system (2.19).

2.2.4 Transcritical bifurcations

Similar to what was done in Section 2.1.4, we also verify the transversality conditions required for the transcritical bifurcations involving the equilibria of model (2.19).

The pairs $P_{11}^{[p\_eep]} - P_9^{[p\_eep]}$ and $P_{11}^{[p\_eep]} - P_{10}^{[p\_eep]}$

The equilibrium point $P_{11}^{[p\_eep]}$ coincides with the equilibrium $P_9^{[p\_eep]}$ and with equilibrium $P_{10}^{[p\_eep]}$ respectively at the parametric thresholds

$$s^* = \frac{aberK}{a^2eK + mr}, \quad r^* = \frac{abesH}{b^2eH + ms}, \tag{2.40}$$

when we compare the second feasibility condition (2.24) and the first stability condition (2.22) and, similarly, the second feasibility condition (2.24) and the stability condition (2.23).

The Jacobian of (2.19) evaluated at $P_{11}^{[p\_eep]}$ with $s = s^*$ is

$$J_{P_{11}}^{[p\_eep]}(s^*) = \begin{pmatrix} -\frac{mr^2}{mr+a^2eK} & -\frac{mr\lambda K}{mr+a^2eK} & 0 & -\frac{amrK}{mr+a^2eK} \\ 0 & \frac{mr\lambda K+mr\mu-acerK-a^2e\mu K}{mr+a^2eK} & 0 & 0 \\ 0 & 0 & 0 & 0 \\ \frac{a^2e^2rK}{mr+a^2eK} & \frac{ace^2rK}{mr+a^2eK} & \frac{abe^2rK}{mr+a^2eK} & -\frac{aemrK}{mr+a^2eK} \end{pmatrix}$$

and its right and left eigenvectors, corresponding to zero eigenvalue, are given by $V_3 = \varphi_3(1, 0, -(mr+a^2eK)/abeK, -r/aK)^T$ and $Q_3 = \omega_3(0, 0, 1, 0)^T$, where φ_3 and ω_3 are any nonzero real number. Differentiating partially the right hand sides of the system equations (2.19) with respect to s and calculating its Jacobian matrix we find

$$f_s = \begin{pmatrix} 0 \\ 0 \\ Y_{11}^{[p\_eep]}(1 - Y_{11}^{[p\_eep]}/H) \\ 0 \end{pmatrix}, \quad Df_s = \begin{pmatrix} 0 & 0 & 0 & 0 \\ 0 & 0 & 0 & 0 \\ 0 & 0 & 1 - \frac{2}{H}Y_{11}^{[p\_eep]} & 0 \\ 0 & 0 & 0 & 0 \end{pmatrix}.$$

Denoting by $P = (X, U, Y, Z)^T$ the population vector and by $f = (f_1, f_2, f_3, f_4)^T$ the right hand side of (2.19), by ψ a generic threshold parameter and by $\xi_1, \xi_2, \xi_3, \xi_4$ the components of the eigenvector $V = (\xi_1, \xi_2, \xi_3, \xi_4)^T$ of variations in X, U, Y and Z, let us define $D^2 f(P, \psi)(V, V)$ by

$$D^2 f(P, \psi)(V, V) = \begin{pmatrix} D_{11}^2 \\ D_{21}^2 \\ D_{31}^2 \\ D_{41}^2 \end{pmatrix}, \tag{2.41}$$

where

$$\begin{aligned} D_{11}^2 &= \frac{\partial^2 f_1}{\partial X^2}\xi_1^2 + \frac{\partial^2 f_1}{\partial U^2}\xi_2^2 + \frac{\partial^2 f_1}{\partial Y^2}\xi_3^2 + \frac{\partial^2 f_1}{\partial Z^2}\xi_4^2 + 2\frac{\partial^2 f_1}{\partial X\partial U}\xi_1\xi_2 + 2\frac{\partial^2 f_1}{\partial X\partial Y}\xi_1\xi_3 \\ &+ 2\frac{\partial^2 f_1}{\partial X\partial Z}\xi_1\xi_4 + 2\frac{\partial^2 f_1}{\partial U\partial Y}\xi_2\xi_3 + 2\frac{\partial^2 f_1}{\partial U\partial Z}\xi_2\xi_4 + 2\frac{\partial^2 f_1}{\partial Y\partial Z}\xi_3\xi_4, \end{aligned}$$

$$\begin{aligned} D_{21}^2 &= \frac{\partial^2 f_2}{\partial X^2}\xi_1^2 + \frac{\partial^2 f_2}{\partial U^2}\xi_2^2 + \frac{\partial^2 f_2}{\partial Y^2}\xi_3^2 + \frac{\partial^2 f_2}{\partial Z^2}\xi_4^2 + 2\frac{\partial^2 f_2}{\partial X\partial U}\xi_1\xi_2 + 2\frac{\partial^2 f_2}{\partial X\partial Y}\xi_1\xi_3 \\ &+ 2\frac{\partial^2 f_2}{\partial X\partial Z}\xi_1\xi_4 + 2\frac{\partial^2 f_2}{\partial U\partial Y}\xi_2\xi_3 + 2\frac{\partial^2 f_2}{\partial U\partial Z}\xi_2\xi_4 + 2\frac{\partial^2 f_2}{\partial Y\partial Z}\xi_3\xi_4, \end{aligned}$$

$$D_{31}^2 = \frac{\partial^2 f_3}{\partial X^2}\xi_1^2 + \frac{\partial^2 f_3}{\partial U^2}\xi_2^2 + \frac{\partial^2 f_3}{\partial Y^2}\xi_3^2 + \frac{\partial^2 f_3}{\partial Z^2}\xi_4^2 + 2\frac{\partial^2 f_3}{\partial X \partial U}\xi_1\xi_2 + 2\frac{\partial^2 f_3}{\partial X \partial Y}\xi_1\xi_3$$
$$+ 2\frac{\partial^2 f_3}{\partial X \partial Z}\xi_1\xi_4 + 2\frac{\partial^2 f_3}{\partial U \partial Y}\xi_2\xi_3 + 2\frac{\partial^2 f_3}{\partial U \partial Z}\xi_2\xi_4 + 2\frac{\partial^2 f_3}{\partial Y \partial Z}\xi_3\xi_4,$$

$$D_{41}^2 = \frac{\partial^2 f_4}{\partial X^2}\xi_1^2 + \frac{\partial^2 f_4}{\partial U^2}\xi_2^2 + \frac{\partial^2 f_4}{\partial Y^2}\xi_3^2 + \frac{\partial^2 f_4}{\partial Z^2}\xi_4^2 + 2\frac{\partial^2 f_4}{\partial X \partial U}\xi_1\xi_2 + 2\frac{\partial^2 f_4}{\partial X \partial Y}\xi_1\xi_3$$
$$+ 2\frac{\partial^2 f_4}{\partial X \partial Z}\xi_1\xi_4 + 2\frac{\partial^2 f_4}{\partial U \partial Y}\xi_2\xi_3 + 2\frac{\partial^2 f_4}{\partial U \partial Z}\xi_2\xi_4 + 2\frac{\partial^2 f_4}{\partial Y \partial Z}\xi_3\xi_4.$$

After calculating $D^2 f$ from (2.41) evaluated at $P_{11}^{[p\_eep]}$, at the threshold s^* and using the eigenvector V_3 we can verify the following three conditions

$$Q_3^T f_s(P_{11}^{[p\_eep]}, s^*) = 0, \quad Q_3^T[Df_s(P_{11}^{[p\_eep]}, s^*)V_3] = -\varphi_3\omega_3(\frac{mr + a^2 eK}{abeK}) \neq 0$$
$$Q_3^T[D^2 f_s(P_{11}^{[p\_eep]}, s^*)(V_3, V_3)] = -2\omega_3\varphi_3{}^2 \left(\frac{bmr^2}{a^2 beK^2} + \frac{r}{K} + \frac{mr^2}{abeHK} + \frac{ar}{bH} \right) \neq 0.$$

Now, a similar calculation when $P_{11}^{[p\_eep]}$ coincides with $P_{10}^{[p\_eep]}$ for $r = r^*$, using the Jacobian

$$J_{P_{11}}^{[p\_eep]}(r^*) = \begin{pmatrix} 0 & 0 & 0 & 0 \\ 0 & \frac{-bcesH - b^2 e\mu H + ms\mu}{b^2 eH + ms} & 0 & 0 \\ 0 & 0 & -\frac{ms^2}{b^2 eH + ms} & -\frac{bmsH}{b^2 eH + ms} \\ \frac{abe^2 sH}{b^2 eH + ms} & \frac{abce^2 HK}{(a^2 beH + amr)K + bmrH} & \frac{b^2 e^2 sH}{b^2 eH + ms} & -\frac{bems}{b^2 eH + ms} \end{pmatrix},$$

the right and left eigenvectors of the zero eigenvalue $V_4 = \varphi_4(1, 0, -abeH/(b^2 eH + ms), aes/(b^2 eH + ms))^T$ and $Q_4 = \omega_4(1, 0, 0, 0)^T$, produces

$$f_r = \begin{pmatrix} X_{11}^{[p\_eep]}(1 - X_{11}^{[p\_eep]}/K) \\ 0 \\ 0 \\ 0 \end{pmatrix}, \quad Df_r = \begin{pmatrix} 1 - \frac{2}{K}X_{11}^{[p\_eep]} & 0 & 0 & 0 \\ 0 & 0 & 0 & 0 \\ 0 & 0 & 0 & 0 \\ 0 & 0 & 0 & 0 \end{pmatrix}$$

so that evaluating $D^2 f$ from (2.41) the following three conditions are satisfied:

$$Q_4^T f_r(P_{11}^{[p\_eep]}, r^*) = 0, \quad Q_4^T[Df_r(P_{11}^{[p\_eep]}, r^*)V_4] = \varphi_4\omega_4 \neq 0,$$
$$Q_4^T[D^2 f_r(P_{11}^{[p\_eep]}, r^*)(V_4, V_4)] = 2\omega_4\varphi_4{}^2 \left(\frac{abesH}{msK + b^2 eHK} \right) \neq 0.$$

These transcritical bifurcations are illustrated, respectively, in Figure 4.2 which occur for $s^* \approx 0.6$, $r^* \approx 0.6$, (2.40).
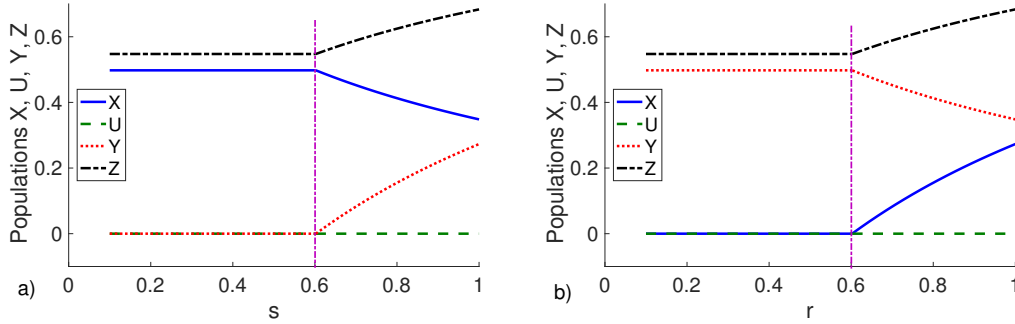
Figure 2.2: a) Transcritical bifurcation between $P_{11}^{[p\_eep]}$ and $P_9^{[p\_eep]}$ for the parameters values $r = K = a = c = \mu = H = b = m = e = 1.1$, $\lambda = 0.5$. The equilibrium $P_9^{[p\_eep]}$ is stable for $s \in [0.1, 0.602]$ while $P_{11}^{[p\_eep]}$ is stable for $s > 0.602$. The vertical line indicates the threshold. b) Transcritical bifurcation between $P_{11}^{[p\_eep]}$ and $P_{10}^{[p\_eep]}$ for $s = K = a = c = \mu = H = b = m = e = 1.1$, $\lambda = 0.5$. The equilibrium $P_{10}^{[p\_eep]}$ is stable for $r \in [0.1, 0.603]$, $P_{11}^{[p\_eep]}$ is stable for $r > 0.603$; the vertical line indicates the threshold.

The pairs $P_{13}^{[p\_eep]} - P_{11}^{[p\_eep]}$ and $P_{13}^{[p\_eep]} - P_{12}^{[p\_eep]}$

$P_{13}^{[p\_eep]}$ coincides with $P_{11}^{[p\_eep]}$ at the threshold λ^* and with $P_{12}^{[p\_eep]}$ at the threshold b^*, comparing (2.34) and the stability condition (2.27) of $P_{11}^{[p\_eep]}$, as well as (2.34) with the stability condition (2.31) of $P_{12}^{[p\_eep]}$, respectively.

The transcritical bifurcations proofs at $P_{13}^{[p\_eep]}$ are analogous to those presented earlier in this section and therefore omitted.

Figure 4.3 illustrates the simulation explicitly showing the transcritical bifurcation between $P_{13}^{[p\_eep]}$ with respectively $P_{11}^{[p\_eep]}$ and $P_{12}^{[p\_eep]}$ for the parameters values given in the caption of Fig. 4.3, respectively for $\lambda^* \approx 1.57$, $b^* \approx 2.7$, (2.40).

In Table 4.3 we summarize the transcritical bifurcations of the models (2.1) and (2.19).

2.3 Comparison between the models with hidden and explicit resources

In this Section, we investigate the behaviour of the models (2.1) and (2.19) from the comparison of their equilibrium points.

In Table (4) 4.4 we present all the possibilities of comparison between equilibria.

The populations in both ecosystems cannot completely disappear, as the origin in both systems is unstable. Note that the equilibria with the presence only of infected prey and predators, while the healthy prey population is ab-
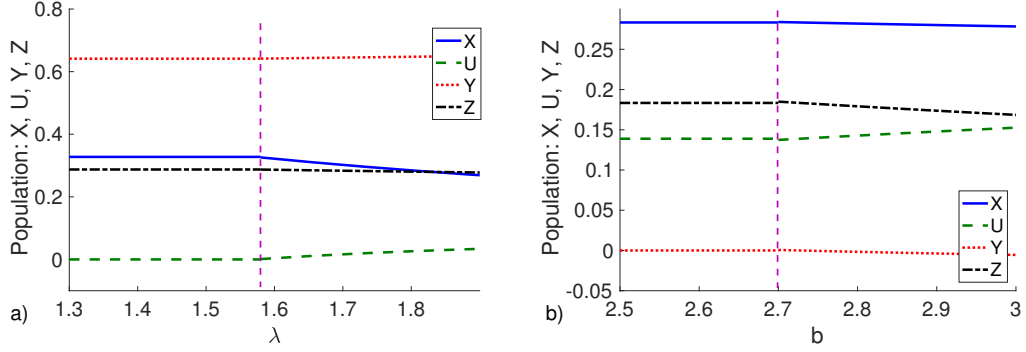
Figure 2.3: a) Transcritical bifurcation between $P_{13}^{[p\_eep]}$ and $P_{11}^{[p\_eep]}$ for $s = K = b = e = r = 0.5$, $a = 0.6$, $c = \mu = 0.4$, $H = m = 0.9$. The point $P_{11}^{[p\_eep]}$ is stable for $\lambda \in [0.1, 1.572]$ and $P_{13}^{[p\_eep]}$ is stable for $\lambda > 1.572$. The vertical line indicates the threshold. b) Transcritical bifurcation between $P_{13}^{[p\_eep]}$ and $P_{12}^{[p\_eep]}$ for $r = K = a = H = m = e = s = 0.5$, $\mu = 0.2$, $c = 0.3$ and $\lambda = 0.9$. $P_{13}^{[p\_eep]}$ is stable for $b \in [0.1, 2.7]$, $P_{12}^{[p\_eep]}$ is stable for $b > 2.7$; the vertical line indicates the threshold.

Table 2.3: Trancritical bifurcations of the models (2.1) and (2.19). The threshold b^* arises after modifications in (2.31) and (2.35) and the threshold λ^* arises from modifications in (2.27) and (2.34).

Model	Threshold	Equilibria
(2.1)	$r^\dagger = aL$	$P_6^{[p\_ehp]} = P_5^{[p\_ehp]}$
(2.1)	$\lambda^\dagger = \dfrac{aeKL(cr+a\mu)+ur(\mu+eL)}{uK(r-aL)}$	$P_6^{[p\_ehp]} = P_7^{[p\_ehp]}$
(2.19)	$s^* = \dfrac{aberK}{a^2eK+mr}$	$P_{11}^{[p\_eep]} = P_9^{[p\_eep]}$
(2.19)	$r^* = \dfrac{abesH}{b^2eH+ms}$	$P_{11}^{[p\_eep]} = P_{10}^{[p\_eep]}$
(2.19)	$\lambda^* = \dfrac{aecrsK+a^2es\mu K+becrsH+b^2er\mu H+mrs\mu}{b^2erHK-abesHK+mrsK}$	$P_{13}^{[p\_eep]} = P_{11}^{[p\_eep]}$
(2.19)	$b^* = \dfrac{c^2ers+ms\lambda^2K}{cer(\lambda K-\mu)+ae\mu\lambda K}$	$P_{13}^{[p\_eep]} = P_{12}^{[p\_eep]}$

Table 2.4: Comparison between similar equilibria of systems (2.1) and (2.19) in which have the same biological behaviour and u=unstable, s=stable, cs=conditionally stable, i=unfeasible, uf=unstable if feasible, sf=stable if feasible. The $\bullet$ corresponds to a nonvanishing population. Note that $P_9^{[p\_eep]} = (\bullet, 0, 0, \bullet)$ of (2.19) is absent since it does not really correspond to any equilibrium of the hidden resource model (2.1).

Eq. of (2.1)	Eq. of (2.19)	Interpretation
$P_1^{[p\_ehp]} = (0,0,0)$ (u)	$P_1^{[p\_eep]} = (0,0,0,0)$ (uu)	ecosystem collapse
	$P_3^{[p\_eep]} = (0,0,\bullet,0)$ (u)	
$P_2^{[p\_ehp]} = (\bullet,0,0)$ (u)	$P_2^{[p\_eep]} = (\bullet,0,0,0)$ (uu)	
	$P_3^{[p\_eep]} = (0,0,\bullet,0)$ (u)	healthy prey-only
	$P_4^{[p\_eep]} = (\bullet,0,\bullet,0)$ (u)	
$P_3^{[p\_ehp]} = (\bullet,\bullet,0)$ (u)	$P_5^{[p\_eep]} = (\bullet,\bullet,0,0)$ (u)	predator-free
	$P_8^{[p\_eep]} = (\bullet,\bullet,\bullet,0)$ (uf)	
$P_4^{[p\_ehp]} = (0,\bullet,\bullet)$ (i)	$P_6^{[p\_eep]} = (0,\bullet,0,\bullet)$ (i)	healthy prey-free
	$P_7^{[p\_eep]} = (0,\bullet,\bullet,\bullet)$ (i)	
$P_5^{[p\_ehp]} = (0,0,\bullet)$ (s)	$P_{10}^{[p\_eep]} = (0,0,\bullet,\bullet)$ (cs)	predator-only
$P_6^{[p\_ehp]} = (\bullet,0,\bullet)$ (cs)	$P_{11}^{[p\_eep]} = (\bullet,0,\bullet,\bullet)$ (cs)	disease-free
$P_7^{[p\_ehp]} = (\bullet,\bullet,\bullet)$ (sf)	$P_{12}^{[p\_eep]} = (\bullet,\bullet,0,\bullet)$ (cs)	coexistence
	$P_{13}^{[p\_eep]} = (\bullet,\bullet,\bullet,\bullet)$ (sf)	

sent, are impossible in both models. This is illustrated in table 4.4 by the comparison of points $P_4^{[p\_ehp]}$ with $P_6^{[p\_eep]}$ and $P_7^{[p\_eep]}$.

The predator-free environment, with endemic disease in the prey, is feasible but unstable in both models, comparing equilibria $P_3^{[p\_ehp]}$ with $P_5^{[p\_eep]}$ and $P_8^{[p\_eep]}$.

Observe that the healthy-prey-only equibrium $P_2^{[p\_ehp]}$ in (2.1) has several counterparts in the system with alternative resources, namely $P_2^{[p\_eep]}$, healthy-prey-only environment, $P_3^{[p\_eep]}$, alternative resource-only point, and $P_4^{[p\_eep]}$ healthy-prey and alternative resource equilibrium. All these states are however unachievable, since they all are unconditionally unstable.

The predator-only state arises at $P_5^{[p\_ehp]}$ in the simpler model, and has its counterpart in the point $P_{10}^{[p\_eep]}$. Both are always feasible. The stability conditions (2.7) and (2.23) express the same idea, that the prey reduced growth rate, i.e. the ratio between the reproduction rate of the healthy prey and the rate at which they are captured by the predators, is bounded above by the predators' population size at equilibrium.

The disease-free equilibrium in (2.1) is $P_6^{[p\_ehp]}$. Two points could be related to it, namely $P_9^{[p\_eep]}$ and $P_{11}^{[p\_eep]}$. The former, however, does not contain the alternative resource, so it is not really comparable. This would be possible only if in the model with alternative food supply we let $L \to 0$, but in such case $P_6^{[p\_ehp]}$ reduces to $P_2^{[p\_ehp]}$.

For feasibility of $P_6^{[p\_ehp]}$ and $P_{11}^{[p\_eep]}$ in both cases the opposite conditions that ensure stability for $P_5^{[p\_ehp]}$ and $P_{10}^{[p\_eep]}$ are required, thereby indicating transcritical bifurcations among the pairs of points belonging to the same model.

Analogously, we can compare the equilibria $P_6^{[p\_ehp]}$ and $P_{11}^{[p\_eep]}$ with the pair $P_7^{[p\_ehp]}$ and $P_{13}^{[p\_eep]}$. The stability conditions of $P_6^{[p\_ehp]}$ and $P_{11}^{[p\_eep]}$ are the opposite conditions that ensure stability for the coexistence equilibria $P_7^{[p\_ehp]}$ and $P_{13}^{[p\_eep]}$, thereby indicating transcritical bifurcations among the pairs of points belonging to the same model (see Table 4.5).

The coexistence equilibrium $P_7^{[p\_ehp]}$ of the hidden resource system has two counterparts in the explicit resource model, $P_{12}^{[p\_eep]}$ and $P_{13}^{[p\_eep]}$, the difference being that in the former the alternative resource is absent, so in reality is not really a "coexistence" equilibrium of the explicit resource model. But in all three equilibria, the first prey with endemic disease and the predators persist.

2.4 Results and conclusions

In this Chapter, we have compared the dynamics between two predator-prey models where the predador is generalist in the first model and specialist on two prey species in the second one; further, a transmissible disease spreads

Table 2.5: Transcritical bifurcations among the pairs of equilibria belonging to the same model.

comparable points of models	Comparable points of models
$P_6^{[p\_ehp]} \equiv P_{11}^{[p\_eep]}$	$P_5^{[p\_ehp]} \equiv P_{10}^{[p\_eep]}$
$P_6^{[p\_ehp]} \equiv P_{11}^{[p\_eep]}$	$P_7^{[p\_ehp]} \equiv P_{13}^{[p\_eep]}$

among the primary population resource. The alternative prey for the predator is implicit in the first model, but in the second one we have made it explicit.

In the first model the infection rate λ on the healthy prey population and the mortality rate of infected prey μ determine the stable coexistence of healthy prey, infected prey and predator when the predator has an alternative resource, see condition (2.12). However, in the second model, when we consider the explicit resource for the predator species, in addition to the infection rate λ and the mortality rate μ, also an extra condition involving the growth rate r of the healthy prey X plays an essential role for the stable coexistence, compare conditions (2.34), (2.35) and (2.36). In these cases the ranges of possible values for the contact rate are, respectively, provided in (2.14) and (2.38).

Due to the presence of the alternative food resource for the generalist predator in model (2.1) we cannot observe any predator's extinction scenario because the equilibria $P_2^{[p\_ehp]}$ and $P_3^{[p\_ehp]}$ are unstable. The same scenario exists in model (2.19) because the equilibria with no predators, namely $P_2^{[p\_eep]}$, $P_3^{[p\_eep]}$, $P_4^{[p\_eep]}$, $P_5^{[p\_eep]}$ and $P_8^{[p\_eep]}$, are all always unstable.

The main features in the behaviour of the systems (2.1) and (2.19) include switching of stability, extinction and persistence for the various populations. The bifurcation analysis and the comparison of the results of these models, summarized in Table 4.3, indicate that the most important parameters in these systems are the reproduction rate of the main prey r, the infection rate of the main prey λ, the mortality rate of infected prey and the reproduction rate of the alternative prey s. Note however, that the last two, in particular, appear only in system (2.19). This remark shows that the more comprehensive formulation allows a finer tuning for the ecosystem behaviour. Indeed this has already been observed earlier, see Table 4.4, when we found that the equilibrium $P_9^{[p\_eep]}$ of (2.19) with neither disease nor alternative prey does not have any counterpart in the hidden resource model (2.1).

If the reproduction rate r of the prey X is low, it will cause the simultaneous extinction of the healthy prey X and the infected prey U in both systems (2.1) and (2.19). This situation is represented by equilibria $P_5^{[p\_ehp]}$ and $P_{10}^{[p\_eep]}$ for which the stability conditions are respectively given by (2.7) and (2.23). However, if the main prey growth rate r is high, the primary prey invade the system and the models will display the infected-prey-only extinction (equilibria $P_6^{[p\_ehp]}$ and $P_{11}^{[p\_eep]}$), compare their feasibility conditions (2.8) and the first

condition in (2.24), respectively.

In addition, when the growth rate s of the alternative prey Y is low in model (2.19), extinction of U and Y occurs (see the first condition of (2.22)). However, if this rate is high, only the infected prey disappears (see the second condition of (2.24)).

A further consideration concerns the infection rate among prey λ. If it is low, extinction of the infected prey U occurs in both ecosystems (equilibria $P_6^{[p\_ehp]}$ and $P_{11}^{[p\_eep]}$), see (2.9) and (2.26), but otherwise both ecosystems will exhibit a coexistence scenario with all the species present, equilibria $P_7^{[p\_ehp]}$ and $P_{13}^{[p\_eep]}$. For both situations see Figures 4.1-b and 4.3-a. In models (2.1) and (2.19) feasibility and local asymptotic stability of the equilibria imply also their global asymptotic stability. Thus if disease eradication is the goal, a low transmission rate λ is desirable.

Another result that we can highlight is associated with the purely demographic system presented in [5], where the same dynamical systems are investigated, but excluding the possibility of an epidemic in the main prey X. As in our present situation, the models proposed in [5] present a logistic growth for both the X and Y prey populations and a quadratic mortality for the Z predator population when the alternative resource is explicit. When it is hidden, to take it into account, also the predators exhibit logistic growth. Table 4.6 illustrates the comparison between models with hidden and explicit prey for the predator, considering an environment with and without the possibility of a transmissible disease among individuals of prey population X. There is no possibility of a scenario in which in the ecoepidemic models, i.e. with a transmissible disease affecting the first prey, the infected prey thrive without the presence of the susceptible prey. This occurs both in the case of the hidden prey as well as of the explicit prey. This situation is represented by the healthy-prey-free equilibria. Note that this remark of course hinges on the assumption that the infected prey do not reproduce.

The scenario in which the predator Z survives is possible in both scenarios, i.e., with and without the infected population U. In both cases, clearly this result is guaranteed in the models (2.1) and (2.19). Finally, the existence of a transmissible disease among individuals X does not compromise the coexistence of prey and predator species. In addition, the disease-free equilibrium points represented by $P_6^{[p\_ehp]}$ and $P_{11}^{[p\_eep]}$, when represented in the same dynamic but without a transmissible disease among individuals X, clearly reduce to the equilibria representing coexistence.

This study ultimately indicates that the simpler formulation with the hidden resource already captures the salient features of the ecosystem. Therefore modeling explicitly the substitute prey is not necessary unless a particular emphasys is placed on the behavior and the possible consequences that involve the alternative resource. In such case the extended model is preferable, but this of course as expected complicates the model formulation and entails a

Table 2.6: Systems dynamics considering an environment with and without a transmissible disease among individuals of the main prey X. The column representing the biological interpretation in the table refers to the equilibrium points obtained in both models (2.1) and (2.19) that are biologically equivalent.

Biological interpretation	Environment **with** disease transmission in prey X	Environment **without** disease transmission in prey X, [5]
ecosystem collapse	not possible	not possible
healthy-prey-only	not possible	not possible
predator-free	not possible	not possible
healthy-prey-free	not possible	possible
predator-only	possible	possible
disease-free	possible	possible
coexistence	possible	possible

rather more complicated analysis. The bottom line of these remarks is therefore that the model to be used should be guided by the questions that prompt its formulation and the answers that are sought.

CHAPTER 3

COMPARING PREDATOR-PREY MODELS WITH HIDDEN AND EXPLICIT RESOURCES WITH A TRANSMISSIBLE DISEASE IN THE PREDATOR SPECIES

Ecology is an area of biology that seeks to understand the relationships existing between living beings in a given environment and to ensure the maintenance of ecological balance. To protect species from extinction it is fundamental to understand the interaction dynamics between different populations, usually related through food links [57, 22, 44, 84]. Important tools to investigate the dynamics among populations are mathematical models that seek to describe this type of interaction. As an instance we can cite the dynamics of predator-prey type biological systems [56, 86, 66], whose scientific foundations provide solid results that allow the expansion of research in the area ([33, 82, 87, 17].

In this Chapter, we extend the results of earlier investigations on predators feeding on a main resource and on an additional prey, when the latter is implicitly and explicitly modeled in the system [5] and in addition when the prey is subject to a transmissible disease [54], presented as Chapters 1 and 2.

Two models are here proposed to investigate a similar situation when the epidemics affects the predators, such as in [42, 41]. We investigate the dynamics between predator and prey in two different scenarios. In the first one, we consider a generalist predator that has two different prey for own survival, the main prey and an alternative one which is not explicitly built in as a model variable. In the second scenario, the predator becomes a type of specialist with only two explicit prey. The results of [5] show that the grazing pressure on

the preferred prey and carrying capacity of the predator determine the stable coexistence of prey and predator when the alternative resource is implicit.

The Chapter is organized as follows: the mathematical models are formulated in Section 3.1. The boundedness of both systems are discussed in Section 3.1.1. The existence of equilibria and the stability are examined in Section 3.1.2 and the theoretical results for bifurcations are discussed in Section 3.1.3. The numerical simulations of Section 3.1.4 give detailed results about the onset of bifurcations. In Sections 3.2 and 3.3 we compare the models and their results, respectively. Transcritical bifurcations present in both models are illustrated with the help of numerical examples.

3.1 Basic assumptions and models formulation

This ecoepidemic model considers the following three populations: the prey X, the healthy predator population Z and the infected predators W. The model with the alternative food supply, in which the prey population is represented by Y, is denoted $[ep\_hp]$, where "ep" denotes ecoepidemic in predator and "hp" denotes hidden prey that substitute resource not explicitly modeled in the equations [5], is well known in the literature, see Chapter 3 of [65]:

$$
\begin{aligned}
\frac{dX}{dt} &= rX\left(1 - \frac{X}{K}\right) - aZX - gXW, \\
\frac{dZ}{dt} &= uZ\left(1 - \frac{Z+W}{L}\right) + eX(aZ + gW) - \beta ZW, \\
\frac{dW}{dt} &= \beta ZW - \nu W.
\end{aligned}
\tag{3.1}
$$

Now, we consider a disease-affected predator, which is specialist for two prey species. The model in this case is denoted by $[ep\_ep]$ where the first "ep" denotes ecoepidemic in predator and the second one denotes explicit prey:

$$
\begin{aligned}
\frac{dX}{dt} &= rX\left(1 - \frac{X}{K}\right) - aZX - gXW, \\
\frac{dY}{dt} &= sY\left(1 - \frac{Y}{H}\right) - bZY - \kappa YW, \\
\frac{dZ}{dt} &= -mZ^2 + eZ(aX + bY) + eW(gX + \kappa Y) - \beta ZW, \\
\frac{dW}{dt} &= \beta ZW - \nu W.
\end{aligned}
\tag{3.2}
$$

In both models all the parameters are assumed to be nonnegative. Their biological meaning is rather obvious, as these are kind of standard models: r, u and s are growth rates, K, L, H denote carrying capacities, a, g, b and κ are hunting rates, β is the disease horizontal transmission rate ν the natural

plus disease-induced mortality, m is the predators' mortality rate, e is the conversion factor, i.e., the fraction of captured prey that is used to produce new predators. In particular note that for the latter, if the biomass is measured in kilograms and in any case taking into account that the whole prey is never entirely converted into predators' mass, we take

$$e \leq 1 \qquad (3.3)$$

The Jacobians are,

$$J^{[ep\_hp]} = \begin{pmatrix} J_{11}^{[ep\_hp]} & -aX & -gX \\ aeZ + egW & J_{22}^{[ep\_hp]} & -\frac{u}{L}Z + egX - \beta Z \\ 0 & \beta W & \beta Z - \nu \end{pmatrix} \qquad (3.4)$$

with

$$J_{11}^{[ep\_hp]} = r - \frac{2r}{K}X - aZ - gW, \quad J_{22}^{[ep\_hp]} = u - \frac{2u}{L}Z - \frac{u}{L}W + aeX - \beta W$$

and

$$J^{[ep\_ep]} = \begin{pmatrix} J_{11}^{[ep\_ep]} & 0 & -aX & -gX \\ 0 & J_{22}^{[ep\_ep]} & -bY & -\kappa Y \\ aeZ + egW & ebZ + e\kappa W & J_{33}^{[ep\_ep]} & egX + e\kappa Y - \beta Z \\ 0 & 0 & \beta W & \beta Z - \nu \end{pmatrix} \qquad (3.5)$$

with

$$J_{11}^{[ep\_ep]} = r - \frac{2r}{K}X - aZ - gW, \quad J_{22}^{[ep\_ep]} = s - \frac{2s}{H}Y - bZ - \kappa W,$$

$$J_{33}^{[ep\_ep]} = -2mZ + eaX + ebY - \beta W,$$

respectively.

The first equation of model (3.1) describes the healthy prey propulation dynamics. The first term on the right hand side expresses logistic growth with r being the per capita net reproduction rate and K the environment carrying capacity. The second and third terms describe the process where the healthy individual is hunted by healthy predator Z and infected predator W, respectively. The second equation of model (3.1) contains the dynamics of the healthy predator,that in absence of prey X has an alternative resource, that is hidden in this model. It is implicitly represented in the model by the carrying capacity L, whereas the predators per capita net reproduction rate is u, respectively. The term $eX(aZ + gW)$ expresses the increase of the predator Z population due to successful hunting of the prey, by healthy and infected predators. The term βZW models the infection process of susceptible predators by contact with other infected individuals. The third equation of

model (3.1) describes the infected predator W evolution, recruited as explained in the previous equation and subject to disease-related mortality ν.

The first and fourth equations of model (3.2) represent the healthy prey X and infected predator W dynamics. They are the same as for model (3.1). The second equation of model (3.2) describes the alternative prey population dynamics which now becomes an explicit variable of the system.

The first term on the right hand side expresses logistic growth with per capita net reproduction rate s and carrying capacity H. The second and third terms model the process where the individual of population Y is hunted by healthy predator Z and infected predator W, respectively. The third equation of model (3.2) describes the healthy predator population dynamics. In this equation, first term on the right hand side assumes mortality in the quadratic form $-mZ^2$ since this term is related to the intraspecific competition term $-uL^{-1}Z^2$ of the system (3.1). Predators mortality clearly occurs in the absence of both their food resources X and Y because in this model the predator is assumed to be a specialist on both of them. The term $eZ(aX+bY)$ corresponds the population increase of predator Z due to hunting the prey X and Y. Finally, the term βZW accounts for individuals of the population Z that become infected.

3.1.1 Boundedness of models

In order to have a well-posed model, the systems trajectories must be contained in a compact set. First of all, note that the populations cannot become negative because they start from positive initial values, for obvious biological reasons, and systems (3.1) and (3.2) are homogeneous, so that the coordinate subspaces are solution trajectories and, by the uniqueness theorem, they cannot be crossed by other trajectories. Indeed $\dot{X} = 0$ if $X(0) = 0$, $\dot{Y} = 0$ if $Y(0) = 0$, $\dot{Z} \geq 0$ if $Z(0) = 0$, $\dot{W} = 0$ if $W(0) = 0$ and when nonvanishing, the initial conditions should always be positive to make biological sense.

Proposition 3.1.1. *Consider the total environment population $\varphi(t) = X(t) + Z(t) + W(t)$, in model (3.1). Then there exists $\eta \in \mathbb{R}_+$ for which*

$$\varphi(t) \leq \left(\varphi(0) - \frac{M}{\eta}\right) e^{-\eta t} + \frac{M}{\eta} \leq \max\left\{\varphi(0), \frac{M}{\eta}\right\}. \tag{3.6}$$

Thus for model (3.1) the solutions are always nonnegative.

Proof. Taking an arbitrary $0 < \eta < \nu$, summing the equations in model (3.1), we obtain:

$$\begin{aligned}
\frac{d\varphi(t)}{dt} &= rX\left(1 - \frac{X}{K}\right) + uZ\left(1 - \frac{Z+W}{L}\right) - \nu W \\
&+ (e-1)(aXZ + gXW).
\end{aligned} \tag{3.7}$$

Recalling (3.3), the last term in (3.7) can be dropped, as well as the term $-uL^{-1}WZ$, to obtain:

$$\frac{d\varphi(t)}{dt} \leq rX\left(1 - \frac{X}{K}\right) + uZ\left(1 - \frac{Z}{L}\right) - \nu W. \tag{3.8}$$

Then, adding $\eta\varphi(t)$ and using the definition of φ on both sides of the inequality (3.8) we find the estimate:

$$\frac{d\varphi(t)}{dt} + \eta\varphi(t) \leq rX\left(1 - \frac{X}{K} + \frac{\eta}{r}\right) + uZ\left(1 - \frac{Z}{L} + \frac{\eta}{u}\right)$$
$$+(\eta - \nu)W \leq p_1(X) + p_2(Z),$$
$$p_1(X) = rX\left(1 - \frac{X}{K} + \frac{\nu}{r}\right), \quad p_2(Z) = uZ\left(1 - \frac{Z}{L} + \frac{\nu}{u}\right).$$

The functions $p_1(X)$ and $p_2(Z)$ are concave parabolae, with maxima located at X^*, Z^*, and corresponding maximum values

$$M_1 = p_1(X^*) = \frac{rK}{4}\left(1 + \frac{\nu}{r}\right)^2, \quad M_2 = p_2(Z^*) = \frac{uL}{4}\left(1 + \frac{\nu}{u}\right)^2.$$

Thus,

$$\frac{d\varphi(t)}{dt} + \eta\varphi(t) \leq M; \quad M_1 + M_2 = M.$$

Integrating the differential inequality, we find (3.6). From this result, since $0 \leq X, Z, W \leq \varphi$, the boundedness of the original ecosystem populations is immediate. From the nonnegativity of the trajectories, remarked before the proof, and this result, the solution of model (3.1) remains bounded and the trajectories remain nonnegative. □

Proposition 3.1.2. *Consider the total environment population $\psi(t) = X(t) + Y(t) + Z(t) + W(t)$ in model (3.2). Then there exists $\eta_1 \in \mathbb{R}_+$ for which*

$$\psi(t) \leq \left(\varphi(0) - \frac{M}{\eta_1}\right)e^{-\eta_1 t} + \frac{M}{\eta_1} \leq \max\left\{\psi(0), \frac{M}{\eta_1}\right\}. \tag{3.9}$$

Thus for model (3.2) the solutions are always nonnegative.

Proof. We proceed in a similar way as for the proof of Proposition 3.1.1. Taking an arbitrary $0 < \eta_1 < \nu$, summing the equations in model (3.2), we obtain:

$$\frac{d\psi(t)}{dt} = rX\left(1 - \frac{X}{K}\right) + sY\left(1 - \frac{Y}{H}\right) - mZ^2 - \nu W \tag{3.10}$$
$$+ (e-1)(aXZ + bYZ + gXW + \kappa YW).$$

Since $e \leq 1$ by (3.3), from (3.10) we can obtain:

$$\frac{d\psi(t)}{dt} \leq rX\left(1 - \frac{X}{K}\right) + sY\left(1 - \frac{Y}{H}\right) - mZ^2 - \nu W. \qquad (3.11)$$

Adding $\eta_1 \psi(t)$ on both sides of inequality (3.8) we find the estimate:

$$\frac{d\psi(t)}{dt} + \eta_1 \psi(t) \leq rX\left(1 - \frac{X}{K} + \frac{\eta_1}{r}\right) + sY\left(1 - \frac{Y}{H} + \frac{\eta_1}{s}\right)$$
$$+ Z(\eta_1 - mZ) + (\eta_1 - \nu)W \leq q_1(X) + q_2(Y) + q_3(Z),$$
$$q_1(X) = rX\left(1 - \frac{X}{K} + \frac{\nu}{r}\right),$$
$$q_2(Z) = sY\left(1 - \frac{Y}{H} + \frac{\nu}{s}\right), \quad q_3(Z) = Z(\nu - mZ)$$

The functions $q_1(X)$, $q_2(Y)$ and $q_3(Z)$ are concave parabolae, with maxima located at X^*, Y^*, Z^*, and corresponding maximum values

$$M_1 = q_1(X^*) = \frac{rK}{4}\left(1 + \frac{\nu}{r}\right)^2,$$
$$M_2 = q_2(Y^*) = \frac{sH}{4}\left(1 + \frac{\nu}{s}\right)^2, \quad M_3 = q_3(Z^*) = \frac{\nu^2}{4m}.$$

Thus,

$$\frac{d\psi(t)}{dt} + \eta_1 \psi(t) \leq M; \quad M_1 + M_2 + M_3 = M.$$

Integrating the differential inequality, we find (3.9). From this result, since $0 \leq X, Y, Z, W \leq \psi$, the boundedness of the original ecosystem populations is immediate. $\qquad \square$

3.1.2 Equilibria and stability analysis

•The purely demographic model (3.1)

As illustrated in the following propositions, there are six equilibria for the model (3.1), two of which are unconditionally unstable while the remaining four are stable subject to suitable conditions on the system parameters. We are concerned with two main issues in this respect, namely feasibility and stability of these stationary points. The former refers to the fact that the population values are all nonnegative. This is a key issue for biological reasons. As for the latter, stability ensures that trajectories originating nearby an equilbrium, do indeed tend to it.

Proposition 3.1.3. *The trivial equilibrium point $P_1^{[ep\_hp]} = (0,0,0)$ and the point $P_2^{[ep\_hp]} = (K,0,0)$ are always feasible and unstable.*

Proof. Since the the system (3.1) is homogeneous, the origin $P_1^{[ep\_hp]}$ is a solution. The eigenvalues of the Jacobian matrix (3.4) evaluated at $P_1^{[ep\_hp]}$ are $r, u, -\nu$. As two eigenvalues are positive, the origin is unstable.

For $Z = W = 0$, the equilibrium equations of (3.1) give $X_2 = K$, i.e. the equilibrium $P_2^{[ep\_hp]}$, which is always feasible. The eigenvalues of the Jacobian evaluated at the $P_2^{[ep\_hp]}$ are $-r, -\nu, u+aeK > 0$, again showing instability. $\quad\square$

Proposition 3.1.4. *The healthy predator-only point* $P_3^{[ep\_hp]} = (0, L, 0)$ *is always feasible. It is stable for*

$$r < aL, \quad \nu > \beta L \tag{3.12}$$

.

Proof. For $X = W = 0$ in the system (3.1) we obtain the equilibrium $P_3^{[ep\_hp]}$, which is always feasible. The Jacobian (3.4) at $P_3^{[ep\_hp]}$ becomes

$$J_{P_3}^{[ep\_hp]} = \begin{pmatrix} r - aL & 0 & 0 \\ aeL & -u & -(u + \beta L) \\ 0 & 0 & \beta L - \nu \end{pmatrix}$$

and provides explicitly the eigenvalues, one of which $-u$ is negative, while the remaining ones give conditions (3.12). $\quad\square$

Proposition 3.1.5. *The disease-free point*

$$P_4^{[ep\_hp]} = \left(\frac{urK - auKL}{a^2eKL + ur}, \frac{aerKL + urL}{a^2eKL + ur}, 0 \right)$$

is feasible for

$$r \geq aL, \tag{3.13}$$

and stable when the following condition holds:

$$\beta < \nu \frac{ur + a^2eKL}{urL + aerKL} \tag{3.14}$$

Proof. The above equilibrium expression is easily obtained setting $W = 0$ in the system (3.1). From $X_4^{[ep\_hp]} \geq 0$ provides the feasibility condition (3.13). The Jacobian matrix (3.4) evaluated at $P_4^{[ep\_hp]}$ gives one explicit eigenvalue, from which (3.14) follows. In addition, since

$$-\mathrm{tr}\left(\overline{J}_{P4}^{[ep\_hp]} \right) = \frac{r}{K} X_4^{[ep\_hp]} + \frac{u}{L} Z_4^{[ep\_hp]} > 0$$

and

$$\det\left(\overline{J}_{P4}^{[ep\_hp]} \right) = \left(\frac{ru}{KL} + a^2e \right) X_4^{[ep\_hp]} Z_4^{[ep\_hp]} > 0,$$

the Routh-Hurwitz conditions on the remaining minor

$$\overline{J}_{P4}^{[ep\_hp]} = \begin{pmatrix} -\frac{r}{K}X_4^{[ep\_hp]} & -aX_4^{[ep\_hp]} \\ aeZ_4^{[ep\_hp]} & -\frac{u}{L}Z_4^{[ep\_hp]} \end{pmatrix}$$

are always satisfied, and thus (3.14) is the only condition for stability. $\square$

Proposition 3.1.6. *The point*

$$P_5^{[ep\_hp]} = \left(0, \frac{\nu}{\beta}, \frac{u\beta L - u\nu}{\beta u + \beta^2 L}\right)$$

is feasible if

$$\nu \leq \beta L \tag{3.15}$$

and stable for

$$ur\beta + r\beta^2 L + gu\nu < au\nu + a\nu\beta L + gu\beta L. \tag{3.16}$$

Proof. This equilibrium point is feasible for $W_5^{[ep\_hp]} \geq 0$ which gives explicitly (3.15). One eigenvalue gives the stability condition (3.16), while for the remaining minor

$$\overline{J}_{P5}^{[ep\_hp]} = \begin{pmatrix} -\frac{u\nu}{\beta L} & -\frac{u\nu}{\beta L} - \nu \\ \frac{u\beta L - u\nu}{u + \beta L} & 0 \end{pmatrix}$$

the Routh-Hurwitz conditions are unconditionally satisfied:

$$-\mathrm{tr}\left(\overline{J}_{P5}^{[ep\_hp]}\right) = \frac{u\nu}{\beta L} > 0, \quad \det\left(\overline{J}_{P5}^{[ep\_hp]}\right) = \beta\left(\frac{u}{L} + \beta\right)Z^{[ep\_hp]}W^{[ep\_hp]} > 0.$$

$\square$

Proposition 3.1.7. *Coexistence,* $P_6^{[ep\_hp]} = (X_6^{[ep\_hp]}, Z_6^{[ep\_hp]}, W_6^{[ep\_hp]})$, *whose population values are given below (3.19), exists as a double equilibrium for (3.20), (3.21) and (3.22), or as a single point, whenever (3.20) and (3.23) are satisfied, with the additional feasibility condition*

$$\beta \geq \frac{a\nu K + r\beta X_6^{[ep\_hp]}}{rK} \tag{3.17}$$

and it is stable for

$$K > \frac{(a\nu\beta L + ug\beta L + au\nu)K + (aeg\beta KL + r\beta^2 L + ru\beta)X_6^{[ep\_hp]}}{r\beta^2 L + 2gu\nu + ru\beta} \tag{3.18}$$

Proof. Explicitly, the coordinates of $P_6^{[ep\_hp]}$ are

$$Z_6^{[ep\_hp]} = \frac{\nu}{\beta}, \quad W_6^{[ep\_hp]} = \frac{r}{g} - \frac{a\nu}{g\beta} - \frac{r}{gK} X_6^{[ep\_hp]} \tag{3.19}$$

where $X_6^{[ep\_hp]}$ is a root of the quadratic function

$$\Phi(X_6^{[ep\_hp]}) = \alpha_2 (X_6^{[ep\_hp]})^2 + \alpha_1 X_6^{[ep\_hp]} + \alpha_0,$$

with

$$\alpha_2 = -\frac{er}{K}, \quad \alpha_1 = er + \frac{ur\nu}{g\beta KL} + \frac{r\nu}{gK},$$

$$\alpha_0 = \frac{u\nu}{\beta} - \frac{r\nu}{g} + \frac{au\nu^2}{g\beta^2 L} - \frac{u\nu^2}{\beta^2 L} - \frac{ur\nu}{g\beta L} + \frac{a\nu^2}{g\beta}.$$

Besides that, $P_6^{[ep\_hp]}$ is feasible if $W_6^{[ep\_hp]} \geq 0$, i.e. (3.17), and, for $X_6^{[ep\_hp]} \geq 0$ we have conditions for two positive roots

$$\Delta = \alpha_1^2 - 4\alpha_2\alpha_0 > 0, \quad -\alpha_1\alpha_2^{-1} > 0, \quad \alpha_0\alpha_2^{-1} > 0,$$

that are equivalent to

$$r\nu^2\beta^2 L + 4aeg\nu^2\beta KL^2 + 4eg^2uv\beta KL^2 + e^2g^2r\beta^2 K^2 L^2 + 2ruv^2\beta L \tag{3.20}$$
$$+4aegu\nu^2 KL + ru^2\nu^2 > 2egr\nu\beta^2 KL^2 + 4eg^2u\nu^2 KL + 2egru\nu\beta KL,$$

$$\frac{L(eg\beta K + \nu\beta) + u\nu}{eg\beta L} > 0 \tag{3.21}$$

and

$$ur\beta + r\beta^2 L + gu\nu > au\nu + a\nu\beta L + gu\beta L. \tag{3.22}$$

For one positive root we have the conditions

$$\Delta = \alpha_1^2 - 4\alpha_2\alpha_0 > 0, \quad \alpha_0\alpha_2^{-1} < 0,$$

that correspond to (3.20), again, and

$$ur\beta + r\beta^2 L + gu\nu < au\nu + a\nu\beta L + gu\beta L, \tag{3.23}$$

respectively.

The Jacobian matrix of $P_6^{[ep\_hp]}$ is

$$J_{P_6}^{[ep\_hp]} = \begin{pmatrix} -\frac{r}{K} X_6^{[ep\_hp]} & -aX_6^{[ep\_hp]} & -gX_6^{[ep\_hp]} \\ \frac{ea\nu}{\beta} + egW_6^{[ep\_hp]} & J_{22}^{[ep\_hp]} & J_{23}^{[ep\_hp]} \\ 0 & \beta W_6^{[ep\_hp]} & 0 \end{pmatrix}$$

63

with

$$J_{22}^{[ep\_hp]} = u - \frac{2u\nu}{\beta L} + eaX_6^{[ep\_hp]} - \left(\frac{u}{L} + \beta\right)W_6^{[ep\_hp]},$$

$$J_{23}^{[ep\_hp]} = -\nu - \frac{u\nu}{\beta L} + egX_6^{[ep\_hp]}.$$

Requiring the condition $J_{22}^{[ep\_hp]} < 0$, that is, (3.18), the principal minors of $-J_{P_6}^{[ep\_hp]}$ are all positive:

$$\frac{r}{K}X_6 > 0, \quad -\frac{r}{K}J_{22}^{[ep\_hp]}X_6^{[ep\_hp]} + aX_6^{[ep\_hp]}\left(\frac{ea\nu}{\beta} + egW_6^{[ep\_hp]}\right) > 0,$$

$$eag\nu X_6^{[ep\_hp]}W_6^{[ep\_hp]} + eg^2\beta X_6^{[ep\_hp]}(W_6^{[ep\_hp]})^2$$

$$+\frac{ur\beta}{KL}X_6^{[ep\_hp]}Z_6^{[ep\_hp]}W_6^{[ep\_hp]} + \frac{r}{K}\beta^2 X_6^{[ep\_hp]}Z_6^{[ep\_hp]}W_6^{[ep\_hp]}$$

$$-\frac{egr\beta}{K}X_6^{[ep\_hp]}W_6^{[ep\_hp]} > 0.$$

Thus, $P_6^{[ep\_hp]}$ is feasible and stable, respectively, if (3.17), (3.20), (3.21), (3.22), (3.23) and (3.18) hold. □

In Table 3.1 we summarize the equilibria of model (3.1).

Table 3.1: Behaviour and conditions of feasibility and stability of equilibria for the model (3.1).

Equilibria	Admissibility	Stability
$P_1^{[ep\_hp]}$	always	unstable
$P_2^{[ep\_hp]}$	always	unstable
$P_3^{[ep\_hp]}$	always	$r < aL, \quad \nu > \beta L$
$P_4^{[ep\_hp]}$	$r \geq aL$	(3.14)
$P_5^{[ep\_hp]}$	$\nu \leq \beta L$	(3.16)
$P_6^{[ep\_hp]}$	(3.17), (3.20), (3.21), (3.22) - 2 positive roots	(3.18)
	(3.17), (3.20), (3.21), (3.23) - 1 positive root	

•**Model (3.2)**

The study of local stability analysis of model (3.2) gives 11 equilibria, four of which are unconditionally unstable, one unfeasible and six are conditionally stable. The details follow.

Proposition 3.1.8. *The equilibria $P_1^{[ep\_ep]} = (0,0,0,0)$, $P_2^{[ep\_ep]} = (K,0,0,0)$, $P_3^{[ep\_ep]} = (0,H,0,0)$, $P_4^{[ep\_ep]} = (K,H,0,0)$ are feasible and unstable and the equilbrium $P_5^{[ep\_ep]} = (0,0,\nu\beta^{-1},-m\nu\beta^{-2})$ is unfeasible.*

Proof. For $X = Y = Z = W = 0$ in the system (3.2) we obtain that the origin $P_1^{[ep\_ep]}$ exists and is feasible. The eigenvalues of the Jacobian matrix (3.5) evaluated at $P_1^{[ep\_ep]}$ are $-\nu$, r, s, 0. As two eigenvalues are positive, the origin is unstable.

For $Y = Z = W = 0$ in the system (3.2) we obtain the equilibrium $P_2^{[ep\_ep]}$, which exists and is feasible. The eigenvalues of the Jacobian matrix (3.5) evaluated at $P_2^{[ep\_ep]}$ are $-r$, $-\nu$, s, eaK. As two eigenvalues are positive, $P_2^{[ep\_ep]}$ is unstable.

For $X = Z = W = 0$ in the system (3.2) we obtain the equilibrium $P_3^{[ep\_ep]}$, which exists and is feasible. The eigenvalues of the Jacobian matrix (3.5) evaluated at $P_3^{[ep\_ep]}$ are $-s$, $-\nu$, r, ebH. As two eigenvalues are positive, $P_3^{[ep\_ep]}$ is unstable.

For $Z = W = 0$ in the system (3.2) we obtain the equilibrium $P_4^{[ep\_ep]}$, which exists and is feasible. The eigenvalues of the Jacobian matrix (3.5) evaluated at $P_4^{[ep\_ep]}$ are $-\nu$, $-s$, $-r$, $eaK + ebH$. As one eigenvalue is positive, $P_4^{[ep\_ep]}$ is unstable.

Finally, for $X = Y = 0$ in the system (3.2) we obtain the equilibrium $P_5^{[ep\_ep]} = (0,0,\nu\beta^{-1},-m\nu\beta^{-2})$ which is unfeasible. $\square$

Proposition 3.1.9. *The point*

$$P_6^{[ep\_ep]} = \left(\frac{mrK}{a^2eK + mr}, 0, \frac{aerK}{a^2eK + mr}, 0 \right)$$

is always feasible and stable for

$$\beta < \frac{mr\nu + a^2e\nu K}{aerK}, \quad b > \frac{mrs + a^2esK}{aerK}. \tag{3.24}$$

Proof. Considering $Y = W = 0$ in the system (3.2) we obtain the equilibrium $P_6^{[ep\_ep]} = (\frac{mrK}{a^2eK+mr}, 0, \frac{aerK}{a^2eK+mr}, 0)$. Two eigenvalues of the Jacobian (3.5) evaluated at the $P_6^{[ep\_ep]}$ are explicit, giving the stability conditions (3.24). No other conditions arise since $-\overline{J}_{P_6}^{[ep\_ep]}$ with

$$\overline{J}_{P_6}^{[ep\_ep]} = \begin{pmatrix} -\frac{r}{K}X_6^{[ep\_ep]} & -aX_6^{[ep\_ep]} \\ aeZ_6^{[ep\_ep]} & -mZ_6^{[ep\_ep]} \end{pmatrix}$$

is positive definite, because its principal minors are

$$\frac{r}{K}X_6^{[ep\_ep]} > 0, \quad \frac{rm}{K}X_6^{[ep\_ep]}Z_6^{[ep\_ep]} + a^2eX_6^{[ep\_ep]}Z_6^{[ep\_ep]} > 0.$$

$\square$

Proposition 3.1.10. *The point*

$$P_7^{[ep\_ep]} = \left(0, \frac{msH}{b^2eH + ms}, \frac{besH}{b^2eH + ms}, 0\right)$$

is always feasible and stable whenever

$$\beta < \frac{ms\nu + b^2e\nu H}{besH}, \quad a > \frac{mrs + b^2erH}{besH}, \tag{3.25}$$

Proof. Substituting $X = W = 0$ in the system (3.2) we obtain the components of $P_7^{[ep\_ep]}$ by solving the equilibrium equations. It is stable for the conditions (3.25), given by two explicit eigenvalues. Nothing else is required, because $-\overline{J}_{P_7}^{[ep\_ep]}$ is positive definite with

$$\overline{J}_{P_7}^{[ep\_ep]} = \begin{pmatrix} -\frac{s}{H}Y_7^{[ep\_ep]} & -bY_7^{[ep\_ep]} \\ ebZ_7^{[ep\_ep]} & -mZ_7^{[ep\_ep]} \end{pmatrix}$$

since its principal minors are

$$\frac{s}{H}Y_7^{[ep\_ep]} > 0, \quad \frac{sm}{H}Y_7^{[ep\_ep]}Z_7^{[ep\_ep]} + b^2eY_7^{[ep\_ep]}Z_7^{[ep\_ep]} > 0.$$

$\square$

Proposition 3.1.11. *The point* $P_8^{[ep\_ep]} = \left(X_8^{[ep\_ep]}, Y_8^{[ep\_ep]}, Z_8^{[ep\_ep]}, 0\right)$ *with*

$$X_8^{[ep\_ep]} = \frac{b^2erHK + mrsK - abesHK}{a^2esK + b^2erH + mrs}, \quad Z_8^{[ep\_ep]} = \frac{aersK + bersH}{a^2esK + b^2erH + mrs},$$

$$Y_8^{[ep\_ep]} = \frac{a^2esHK + mrsH - aberHK}{a^2esK + b^2erH + mrs}.$$

is feasible if

$$a \leq \frac{b^2erH + mrs}{besH}, \tag{3.26}$$

$$b \leq \frac{a^2esK + mrs}{aerK}. \tag{3.27}$$

and is conditionally stable for

$$\beta < \frac{a^2es\nu K + b^2er\nu H + mrs\nu}{aersK + bersH}. \tag{3.28}$$

Proof. $P_8^{[ep\_ep]}$ is obtained setting $W = 0$ in the system (3.2). It is feasible for $X_8^{[ep\_ep]} \geq 0$, giving (3.26) and for $Y_8^{[ep\_ep]} \geq 0$, giving (3.27). One explicit eigenvalue of the Jacobian matrix gives the stability condition (3.28), No further stability conditions arise, because $-\overline{J}_{P_8}^{[ep\_ep]}$ is positive definite, where

$$\overline{J}_{P_8}^{[ep\_ep]} = \begin{pmatrix} -\frac{r}{K}X_8^{[ep\_ep]} & 0 & -aX_8^{[ep\_ep]} \\ 0 & -\frac{s}{H}Y_8^{[ep\_ep]} & -bY_8^{[ep\_ep]} \\ aeZ_8 & ebZ_8^{[ep\_ep]} & -mZ_8^{[ep\_ep]} \end{pmatrix}.$$

Indeed its principal minors are

$$\frac{r}{K}X_8^{[ep\_ep]} > 0, \quad \frac{rs}{HK}X_8^{[ep\_ep]}Y_8^{[ep\_ep]} > 0,$$

$$\left(\frac{mrs}{HK} + \frac{a^2es}{H} + \frac{b^2er}{K}\right)X_8Y_8Z_8 > 0.$$

$\square$

Proposition 3.1.12. *The main prey-free equilibrium point*

$$P_9^{[ep\_ep]} = \left(0, Y_9^{[ep\_ep]}, Z_9^{[ep\_ep]}, W_9^{[ep\_ep]}\right)$$

is conditionally feasible see (3.29), (3.31) below and stable, (3.33).

Proof. We have explicitly

$$Z_9^{[ep\_ep]} = \nu\beta^{-1}, \quad Y_9^{[ep\_ep]} = H - \frac{b\nu H}{s\beta} - \frac{\kappa H}{s}W_9^{[ep\_ep]},$$

and $W_9^{[ep\_ep]}$ is given by the roots of the quadratic function

$$\Phi(W_9^{[ep\_ep]}) = \alpha_2(W_9^{[ep\_ep]})^2 + \alpha_1 W_9^{[ep\_ep]} + \alpha_0,$$

with

$$\alpha_2 = -\frac{e\kappa^2 H}{s}, \quad \alpha_1 = -\frac{2be\nu\kappa H}{s\beta} + e\kappa H - \nu, \quad \alpha_0 = -\frac{b^2e\nu^2 H}{s\beta^2} + \frac{be\nu H}{\beta} - \frac{m\nu^2}{\beta^2}.$$

The point $P_9^{[ep\_ep]}$ is feasible if $Y_9^{[ep\_ep]} \geq 0$, which becomes

$$s \geq \frac{b\nu}{\beta} + \kappa W_9^{[ep\_ep]}, \tag{3.29}$$

and also, two positive values for $W_9^{[ep\_ep]}$ are obtained if

$$\Delta = \alpha_1^2 - 4\alpha_2\alpha_0 > 0, \quad -\alpha_1\alpha_2^{-1} > 0, \quad \alpha_0\alpha_2^{-1} > 0,$$

that are equivalent to

$$\nu < \frac{e^2s\kappa^2\beta^2 H^2 + 4be\nu^2\beta\kappa H + \beta^2 s\nu^2}{4em\nu\kappa H + 2es\beta^2\kappa H}, \tag{3.30}$$

and

$$\nu < \frac{es\kappa\beta H}{s\beta + 2be\kappa H}, \quad \beta < \frac{b^2e\nu H + ms\nu}{besH}, \tag{3.31}$$

respectively. For one positive root $W_9^{[ep\_ep]}$, instead the following conditions must hold

$$\Delta = \alpha_1^2 - 4\alpha_2\alpha_0 > 0, \quad \alpha_0\alpha_2^{-1} < 0,$$

which are equivalent to the first condition (3.30) and

$$\beta > \frac{b^2 e\nu H + ms\nu}{besH}. \tag{3.32}$$

Besides that, $P_9^{[ep\_ep]}$ is stable for

$$r < \frac{a\nu}{\beta} + gW_9^{[ep\_ep]} \tag{3.33}$$

given by an explicit eigenvalue of the Jacobian matrix.

In addition,

$$\overline{J}_{P_9}^{[ep\_ep]} = \begin{pmatrix} -\frac{s}{H}Y_9^{[ep\_ep]} & -bY_9^{[ep\_ep]} & -\kappa Y_9^{[ep\_ep]} \\ \frac{be\nu}{\beta} + e\kappa W_9^{[ep\_ep]} & \overline{J}_{22}^{[ep\_ep]} & \overline{J}_{23}^{[ep\_ep]} \\ 0 & \beta W_9^{[ep\_ep]} & 0 \end{pmatrix},$$

with

$$\overline{J}_{22}^{[ep\_ep]} = J_{33}^{[ep\_ep]}, \quad \overline{J}_{23}^{[ep\_ep]} = J_{34}^{[ep\_ep]},$$

is negative definite, if we require the conditions $J_{33}^{[ep\_ep]} < 0$, $J_{34}^{[ep\_ep]} < 0$, i.e.

$$b < \frac{2m\nu}{e\beta H} + \frac{b^2\nu}{s\beta} + \left(\frac{b\kappa}{s} + \frac{\beta}{eH}\right)W_9^{[ep\_ep]} \tag{3.34}$$

and

$$e < \frac{eb\nu}{s\beta} + \frac{\nu}{\kappa H} + \frac{e\kappa}{s}W_9^{[ep\_ep]}, \tag{3.35}$$

respectively. Indeed, in this way the principal minors of $-\overline{J}_{P9}$ turn out to be all positive,

$$\frac{s}{H}Y_9^{[ep\_ep]} > 0, \quad \frac{s}{H}\overline{J}_{22}^{[ep\_ep]}Y_9^{[ep\_ep]} + bY_9^{[ep\_ep]}\left(\frac{be\nu}{\beta} + e\kappa W_9^{[ep\_ep]}\right) > 0,$$

$$(\beta\kappa Y_9^{[ep\_ep]}W_9^{[ep\_ep]})\overline{J}_{22}^{[ep\_ep]} + \frac{s\beta}{H}Y_9^{[ep\_ep]}W_9^{[ep\_ep]}\overline{J}_{23}^{[ep\_ep]} > 0.$$

$\square$

Proposition 3.1.13. *The equilibrium point $P_{10}^{[ep\_ep]} = (X_{10}^{[ep\_ep]}, 0, Z_{10}^{[ep\_ep]}, W_{10}^{[ep\_ep]})$ is unique and feasible if the conditions (3.36) and (3.39) hold; it is conditionally stable when (3.40), (3.41) and (3.42) hold.*

Proof. Setting $Y = 0$ in the system (3.2) we obtain the population values

$$X_{10}^{[ep\_ep]} = K - \frac{a\nu K}{r\beta} - \frac{gK}{r} W_{10}^{[ep\_ep]}, \quad Z_{10}^{[ep\_ep]} = \frac{\nu}{\beta}$$

where $W_{10}^{[ep\_ep]}$ is a root of the quadratic

$$\Phi(W_{10}^{[ep\_ep]}) = \alpha_2 (W_{10}^{[ep\_ep]})^2 + \alpha_1 W_{10}^{[ep\_ep]} + \alpha_0,$$

with

$$\alpha_2 = -\frac{eg^2 K}{r}, \quad \alpha_1 = egK - \frac{2aeg\nu K}{r\beta} - \nu, \quad \alpha_0 = \frac{ae\nu K}{\beta} - \frac{a^2 e\nu^2 K}{r\beta^2} - \frac{m\nu^2}{\beta^2}.$$

For feasibility we need to require $X_{10}^{[ep\_ep]} \geq 0$, that is,

$$r \geq \frac{a\nu}{\beta} + gW_{10}^{[ep\_ep]}, \tag{3.36}$$

and $W_{10}^{[ep\_ep]} \geq 0$. In this case, two positive roots arise if

$$\Delta = \alpha_1^2 - 4\alpha_2\alpha_0 > 0, \quad -\alpha_1 \alpha_2^{-1} > 0, \quad \alpha_0 \alpha_2^{-1} > 0,$$

that are equivalent to

$$\nu < \frac{r\nu^2\beta^2 + 4aeg\nu^2\beta K + e^2 g^2 r\beta^2 K^2}{4eg^2 m\nu K + 2egr\beta^2 K} \tag{3.37}$$

$$\beta > \frac{r\nu\beta + 2aeg\nu K}{egrK}, \quad \beta < \frac{mr\nu + a^2 e\nu K}{aerK}, \tag{3.38}$$

respectively. One positive root is found whenever the conditions

$$\Delta = \alpha_1^2 - 4\alpha_2\alpha_0 > 0, \quad \alpha_0 \alpha_2^{-1} < 0,$$

hold, which are equivalent to (3.36) and

$$\beta > \frac{mr\nu + a^2 e\nu K}{aerK}. \tag{3.39}$$

One explicit eigenvalue of the Jacobian at $P_{10}^{[ep\_ep]}$ is $J_{22}^{[ep\_ep]}$, which must be negative for stability, giving

$$s < \frac{b\nu}{\beta} + \kappa W_{10}^{[ep\_ep]} \tag{3.40}$$

given by one explicit eigenvalue of $J_{P_{10}}^{[ep\_ep]}$.

69

In addition,

$$\overline{J}_{P_{10}}^{[ep\_ep]} = \begin{pmatrix} -\frac{r}{K}X_{10}^{[ep\_ep]} & -aX_{10}^{[ep\_ep]} & -gX_{10}^{[ep\_ep]} \\ \frac{ae\nu}{\beta} + egW_{10}^{[ep\_ep]} & J_{33}^{[ep\_ep]} & egX_{10}^{[ep\_ep]} - \nu \\ 0 & \beta W_{10}^{[ep\_ep]} & 0 \end{pmatrix}$$

is negative definite, if we require the conditions $J_{33}^{[ep\_ep]} < 0$ and $J_{34}^{[ep\_ep]} < 0$, that is, respectively

$$a < \frac{2m\nu}{e\beta K} + \frac{a^2\nu}{r\beta} + (\frac{ag}{r} - \beta)W_{10}^{[ep\_ep]} \qquad (3.41)$$

and

$$\nu > egX_{10}^{[ep\_ep]}, \qquad (3.42)$$

because its principal minors of $-\overline{J}_{P_{10}}$ become

$$\frac{r}{K}X_{10}^{[ep\_ep]} > 0, \quad \frac{r}{K}J_{33}^{[ep\_ep]}X_{10} + aX_{10}^{[ep\_ep]}(\frac{ae\nu}{\beta} + egW_{10}^{[ep\_ep]}) > 0,$$

$$g\beta X_{10}^{[ep\_ep]}W_{10}^{[ep\_ep]}(\frac{ae\nu}{\beta} + egW_{10}^{[ep\_ep]}) + \frac{r\beta}{K}X_{10}^{[ep\_ep]}W_{10}^{[ep\_ep]}(\nu - egX_{10}^{[ep\_ep]}) > 0.$$

$\square$

Proposition 3.1.14. *The coexistence* $P_{11}^{[ep\_ep]} = (X_{11}^{[ep\_ep]}, Y_{11}^{[ep\_ep]}, Z_{11}^{[ep\_ep]}, W_{11}^{[ep\_ep]})$ *is unique if (3.43) and (3.46) hold and is conditionally stable for (3.47).*

Proof. For the coexistence $P_{11}^{[ep\_ep]}$ we have

$$Z_{11}^{[ep\_ep]} = \nu\beta^{-1}, \quad X_{11}^{[ep\_ep]} = K - \frac{a\nu K}{r\beta} - \frac{gK}{r}W_{11}^{[ep\_ep]},$$

$$Y_{11}^{[ep\_ep]} = H - \frac{b\nu H}{s\beta} - \frac{\kappa H}{s}W_{11}^{[ep\_ep]},$$

with $W_{11}^{[ep\_ep]}$ given by root of the quadratic function:

$$\Phi(W_{11}^{[ep\_ep]}) = \alpha_2(W_{11}^{[ep\_ep]})^2 + \alpha_1 W_{11}^{[ep\_ep]} + \alpha_0,$$

with

$$\alpha_2 = -\frac{eg^2K}{r} - \frac{e\kappa^2H}{s}, \quad \alpha_1 = e\kappa H + egK - \nu - \frac{2be\nu\kappa H}{s\beta} - \frac{2aeg\nu K}{r\beta},$$

$$\alpha_0 = \frac{be\nu H}{\beta} + \frac{ae\nu K}{\beta} - \frac{m\nu^2}{\beta^2} - \frac{a^2e\nu^2K}{r\beta^2} - \frac{b^2e\nu^2H}{s\beta^2}.$$

The equilibrium $P_{11}^{[ep\_ep]}$ is feasible if $X_{11}^{[ep\_ep]} \geq 0$ and $Y_{11}^{[ep\_ep]} \geq 0$, i.e. for

$$r \geq \frac{a\nu}{\beta} + gW_{11}^{[ep\_ep]}, \quad s \geq \frac{b\nu}{\beta} + \kappa W_{11}^{[ep\_ep]} \qquad (3.43)$$

respectively, and if $W_{11}^{[ep\text{-}ep]} \geq 0$. There are two positive roots if

$$\Delta = \alpha_1^2 - 4\alpha_2\alpha_0 > 0, \quad -\alpha_1\alpha_2^{-1} > 0, \quad \alpha_0\alpha_2^{-1} > 0,$$

that are equivalent to

$$e^2 rs\beta^2\kappa^2 H^2 + 8abe^2 g\nu^2\kappa KH + 4ber\nu^2\kappa\beta H + 4ae^2 r\nu\kappa^2\beta KH \qquad (3.44)$$
$$+4be^2 g^2 s\nu\beta KH + 2e^2 grs\kappa\beta^2 KH + 4aegs\nu^2\beta K + e^2 g^2 rs\beta^2 K$$
$$+rs\nu^2\beta^2 > 4a^2 e^2\nu^2\kappa^2 KH + 4b^2 e^2 g^2\nu^2 KH + 4be^2 gr\nu\kappa\beta KH$$
$$+4emr\nu^2\kappa^2 H + 4ae^2 gs\nu\kappa\beta KH + 2ers\nu\kappa\beta^2 H + 4eg^2 ms\nu^2 K + 2egrs\nu\beta^2 K,$$

$$\nu < \frac{ers\beta\kappa H + egrs\beta K}{2ber\kappa H + rs\beta + 2aegsK}, \quad \beta < \frac{b^2 er\nu H + mrs\nu + a^2 es\nu K}{bersH + aersK}, \quad (3.45)$$

respectively. For one positive root the conditions are

$$\Delta = \alpha_1^2 - 4\alpha_2\alpha_0 > 0, \quad \alpha_0\alpha_2^{-1} < 0,$$

or, explicitly, (3.44) and

$$\beta > \frac{b^2 er\nu H + mrs\nu + a^2 es\nu K}{bersH + aersK}. \qquad (3.46)$$

In addition, $J_{P_{11}}^{[ep\text{-}ep]}$ is negative definite if we require the condition $J_{34}^{[ep\text{-}ep]} < 0$ which explicitly becomes

$$egX_{11}^{[ep\text{-}ep]} + e\kappa Y_{11}^{[ep\text{-}ep]} < \nu. \qquad (3.47)$$

Indeed, the Jacobian of $P_{11}^{[ep\text{-}ep]}$ simplifies to

$$J_{P_{11}}^{[ep\text{-}ep]} = \begin{pmatrix} -\frac{r}{K}X_{11}^{[ep\text{-}ep]} & 0 & -aX_{11}^{[sp\text{-}ep]} & -gX_{11}^{[ep\text{-}ep]} \\ 0 & -\frac{s}{H}Y_{11}^{[ep\text{-}ep]} & -bY_{11}^{[ep\text{-}ep]} & -\kappa Y_{11}^{[ep\text{-}ep]} \\ J_{31}^{[ep\text{-}ep]} & J_{32}^{[ep\text{-}ep]} & -\frac{m\nu}{\beta} & J_{34}^{[ep\text{-}ep]} \\ 0 & 0 & \beta W_{11}^{[ep\text{-}ep]} & 0 \end{pmatrix},$$

with

$$J_{31}^{[ep\text{-}ep]} = \frac{ae\nu}{\beta} + egW_{11}^{[ep\text{-}ep]}, \quad J_{32}^{[ep\text{-}ep]} = \frac{be\nu}{\beta} + e\kappa W_{11}^{[ep\text{-}ep]},$$
$$J_{34}^{[ep\text{-}ep]} = egX_{11}^{[ep\text{-}ep]} + e\kappa Y_{11}^{[ep\text{-}ep]} - \nu.$$

The first three principal minors of $-J_{P_{11}}^{[ep\text{-}ep]}$ are all positive:

$$\frac{r}{K}X_{11}^{[ep\text{-}ep]} > 0, \quad \frac{rs}{HK}X_{11}^{[ep\text{-}ep]}Y_{11}^{[ep\text{-}ep]} > 0,$$

$$X_{11}^{[ep\text{-}ep]}Y_{11}^{[ep\text{-}ep]}\left[\left(\frac{mrs}{HK} + \frac{a^2 es}{H} + \frac{b^2 er}{K}\right)\frac{\nu}{\beta} + \left(\frac{aegs}{H} + \frac{ber\kappa}{K}\right)W_{11}^{[ep\text{-}ep]}\right] > 0,$$

and also the determinant is, as it simplifies to

$$\frac{egs}{H}\left(\frac{a\nu}{\beta} + gW_{11}^{[ep\text{-}ep]}\right) + \frac{e\kappa r}{K}\left(\frac{b\nu}{\beta} + \kappa W_{11}^{[ep\text{-}ep]}\right) - \frac{rs}{HK}J_{34}^{[ep\text{-}ep]} > 0$$

Thus, then feasible, $P_{11}^{[ep\text{-}ep]}$ is stable if (3.47) holds. $\qquad\square$

In the Table 3.2 we summarize the behaviour of the equilibria of model (3.2).

Table 3.2: Behaviour and conditions of feasibility and stability of equilibria for the model (3.2).

Equilibria	Admissibility	Stability
$P_1^{[ep\text{-}ep]}$	always	unstable
$P_2^{[ep\text{-}ep]}$	always	unstable
$P_3^{[ep\text{-}ep]}$	always	unstable
$P_4^{[ep\text{-}ep]}$	always	unstable
$P_5^{[ep\text{-}ep]}$	unfeasible	
$P_6^{[ep\text{-}ep]}$	always	(3.24)
$P_7^{[ep\text{-}ep]}$	always	(3.25)
$P_8^{[ep\text{-}ep]}$	(3.26), (3.27)	(3.28)
$P_9^{[ep\text{-}ep]}$	(3.29), (3.30), (3.31) - 2 positive roots	(3.33), (3.34), (3.35)
	(3.29), (3.30), (3.32) - 1 positive root	
$P_{10}^{[ep\text{-}ep]}$	(3.36), (3.37), (3.38) - 2 positive roots	(3.40), (3.41), (3.42)
	(3.36), (3.37), (3.39) - 1 positive root	
$P_{11}^{[ep\text{-}ep]}$	(3.43), (3.44), (3.45) - 2 positive roots	(3.47)
	(3.43), (3.44), (3.46) - 1 positive root	

3.1.3 Theoretical results for bifurcations of the models (3.1) and (3.2)

The bifurcations presented in this section were found from the conditions of feasibility and stability of equilibria of the systems (3.1) and (3.2). These conditions are summarized in Tables 3.1 and 3.2. We do not claim that the bifurcations found are exhaustive.

To study the local bifurcations of the equilibria of the models (3.1) and (3.2) we use Sotomayor theorem [70].

Proposition 3.1.15. *Consider the continuously differentiable system* (3.1), *then:*

(i) *There is a transcritical bifurcation between equilibria* $P_3^{[ep\_hp]}$ *and* $P_4^{[ep\_hp]}$ *when* r *passes through the critical value* $r^\dagger = aL$.

(ii) *There is a transcritical bifurcation between equilibria* $P_3^{[ep\_hp]}$ *and* $P_5^{[ep\_hp]}$ *when* ν *passes through the critical value* $\nu^\dagger = \beta L$.

Proof.

(i) The equilibrium point $P_3^{[ep\_hp]}$ coincides with the equilibrium $P_4^{[ep\_hp]}$ at the parametric threshold $r^\dagger = aL$, compare the first stability condition (3.12) of $P_3^{[ep\_hp]}$ and the feasibility condition (3.13) of $P_4^{[ep\_hp]}$.

The Jacobian matrix of the system (3.1) evaluated at $P_3^{[ep\_hp]}$ and at the parametric threshold $r^\dagger = aL$, becomes

$$J_{P_3}^{[ep\_hp]}(r^\dagger) = \begin{pmatrix} 0 & 0 & 0 \\ aeL & -u & -u - \beta L \\ 0 & 0 & -\nu + \beta L \end{pmatrix}$$

and its right and left eigenvectors, corresponding to zero eigenvalue, are given by $V_1 = \varphi_1(1, aeL/u, 0)^T$ and $Q_1 = \omega_1(1, 0, 0)^T$, where φ_1 and ω_1 are arbitrary nonzero real numbers. Differentiating with respect to r the right hand sides of the system (3.1), we find

$$f_r = \begin{pmatrix} X_3^{[ep\_hp]}(1 - X_3^{[ep\_hp]}/K) \\ 0 \\ 0 \end{pmatrix}.$$

Its Jacobian matrix is

$$Df_r = \begin{pmatrix} 1 - \frac{2}{K}X_3^{[ep\_hp]} & 0 & 0 \\ 0 & 0 & 0 \\ 0 & 0 & 0 \end{pmatrix}.$$

Calculating $D^2 f$ we find

$$D^2 f(P, \psi)(V, V)$$
$$= \begin{pmatrix} (\frac{\partial^2 f_1}{\partial X^2}\xi_1^2 + \frac{\partial^2 f_1}{\partial Z^2}\xi_2^2 + \frac{\partial^2 f_1}{\partial W^2}\xi_3^2 + 2\frac{\partial^2 f_1}{\partial X\partial Z}\xi_1\xi_2 + 2\frac{\partial^2 f_1}{\partial X\partial W}\xi_1\xi_3 + 2\frac{\partial^2 f_1}{\partial Z\partial W}\xi_2\xi_3 \\ \frac{\partial^2 f_2}{\partial X^2}\xi_1^2 + \frac{\partial^2 f_2}{\partial Z^2}\xi_2^2 + \frac{\partial^2 f_2}{\partial W^2}\xi_3^2 + 2\frac{\partial^2 f_2}{\partial X\partial Z}\xi_1\xi_2 + 2\frac{\partial^2 f_2}{\partial X\partial W}\xi_1\xi_3 + 2\frac{\partial^2 f_2}{\partial Z\partial W}\xi_2\xi_3 \\ \frac{\partial^2 f_3}{\partial X^2}\xi_1^2 + \frac{\partial^2 f_3}{\partial Z^2}\xi_2^2 + \frac{\partial^2 f_3}{\partial W^2}\xi_3^2 + 2\frac{\partial^2 f_3}{\partial X\partial Z}\xi_1\xi_2 + 2\frac{\partial^2 f_3}{\partial X\partial W}\xi_1\xi_3 + 2\frac{\partial^2 f_3}{\partial Z\partial W}\xi_2\xi_3 \end{pmatrix},$$

73

where $P = (X, Z, W)^T$, while the components of $f = (f_1, f_2, f_3)^T$ are given by the right hand sides of (3.1), ψ represents the parametric thresold and ξ_1, ξ_2, ξ_3 are the components of the eigenvector $V = (\xi_1, \xi_2, \xi_3)^T$ of the variations in X, Z and W.

We can thus verify the following three conditions

$$Q_1^T f_r(P_3^{[ep\_hp]}, r^\dagger) = 0,$$
$$Q_1^T [Df_r(P_3^{[ep\_hp]}, r^\dagger)V_1] = \varphi_1\omega_1 \neq 0$$
$$Q_1^T [D^2 f(P_3^{[ep\_hp]}, r^\dagger)(V_1, V_1)] = -\omega_1\varphi_1^2 \left(\frac{2aL}{K} + a^2 eL\right) \neq 0.$$

(ii) When the equilibrium point $P_3^{[ep\_hp]}$ coincides with the equilibrium $P_5^{[ep\_hp]}$ at the threshold $\nu^\dagger = \beta L$ (compare the second stability condition (3.12) of $P_3^{[ep\_hp]}$ and the feasibility condition (3.15) of equilibrium $P_5^{[ep\_hp]}$), the Jacobian matrix of the system (3.1) evaluated at $P_3^{[ep\_hp]}$ and at the parametric threshold $\nu^\dagger$, becomes

$$J_{P_3}^{[ep\_hp]}(\nu^\dagger) = \begin{pmatrix} r - aL & 0 & 0 \\ aeL & -u & -u - \beta L \\ 0 & 0 & 0 \end{pmatrix}.$$

Its right and left eigenvectors, corresponding to the zero eigenvalue, are given by $V_2 = \varphi_2(0, 1, -u/(u + \beta L))^T$ and $Q_2 = \omega_2(0, 0, 1)^T$, where φ_2 and ω_2 are any nonzero real numbers. Differentiating with respect to $\nu^\dagger$ the right hand sides of (3.1), we find

$$f_\nu = \begin{pmatrix} 0 \\ 0 \\ -W_3^{[ep\_hp]} \end{pmatrix},$$

and calculating its Jacobian matrix, we get

$$Df_\nu = \begin{pmatrix} 0 & 0 & 0 \\ 0 & 0 & 0 \\ 0 & 0 & -1 \end{pmatrix}.$$

From $D^2 f$ we can finally verify the following three conditions

$$Q_2^T f_\nu(P_3^{[ep\_hp]}, \nu^\dagger) = 0,$$
$$Q_2^T [Df_\nu(P_3^{[ep\_hp]}, \nu^\dagger)V_2] = \varphi_2\omega_2 \frac{u}{u + \beta L} \neq 0$$
$$Q_2^T [D^2 f(P_3^{[ep\_hp]}, \nu^\dagger)(V_2, V_2)] = -\omega_2\varphi_2^2 \left(\frac{2u\beta}{u + \beta L}\right) \neq 0.$$

Hence all the conditons for transcritical bifurcation are satisfied. □

Proposition 3.1.16. *Consider the continuously differentiable system of equations (3.2), then:*

(i) *There is a transcritical bifurcation between equilibria $P_8^{[ep\text{-}ep]}$ and $P_6^{[ep\text{-}ep]}$ when b crosses the critical value $b^\dagger = (mrs + a^2 esK)/aerK$.*

(ii) *There is a transcritical bifurcation between equilibria $P_8^{[ep\text{-}ep]}$ and $P_7^{[ep\text{-}ep]}$ when a passes through the critical value $a^\dagger = (mrs + b^2 erH)/besH$.*

Proof.

(i) When the equilibria $P_8^{[ep\text{-}ep]}$ and $P_6^{[ep\text{-}ep]}$ coincide at the parametric threshold $b^\dagger = (mrs + a^2 esK)/aerK$ (compare the second condition condition of (3.24) and the condition (3.27)), the Jacobian of the system (3.1) evaluated at $P_8^{[ep\text{-}ep]}$ and at the parametric threshold $b^\dagger$, is

$$J_{P_8}^{[ep\text{-}ep]}(b^\dagger) = \begin{pmatrix} -\frac{mr^2}{mr+a^2eK} & 0 & -\frac{amrK}{mr+a^2eK} & -\frac{gmrK}{mr+a^2eK} \\ 0 & 0 & 0 & 0 \\ \frac{a^2e^2rK}{mr+a^2eK} & es & -\frac{aemrK}{mr+a^2eK} & \frac{egmrK-aer\beta K}{mr+a^2eK} \\ 0 & 0 & 0 & \frac{-mr\nu-a^2e\nu K+aer\beta K}{mr+a^2eK} \end{pmatrix}$$

and its right and left eigenvectors, corresponding to the zero eigenvalue, are given by $V_3 = \varphi_3(1, -r/s, -r/(aK), 0)^T$ and $Q_3 = \omega_3(0, 1, 0, 0)^T$, where φ_3 and ω_3 are any nonzero real numbers. Differentiating partially the right hand sides of the system equations (3.2) with respect to b, we find

$$f_b = \begin{pmatrix} 0 \\ -Y_8^{[ep\text{-}ep]} Z_8^{[ep\text{-}ep]} \\ eY_8^{[ep\text{-}ep]} Z_8^{[ep\text{-}ep]} \\ 0 \end{pmatrix},$$

and calculating its Jacobian matrix, we get

$$Df_b = \begin{pmatrix} 0 & 0 & 0 & 0 \\ 0 & -Z_8^{[ep\text{-}ep]} & -Y_8^{[ep\text{-}ep]} & 0 \\ 0 & eZ_8^{[ep\text{-}ep]} & eZ_8^{[ep\text{-}ep]} & 0 \\ 0 & 0 & 0 & 0 \end{pmatrix}.$$

From the calculation of D^2f the following three conditions are verified:

$$Q_3{}^T f_b(P_8^{[ep\text{-}ep]}, b^\dagger) = 0,$$
$$Q_3{}^T [Df_b(P_8^{[ep\text{-}ep]}, b^\dagger)V_3] = \varphi_3\omega_3\rho \neq 0,$$
$$Q_3^T [D^2 f_b(P_8^{[ep\text{-}ep]}, b^\dagger)(V_3, V_3)] = -2\omega_3\varphi_3{}^2(\frac{mr^2H + a^2erHK + a^2er^2K}{a^2esHK}) \neq 0,$$

75

3 Comparing predator-prey models with hidden and explicit resources with a transmissible disease in the predator species

Since the feasibility condition of the $P_8^{[ep\_ep]}$ for $Y_8^{[ep\_ep]}$ is given by (3.27), and

$$\rho = \frac{r(a^2 esHK - aberHK + mrsH)}{aK} + \frac{r(arrK + berH)}{a^2 esK + b^2 erH + mrs},$$

we have $\frac{r(a^2 esHK - aberHK + mrsH)}{aK} \geq 0$ and thus $\rho \neq 0$.

(ii) When the equilibrium point $P_8^{[ep\_ep]} = P_7^{[ep\_ep]}$ at the threshold $a^\dagger = (mrs + b^2 erH)/besH$ (compare the second condition of (3.25) and the condition (3.26)), the Jacobian of (3.2) evaluated at $P_8^{[ep\_ep]}$ and at the parametric threshold $a^\dagger$, is

$$J_{P_8}^{[ep\_ep]}(a^\dagger) = \begin{pmatrix} 0 & 0 & 0 & 0 \\ 0 & -\frac{ms^2}{ms+b^2 eH} & -\frac{bmsH}{ms+b^2 eH} & 0 \\ er & \frac{b^2 e^2 sH}{ms+b^2 eH} & -\frac{bemsH}{ms+b^2 eH} & \frac{(em\kappa - eb\beta)sH}{ms+b^2 eH} \\ 0 & 0 & 0 & \frac{-b^2 e\nu H + bes\beta H - ms\nu}{ms+b^2 eH} \end{pmatrix}$$

and its right and left eigenvectors, corresponding to the zero eigenvalue, are given by $V_4 = \varphi_4(1, -r/s, r/(bH), 0)^T$ and $Q_4 = \omega_4(1, 0, 0, 0)^T$, where φ_4 and ω_4 are any nonzero real numbers. Differentiating partially with respect to $a^\dagger$ the right hand sides of (3.2), we find

$$f_a = \begin{pmatrix} -X_8^{[ep\_ep]} Z_8^{[ep\_ep]} \\ 0 \\ eX_8^{[ep\_ep]} Z_8^{[ep\_ep]} \\ 0 \end{pmatrix},$$

and calculating its Jacobian, we get

$$Df_a = \begin{pmatrix} -Z_8^{[ep\_ep]} & 0 & 0 & 0 \\ 0 & 0 & 0 & 0 \\ eZ_8^{[ep\_ep]} & 0 & eX_8^{[ep\_ep]} & 0 \\ 0 & 0 & 0 & 0 \end{pmatrix}.$$

Evaluation of $D^2 f$ verifies the following three conditions

$$Q_4^T f_a(P_8^{[ep\_ep]}, a^\dagger) = 0,$$

$$Q_4^T[Df_a(P_8^{[ep\_ep]}, a^\dagger)V_4] = -\varphi_4\omega_4\frac{besH}{ms+b^2 eH} \neq 0$$

$$Q_4^T[D^2 f_a(P_8^{[ep\_ep]}, a^\dagger)(V_4, V_4)] = -2\omega_4\varphi_4{}^2\left(\frac{b^2 ersH^2 + b^2 er^2 K + mr^2 sK}{b^2 esH^2 K}\right) \neq 0.$$

Hence all the conditons for a transcritical bifurcation are satisfied. The computation of $D^2 f(P, \psi)(V, V)$ of the (3.2) is analogous to the formula for the model (3.1). $\qquad\square$

Figure 3.1: a) Transcritical bifurcation between $P_3^{[ep\_hp]}$ and $P_5^{[ep\_hp]}$. The equilibrium $P_5^{[ep\_hp]}$ is stable for $0.1 < \nu < 1.6$ and $P_3^{[ep\_hp]}$ is stable for $\nu > 1.6$. The vertical line corresponds to the transcritical bifurcation threshold $\nu^\dagger = 1.6$ between the equilibria. b) Transcritical bifurcation between $P_5^{[ep\_hp]}$ and $P_6^{[ep\_hp]}$. The equilibrium $P_6^{[ep\_hp]}$ is stable for $0.1 < \nu < 0.4009$ and $P_5^{[ep\_hp]}$ is stable for $\nu > 0.4009$. The vertical line corresponds to the transcritical bifurcation threshold $\nu^\dagger = 0.4009$. The parameter values for (a) and (b) are $r = u = 1$, $L = 2$, $K = 10$, $e = 0.75$, $g = 0.56$, $a = 1.75$. For (a) $\beta = 0.8$ and (b) $\beta = 1$.

3.1.4 Numerical results for bifurcations of the models (3.1) and (3.2)

In Section 3.1.3 we performed theoretical analysis for transcritical bifurcation of models (3.1) and (3.2). In this Section, we illustrate these transcritical bifurcations and further investigate the possibilities for transcritical bifurcations about other equilibria of the systems by means of numerical simulations, by suitably adapting the standard ode45 Matlab routine for our purposes.

•Numerical results for model (3.1)

Here, we performed the investigation for transcritical bifurcations in terms of the bifurcation parameters ν and r. Considering ν as bifurcation parameter we find transcritical bifurcations between the equilibria: $P_3^{[ep\_hp]}$ and $P_5^{[ep\_hp]}$ for $\nu^\dagger = \beta L = 1.6$ as well as between $P_5^{[ep\_hp]}$ and $P_6^{[ep\_hp]}$ for $\nu^\dagger = \frac{\beta(ur + r\beta L - guL)}{au + a\beta L - gu} = 0.4009$, see Figure 3.1 frames (a) and (b), respectively.

The frames (a) and (b) of Figure 3.2 illustrate the transcritical bifurcation between $P_3^{[ep\_hp]}$ and $P_4^{[ep\_hp]}$ taking r as a bifurcation parameter, with threshold $r^\dagger = aL = 0.5$ and between $P_6^{[ep\_hp]}$ and $P_4^{[ep\_hp]}$ for the threshold $\nu^\dagger = \frac{\beta(urL + aerK)}{ur + a^2 eKL} = 0.9747$, respectively.

Table 3.3 presents a summary of all bifurcations results in our numerical simulations.

•Numerical results for model (3.2)

Here, we take β, a and b as bifurcation parameters in the model (3.2).
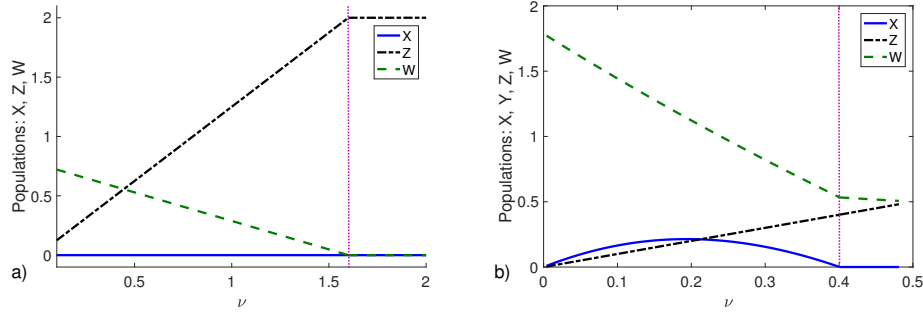
77
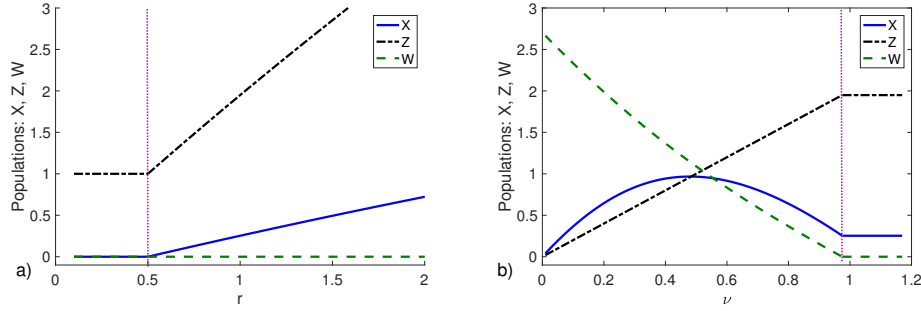
Figure 3.2: a) Transcritical bifurcation between $P_3^{[ep\_hp]}$ and $P_4^{[ep\_hp]}$. The equilibrium $P_3^{[ep\_hp]}$ is stable for $0.1 < r < 0.5$ and $P_4^{[ep\_hp]}$ is stable for $r > 0.5$. The vertical line corresponds to the transcritical bifurcation threshold $r^\dagger = 0.5$ with $\nu = 0.9747$. b) Transcritical bifurcation between $P_6^{[ep\_hp]}$ and $P_4^{[ep\_hp]}$. The equilibrium $P_6^{[ep\_hp]}$ is stable for $0.1 < \nu < 0.9747$ and $P_4^{[ep\_hp]}$ is stable for $\nu > 0.9747$. The vertical line denotes the transcritical bifurcation threshold $\nu^\dagger = 0.9747$ between the equilibria and $r = 1$. The parameter values for (a) and (b) are: $L = 1$, $K = 10$, $e = 0.75$, $a = \beta = 0.5$, $u = 0.1$, $g = 0.37$.

Table 3.3: Behaviour of equilibria of the model (3.1) considering ν and r as variation parameters. Notation: tb=transcritical bifurcation

Behaviour of the model (3.1)	Equilibria involved	Parameter threshold
tb	$P_3^{[ep\_hp]} - P_5^{[ep\_hp]}$	$\nu^\dagger = \beta L = 1.6$
tb	$P_5^{[ep\_hp]} - P_6^{[ep\_hp]}$	$\nu^\dagger = \frac{\beta(ur + r\beta L - guL)}{au + a\beta L - gu} = 0.4009$
tb	$P_3^{[ep\_hp]} - P_4^{[ep\_hp]}$	$r^\dagger = aL = 0.5$
tb	$P_4^{[ep\_hp]} - P_6^{[ep\_hp]}$	$\nu^\dagger = \frac{\beta(urL + aerKL)}{ur + a^2 eKL} = 0.9747$
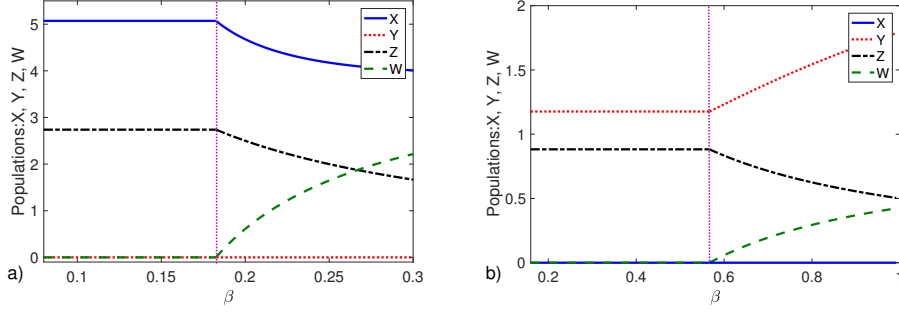
Figure 3.3: The common parameter values for both (a) and (b) are: $r = 1$, $K = 10$, $e = 0.75$, $\nu = 0.5$, $g = 0.937$, $m = s = b = 0.25$, $H = 10$, $\kappa = 0.187$. a) Transcritical bifurcation between $P_6^{[ep\_ep]}$ and $P_{10}^{[ep\_ep]}$. The equilibrium $P_6^{[ep\_ep]}$ is stable for $0.1 < \beta < 0.1826$ and $P_{10}^{[ep\_ep]}$ is stable for $\beta > 0.1826$. The vertical line corresponds at the transcritical bifurcation threshold $\beta^\dagger = 0.1826$ between the equilibria. Here we have $a = 0.18$. b) Transcritical bifurcation between $P_7^{[ep\_hp]}$ and $P_9^{[ep\_ep]}$. The equilibrium $P_7^{[ep\_ep]}$ is obtained for $0.1 < \beta < 0.5667$ while $P_9^{[ep\_ep]}$ is found for $\beta > 0.5667$. The vertical line corresponds at the transcritical bifurcation threshold $\beta^\dagger = 0.5667$ between the equilibria. In this case we take $a = 1.25$.

Figures 3.3, 3.4, 3.5 illustrate all the possibilities that we have found. All the different behaviours of the system are summarized in Table 3.4.

Note that considering β as bifurcation parameter the system has several possible different behaviours.

Figure 3.3 (a) illustrates the transcritical bifurcation between $P_6^{[ep\_ep]}$ and $P_{10}^{[ep\_ep]}$ and (b) illustrates a transcritical bifurcation between $P_7^{[ep\_ep]}$ and $P_9^{[ep\_ep]}$ for

$$\beta^\dagger = \frac{\nu(mr + a^2 eK)}{aerK} = 0.1826, \qquad \beta^\dagger = \frac{ms\nu + b^2 e\nu H}{besH} = 0.5667,$$

respectively.

Figure 3.4 illustrates the transcritical bifurcation between $P_8^{[ep\_ep]}$ and $P_{11}^{[ep\_ep]}$ with critical threshold

$$\beta^\dagger = \frac{\nu(a^2 esK + b^2 erH + mrs)}{aersK + bersH} = 0.3884.$$

Figure 3.5 (a), (b) illustrates a numerical simulations when we consider b and a as a bifurcation parameters. There is a transcritical bifurcation between $P_6^{[ep\_ep]}$ and $P_8^{[ep\_ep]}$ and another one between $P_7^{[ep\_ep]}$ and $P_8^{[ep\_ep]}$ for

$$b^\dagger = \frac{mrs + a^2 esK}{aerK} = 1.5, \qquad a^\dagger = \frac{mrs + b^2 erH}{besH} = 2.17,$$

respectively. .

79
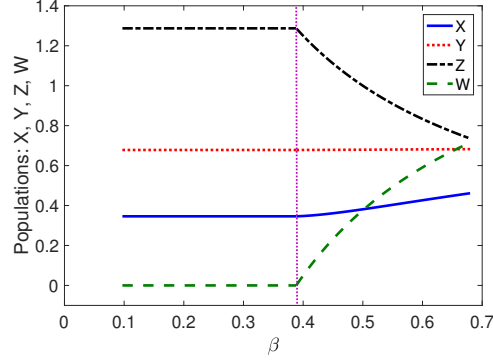
Figure 3.4: Transcritical bifurcation between $P_8^{[ep\_ep]}$ and $P_{11}^{[ep\_ep]}$. The equilibrium $P_8^{[ep\_ep]}$ is stable for $0.1 < \beta < 0.3884$ while $P_{11}^{[ep\_ep]}$ is obtained for $0.3884 < \beta < 0.67$. The vertical line corresponds to the transcritical bifurcation threshold $\beta^\dagger = 0.3884$. The remaining parameter values are: $r = 1$, $K = 10$, $e = 0.75$, $\nu = 0.5$, $g = 0.5625$, $m = b = 0.25$, $\kappa = 0.187$, $a = 0.75$, $s = H = 1$.
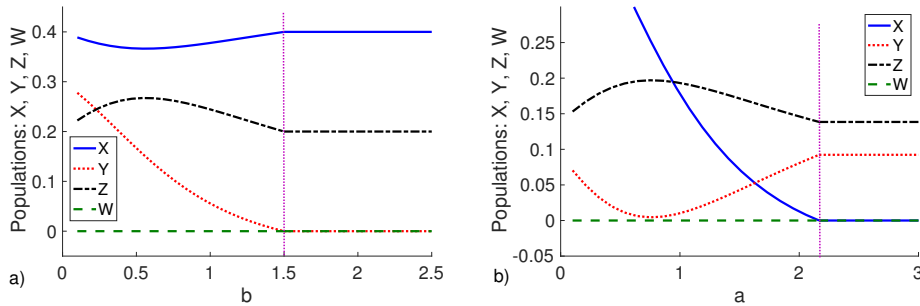
Figure 3.5: a) Transcritical bifurcation between $P_8^{[ep\_ep]}$ and $P_6^{[ep\_ep]}$ for the parameter values: $r = K = a = e = m = 0.5$, $g = 0.8$, $s = H = \beta = 0.3$ and $\nu = \kappa = 0.9$. Initial conditions $X_0 = Z_0 = W_0 = 0.01$. The equibrium $P_8^{[ep\_ep]}$ is found for $0.1 \leq b < 1.5$ and $P_6^{[ep\_ep]}$ arises for $b > 1.5$. The vertical line corresponds to the transcritical bifurcation threshold $b^\dagger = 1.5$. b) Transcritical bifurcation between $P_8^{[ep\_ep]}$ and $P_7^{[ep\_ep]}$ for the parameter values: $K = e = m = 0.5$, $g = 0.8$, $r = s = H = \beta = 0.3$, $b = 1.5$ and $\nu = \kappa = 0.9$. Initial conditions and populations are the same. The equibrium $P_8^{[ep\_ep]}$ is found for $0.1 \leq a < 2.17$ while $P_7^{[ep\_ep]}$ exists in the range $a > 2.17$. The vertical line corresponds to the transcritical bifurcation threshold $a^\dagger = 2.17$.

Table 3.4: Behaviour of equilibria of the model (3.2) considering β, b and s as bifurcation parameters. Notation: tb=transcritical bifurcation

Behaviour of the model (3.2)	Equilibria involved	Parameter threshold
tb	$P_7^{[ep\_ep]} - P_9^{[ep\_ep]}$	$\beta^\dagger = \frac{ms\nu + b^2 e\nu H}{besH} = 0.5667$
tb	$P_6^{[ep\_ep]} - P_{10}^{[ep\_ep]}$	$\beta^\dagger = \frac{\nu(a^2 eK + mr)}{aerK} = 0.1826$
tb	$P_{11}^{[ep\_ep]} - P_8^{[ep\_ep]}$	$\beta^\dagger = \frac{a^2 e\nu sK + b^2 er\nu H + mrs\nu}{aersK + bersH} = 0.3884$
tb	$P_6^{[ep\_ep]} - P_8^{[ep\_ep]}$	$b^\dagger = \frac{mrs + b^2 erH}{aerK} = 1.5$
tb	$P_7^{[ep\_ep]} - P_8^{[ep\_ep]}$	$a^\dagger = \frac{mrs + b^2 erH}{besH} = 2.17$

3.2 Comparing analytical findings for the models (3.1) and (3.2)

In this Section, we compare the behaviour of the models (3.1) and (3.2), summarizing in Table 3.5 all the possibilities.

As we can see in Table 3.5, both ecosystems cannot completely disappear. Note that to the origin $P_1^{[ep\_hp]}$ in model (3.1) corresponds also the point $P_3^{[ep\_ep]}$ of model (3.2), in which only the alternative prey thrives. The prey-only equilibria $P_2^{[ep\_hp]}$ and $P_2^{[ep\_ep]}$, $P_3^{[ep\_ep]}$ and $P_4^{[ep\_ep]}$ are all unstable.

The healthy-predator-only equilibrium $P_3^{[ep\_hp]}$ has its counterpart in the point $P_7^{[ep\_ep]}$. The equilibrium $P_3^{[ep\_hp]}$ can be achieved stably in the simpler model, provided (3.12) is satisfied and $P_7^{[ep\_ep]}$ can also be stably attained, if the stability condition (3.25) holds.

The disease-free equilibrium point in model (3.1) is $P_4^{[ep\_hp]}$. Three points of model (3.2) could be related to it, namely $P_6^{[ep\_ep]}$, $P_7^{[ep\_ep]}$ and $P_8^{[ep\_ep]}$, differing in that either the extra source or the main prey are absent, or that both preys thrive, together with the healthy predators.

The main-prey-free point $P_5^{[ep\_hp]}$ in model (3.1) cannot be compared with the equilibrium $P_5^{[ep\_ep]}$ of model (3.2) because $P_5^{[ep\_ep]}$ does not contain the alternative resource and the predador can only survive if the alternative prey thrives in the absence of the main prey. Its counterpart is thus just the equilibrium $P_9^{[ep\_ep]}$.

Finally, the coexistence equilibria in both models are conditionally stable. Table 3.5, shows that the $P_6^{[ep\_hp]}$ in model (3.1) can be related with equilibria $P_{10}^{[ep\_ep]}$ and $P_{11}^{[ep\_ep]}$ of model (3.2). Thus, for both models there is the possibility of the survival of all predators and preys.

Table 3.5: Possibilities of comparison between equilibria of systems (3.1) and (3.2) that have the same biological behaviour. Notation: u=unstable, s=stable, cs=conditionally stable, uf=unstable if feasible, sf=stable if feasible. Note that the second and third components of system (3.1) correspond to the third and fourth components of system (3.2), respectively, while in this latter system the second one represents the explicit resource that was hidden in the model (3.1).

Equilibrium - model (3.1)	Equilibrium - model (3.2)	Interpretation
$P_1^{[ep\_hp]} = (0,0,0)$ (u)	$P_1^{[ep\_ep]} = (0,0,0,0)$ (u)	ecosystem collapse
	$P_3^{[ep\_ep]} = (0,\bullet,0,0)$ (u)	
$P_2^{[ep\_hp]} = (\bullet,0,0)$ (u)	$P_2^{[ep\_ep]} = (\bullet,0,0,0)$ (u)	
	$P_3^{[ep\_ep]} = (0,\bullet,0,0)$ (u)	prey-only
	$P_4^{[ep\_ep]} = (\bullet,\bullet,0,0)$ (u)	
$P_3^{[ep\_hp]} = (0,\bullet,0)$ (cs)	$P_7^{[ep\_ep]} = (0,\bullet,\bullet,0)$(cs)	healthy-predator-only
$P_4^{[ep\_hp]} = (\bullet,\bullet,0)$ (cs)	$P_6^{[ep\_ep]} = (\bullet,0,\bullet,0)$ (cs)	
	$P_7^{[ep\_ep]} = (0,\bullet,\bullet,0)$ (cs)	disease-free
	$P_8^{[ep\_ep]} = (\bullet,\bullet,\bullet,0)$ (cs)	
$P_5^{[ep\_hp]} = (0,\bullet,\bullet)$ (cs)	$P_5^{[ep\_ep]} = (0,0,\bullet,\bullet)$ (u)	main-prey-free
	$P_9^{[ep\_ep]} = (0,\bullet,\bullet,\bullet)$ (cs)	
$P_6^{[ep\_hp]} = (\bullet,\bullet,\bullet)$ (cs)	$P_{10}^{[ep\_ep]} = (\bullet,0,\bullet,\bullet)$ (cs)	coexistence
	$P_{11}^{[ep\_ep]} = (\bullet,\bullet,\bullet,\bullet)$ (cs)	

3.3 Results

In this Chapter, we have compared the dynamics between two predator-prey models where a transmissible disease spreads among the predators. The alternative prey for the predator is implicit in the first model, but in the second one we have made it explicit.

The most important parameters determining the type of possible changes in the system behaviour, leading to transcritical bifurcations, are the growth rate r of the prey population X and the mortality of the infected predator ν. In the case where the mortality rate ν of the infected predator exceeds the infection rate β of healthy predator Z, the environment becomes infection-free due to the extinction of the infected predators W. However, two distinct scenarios arise: in the first one, if we the growth rate of the prey X is smaller than the predator efficiency Z in converting resource into new predators as well as its carrying capacity L (see Proposition 3.1.4), the resulting dynamics is composed only of healthy predators Z; their survival is guaranteed by the existence of an alternative resource. However, if the growth rate of the prey X exceeds the predation efficiency as well as the carrying capacity of the healthy predator Z, the main prey survives in the environment. This result is guaranteed by the existence of a transcritical bifurcation between the equilibria $P_3^{[ep\_hp]}$ and $P_4^{[ep\_hp]}$. Continuing along the same lines, the study of transcritical bifurcation between the equilibria $P_3^{[ep\_hp]}$ and $P_5^{[ep\_hp]}$ shows that if the mortality rate ν of the infected predator W is smaller than the infection rate β and the carrying capacity L of the healthy-predator, the ecosystem will be composed just of the populations of healthy-predators Z and infected-predators W; their survival is in this case guaranteed by the available alternative resource (see the feasibility and stability conditions (3.15) and (3.16)).

For the second model (3.2), where the alternative resource is explicit, the main parameters defining the system dynamics are the predation rates a and b on the main prey X and on the alternative prey Y as well as the infection rate β of the healthy predator Z, respectively. In an infection-free scenario, the analysis of the transcritical bifurcation between equilibria $P_6^{[ep\_ep]}$ and $P_8^{[ep\_ep]}$ indicates the predation rate b as an important factor to guarantee the survival of the predator, i.e. b determines if the predator will feed only on the main prey or on both main and alternative prey, see the second condition of (3.24) and (3.27). Similarly, the transcritical bifurcation between $P_7^{[ep\_ep]}$ and $P_8^{[ep\_ep]}$ indicates that the mortality a characterizes the predator survival only. The second condition of (3.25) shows that the healthy predator Z has only the alternative prey Y as source of food represented by the stable equilibrium point $P_7^{[ep\_ep]}$. But, when a transcritical bifurcation occurs with the equilibrium point $P_8^{[ep\_ep]}$ considering the same value of the bifurcation parameter a (see condition (3.26)), the healthy predator Z has two sources of food, i.e., the main prey X and the alternative prey Y. Thus, the predator thrive on both

resources.

Our numerical analysis indicates that the disease transmission rate β plays a fundamental role for obtaining an environment with persistent disease, see Section 3.1.4.

Table 3.6 illustrates the comparison between models with hidden and explicit prey for the predator, considering an environment with and without the possibility of a transmissible disease among the predators.

Table 3.6: Systems dynamics considering an environment with and without a transmissible disease among the predator population Z. The column representing the biological interpretation in the table refers to the equilibrium points obtained in both models (3.1) and (3.2) that are biologically equivalent.

Biological interpretation	Environment **with** disease transmission in predator Z	Environment **without** disease transmission in predator Z, [5]
ecosystem collapse	not possible	not possible
prey-only	not possible	not possible
healthy-predator-only	possible	possible
disease-free	possible	possible
main-prey-free/ predator-only	possible	possible
coexistence	possible	possible

There is no possibility of a scenario where in the ecoepidemic model (3.2), the infected predators thrive without the presence of the main and of the alternative prey because $P_5^{[ep\_ep]}$ is unstable. However, healthy and infected predators survive without the presence of the main prey in both systems (3.1) and (3.2). In this case, the alternative prey provides the food for predators in both models. This situation is represented by the main-prey-free equilibria $P_5^{[ep\_hp]}$ and $P_9^{[ep\_ep]}$.

The environment in which only the healthy predator Z survives in the absence of the main prey is possible in both scenarios, i.e., at the equilibria $P_3^{[ep\_hp]}$ and $P_7^{[ep\_ep]}$. The disease-free equilibrium points represented by $P_4^{[ep\_hp]}$ and $P_8^{[ep\_ep]}$ when represented in the same dynamics but without a transmissible disease among individuals Z, [5], clearly can represent the coexistence between X and Z populations. In this situation, investigated in [5], the same feasibility conditions for these equilibria hold. The coexistence also has the same behaviour in both environments, i.e. with and without a transmissible disease among the predator population Z.

CHAPTER 4

A MATHEMATICAL MODEL TO DESCRIBE THE BOVINE TUBERCULOSIS AMONG BUFFALOES AND LIONS IN THE KRUGER NATIONAL PARK

Bovine Tuberculosis (BT) is a threat to wildlife health. For instance, in the Kruger National Park in South Africa, at least 21 species of wild mammals were diagnosed [72, 62]. There are species that are "maintenance" hosts for BT and those that are considered "spillovers". The former are species in which the infection is endemic, without introduction from an external source. Indeed, the BT bacterium *M. bovis* has been found in African buffalo and possibly also in the Greater kudu (*Tragelaphus strepsiceros*) and in the lions. In view of their multiple interactions, variable susceptibility and the influence of environmental factors, [72], the presence of several susceptible hosts complicates the management and control of BT. Further, with diminishing habitats, there are increased wildlife-livestock-human interfaces and a growing threat of disease transmission through the species barrier. Indeed, the transmission of BT between herd individuals occurs most frequently by aerosol, [9]. However, predators contract the disease mostly by ingestion of infected tissues [61]. BT directly impacts animal productivity and fitness and can lead to a mortality rate increase.

Wild animals appear to be able to harbour mycobacteria for months or even years. As infection progresses, there is evidence that BT may decrease their reproductive and other fitness parameters, but it may not significantly affect them unless they experience other stressors, such as drought or concurrent

disease, suggesting that infected animals may remain in the population for prolonged periods [61, 62]. For instance, buffalo herds with a higher prevalence of BT had worse body condition in the dry season than those with lower BT prevalence. Consequently, affected buffalo might be more susceptible to predation by lions, [20]. In addition the loss of these prey animals may influence the predators. A simulation over 50 years of the the impact of BT on lions shows a scenario suggesting a serious threat to the species survival, with a possible 35%-75% decline with respect to the present population, [62].

To study the impact of BT on wild animals, we present a predator-prey model involving buffaloes and lions, both subject to the disease, which is horizontally as well as vertically transmitted. Because the wild buffalo congregates in huge herds, the border individuals are usually captured. Mathematically, this can be modeled via a square root response function, [3, 2, 83, 18]. Indeed since the total prey population P occupies a certain area A on the ground, the number of the individuals who are found at the border is proportional to the length of the perimeter of the patch A, which in turn is proportional to $\sqrt{P}$.

The chapter is organized as follows. In the next section, we formulate the model, show that trajectories are bounded and nondimensionalize it. The feasibility and stability analysis are performed in Section 4.3. Section 4.4 contains a study about the basic reproduction number $\mathcal{R}_0$ where we focus the discussion on conditions for disease eradication. Transcritical and Hopf bifurcations are investigated in Section 4.5. Section 4.6 shows that the predators mortality m is crucial for the feasibility and stability of the prey-only point E_1 and the disease-free equilibrium E_2, respectively. Endemicity of the disease is directly related to the value of $\mathcal{R}_0$ at both points. To investigate the behaviour of model (4.2) in relation to the parameters, we first separate the simulations in two specific cases, considering also the predation rate a. In the first case, E_1 is stable and E_2 is unstable; the ecosystem thus attains the prey-only equilibrium, if the predators mortality exceeds their hunting rate, i.e. $m > a$. Alternatively when the mortality falls below the hunting rate, but not too much, namely for $a/\sqrt{3} < m < a$, the disease-free point becomes feasible and E_1 is unstable. A final discussion concludes the chapter.

4.1   Model Formulation

We consider a model for species interactions, subject to a BT that can infect both the buffaloes and lions. Once infected, an animal remains infected for its life, so that the disease is of type SI. Infected prey $\widehat{I}$ become weak and are left behind the herd. Let further $\widehat{R}$ denote the susceptible prey population, $\widehat{F}$ and $\widehat{W}$ r the susceptible and infected predators, respectively. The prey have a highly socialized "herd behaviour", in that they live together wandering in search of pastures. They are generally followed in their wanderings by the predators. If the hunt is successful for the predator, generally the prey indi-

viduals residing on the boundary of herd are harmed. The model, accounting for all the possible population interactions described below, reads as follows:

$$
\begin{aligned}
\frac{d\widehat{R}}{d\tau} &= \tilde{r}\widehat{R} + \bar{r}\left(1 - \widehat{\alpha}\right)\widehat{I} - k\widehat{R}\left(\widehat{R} + \widehat{g}\widehat{I}\right) - \widehat{\lambda}\widehat{R}\widehat{I} - \widehat{cp}\sqrt{\widehat{R}}\widehat{W} - \widehat{a}\sqrt{\widehat{R}}\widehat{F} \quad (4.1) \\
&\quad - \widehat{\theta}\left(1 - \widehat{p}\right)\widehat{c}\sqrt{\widehat{R}}\widehat{W}, \\
\frac{d\widehat{I}}{d\tau} &= \bar{r}\widehat{\alpha}\widehat{I} + \widehat{I}\left(\widehat{\lambda}\widehat{R} - \widehat{b}\widehat{F} - \widehat{\mu} - \widehat{\ell W}\right) + \widehat{\theta}(1 - \widehat{p})\widehat{c}\sqrt{\widehat{R}}\widehat{W} - k\widehat{I}(\widehat{u}\widehat{R} + \widehat{q}\widehat{I}), \\
\frac{d\widehat{F}}{d\tau} &= \widehat{ae}\sqrt{\widehat{R}}\widehat{F} + (1 - \widehat{\sigma})\widehat{be}\widehat{I}\widehat{F} + (1 - \widehat{\gamma})\widehat{W}(\widehat{cep}\sqrt{\widehat{R}} + \widehat{\ell e}\widehat{I}) - \widehat{m}\widehat{F} - \widehat{\beta}\widehat{F}\widehat{W}, \\
\frac{d\widehat{W}}{d\tau} &= \widehat{W}\left(\widehat{\gamma}\widehat{cep}\sqrt{\widehat{R}} + \widehat{\gamma}\widehat{\ell e}\widehat{I} - \widehat{\nu}\right) + \widehat{\sigma}\widehat{be}\widehat{I}\widehat{F} + \widehat{\beta}\widehat{F}\widehat{W}.
\end{aligned}
$$

The first equation describes the dynamics of $\widehat{R}$ (susceptible prey). The term $\tilde{r}\widehat{R}$ expresses growth rate of $\widehat{R}$ due to their own reproduction and $\bar{r}(1 - \widehat{\alpha})\widehat{I}$ is the fraction of $\widehat{I}$ that are born healthy (vertical transmission). The term $k\widehat{R}\left(\widehat{R} + \widehat{g}\widehat{I}\right)$ is the mortality by intraspecific competition between $\widehat{R}$ individuals among themselves and with $\widehat{I}$ individuals. The term $\widehat{\lambda}\widehat{R}\widehat{I}$ represents the susceptible prey, that become infected (horizontal transmission). The term $\widehat{cp}\sqrt{\widehat{R}}\widehat{W}$ represents the prey individuals that are captured by infected predators and $\widehat{a}\sqrt{\widehat{R}}\widehat{F}$ is the capture rate of $\widehat{R}$ by $\widehat{F}$. Finally, $\widehat{\theta}\left(1 - \widehat{p}\right)\widehat{c}\sqrt{\widehat{R}}\widehat{W}$ are the new infections by an unsuccessful attack of infected predator $\widehat{W}$ on healthy prey $\widehat{R}$, and then latter gets disease. Note that, we have a fraction $(1 - \widehat{\theta})(1 - \widehat{p})$ of healthy prey that are not captured, but do not get the disease from predators.

The second equation describes the dynamics of $\widehat{I}$ (infected prey). The term $\bar{r}\widehat{\alpha}\widehat{I}$ is the fraction of the reproduction rate of $\widehat{I}$ that is born infected (possibility of vertical transmission), $\widehat{\lambda}\widehat{R}\widehat{I}$ represents the susceptibles prey, that become infected (horizontal transmission), $\widehat{b}\widehat{I}\widehat{F}$ is the predation of $\widehat{I}$ by $\widehat{F}$, $\widehat{\mu}\widehat{I}$ is the mortality of $\widehat{I}$ (disease-related) and $\widehat{\ell I}\widehat{W}$ is the predation of $\widehat{I}$ by $\widehat{W}$. Finally, $\widehat{\theta}\left(1 - \widehat{p}\right)\widehat{c}\sqrt{\widehat{R}}\widehat{W}$ are the new infections by an unsuccessful attack of infected predator $\widehat{W}$ on healthy prey $\widehat{R}$, and then latter gets disease and $k\widehat{I}(\widehat{u}\widehat{R} + \widehat{q}\widehat{I})$ is the mortality by intraspecific competition of $\widehat{I}$ among themselves and with $\widehat{R}$. Note that, in the model, infected prey do not benefit from the effects of herd behaviour.

The third equation describes the dynamics of $\widehat{F}$ (susceptible predator). The term $\widehat{ae}\sqrt{\widehat{R}}\widehat{F}$ expresses the increase of $\widehat{F}$ due to the consumption of $\widehat{R}$ on the boundary with conversion factor $0 < \widehat{e} < 1$. The term $(1 - \widehat{\sigma})\widehat{be}\widehat{I}\widehat{F}$ represents the growth rate of $\widehat{F}$ due to the consumption of $\widehat{I}$, that is, predators that consume infected prey but do not become infected. The term $(1 - \widehat{\gamma})\widehat{W}(\widehat{cep}\sqrt{\widehat{R}})$

87

expresses the fraction of the reproduction rate of $\widehat{W}$ that is born as a healthy predator due to the consumption $\widehat{R}$ on boundary. Besides that, $(1-\widehat{\gamma})\widehat{W}(\widehat{\ell e}\widehat{I})$ is the analogous term, but due to the consumption of infected prey $\widehat{I}$. Now, the term $\widehat{m}\widehat{F}$ is the mortality of $\widehat{F}$, $\widehat{\beta}\widehat{F}\widehat{W}$ represents the predator who moves from one class to another, that is, susceptibles become infected by contact with another infected predator $\widehat{W}$ (horizontal transmission).

The fourth equation describes the dynamics of $\widehat{W}$ (infected predator). The term $\widetilde{\gamma c e p}\sqrt{\widehat{R}}\widehat{W}$ represents the vertical transmission of $\widehat{W}$ in converting captured $\widehat{R}$ on boundary in infected predators $\widehat{W}$. The term $\widehat{\gamma}\widehat{\ell e}\widehat{I}\widehat{W}$ is the vertical transmission of $\widehat{W}$ due to the consumption of $\widehat{I}$, $\widehat{\nu}\widehat{W}$ is the mortality of $\widehat{W}$ (disease-related) and $\widehat{\sigma b e}\widehat{I}\widehat{F}$ is the fraction of healthy predators that gives birth to infected offspring by eating $\widehat{I}$ (vertical transmission). Finally, $\widehat{\beta}\widehat{F}\widehat{W}$ represents the predator who moves from one class to another, that is, susceptibles become infected by contact with another infected predator $\widehat{W}$ (horizontal transmission). All parameters are non-negative and listed in Table 4.1.

Following closely [83], the system's trajectories are confined within a compact set. For the total environment population $\varphi(\tau) = \widehat{R}(\tau) + \widehat{I}(\tau) + \widehat{F}(\tau) + \widehat{W}(\tau)$, summing equations (4.1),

$$\frac{d\varphi(\tau)}{d\tau} = \left(\tilde{r}\widehat{R} + \bar{r}\widehat{I}\right) - k\widehat{R}\left(\widehat{R} + \widehat{g}\widehat{I}\right) - k\widehat{I}\left(\widehat{u}\widehat{R} + \widehat{q}\widehat{I}\right) \\ + (\widehat{e} - 1)\left(\widetilde{cp}\sqrt{\widehat{R}}\widehat{W} + \widehat{a}\sqrt{\widehat{R}}\widehat{F} + \widetilde{\ell I}\widehat{W}\right) - \left(\widehat{\mu}\widehat{I} + \widehat{m}\widehat{F} + \widehat{\nu}\widehat{W}\right).$$

Using $(\widehat{e} - 1) \le 0$ we can drop the term that contains it, to get

$$\frac{d\varphi(\tau)}{d\tau} \le (\tilde{r}\widehat{R} + \bar{r}\widehat{I}) - k\widehat{R}(\widehat{R} + \widehat{g}\widehat{I}) - k\widehat{I}(\widehat{u}\widehat{R} + \widehat{q}\widehat{I}) - (\widehat{\mu}\widehat{I} + \widehat{m}\widehat{F} + \widehat{\nu}\widehat{W})$$

Letting M be the maximum value of the parabola $\Phi(\widehat{R} + \widehat{I}) = -k\eta_2(\widehat{R} + \widehat{I})^2 + (\eta_1 + \eta_3)(\widehat{R} + \widehat{I})$, with $\eta_1 = \max\{\tilde{r}, \bar{r}\}$, $\eta_2 = \min\{1, \widehat{g}, \widehat{u}, \widehat{q}\}$, $\eta_3 = \min\{\widehat{\mu}, \widehat{m}, \widehat{\nu}\}$, we find the estimate

$$\frac{d\varphi(\tau)}{d\tau} + \eta_3\varphi(\tau) \le \Phi(\widehat{R} + \widehat{I}) \le \bar{M} = \frac{(\eta_1 + \eta_3)^2}{4\eta_2 k},$$

from which we establish the boundedness result

$$\varphi(\tau) \le \frac{M}{\eta_3} + \varphi(0)(\widehat{e})^{-\eta_3\tau} \le \frac{M}{\eta_3} + \varphi(0) = \bar{M}$$

Note also that from below, the coordinate hyperplanes cannot be crossed toward negative values, although the system is not homogeneous. For instance, the first equation for $\widehat{R} = 0$ gives $\widehat{R}'(\tau) = \bar{r}(1 - \widehat{\alpha})\widehat{I} \ge 0$ because the parameters are nonnegative and $1 - \widehat{\alpha} \ge 0$.

Table 4.1: Parameters of model (4.1) and their biological meanings

Parameter	Biological meaning
$\tilde{r}$	Specific growth rate of healthy prey $\widehat{R}$
$\bar{r}$	Specific growth rate of infected prey I ($\bar{r} \leq \tilde{r}$)
$\widehat{\alpha}$	Non-dimensional parameter that represents the fraction of prey $\widehat{R}$ that born infected (vertical transmission)
$1 - \widehat{\alpha}$	Non-dimensional parameter that represents the fraction of prey $\widehat{R}$ that born no infected
k	Mortality of healthy prey $\widehat{R}$ due intraspecific competition ($k = \frac{r}{K}$)
K	Carrying capacity of prey $\widehat{R}$ in absence of predator
$\widehat{g}$	Parameter that regulates competition among infected prey $\widehat{I}$ with healthy prey $\widehat{R}$
$\widehat{\lambda}$	Infection rate in healty prey $\widehat{R}$ (horizontal transmission)
$\widehat{\theta}$	Probability that healthy prey $\widehat{R}$, not captured by infected predator $\widehat{W}$, becomes infected
$\widehat{p}$	Probability that represents the fraction of captured prey $\widehat{R}$
$1 - \widehat{p}$	Probability that represents the fraction of no captured prey $\widehat{R}$
$\widehat{a}$	Predation rate of healthy prey $\widehat{R}$ by healthy predator $\widehat{F}$
$\widehat{c}$	Predation rate of healthy prey $\widehat{R}$ by infected predator $\widehat{W}$
$\widehat{b}$	Predation rate of infected prey $\widehat{I}$ by healthy predator $\widehat{F}$
$\widehat{\mu}$	Mortality rate of infected prey $\widehat{I}$
$\widehat{\ell}$	Predation rate of infected prey $\widehat{I}$ by infected predator $\widehat{W}$
$\widehat{u}$	Non-dimensional parameter that regulates how infected prey $\widehat{I}$ compete with healthy prey $\widehat{R}$
$\widehat{q}$	Non-dimensional parameter that regulates how infected prey $\widehat{I}$ compete with infected prey $\widehat{I}$
$\widehat{e}$	Efficiency of the predator in converting captured prey into reproductive success
$\widehat{\sigma}$	Non-dimensional parameter that regulates the infection rate in predator $\widehat{F}$ (vertical transmission)
$1 - \widehat{\sigma}$	Non-dimensional parameter that represents the fraction of no infection of $\widehat{F}$ in the vertical transmission for the case where there is consumption of infected prey
$\widehat{m}$	Mortality rate of healthy predator $\widehat{F}$
$\widehat{\beta}$	Infection rate in healty predator $\widehat{F}$ (horizontal transmission)
$\widehat{\gamma}$	Probalility of vertical transmission in predator $\widehat{F}$
$1 - \widehat{\gamma}$	Non-dimensional parameter that describes the fraction that rate of no infection in $\widehat{F}$ (no infected individual)
$\widehat{\nu}$	Mortality rate of infected predator $\widehat{W}$

4.2 Non-dimensional model

The model (4.1) can be nondimensionalized via $R(t) = \frac{k}{\tilde{r}}\widehat{R}(\tau)$, $I(t) = \frac{k}{\tilde{r}}\widehat{I}(\tau)$, $F(t) = \frac{k}{e\tilde{r}}\widehat{F}(\tau)$, $W(t) = \frac{k}{e\tilde{r}}\widehat{W}(\tau)$, $t = \tilde{r}\tau$, and

$$r = \frac{\bar{r}}{\tilde{r}}, \quad g = \widehat{g}, \quad \lambda = \frac{\widehat{\lambda}}{k}, \quad c = \frac{\widetilde{ce}}{\sqrt{\tilde{r}k}}, \quad a = \frac{\widehat{ae}}{\sqrt{\tilde{r}k}}, \quad b = \frac{\widehat{be}}{k}, \quad \mu = \frac{\widehat{\mu}}{\tilde{r}},$$

$$\ell = \frac{\widehat{\ell e}}{k}, u = \widehat{u}, \quad q = \widehat{q}, \quad m = \frac{\widehat{m}}{\tilde{r}}, \quad \frac{\widehat{\beta e}}{k},$$

to get re-scaled system:

$$\frac{dX}{dt} = f(X), \quad X = (R, I, F, W)^T, \quad f = (f_1, f_2, f_3, f_4)^T, \tag{4.2}$$

$$
\begin{aligned}
f_1 &= R + r(1-\alpha)I - R(R+gI) - \lambda RI - cp\sqrt{R}W - a\sqrt{R}F \\
&\quad - \theta(1-p)c\sqrt{R}W, \\
f_2 &= \alpha I + I(\lambda R - bF - \mu - \ell W) + \theta(1-p)c\sqrt{R}W - I(uR + qI), \\
f_3 &= a\sqrt{R}F + (1-\sigma)bIF + (1-\gamma)cp\sqrt{R}W - mF + (1-\gamma)\ell IW \\
&\quad - \beta FW, \\
f_4 &= \gamma cp\sqrt{R}W + \gamma\ell IW - \nu W + \sigma bIF + \beta FW.
\end{aligned}
$$

4.3 System's equilibria

Model (4.2) has five equilibria. The origin E_0, two disease-free equilibria, $E_1 = (1, 0, 0, 0)$, and $E_2 = (R_2, 0, F_2, 0)$, the predator-free $E_3 = (R_3, I_3, 0, 0)$ and coexistence $E_4 = (R_4, I_4, F_4, W_4)$ which is studied numerically. Their components are:

$$R_2 = \frac{m^2}{a^2}, \quad F_2 = \frac{m^2}{a^2}\left(\frac{1}{m} - \frac{m}{a^2}\right), \quad I_3 = \frac{\alpha - \mu}{q} + \frac{\lambda - u}{q}R_3 \tag{4.3}$$

and R_3 given by the roots of the quadratic equation

$$\Phi(R_3) = \alpha_2 R_3^2 + \alpha_1 R_3 + \alpha_0 = 0 \tag{4.4}$$

with

$$\alpha_2 = \frac{(g+\lambda)(u-\lambda) - q}{q}, \quad \alpha_0 = \frac{r(\alpha-1)(\mu-\alpha)}{q},$$

$$\alpha_1 = \frac{(1-\alpha)r(\lambda-u) + (\mu-\alpha)(\lambda+g) + q}{q}.$$

4.3.1   Feasibility

Feasibility for E_2 is ensured by

$$m \leq a \tag{4.5}$$

and in case of E_3 the feasibility conditions are for $I_3 \geq 0$

$$\alpha + \lambda R_3 \geq \mu + u R_3 \tag{4.6}$$

and for $R_3 \geq 0$ two positive roots exist if

$$\Delta = \alpha_1^2 - 4\alpha_2\alpha_0 > 0, \quad -\alpha_1\alpha_2^{-1} > 0, \quad \alpha_0\alpha_2^{-1} > 0$$

while at least one positive root is ensured by

$$\Delta = \alpha_1^2 - 4\alpha_2\alpha_0 > 0, \quad \alpha_0\alpha_2^{-1} < 0.$$

The viability conditions for $R_3 \geq 0$ of E_3 are explicit in the appendix 4.7. A feasible equilibrium solution for system (4.2) with $F = 0$ and $W = 0$ is an intersection in the first quadrant of the two curves:

$$f(R) = \frac{(R-1)R}{(1-\alpha)r - (g+\lambda)R}, \quad h(R) = \frac{(\alpha - \mu) + (\lambda - u)R}{q}.$$

Note that the function $f(R)$ has an asymptote in $R = p^* = r(1-\alpha)/(g+\lambda)$, thus there are two cases: $p^* > 1$ and $p^* < 1$, which respectively give:

$$f(R) : \begin{cases} < 0 & \text{if } 0 < R < p^* \\ > 0 & \text{if } p^* < R < 1 \\ < 0 & \text{if } 1 < R \end{cases} \qquad f(R) : \begin{cases} < 0 & \text{if } 0 < R < 1 \\ > 0 & \text{if } 1 < R < p^* \\ < 0 & \text{if } p^* < R \end{cases}.$$

Assume

$$\lambda + \alpha > \mu + u. \tag{4.7}$$

It follows thay $f(1) = 0$ and f is unbounded around $(p^* - \epsilon, p^* + \epsilon)$, $\epsilon > 0$, since $h(R)$ is bounded in any closed interval in $(0, \infty)$ it follows that $f(R)$ and $h(R)$ must intersect at a point in $(p^*, 1)$ if $p^* < 1$ or in the interval $(1, p^*)$ if $p^* > 1$. Since $f(R)$ is convex in such intervals and negative outside them, uniqueness of the intersection is assured. In Figure 4.1 we present a sketch with the two cases.

4.3.2   Local stability analysis

The Jacobian of the system (4.2) is given by
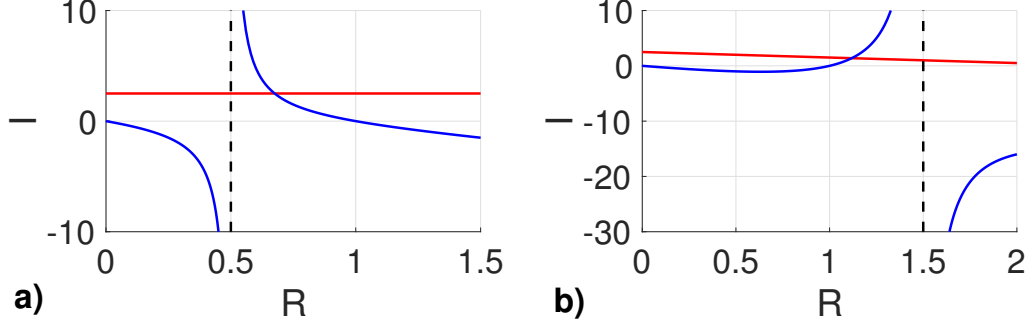
Figure 4.1: Nullclines in the plane $R - I$, considering $F = W = 0$. If $\lambda + \alpha > u + \mu$ ($\lambda_1^{E_1} > 1$), there is a unique feasible equilibrium point in the form $(R_3, I_3, 0, 0)$. a) Parameter values: $\alpha = 0.5$, $q = 0.1$, $r = 0.5$ and $g = u = \mu = 0.25$ we obtain $p^* = 0.5$. b) Parameter values: $\alpha = 0.5$, $q = g = 0.1$, $r = 0.75$ and $u = \mu = 0.25$ we obtain $p^* = 1.5$.

$$
J = \begin{pmatrix}
J_{11} & -\lambda R - gR + (1-\alpha)r & -a\sqrt{R} & -\theta(1-p)c\sqrt{R} - cp\sqrt{R} \\
J_{21} & J_{22} & -bI & \theta(1-p)c\sqrt{R} - \ell I \\
J_{31} & J_{32} & J_{33} & (1-\gamma)(\ell I + cp\sqrt{R}) - \beta F \\
\frac{c\gamma pW}{2\sqrt{R}} & \ell\gamma W + b\sigma F & \beta W + b\sigma I & cp\gamma\sqrt{R} + \gamma\ell I + \beta F - \nu
\end{pmatrix}
$$

with

$$
J_{11} = -\lambda I - \frac{\theta(1-p)cW}{2\sqrt{R}} - \frac{cpW}{2\sqrt{R}} - 2R - \frac{aF}{2\sqrt{R}} - gI + 1, \quad J_{31} = \frac{c(1-\gamma)pW}{2\sqrt{R}} + \frac{aF}{2\sqrt{R}},
$$

$$
J_{22} = \lambda R - \ell W - 2qI - uR - bF + \alpha - \mu, \quad J_{21} = \lambda I + \frac{\theta(1-p)cW}{2\sqrt{R}} - uI,
$$

$$
J_{32} = (1-\gamma)\ell W + b(1-\sigma)F, \quad J_{33} = -\beta W + a\sqrt{R} + b(1-\sigma)I - m.
$$

The origin for this model presents a particular behaviour. Although unstable in the Lyapunov sense [70], it is still capable of attracting trajectories over a set of initial condition with positive measure in $\mathbb{R}^4$. The instability of the origin can be seen, by observing that any trajectory starting in the line defined by $I = F = W = 0$ remains in it, since $\dot{I} = \dot{F} = \dot{W} = 0$. The equation for $\dot{R}$ on the line is simply $\dot{R} = R(1 - R)$ which implies that the origin is unstable, since any trajectory with initial condition $0 < \epsilon = R_0 < 1$ moves away from the origin.

This particular behaviour of the origin is caused by the predation term which is proportional to the square root of the healthy prey population. When $R \to 0$, such term has a higher order when compared to the reproduction term (R). In fact such proportionality to the square root of R is adequate

for "large" population, since the group defense effect is negligible when the population is "small". Also, in the present model we seek to analyze the biological situations which are relevant to the analysis to the spread of the disease, that is, the scenarios where at least one of the populations is present.

However, a particular phenomenon has been observed in similar models in these conditions, [85, 34, 52, 7]. The right hand side of the system is not Lipschitz-continuous because of the presence of the square root in every component, so that the uniqueness theorem does not hold. In [85] this has been investigated, showing that trajectories lying in a narrow stripe may well end up on the prey axis in finite time, and from there they move toward the origin, with ecosytem collapse. This has been further investigated in [34, 52, 7], showing that it entails a wealth of bifurcation phenomena. For a generalization to an arbitrary power instead of the square root, see [15].

At E_1 the eigenvalues are easily found and given by $\lambda_1 = cp\gamma - \nu$, $\lambda_2 = a - m$, $\lambda_3 = -1$ and $\lambda_4 = \lambda + \alpha - \mu - u$. E_1 is stable if and only if

$$cp\gamma < \nu, \quad a < m, \quad \lambda + \alpha < \mu + u. \tag{4.8}$$

For E_2 the product of two quadratic equations is obtained. The first one has the Routh-Hurwitz conditions $\mathrm{tr}(\overline{J}^1_{E_2}) = (a^2 - 3m^2)(2a)^{-2} < 0$, $\det(\overline{J}^1_{E_2}) = (ma^2 - m^3)(2a)^{-2} > 0$, the stability conditions

$$\frac{a}{\sqrt{3}} < m < a. \tag{4.9}$$

The second quadratic has more complicated Routh-Hurwitz conditions that provide the second set of stability conditions

$$a^4\nu + a^2m^2u + a^4\mu + \beta m^3 + bma^2 > am^2\lambda + cmp\gamma a^3 + bm^3 + \beta ma^2 + \alpha a^4 \tag{4.10}$$

and

$$\begin{aligned}
a^5 c\gamma m^3 p\lambda + a^4\beta m^3\lambda + a^6 m^2 u\nu + a^8\mu\nu + a^6 bm\nu + a^2\beta m^5 u \\
+ a^5 bcpm^2\theta\sigma + a^3 bcm^4\theta\sigma + a^3 bcpm^4\gamma + a^7 cmp\alpha\gamma + a^4\beta m^3\mu \\
+ a^2 2b\beta m^4 + a^6\beta m\alpha > a^6 m^2\nu\lambda + a^2\beta m^5\lambda + a^4 bm^3\nu + a^8\alpha\nu \\
+ a^5 cpu\gamma m^3 + a^3 bcpm^4\theta\sigma + a^4\beta m^3 u + a^5 bcm^2\theta\sigma + a^7 cmp\mu\gamma \\
+ a^5 bcpm^2\gamma + a^6\beta m\mu + \beta bm^6 + a^4\beta m^3\alpha + a^4\beta bm^2.
\end{aligned} \tag{4.11}$$

At E_3 again the characteristic equation factorizes into the product of two quadratic equations, that have the Routh-Hurwitz conditions

$$\mathrm{tr}(\overline{J}^1_{E_3}) = (\lambda R_3 - \lambda I_3 - 2qI_3 - gI_3 - uR_3 - 2R_3 + \alpha + 1 - \mu < 0,$$

$$\begin{aligned}
\det(\overline{J}^1_{E_3}) &= -2\lambda R_3{}^2 + \lambda R_3 + 2q\lambda I_3{}^2 + 2gqI_3{}^2 - 2r\lambda I_3 - g\mu I_3 - 2uR_3{}^2 \\
&+ 4qR_3 I_3 - 2qI_3 - rukR_3 - r\alpha uI_3 - ruI_3 - 2\mu R_3 - r\lambda I_3 \\
&+ \mu\lambda I_3 - \alpha\lambda I_3 - g\alpha I_3 - 2\alpha r - \mu + \alpha > 0,
\end{aligned}$$

from which the stability conditions follow

$$\lambda I_3 + 2q I_3 + g I_3 + u R_3 + 2 R_3 + \mu > \lambda R_3 + \alpha + 1,$$

$$2\lambda R_3{}^2 + \lambda R_3 + 2q\lambda I_3{}^2 + 2gq I_3{}^2 + 4q R_3 I_3 + \mu\lambda I_3 + \alpha > 2r\lambda I_3 + g\mu I_3 + 2u R_3{}^2$$
$$+2q I_3 + ruk R_3 + r\alpha u I_3 + ru I_3 + 2\mu R_3 + r\lambda I_3 + \alpha\lambda I_3 + g\alpha I_3 + 2\alpha r + \mu.$$

The second quadratic instead gives the Routh-Hurwitz conditions

$$\mathrm{tr}(\overline{J}_{E_3}^2) = cp\gamma\sqrt{R_3} + a\sqrt{R_3} - b\sigma I_3 + \gamma\ell I_3 + b I_3 - \nu - m < 0,$$

$$\begin{aligned}
\det(\overline{J}_{E_3}^2) &= acp\gamma R_3 - bcp\sigma\sqrt{R_3}I_3 + bc\gamma p\sqrt{R_3}I_3 + a\gamma\ell\sqrt{R_3}I_3 - a\nu\sqrt{R_3} \\
&- cmp\gamma\sqrt{R_3} - b\sigma\ell I_3{}^2 + b\ell\gamma I_3{}^2 + b\sigma\nu I_3 - b\nu I_3 - m\ell\gamma I_3 + m\nu > 0,
\end{aligned}$$

once again providing the stability conditions

$$\begin{aligned}
b\sigma I_3 + \nu + m &> cp\gamma\sqrt{R_3} + a\sqrt{R_3} + \gamma\ell I_3 + b I_3 acp\gamma R_3 + bc\gamma p\sqrt{R_3}I \\
&+ a\gamma\ell\sqrt{R_3}I_3 + b\ell\gamma I_3{}^2 + b\sigma\nu I_3 + m\nu > bcp\sigma\sqrt{R_3} + a\nu\sqrt{R_3}I_3 \\
&+ cmp\gamma\sqrt{R_3} + b\sigma\ell I_3{}^2 + b\nu I_3 + m\ell\gamma I_3.
\end{aligned}$$

4.4 The basic reproduction number

Conditions for the eradication of the disease can be obtained from the basic reproduction number $\mathcal{R}_0$, the spectral radius of the next generation matrix at each disease-free equilibrium [26, 12].

Let F_I, F_W be the corresponding new infectious rates and V_I, V_W the analogous flows, the dynamics of the infectious classes I and W can be written as:

$$\frac{dI}{dt} = F_I - V_I = F_I - (V_I^- - V_I^+), \quad \frac{dW}{dt} = F_W - V_W = (V_W^- - V_W^+), \quad (4.12)$$

where

$$\begin{aligned}
F_I &= \alpha I + \lambda R I + \theta(1-p)c\sqrt{R}W, \\
F_W &= b\sigma IF + \beta FW + cp\gamma\sqrt{R}W + l\gamma IW, \\
V_I^- &= bIF + \mu I + lIW + uRI + qI^2, \\
V_I^+ &= 0, \\
V_W^- &= \nu W, \\
V_W^+ &= 0.
\end{aligned}$$

Letting

$$F = \begin{pmatrix} \frac{\partial F_I}{\partial I} & \frac{\partial F_W}{\partial I} \\ \frac{\partial F_I}{\partial W} & \frac{\partial F_W}{\partial W} \end{pmatrix} = \begin{pmatrix} \alpha + \lambda R & \gamma\ell W + b\sigma F \\ \theta(1-p)c\sqrt{R} & pc\gamma\sqrt{R} + \ell\gamma I + \beta F \end{pmatrix}$$

and

$$V = \begin{pmatrix} \frac{\partial V_I}{\partial I} & \frac{\partial V_W}{\partial I} \\ \frac{\partial V_I}{\partial W} & \frac{\partial V_W}{\partial W} \end{pmatrix} = \begin{pmatrix} bF + \mu + \ell W + uR + 2qI & 0 \\ \ell I & \nu \end{pmatrix},$$

the next generation matrix is

$$G = FV^{-1} =$$

$$\begin{pmatrix} \dfrac{\alpha\nu + \lambda\nu R - \ell\gamma IW - b\ell\sigma IF}{\nu(\ell W + uR + 2qI + bF + \mu)} & \dfrac{\ell\gamma W + b\sigma F}{\nu} \\ \dfrac{\theta(1-p)c\nu\sqrt{R} - pc\ell\gamma I\sqrt{R} - \ell^2\gamma I^2 - \beta\ell IF}{\nu(\ell W + uR + 2qI + bF + \mu)} & \dfrac{\beta F + \ell\gamma I + cp\gamma\sqrt{R}}{\nu} \end{pmatrix}.$$

$\mathcal{R}_0$ is defined in each disease-free equilibrium as the spectral radius of G. For model (4.2) the only feasible disease-free equilibria are E_0, E_1 and E_2. Therefore, we proceed the analysis of the disease-free equilibria.

4.4.1 Stability analysis of disease-free equilibria

The methodology requires five conditions to be applied [26], one of them is that disease-free equilbrium should be stable if the number of new cases are set to zero. Considering $F_I = 0$ and $F_W = 0$ in model (4.2) we obtain:

$$\begin{aligned} \frac{dR}{dt} &= R + r(1-\alpha)I - R(R + gI) - \lambda RI - cp\sqrt{R}W \\ &\quad - a\sqrt{R}F - \theta(1-p)c\sqrt{R}W, \\ \frac{dI}{dt} &= -bIF - \mu I - lIW - uRI - qI^2, \\ \frac{dF}{dt} &= a\sqrt{R}F + (1-\sigma)bIF + (1-\gamma)W(cp\sqrt{R} + \ell I) \\ &\quad - mF - \beta FW, \\ \frac{dW}{dt} &= -vW. \end{aligned} \tag{4.13}$$

The Jacobian of the system (4.13) is given by

$$J = \begin{pmatrix} J_{11} & -\lambda R - gR + (1-\alpha)r & -a\sqrt{R} & J_{14} \\ -uI & J_{22} & -bI & -\ell I \\ \frac{cp(1-\gamma)W + aF}{2\sqrt{R}} & J_{32} & J_{33} & J_{34} \\ 0 & 0 & 0 & -v \end{pmatrix}$$

with

$$J_{11} = -\lambda I - \frac{\theta(1-p)cW}{2\sqrt{R}} - \frac{cpW}{2\sqrt{R}} - gI - 2R - \frac{aF}{2\sqrt{R}} + 1,$$

$$J_{14} = -\theta(1-p)c\sqrt{R} - cp\sqrt{R}, \quad J_{22} = -bF - \mu - \ell W - uR - 2qI,$$

$$J_{32} = (1-\gamma)\ell W + b(1-\sigma)F,$$

$$J_{33} = a\sqrt{R} + (1-\sigma)bI - m - \beta W, \quad J_{34} = (1-\gamma)(\ell I + cp\sqrt{R}) - \beta F.$$

Disease-free equilibrium E_1

For this point the stability condition under $F_I = F_W = 0$ is

$$m > a.$$

The eigenvalues of G in E_1 are:

$$\lambda_1^{E_1} = \frac{\alpha + \lambda}{u + \mu}, \quad \lambda_2^{E_1} = \frac{cp\gamma}{\nu}. \tag{4.14}$$

Since $\lambda_1^{E_1}$ and $\lambda_2^{E_1}$ are both positive, the value of $\mathcal{R}_0$ in E_1 is simply $\mathcal{R}_0^{E_1} = \max\{\lambda_1^{E_1}, \lambda_2^{E_1}\}$. Disease-induced instability occurs if $\mathcal{R}_0 > 1$.

If $\nu \geq m$, that is, the rate of mortality of infected predators is greater than non-infected ones, then we can write:

$$\nu \geq m > a \geq c \geq cp\gamma,$$

because we consider $a \geq c$ (healthy predators are more efficient in hunting than infected ones) and $p, \gamma \leq 1$. Therefore, $\lambda_2^{E_1} < 1$ if E_1 is stable in the absence of disease.

The condition for $\mathcal{R}_0 < 1$ coming from $\lambda_1^{E_1}$ can be written as

$$\alpha + \lambda < u + \mu.$$

The left side of the inequality represents rates that are favorable to the permanence of the disease, i.e, reproduction rate of infectious prey and generation of new infectious cases at the equilibrium. In the right side of inequality are the factors that contribute to the eradication of the disease, i.e, the mortality rates of infected prey and mortality due to competition with healthy prey at the equilibrium. In this case stability in the absence of the disease does not imply $\lambda_1^{E_1} < 1$. For instance, even if $\alpha = 0$ it is sufficient to take $\lambda > u + \mu$ to obtain $\mathcal{R}_0 > 1$.

Disease-free equilibrium E_2

Considering $F_I = F_W = 0$, the viability condition for the equilibrium E_2 is given by

$$m \leq a$$

and the stability conditions for it are

$$\frac{a}{\sqrt{3}} < m < a.$$

The matrix G in E_2 is

$$G(E_2) = \begin{pmatrix} \dfrac{\alpha a^4 + \lambda m^2 a^2}{um^2 a^2 + bma^2 - bm^3 + \mu a^4} & \dfrac{\sigma ba^2 m - \sigma bm^3}{\nu a^4} \\[3mm] \dfrac{(-cpma^3 + cma^3)\theta}{a^2 m^2 u + \mu a^4 - bm^3 + bma^2} & \dfrac{cpm\gamma a^3 - \beta m^3 + \beta ma^2}{\nu a^4} \end{pmatrix}$$

The formulas for eigenvalues of $G(E_2)$ do not provide any immediate insight on the behaviour of $\mathcal{R}_0$, but through numerical simulations we can state that both $\lambda_1^{E_2}$ and $\lambda_2^{E_2}$ can have absolute values greater than one.

4.5 Bifurcations

To make a study about the local bifurcations near the equilibrium points of model (4.2), we use the Sotomayor theorem [70, 67].

4.5.1 Transcritical bifurcation

Note that the general second order term of the Taylor expansion of f, recall (4.2), is given by

$$D^2 f((R, I, F, W), \psi)(V, V) = (D_{11}, D_{21}, D_{31}, D_{41})^T, \qquad (4.15)$$

taking ψ as bifurcation parameter and $V = (\xi_1, \xi_2, \xi_3, \xi_4)^T$ being the vector of variations in R, I, F and W, with

$$
\begin{aligned}
D_{11} &= \frac{\theta(1-p)cW\xi_1{}^2 + cpW\xi_1{}^2 + aF\xi_1{}^2}{4R\sqrt{R}} - 2\xi_1{}^2 \\
&\quad - 2g\xi_1\xi_2 - 2\lambda\xi_1\xi_2 - \frac{a}{\sqrt{R}}\xi_1\xi_3 - \frac{cp}{\sqrt{R}}\xi_1\xi_4 - \frac{\theta(1-p)c}{\sqrt{R}}\xi_1\xi_4, \\
D_{21} &= -\frac{\theta(1-p)cW}{4R\sqrt{R}}\xi_1{}^2 + 2(\lambda - u)\xi_1\xi_2 - 2b\xi_2\xi_3 - 2\ell\xi_2\xi_4 - 2q\xi_2{}^2 \\
&\quad + \frac{\theta(1-p)c}{\sqrt{R}}\xi_1\xi_4, \\
D_{31} &= -\frac{c(1-\gamma)pW\xi_1{}^2 - aF\xi_1{}^2}{4R\sqrt{R}} + \frac{a}{\sqrt{R}}\xi_1\xi_3 + \frac{c(1-\gamma)p}{\sqrt{R}}\xi_1 l\xi_4 \\
&\quad + 2b(1-\sigma)\xi_2\xi_3 + 2(1-\gamma)\ell\xi_2\xi_4 - 2\beta\xi_3\xi_4, \\
D_{41} &= -\frac{cpW}{4R\sqrt{R}}\xi_1{}^2 + \frac{cp\gamma}{\sqrt{R}}\xi_1\xi_4 + 2b\sigma\xi_2\xi_3 + 2\gamma\ell\xi_2\xi_4 + 2\beta\xi_3\xi_4.
\end{aligned}
$$

Bifurcation between E_1 and E_2

Comparing the second stability condition in (4.8) given by $m > a$ for the
equilibrium point E_1 and, the feasibility condition in (4.5) of E_2, we find
that E_2 we can see a transcritical bifurcation between E_1 and E_2 when the
parameter m crosses the critical value $m^\dagger$ given by

$$m^\dagger = a.$$

Proposition 8. *Assuming that $\alpha + \lambda < u + \mu$ and $cp\gamma < \nu$, when m passes
through the value $m^\dagger = a$, model (4.2) near the disease-free equilibrium $E_1 =
(1, 0, 0, 0)$ has:*

- *no saddle-node bifurcation;*

- *a transcritical bifurcation;*

- *no pitchfork bifurcation.*

Proof. Since $\alpha + \lambda < u + \mu$, $cp\gamma < \nu$ and $m > a$, the equilibrium point E_1 is
stable. The Jacobian matrix of model (4.2) evaluated at E_1 with $m^\dagger = a$, is
given by

$$J_{E_1}(m^\dagger) = \begin{pmatrix} -1 & -\lambda - g + (1-\alpha)r & -a & -\theta(1-p)c - cp \\ 0 & \lambda - u - \mu + \alpha & 0 & \theta(1-p)c \\ 0 & 0 & 0 & c(1-\gamma)p \\ 0 & 0 & 0 & cp\gamma - \nu \end{pmatrix}. \quad (4.16)$$

In this case, we have one eigenvalue equal zero in (4.16), in which the cor-
responding eigenvector is $V_1 = \varphi_1(1, 0, -\frac{1}{a}, 0)^T$ and $Z_1 = \omega_1(0, 0, 1, -p(c\gamma - c)(\nu - c\gamma p)^{-1})^T$ represents the eigenvector corresponding to eigenvalue equal
zero of $(J_{E_1}(m^\dagger))^T$, where φ_1 and ω_1 are any nonzero real number.

Differentiating partially the right hand sides of the equations of system
(4.2) with respect to $m^\dagger = a$, we find

$$\frac{df}{dm} = f_m(E_1, a) = (0, 0, 0, 0)^T,$$

which gives $Z_1^T f_m(E_1, a) = 0$. Thus, according to Sotomayor's theorem for
local bifurcation, model (4.2) has no saddle-node bifurcation near disease-free
equilibrium at $m^\dagger = a$. Besides that,

$$Df_m(E_1, a) = \begin{pmatrix} 0 & 0 & 0 & 0 \\ 0 & 0 & 0 & 0 \\ 0 & 0 & -1 & 0 \\ 0 & 0 & 0 & 0 \end{pmatrix}$$

then,

$$Z_1^T[Df_m(E_1, a).V_1] = \frac{\varphi_1 \omega_1}{a} \neq 0.$$

Now, considering E_1, $m^\dagger = a$ and V_1 in (4.15) we get

$$D^2 f(E_1, a).(V_1, V_1) = \varphi_1^2 (-1, 0, -1, 0)^T.$$

Therefore,

$$Z_1^T[D^2 f(E_1, a).(V_1, V_1)] = -\omega_1 \varphi_1^2 \neq 0.$$

According to Sotomayor's theorem model (4.2) has a transcritical bifurcation at E_1 with parameter $m^\dagger = a$, while the pitchfork bifurcation cannot occur. $\square$

Bifurcation between E_1 and E_3

Comparing the third stability condition in (4.8) for the equilibrium point E_1 and, the feasibility condition in (4.7) for equilibrium point E_3, we have a transcritical bifurcation between E_1 and E_3 when the parameter α crosses the critical value $\alpha^\dagger$ given by

$$\alpha^\dagger = u + \mu - \lambda$$

Proposition 9. *Assuming that $\alpha + \lambda < u + \mu$ and $cp\gamma < \nu$, when α passes through the value $\alpha^\dagger = u + \mu - \lambda$, model (4.2) near the disease-free equilibrium E_1 has:*

- *no saddle-node bifurcation;*

- *a transcritical bifurcation;*

- *no pitchfork bifurcation.*

Proof. Since $\alpha + \lambda < u + \mu$, $cp\gamma < \nu$ and $m > a$, the equilibrium point E_1 is stable. The Jacobian matrix of model (4.2) evaluated at E_1, with $\alpha^\dagger = u + \mu - \lambda$ is

$$J_{E_1}(\alpha^\dagger) = \begin{pmatrix} -1 & \lambda(r-1) + r(1 - u - \mu) - g & -a & -\theta(1-p)c - cp \\ 0 & 0 & 0 & \theta(1-p)c \\ 0 & 0 & a - m & c(1-\gamma)p \\ 0 & 0 & 0 & cp\gamma - \nu \end{pmatrix}.$$

which has one eigenvalue equal zero and the corresponding eigenvector is $V_2 = \varphi_2(1, (\lambda - ru + r - r\mu - g)^{-1}, 0, 0)^T$. For $J_{E_1}(\alpha^\dagger))^T$, the eingenvector is $Z_2 = \omega_2(0, 1, 0, ((cp - c)\theta)(c\gamma p - \nu)^{-1})^T$. We have φ_2 and ω_2 are any nonzero real number.

Differentiating partially the right hand sides of the equations of system
(4.2) with respect to $\alpha^{\dagger} = u + \mu - \lambda$, we find

$$\frac{df}{d\alpha} = f_{\alpha}(E_1, \alpha^{\dagger}) = (0, 0, 0, 0)^{T},$$

which gives $Z_2^{T}.f_{\alpha}(E_1, \alpha^{\dagger}) = 0$. Thus, according to Sotomayor's theorem for
local bifurcation, model (4.2) has no saddle-node bifurcation near disease-free
equilibrium at $\alpha^{\dagger} = u + \mu - \lambda$.

Moreover,

$$Df_{\alpha}(E_1, \alpha^{\dagger}) = \begin{pmatrix} 0 & -r & 0 & 0 \\ 0 & 1 & 0 & 0 \\ 0 & 0 & 0 & 0 \\ 0 & 0 & 0 & 0, \end{pmatrix}$$

then,

$$Z_2^{T}[Df_m(E_1, \alpha^{\dagger})V_2] = \varphi_2 \omega_2 (\lambda - ru + r - r\mu - g)^{-1} \neq 0.$$

Now, considering E_1, $\alpha^{\dagger}$ and V_2 in (4.15) we get with $\Lambda = \lambda - ru + r - r\mu - g$

$$D^2 f(E_1, \alpha^{\dagger}).(V_2, V_2) = \varphi_2^2 \left(\frac{-4\lambda - 2r + 2ru - 2r\mu}{\Lambda}, \frac{2(\lambda - u)}{\Lambda} - \frac{2q}{\Lambda^2}, 0, 0 \right)^{T}.$$

Therefore,

$$Z_2^{T}[D^2 f(E_1, \alpha^{\dagger}).(V_2, V_2)] = \frac{2\omega_2 \varphi_2^2 (\lambda - u)(\lambda - ru + r - r\mu - g)}{(\lambda - ru + r - r\mu - g)^2} \neq 0.$$

So, according to Sotomayor's theorem model (4.2) has a transcritical bifur-
cation at E_1 with parameter $\alpha^{\dagger} = u + \mu - \lambda$, while the pitchfork bifurcation
cannot occur. □

Both theoretical proof made above, can be illustrated in the simulations
presented in Figure 4.2, which (a) shows explicitly the transcritical bifurcation
between E_1 and E_2 for the chosen parameters values (see the caption of Fig. 4.2
(a)) when the parameter m crosses a critical value $m^{\dagger} = a = 1$ and, (b) shows
the transcritical bifurcation between E_1 and E_3 for the chosen parameters
values (see the caption of Fig. 4.2 (b)) when the parameter α crosses a critical
value $\alpha^{\dagger} = u + \mu - \lambda = 1$.

4.5.2 Hopf bifurcation

We now try to establish whether there are parameter combinations giving
sustained population oscillations. For E_1 it is not the case, since the eigenvalues
are all real.

For the equilibrium point E_2 we have a Hopf bifurcation according to the
following proposition.
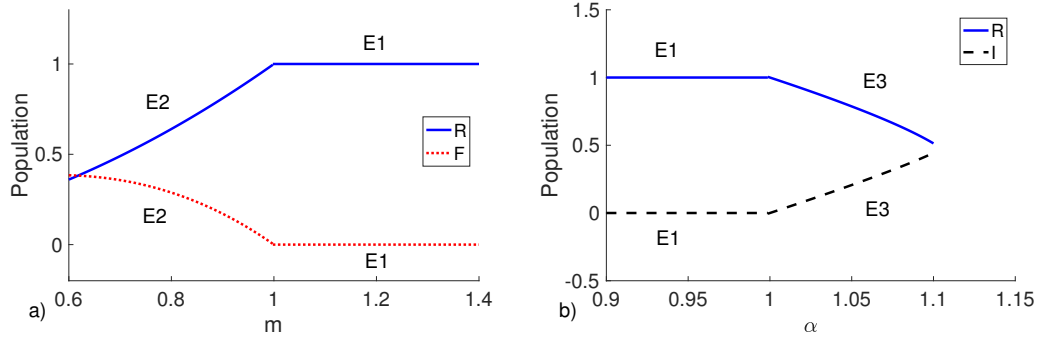
Figure 4.2: a) Transcritical bifurcation between E_1 and E_2 for the parameter values $\lambda = \beta = \ell = \alpha = \sigma = \gamma = \theta = q = c = p = r = g = b = 0.5$, $a = 1$, $u = \mu = 0.75$, $\nu = 2m$. Initial conditions $R_0 = I_0 = F_0 = W_0 = 0.1$ considering R and F populations The equilibrium E_2 is stable from 0.6 to 1 and E_1 is stable past 1. b) Transcritical bifurcation between E_1 and E_3. We have same parameter value and initial conditions for R and I populations, except for $m = 0.5$. The equilibrium E_1 is stable from 0.9 to 1 and E_3 us stable past 1.

Proposition 10. *Assuming that conditions (4.10) and (4.11) hold, then model (4.2) undergoes Hopf bifurcation around the equilibrium point E_2 when parameter m crosses the critical positive value $m^* = a/\sqrt{3}$.*

Proof. For systems in four-dimensional spaces, for a Hopf bifurcation to occur, the following conditions should be satisfied [30, 89, 67]:

- The characteristic equation at E_2 has two real and negative eigenvalues and two complex eigenvalues;

- $\tau_1(m^*) = 0$;

- $(\frac{d}{dm}\tau_1(m))|_{m=m^*}$ (The transversality condition).

The stability analysis of E_2 showed that we obtain two real and negative eigenvalues and another two given by:

$$\Lambda_{\pm} = \frac{\tau_1 \pm \sqrt{P(m)}}{4a^2}, \quad \tau_1 = 3m^2 - a^2, \quad P(m) = 9m^4 + 8a^2 m^3 - 6a^2 m^2 - 8a^4 m + a^4.$$

Thus, since $P(m)$ is continuous, $\tau_1(m^*) = 0$ and $P(m^*) = -16a^5(3\sqrt{3})^{-1} < 0$, there is an interval $T = (m^* - \epsilon, m^* + \epsilon)$ around m^* , such that, $P(x) < 0$ whenever $x \in T$.

101
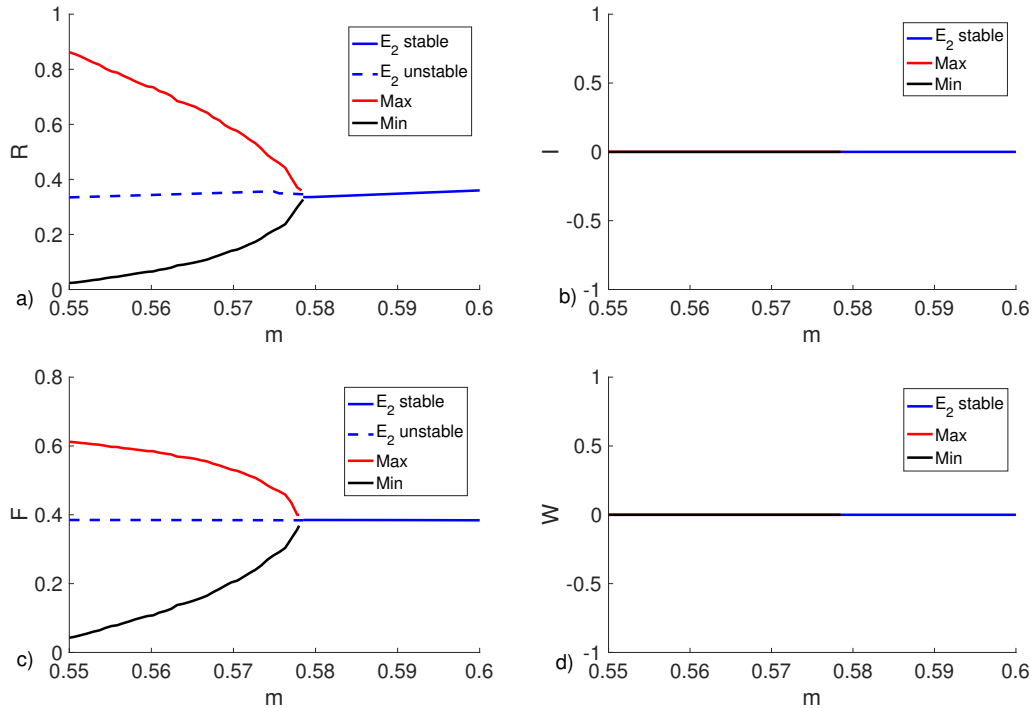
Figure 4.3: Hopf bifurcation for point E_2 for parameter values $\lambda = \beta = \ell = \alpha = \sigma = \gamma = \theta = q = c = p = r = g = b = 0.5$, $a = 1$, $u = \mu = 0.75$, $\nu = 1.157$. Initial conditions $R_0 = I_0 = F_0 = W_0 = 0.1$.

Finally, the transversality condition is satisfied because

$$\frac{d}{dm}\tau_1(m^*) = \frac{3}{2a\sqrt{3}} \neq 0.$$

$\square$

Figure 4.3 illustrates the simulation explicity showing a Hopf bifrucation at E_2.

At E_4 we can only perform numerical simulations. We present two different bifurcation scenarios. In the first, when parameter m crosses from above the critical value $m_1^\star \approx 0.71462$ there is a transcritical bifurcation between E_4 losing feasibility and E_2 becoming stable. Then when $m_2^\star \approx 0.578$ we find a Hopf bifurcation in E_2. With a further decrease of m a four-dimensional limit cycle arises when $m_3^\star \approx 0.56884$, Figure 4.4. The second situation is simply a Hopf bifurcation in E_4 when m crosses from above the critical value of $m_4^\star \approx 0.4626875$, Figure 4.5.
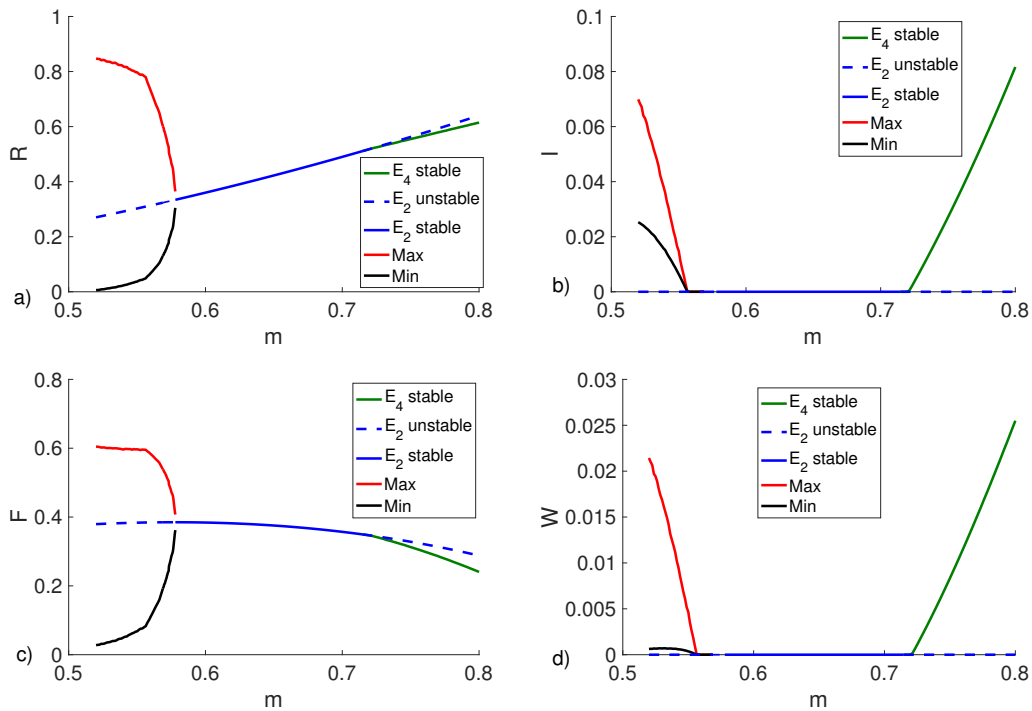
Figure 4.4: a), b), c) and d) illustrate a Transcritical bifurcation between E_4 and E_2 for $m_1^\star \approx 0.71462$; Hopf bifurcation for E_2 when $m_2^\star \approx 0.578$; Loss of stability of the two-dimensional limit cycle and creation of a four-dimensional limit cycle when $m_3^\star \approx 0.56884$. The parameter values are: $\lambda = \sigma = \theta = r = q = g = \mu = 0.5$, $a = 1$, $\alpha = 0.6$, $c = 0.8289$, $\beta = 0.2056$, $\gamma = \ell = 0.99$, $b = 0.5066$, $\nu = 0.8$, $p = 0.7389$ and $u = 0.4$. Initial conditions $R_0 = I_0 = F_0 = W_0 = 0.1$.
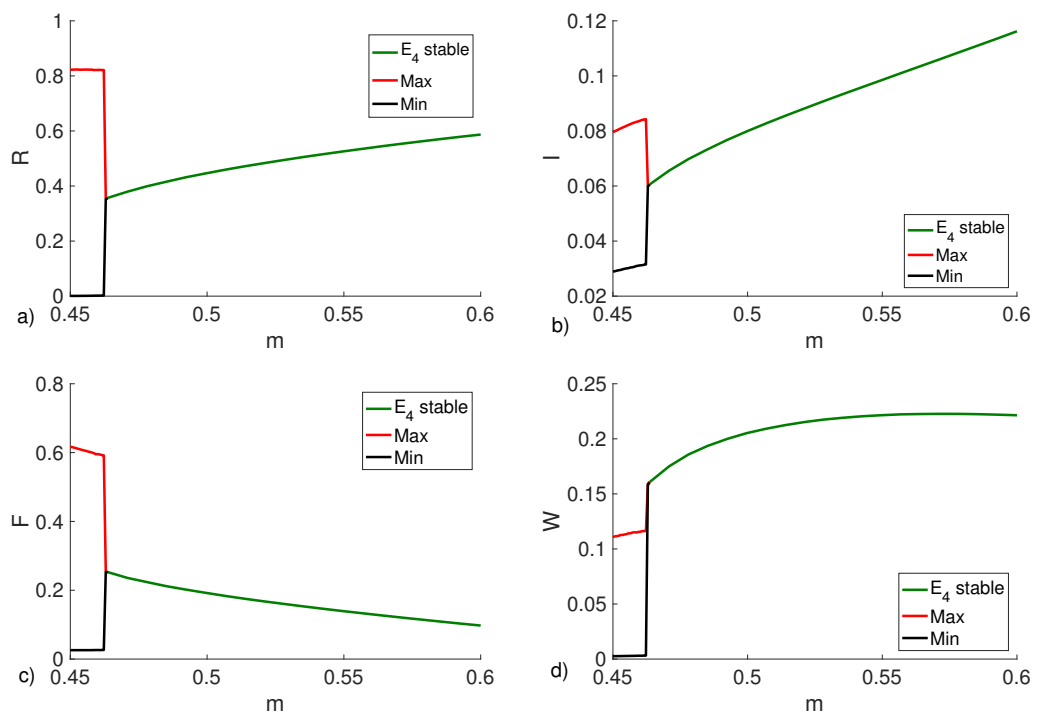
Figure 4.5: Hopf bifurcation for point E_4 for parameter values $\lambda = \sigma = \theta = r = q = g = \mu = 0.5$, $a = 1$, $\alpha = 0.61$, $c = 0.8289$, $\beta = 0.9433$, $\gamma = \ell = 0.99$, $b = 0.5066$, $\nu = 0.6833$, $p = 0.7389$ and $u = 0.4$.

4.6 Numerical results

The analysis of model (4.2), shows that the parameter m is crucial for the feasibility and stability of points E_1 and E_2, respectively. The establishment of the disease is directly related to the value of $\mathcal{R}_0$ at both points. Thus, we conduct an exploration of the parameter space with relation to those fundamental quantities. As it will be shown in this section, the results of the majority of the simulations can be predicted simply by the analysis of m, $\mathcal{R}_0^{E_1}$ and $\mathcal{R}_0^{E_2}$.

4.6.1 Details about the numerical implementation

To investigate the behaviour of model (4.2) in relation to the parameters, we first separate the simulations in two specific cases. In the first case, E_1 is stable and E_2 is unstable, that is, $m > a$. The second case, is obtained when $a/\sqrt{3} < m < a$, in which E_1 is unstable and E_2 is feasible. The reason for the adoption of such thresholds comes from the analysis of the analogous predator-prey model without the presence of disease [15]. In our model a transcritical bifurcation E_1 and E_2 is observed when $m = a$ and Hopf bifurcation occurs when $m = a/\sqrt{3}$ as we can see in subsection 4.5.

Given the high number of parameters (18), we opt for a random exploration of the space. In Table 4.2 represent the distributions adopted for each parameter.

Table 4.2: Distribution for the parameters in simulations using Matlab. Here, we make a random exploration of the space to each parameter. $\mathcal{U}(x,y)$ stands for an uniform distribution between x and y.

Parameters	Distribution
$u, \quad q, \quad g$	50% $\mathcal{U}(0.5,1)$; 50% $\mathcal{U}(1,2)$
$\mu, \quad \beta, \quad \lambda$	50% $\mathcal{U}(0.1,1)$; 50% $\mathcal{U}(1,10)$
$a, \quad b$	50% $\mathcal{U}(0.1,1)$; 50% $\mathcal{U}(1,2)$
c	$\mathcal{U}(0.1,a)$
$m > a$ (case 1)	$\mathcal{U}(1.1a,(2-1.1/\sqrt{3})a)$
$a/\sqrt{3} < m < a$ (case 2)	$\mathcal{U}(1.1a/\sqrt{3},0.9a)$
ν	$\mathcal{U}(m,3m)$
ℓ	$\mathcal{U}(0.1,b)$
$\alpha, \quad \sigma, \quad \gamma, \quad \theta, \quad p$	$\mathcal{U}(0.05,0.95)$
r	$\mathcal{U}(0.05,1)$

When non-dimensional parameters cross the threshold 1, it usually means a transition between two qualitatively distinct scenarios. For this reason, the random sampling is chosen to be half of the time in each situation. For biological reasons, some parameters are linked. For instance, the mortality of

diseased predators (ν) is greater than or equal to the mortality of healthy predators (m).

For the numerical simulation of the system of differential equations we use the Matlab ode45 routine. For each random combination of parameters, a random initial condition was chosen with the distributions: $R_0 \sim \mathcal{U}(0.2, 1)$, $I_0 \sim \mathcal{U}(0.2, 0.6)$, $F_0 \sim \mathcal{U}(0.05, 1.05)$ and $W_0 \sim \mathcal{U}(0.05, 0.1)$ ($\mathcal{U}(x, y)$ stands for an uniform distribution between x and y). The choice of initial conditions with smaller predator populations is made in order to avoid trajectories that converge to the origin, in which the approximation of the predation term by $\sqrt{R}$ is not valid. Given the initial conditions, the system is simulated in the time interval $I_{t_1} = [0, 200]$, if such interval is not enough to find an equilibrium, another try is attempted with $I_{t_2} = [0, 2000]$.

Also, for each combination of parameters the equilibrium points E_1, E_2, E_3 and E_4 are estimated. For E_1 and E_2 the analytical formulae of section 4.3 are used. For the equilibrium point E_3 the quadratic equation (4.17) is numerically solved using the routine ROOTS of Matlab. In sequence, the equation for I_3 (4.3) is employed to establish if there was any feasible equilibrium solution E_3.

For the equilibrium point E_4 we do not have analytic formulae. Thus, we used the routine FMINCON of Matlab, to minimize the sum of the squares of the derivatives subject to the conditions: $R_4 > 2^{-8}$, $I_4 > 2^{-8}$, $F_4 > 2^{-8}$, e $W_4 > 2^{-8}$. Since the results of the minimization process depend on the initial guess, 10 starting points are taken for each parameter combination. The distributions of the initial guesses are taken as: $R_g \sim \mathcal{U}(0, 1)$, $I_g \sim \mathcal{U}(0, 1)$, $F_g \sim \mathcal{U}(0, 1)$ and $W_g \sim \mathcal{U}(0, 1)$. Each time, if the routine obtained with success a solution for the minimization problem, it is stored as a candidate for equilibrium point E_4. After the 10 executions of the routine FMINCON, redundant solutions are removed from the list of equilibrium candidates. Two solutions x_1, $x_2 \in \mathbb{R}^4$ are considered redundant if

$$\frac{\|x_1 - x_2\|}{\|x_1\|} < 0.01.$$

After obtaining the list of all equilibrium candidates (from E_1 to E_4), again all redundant solutions are removed, using the same criterion. For the equilibrium points E_1 and E_2 the values of $\lambda_1^{E_1}$, $\lambda_2^{E_1}$, $\lambda_1^{E_2}$ and $\lambda_2^{E_2}$ are computed. For points E_3 and E_4 (possibly multiple) the stability (eigenvalues of the Jacobian) are computed numerically.

The remaining list of candidates is then used to be compared with the result of the numerical simulation. The relative error between all the candidate solutions and the result of the numerical simulation is calculated. If the smallest error between the simulated solution and the candidate solutions is smaller than 0.001, then the simulation is classified as a success and said to converge to the candidate solution closest to the simulated solution. In figure 4.6 we present a scheme on how each simulation is conducted.
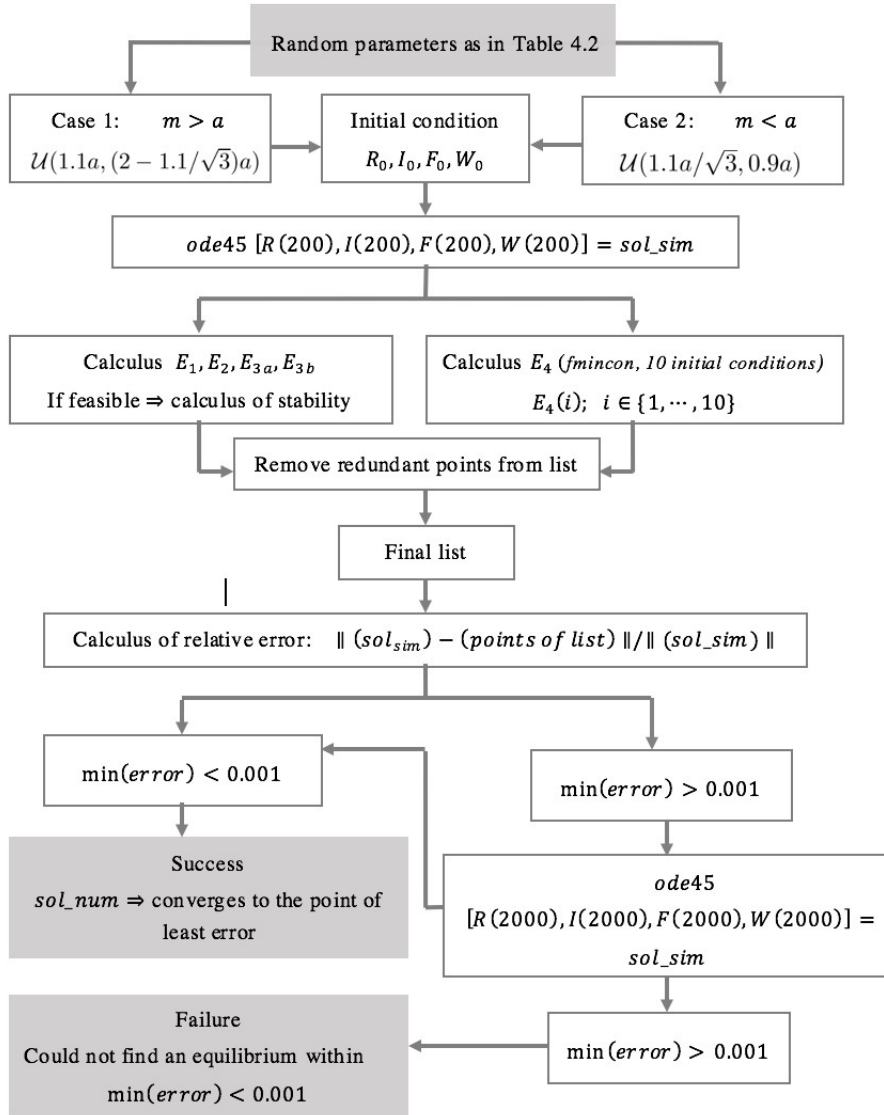
Figure 4.6: Scheme for a numerical simulation of the system. The equilibrium points, their stability and a simulated solution is computed. If the numerical solution converges to any of the computed candidate equilibrium points, the simulation is classified as a success.

As we shall show, from the results of the numerical simulations, the majority of the results of the simulations can be predicted only by analyzing the values of m (which is a critical ecological parameter) and the values related to the spread of the epidemy: $\lambda_1^{E_1}$, $\lambda_2^{E_1}$, $\lambda_1^{E_2}$ and $\lambda_2^{E_2}$. We divide the discussion according to the values of those variables.

4.6.2 Case 1: m > a

We ran 10,000 simulations with random parameters as in Table 4.2, in which $m > a$. Of this total, 9870 (98.7%) were concluded with success in the sense defined in section 4.6.1 and Figure 4.6. The results can be subdivided in two main cases, one when $\mathcal{R}_0^{E_1} < 1$ and the other when $\mathcal{R}_0^{E_1} > 1$.

$\mathcal{R}_0^{E_1} < 1$:

In 6155 (63,26%) of the total 9870 successful simulations, $\mathcal{R}_0^{E_1} < 1$. Of those, in 6143 (99.81%) the system converged to E_1 while in 12 (0.19%) cases it converged to E_3. To understand these results, we analyzed also the feasibility and stability of the other equilibrium points under these conditions.

We have shown that if $m > a$, E_2 is unfeasible, therefore, besides E_1, the system could converge to E_3 or E_4. We map the behaviour of those other two points in the simulations. For each simulation, we classify three possible states for the points E_3 and E_4:

- State 1: There are no feasible points of this type of equilibrium.

- State 2: There is at least one feasible point of this type of equilibrium, but it is unstable.

- State 3: There is at least a feasible and stable point of this type of equilibrium.

In table 4.3 we present the distribution of the results for points E_3 and E_4. It is easy to note that, for the vast majority of the simulations, the only feasible and stable point is E_1, in agreement with the result that 99.81 % of the simulations with $\mathcal{R}_0^{E_1} < 1$ converged to E_1.

The results for point E_3 can be summarized as follows: in 6136 (99.69%) we have two unfeasible points, in two (0.02%) we have two feasible and unstable points and in 17 (0.28 %) we have two feasible points of which one is stable.

The behaviour of E_4 can be summarized as follows. The 6155 simulations with $\mathcal{R}_0^{E_1} < 1$ are distributed as follows: 5301 (86.13 %) no feasible points are found, 628 (10.2%) one feasible and unstable point, 25 (0.41%) two feasible and unstable points, 130 (2.11%) one feasible and stable point, 59 (0.96%) two feasible points with one stable and 12 (0.19%) three feasible points with one stable. Thus, in the vast majority of the simulations, E_4 is either unfeasible or

Table 4.3: Distribution of states of points E_3 and E_4 when $m > a$ and $\mathcal{R}_0^{E_1} < 1$. The rows and columns represent the number of times the points E_3 and E_4, respectively, were in the states 1, 2 or 3. State 1: No feasible points of this type are found in the simulation. State 2: there is at least one feasible point of this type, but it is unstable. State 3: There is at least a feasible and stable point of this type.

E_3 \ E_4	1	2	3
1	5285 (85.87%)	652 (10.59%)	199 (3.23 %)
2	0	0	2 (0.03 %)
3	16 (0.26%)	1 (0.02%)	0

unstable. We may also observe that, since E_4 is calculated numerically it can be very close to other equilibria, but not enough to be eliminated as redundant from the candidate list.

$\mathcal{R}_0^{E_1} > 1$:

In this particular case it is possible to show that there exists a unique feasible point E_3 in the form $(R_3, I_3, 0, 0)$ (see section 4.3.2).

In 3715 (37.64%) of the total 9870 successful simulations, $\mathcal{R}_0^{E_1} > 1$. Of those, in 3567 (96.02%), the system converges to E_3 and in 148 (3.98%) it converges to E_4. In this case, E_1 is unstable, E_2 is unfeasible and the equilibria for which the solution could converge are only E_3 or E_4.

In Table 4.4 we present the distribution of the results for points E_3 and E_4, observing that E_3 can never be unfeasible in this case. It is easy to note that, for the vast majority of the simulations, the only feasible and stable point is E_3, in agreement with the result that 96.02 % of the simulations with $\mathcal{R}_0^{E_1} > 1$ converges to E_3. The only cases in which we have convergence for E_4 is in when E_3 is unstable.

Table 4.4: Distribution of states of points E_3 and E_4 when $m > a$ and $\mathcal{R}_0^{E_1} > 1$.

E_3 \ E_4	1	2	3
2	0	0	148 (3.98%)
3	3050 (82.10%)	302 (8.13%)	215 (5.79%)

The results for point E_3 can be summarized as follows: in 148 (3.98%) simulations we have one feasible and unstable point and in the other 3567 (96.02%) we obtain one feasible and stable point.

The behaviour of E_4 can be summarized as follows. Of the total 3715 simulations with $\mathcal{R}_0^{E_1} > 1$ we have: 3050 (82.10%) no feasible point found, 282 (7.59 %) one feasible and unstable point, 14 (0.38 %) two feasible and unstable

points, 6 (0.16%) three feasible and unstable points, 306 (8.24%) one feasible and stable point, 50 (1.35%) two feasible points with one stable, 2 (0.05%) three feasible points with one stable, 3 (0.08 %) four feasible points with one stable and 2 (0.05%) two stable and feasible points.

Sensitivity analysis

Since $\mathcal{R}_0^{E_1}$ has a fundamental role in the determination of the behaviour of the system, we can discuss its sensibility in relation to the parameters. In the first place, it is worth to note that, as shown in section 4.4.1 in this case, $\lambda_2^{E_1} < 1$. Therefore, point E_1 can only be destabilized through $\lambda_1^{E_1}$. The explicit relation of equation (4.14) indicates that $\lambda_1^{E_1}$ should be sensible to parameters α and λ with a positive correlation and to parameters u and μ with a negative correlation.

For each of the 9870 successful simulations, $\lambda_1^{E_1}$ is computed. Using this collection of values, we calculate the slope of the linear regression of $\lambda_1^{E_1}$ with each of the parameters. In table 4.5 we present the coefficients. As expected, the strongest correlations are those of parameters α, λ, u and μ.

Table 4.5: Regression slopes of $\lambda_1^{E_1}$ for each parameter.

Parameter	α	σ	γ	q	u	g
Slope	0.4576	0.0642	0.1734	-0.0188	-0.6930	-0.0080
Parameter	p	a	c	θ	r	m
Slope	-0.0013	0.0899	0.0503	0.0202	0.0720	0.0643
Parameter	λ	β	ν	μ	ℓ	b
Slope	0.4156	0.0045	0.0283	-0.2584	-0.0103	-0.0153

4.6.3   Case 2: $a/\sqrt{3} < m < a$

We ran 10,000 simulations with random parameters as in table 4.2, in which $m < a$. Of this total, 9001 (90.1%) are successul in the sense defined in section 4.6.1 and Figure 4.6. In this case, E_1 is always unstable, the stability of E_2 hinges on $\mathcal{R}_0^{E_2}$ and the distribution of the convergences is more complex than when $m > a$. Again, we discuss separately the two cases $\mathcal{R}_0^{E_2} < 1$ and $\mathcal{R}_0^{E_2} > 1$.

$\mathcal{R}_0^{E_2} < 1$:

In 4598 (51,08%) of the total 9001 successful simulations, $\mathcal{R}_0^{E_2} < 1$. Of those, in 4581 (99.63%) the system converges to E_2, in 16 (0.35%) cases it converges to E_3 and in 1 (0.02%) case it converges to E_4. To understand these results, we analyze also the feasibility and stability of the other equilibrium points under these conditions.

We have shown that if $m < a$, E_1 is unstable, therefore, besides E_2, the system could converge to E_3 or E_4. Just as in the examples above, we map the behaviour of those other two points in the simulations. In table 4.6 we present the distribution of the results for points E_3 and E_4. It is easy to note that, for the vast majority of the simulations, the only feasible and stable point is E_2, in agreement with the result that 99.63 % of the simulations with $\mathcal{R}_0^{E_2} < 1$ converged to E_2.

Table 4.6: Distribution of states of points E_3 and E_4 when $m < a$ and $\mathcal{R}_0^{E_2} < 1$.

E_3 \ E_4	1	2	3
1	3600 (78.29%)	273 (5.94%)	155 (3.37 %)
2	406 (8.83 %)	63 (1.37 %)	78 (1.70 %)
3	2 (0.04%)	20 (0.43%)	1 (0.02%)

The results for point E_3 can be summarized as follows. Of the total 4598 simulations with $\mathcal{R}_0^{E_2} < 1$ we obtain: 4028 (87.60%) two unfeasible points, 544 (11.83%) one feasible and unstable point, 12 (0.26 %) one feasible and stable point, 3 (0.07%) two feasible and unstable points and 11 (0.24%) two feasible points with one stable.

The behaviour of E_4 can be summarized as follows. The 4598 simulations with $\mathcal{R}_0^{E_2} < 1$ are distributed in this form: 4008 (87.17 %) no feasible points are found, 346 (7.53%) one feasible and unstable point, 9 (0.2%) two feasible and unstable points, 1 (0.02%) three feasible and unstable points, 207 (4.5%) one feasible and stable point, 26 (0.57%) two feasible points with one stable and 1 (0.02%) two feasible and stable points. Thus, in the vast majority of the simulations, E_4 is either unfeasible or unstable.

$\mathcal{R}_0^{E_2} > 1$:

In 4403 (48.92%) of the total 9001 successful simulations, $\mathcal{R}_0^{E_2} > 1$. Of those, in 2255 (51.22%) the system converges to E_4, in 2137 (48.54%) cases it converges to E_3 and in 12 (0.25%) case it converges to E_2. In the cases where the solution converge to E_2, despite its instability, were due to the fact that $\mathcal{R}_0^{E_2}$ is close to one, so the numerical solution remains quasi-stationary close to E_2 for a long period of time, in that time the relative error between E_2 and the numerical solution is estimated and found to be smaller than 0.001. Below, we present the analysis of the stability of the other equilibrium points in those simulations.

In table 4.7 we present the distribution of the results for points E_3 and E_4.

The results for point E_3 can be summarized as follows. Of the total 4403 simulations with $\mathcal{R}_0^{E_2} > 1$ we obtain: 1526 (34.66%) two unfeasible points, in 620 (14.08%) one feasible and unstable point, 2248 (51.06%) one feasible and

Table 4.7: Distribution of states of points E_3 and E_4 when $m < a$ and $\mathcal{R}_0^{E_2} > 1$.

E_3 \ E_4	1	2	3
1	0	8 (0.18%)	1518 (34.48 %)
2	0	0	622 (14.13 %)
3	1483 (33.68%)	346 (7.86%)	426 (9.68%)

stable point, 2 (0.05%) two feasible and unstable points and 7 (0.16%) two feasible points with one stable.

The behaviour of E_4 can be summarized as follows. The 4403 simulations with $\mathcal{R}_0^{E_2} > 1$ are distributed in this form: 1483 (33.68 %) no feasible points are found, 331 (7.52%) one feasible and unstable point, 20 (0.45) two feasible and unstable points, 2 (0.05%) three feasible and unstable points, 1 (0.02%) 5 feasible and unstable points, 2032 (46.15%) one feasible and stable point, 493 (11.20%) two feasible points with one stable, 28 (0.64%) three feasible points with one stable, 4 (0.09%) four feasible points with one stable, 1 (0.02%) five feasible points with one stable, 4 (0.09%) two feasible and stable points, 3 (0.07%) three feasible points with two stable ones and 1 (0.02%) four feasible points with two stable ones.

Sensitivity analysis

In this case, there is not a clear behaviour of convergence dependent only on the value of $\mathcal{R}_0^{E_2}$. In fact, it is possible to predict the vast majority of the results (see section 4.6.4) if we analyze the three eigenvalues $\lambda_1^{E_1}$, $\lambda_1^{E_2}$ and $\lambda_2^{E_2}$. Therefore, we present in Tables 4.8 and 4.9, the analysis of sensitivity for $\lambda_1^{E_2}$, $\lambda_2^{E_2}$. The sensitivity results for $\lambda_1^{E_1}$ are very similar to the case were $m > a$ (case 1).

Table 4.8: Regression slopes of $\lambda_1^{E_2}$ for each parameter.

Parameter	α	σ	γ	q	u	g
Slope	0.4764	0.2535	-1.0134	0.1274	-0.1382	0.1062
Parameter	p	a	c	θ	r	m
Slope	- 0.6685	-4.8558	-3.8989	-0.1514	0.0643	-6.1289
Parameter	λ	β	ν	μ	ℓ	b
Slope	0.0841	0.6735	-2.2916	-0.0819	0.0761	-0.0622

4.6.4 Behaviour based on m, $\lambda_1^{E_1}$, $\lambda_1^{E_2}$ and $\lambda_2^{E_2}$

Based on the results of the simulations and the stability analysis of the equilibrium points it is possible to suggest a prediction rule based on the values

Table 4.9: Regression slopes of $\lambda_2^{E_2}$ for each parameter.

Parameter	α	σ	γ	q	u	g
Slope	0.5313	0.0484	-0.0187	-0.0313	-0.3421	-0.0486
Parameter	p	a	c	θ	r	m
Slope	-0.0726	0.2256	0.1760	0.0122	0.0105	0.3220
Parameter	λ	β	ν	μ	ℓ	b
Slope	0.2590	0.0036	0.1006	-0.1795	-0.2026	-0.2385

of $\lambda_1^{E_1}$, $\lambda_1^{E_2}$ and $\lambda_2^{E_2}$. In Figure 4.7 we present the way in which the behaviour of the system can be classified. We show that, for the vast majority of the parameter space that was explored in this work, a simple analysis of the values of m, $\lambda_1^{E_1}$, $\lambda_1^{E_2}$ and $\lambda_2^{E_2}$ is enough to predict the model's behaviour. The scheme was successful in predicting the outcome of the numerical simulations in 96.35% of the simulations.
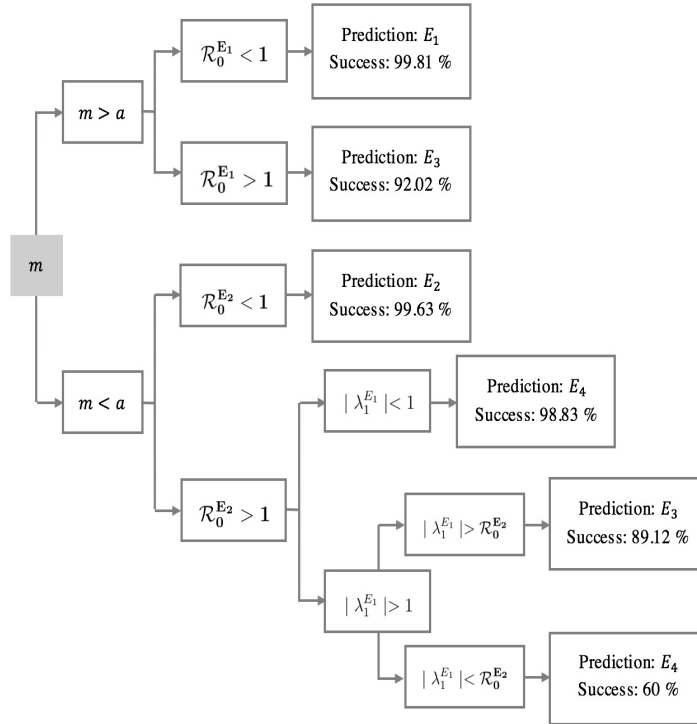

Figure 4.7: Scheme for a numerical simulation of the system. The equilibrium points, their stability and a simulated solution is computed. If the numerical solution converges to any of the computed candidate equilibrium points, the simulation is classified as a success.

4.7 Conclusions

In this work we presented an model for the study of prey-predator dynamics
with the presence of disease and herd behaviour. The theoretical analysis
and the numerical simulations suggest that, in the majority of the parameter
combinations studied, the behaviour of the model can be predicted by the
analysis of just four fundamental quantities in the system (m, $\lambda_1^{E_1}$, $\lambda_1^{E_2}$ and
$\lambda_2^{E_2}$).

The first fundamental quantity is the natural mortality rate of predators,
which is crucial to define the survival of the predator species. Since the mor-
tality of diseased predators is supposed to be equal or higher than the the
mortality of healthy ones, parameter m plays a determinant role in the dy-
namics of the system.

The second, third and fourth fundamental quantities are the values of $\mathcal{R}_0$
(basic reproduction number) calculated in the two disease-free equilibria of
the system (E_1 and E_2): $\mathcal{R}_0^{E_1}$ and $\mathcal{R}_0^{E_2}$. Sensitivity analysis through linear
regression between the parameters has shown that the parameter with the
strongest influence is $\mathcal{R}_0^{E_1}$.

Parameters α and λ are related to the vertical and horizontal transmission
rates, respectively, and have a positive correlation with $\mathcal{R}_0^{E_1}$. Parameters u
(influence intra-specific competition between healthy and diseased prey on the
infected prey population) has a negative effect on the spread of the disease.
Therefore, it is clear that a species with the behaviour of marginalizing or
being hostile to the diseased individuals reduces the chance of permanence of
an epidemics in the population.

The analysis of sensitivity for $\mathcal{R}_0^{E_2}$, involves two eigenvalues $\lambda_1^{E_2}$ and $\lambda_2^{E_2}$.
The strongest positive correlation between the first one and the parameters
occurs for parameters α and β. Thus, again, vertical transmission in prey
plays an important role in the maintenance of the disease. Interestingly, the
horizontal transmission in the predator population (β) plays a more important
role in the destabilization of the disease-free coexistence than the horizontal
transmission between prey (λ). Strong negative correlations were observed for
parameters a and m. For the sensitivity of $\lambda_2^{E_2}$, again, α displayed a strong
positive correlation, followed by parameters m and λ (horizontal transmission).
Parameters u and b (mortality of diseased preys) displayed the strongest ne-
gative correlation.

Given the importance of parameters α, λ and u, our results suggest that
the removal of diseased-prey may be the most effective strategy to lead the
system to a disease-free equilibrium.

Appendix A

In section 4.3.1 we saw that $E_3 = (R_3, I_3, 0, 0)$, where $I_3 = \frac{\alpha - \mu}{q} + \frac{\lambda - u}{q} R_3$ and R_3 given by the roots of the quadratic equation

$$\Phi(R_3) = \alpha_2 R_3^2 + \alpha_1 R_3 + \alpha_0 = 0$$

with

$$\alpha_2 = \frac{-q - g\lambda - \lambda^2 + gu + \lambda u}{q}, \quad \alpha_0 = \frac{(\alpha - 1)\mu r - \alpha^2 r + \alpha r}{q}$$

and

$$\alpha_1 = \frac{(1 - \alpha)r\lambda + \mu\lambda - \alpha\lambda - (1 - \alpha)ru + q + g\mu - \alpha g}{q}.$$

For $R_3 \geq 0$ we have the conditions for two positive roots given by

$$\Delta = \alpha_1^2 - 4\alpha_2\alpha_0 > 0, \quad -\alpha_1\alpha_2^{-1} > 0, \quad \alpha_0\alpha_2^{-1} > 0$$

and for at least one positive root we have

$$\Delta = \alpha_1^2 - 4\alpha_2\alpha_0 > 0, \quad \alpha_0\alpha_2^{-1} < 0.$$

Explicit, $\Delta = \alpha_1^2 - 4\alpha_2\alpha_0 > 0$ is given by

$$\alpha^2 r^2 \lambda^2 + 4gru\mu + 2\alpha\mu r\lambda^2 + 2\alpha r\lambda^2 + 4\alpha r^2 u\lambda + 2\alpha\mu ru\lambda + 2gru\lambda\alpha$$
$$+2gru^2 + \mu^2\lambda^2 + 2\alpha ru\lambda + 2gu\mu\lambda + 2qr\lambda + 2\lambda gr\alpha^2 + 2q\mu\lambda + 2g\lambda\alpha^2$$
$$+r^2 u^2 \alpha^2 + r^2 u^2 + \alpha^2\lambda^2 + g^2 u^2 + 2qru\alpha + r^2\lambda^2 + 4ru\mu + 2gru\alpha^2 + q^2$$
$$+g^2\alpha^2 + 4rq\alpha + 4rq\mu\alpha + 4gr\mu\alpha + 4gr^2\alpha + 4ru\alpha^2 > 2r^2\alpha\lambda^2 + 2\mu r\lambda^2$$
$$+2r\lambda^2\alpha^2 + 2\alpha\mu\lambda^2 + 2q\alpha\lambda + 2r^2 u\lambda + 2ru\mu\lambda + 2gru\alpha\lambda + 2\alpha^2 ru\lambda$$
$$+2\alpha^2 ru\lambda + 2gu\alpha\lambda + 2qr\alpha\lambda + 2\alpha^2 r^2 u\lambda + 2gr\alpha\lambda + 2g\mu\alpha\lambda + 2r^2 u^2\alpha$$
$$+2gru^2 + 2qru + 4gru\mu\alpha + 4gru\mu\alpha + 4ru\mu\alpha + 2gru\alpha + 4ru\alpha$$
$$+2g^2 u\alpha + 4urq + 4rq\alpha^2 + 4gr\mu + 4gr\alpha^2 + 2gq\alpha,$$

for $-\alpha_1\alpha_2^{-1} > 0$ we have

$$r\lambda + \mu\lambda + \alpha ru + q + gu > r\alpha\lambda + \alpha\lambda + ru + \alpha g,$$

$$\lambda^2 + g\lambda + q > u\lambda + gu$$

or

$$r\lambda + \mu\lambda + \alpha ru + q + gu < r\alpha\lambda + \alpha\lambda + ru + \alpha g,$$

$$\lambda^2 + g\lambda + q < u\lambda + gu,$$

for $\alpha_0 \alpha_2^{-1} > 0$ we have

$$\mu < \alpha, \quad \alpha > 1, \quad \lambda^2 + g\lambda + q > u\lambda + gu$$

or

$$\mu > \alpha, \quad \alpha < 1, \quad \lambda^2 + g\lambda + q > u\lambda + gu$$

or

$$\mu > \alpha, \quad \alpha > 1, \quad \lambda^2 + g\lambda + q < u\lambda + gu$$

or

$$\mu < \alpha, \quad \alpha < 1, \quad \lambda^2 + g\lambda + q < u\lambda + gu$$

and , for $\alpha_0 \alpha_2^{-1} < 0$ we have

$$\mu < \alpha, \quad \alpha > 1, \quad \lambda^2 + g\lambda + q < u\lambda + gu$$

or

$$\mu > \alpha, \quad \alpha < 1, \quad \lambda^2 + g\lambda + q < u\lambda + gu$$

or

$$\mu > \alpha, \quad \alpha > 1, \quad \lambda^2 + g\lambda + q > u\lambda + gu$$

or

$$\mu < \alpha, \quad \alpha < 1, \quad \lambda^2 + g\lambda + q > u\lambda + gu.$$

CHAPTER 5

A PROPOSAL FOR MODELING HERD BEHAVIOUR IN POPULATION SYSTEMS

The interactions between two populations can be described using various approaches. In particular, Lotka-Volterra systems have played an important role in the development of mathematical ecology, for example, in the analysis of thophic webs [1]. Lotka-Volterra systems are based on the very simple assumption that intensity of the interactions between the species, be it of symbiosis, competition or of prey-predator type, follow a simple mass action law. Therefore, a natural development of the field was the proposition of alternative "response functions" to describe the interactions, such as the classical Holling Type I and II [45]. In [47] an excellent review of the development of such models is presented.

More recently, new models have been proposed to describe "herd behaviour", [3, 83]. Such models seek to incorporate the effect of group behaviour in the interactions between populations, such as the formation of a boundary that protects the individuals in its interior [40]. The models proposed displayed novel behaviour that was not observed in the traditional Lotka-Volterra systems [2]. In this way, particular qualities of the systems, such as the shape of the herd or the dimension of the space in which the interactions occurs could be modeled implicitly through the interaction term, without explicit spatial description.

Despite such advantages, the proposed models have a drawback: group effects usually require a minimum number of individuals to be observed. In this Chapter we propose a modification of the previous "herd models" to incorporate this factor in the dynamics. Therefore, we include a threshold for which the interactions between the population shift from a Lotka-Volterra type in-

teraction to a "herd type" interaction. In this way, topics of planar continuous piecewise differential systems arise naturally in the analysis of the models.

In this work, we want to clarify some bifurcation phenomena that can appear in planar continuous piecewise differential systems with two zones. In particular, we highlight the simplest case of boundary equilibrium bifurcation, similar to the one introduced in [71].

The Chapter is organized as follows. Section 2 presents a response function for the predator-prey model which is detailed in Section 5.2. In Section 5.2.1 is proved that the trajectories of the model remain confined within a compact set. Section 5.2.2 brings a nondimensionalized version of the model and in Section 5.3 a detailed analysis of local stability is performed, including a topological interpretation of the results. In Section 5.4 the possible bifurcations are analytically investigated and numerical simulations are performed to illustrate the behaviour and in Section 5.5 we present a brief theoretical contribution. A biological interpretation and a discussion of the theoretical results is done in section 5.6. Finally, a brief section of conclusions finishes the Chapter.

5.1   Response function

In [2] a predator-prey model is proposed in which the prey is assumed to be highly sociable while the predator has a more individualistic behaviour. The sociable characteristic of the prey is described as an interaction term proportional to the square root of the total population. Such term represents the effects of group defense in which strongest individuals surround weaker ones, such as calfs. The formation of a herd may restrict the access of the predators to the prey, limiting the attacks to those situated at the boundaries of the group.

Mathematically, this biological behaviour can be represented by assuming that from the total $\widehat{R}$ prey population distributed in a certain area A, only the individuals at the boundary will be exposed to attacks. The total number of individuals in the boundary should be proportional to the perimeter of the area A which, in turn, is proportional to $\sqrt{\widehat{R}}$, the exact constant of proportionality being dependent on the geometry of the herd.

Such interaction term is reasonable if we consider "large" $\widehat{R}$ populations, capable of displaying group defense. If a group is too small it may not be possible to form an appropriate group defense or the boundary of the herd may be composed of the totality of the population. For such small groups it would be more reasonable to adopt a traditional Lotka-Volterra interaction term proportional to the population of prey. Therefore, if $\widehat{F}$ is the population of predators, we could separate the interaction term in two distinct forms: $\widehat{a}\sqrt{\widehat{R}}\widehat{F}$, valid for large populations and $\frac{\widehat{a}}{\sqrt{R^*}}\widehat{R}\widehat{F}$, valid for small populations.

In this manner, the interaction in the model can be described as a piecewise

function:

$$\widehat{g}(\widehat{R}) = \begin{cases} \frac{\widehat{R}}{\sqrt{R^*}} & \text{if } 0 < \widehat{R} \leq R^* \\ \sqrt{\widehat{R}} & \text{if } R^* < \widehat{R} \end{cases} \tag{5.1}$$

where R^* represents a critical threshold of group size for effective defense. Note that in this way g is a C^0 function. In this way, when the prey population size is large, the herd effect is accounted for. When it falls below the threshold R^*, we can say that the herd disperses into a bunch of almost individualistically behaving individuals, so that the hunting occurs classically on a one-to-one basis, and the Mass Action Law is the tool used to model it.

5.2 The predator-prey model

Using the response function defined by (5.1), we propose the following predator-prey model:

$$\begin{aligned} \frac{d\widehat{R}}{d\tau} &= r\left(1 - \frac{\widehat{R}}{K}\right)\widehat{R} - a\widehat{g}(\widehat{R})\widehat{F} \\ \frac{d\widehat{F}}{d\tau} &= -m\widehat{F} + ea\widehat{g}(\widehat{R})\widehat{F} \end{aligned} \tag{5.2}$$

where $\widehat{g}(\widehat{R})$ is given by (5.1) and all the parameters are assumed to be non-negative. In model (5.2) the first equation describes the evolution of the $\widehat{R}$ population.

The dynamics for $\widehat{R}$ contains two components: a logistic growth and a predation term. The logistic growth represents the assumption that, without predation, the prey population will grow up to a carrying capacity. Parameters r and K describe the speed of growth and the total carrying capacity, respectively.

Predation is described by the term $a\widehat{g}(\widehat{R})\widehat{F}$, meaning group defense above the threshold group size R^* and traditional mass action law below it. Parameter a incorporates efficiency of predators and the prey's mechanisms of defense.

The dynamics of $\widehat{F}$ is also composed by two components: a mortality term proportional to the population and a reproduction one dependent on the predation rate. In the absence of prey, the predator is assumed to go extinct, parameter m describes the speed of this process. By modelling the reproduction term as proportional to the predation rate, we are asserting that the predator is a very specialized one that depends exclusively on the specific prey to survive. Parameter e wich has units [units of predator]/[units of prey] represents a "conversion rate" from predation to reproduction.

Similarly to [31], the system (5.2) is Lipschitz and so it satisfies the standard results on existence and uniqueness of solution as well as its continuous depen-

dence with respect to the initial conditions and parameters. Furthermore, the Poincaré-Bendixson's theorem can be extended to cover this system, see [16].

5.2.1 Boundedness of the model

Since we are analysing an ecological model, the variables cannot grow unboundedly. Thus, in order to have a well-posed model, it is necessary to show that the system's trajectories remain confined within a compact set as shown in the following proposition. In the following proof we will assume $e \leq 1$, wich surely is the case it both populations are described in terms of biomass. Consider the total environment population $\varphi(\tau) = \widehat{R}(\tau) + \widehat{F}(\tau)$, then we have the following result.

Proposition 5.2.1. *There exists $m > 0$ for which the solutions of (5.2) are always non-negative and bounded:*

$$\varphi(\tau) \leq \left(\varphi(0) - \frac{M}{m} \right) e^{-m\tau} + \frac{M}{m} \leq \max\left\{ \varphi(0), \frac{M}{m} \right\}. \qquad (5.3)$$

Proof. Now $\varphi(\tau)$ is a differentiable function, then taking $m > 0$, summing the equations in model (5.2) and observing that $e \leq 1$ we find

$$\frac{d\varphi(\tau)}{d\tau} + m\varphi(\tau) = r \left(1 - \frac{\widehat{R}}{K} + \frac{m}{r} \right) \widehat{R} + a\widehat{g}(\widehat{R})\widehat{F}(e - 1)$$

$$\leq r \left(1 - \frac{\widehat{R}}{K} + \frac{m}{r} \right) \widehat{R} = p(\widehat{R}).$$

The function $p(\widehat{R})$ is concave parabola, with maxima located at $\widehat{R}_{max}$, and corresponding maximum value

$$M = p(\widehat{R}_{max}) = \frac{rK}{4} \left(1 + \frac{m}{r} \right)^2.$$

Thus, $\varphi(\tau)' + m\varphi(\tau) \leq M$. Integrating the differential inequality, we find (5.3). Thus, for model (5.2) the solution remains bounded. That trajectories remain non-negative follows directly from the facts that $\widehat{R}' = 0$ if $\widehat{R} = 0$, $\widehat{F}' = 0$ if $\widehat{F} = 0$ and that initial conditions for the model should always be non-negative to make biological sense. $\qquad \square$

5.2.2 Non-dimensional model

Model (5.2) can be nondimensionalized via $R(t) = \frac{1}{K}\widehat{R}(\tau)$, $F(t) = \frac{1}{eK}\widehat{F}(\tau)$, $t = m\tau$ and $\lambda = \frac{r}{m}$, $\theta = \frac{ae\sqrt{K}}{m}$ to get the rescaled system:

$$\frac{dR}{dt} = \lambda R(1 - R) - \theta g(R)F$$
$$\frac{dF}{dt} = -F + \theta g(R)F \qquad (5.4)$$

and the interaction between prey and predators in the non-dimensional model can be described as a piecewise function:

$$g(R) = \begin{cases} \dfrac{R}{\sqrt{\tilde{R}}} & \text{if } 0 < R \leq \tilde{R} \\ \sqrt{R} & \text{if } \tilde{R} < R \end{cases}$$

where $0 < \tilde{R} < 1$ is the critical threshold of group size for effective defense.

5.3   Equilibria and local stability analysis

The vertical and horizontal isoclines are

$$R = 0, \quad F = \frac{\lambda R(1 - R)}{\theta g(R)} \tag{5.5}$$

and

$$F = 0, \quad g(R) = \frac{1}{\theta} = \mu. \tag{5.6}$$

where we introduced the bifurcation parameter μ. Thus we can rewrite the equation $g(R) = \mu$ as

$$R = g^{-1}(\mu) = \begin{cases} \mu\sqrt{\tilde{R}} & \text{if } 0 < \mu \leq \sqrt{\tilde{R}}; \\ \mu^2 & \text{if } \mu > \sqrt{\tilde{R}}. \end{cases}$$

The system equilibria are the ecosystem collapse $E_1 = (0,0)$, the prey-only point $E_2 = (1,0)$ and coexistence:

$$E_3 = \begin{cases} \left(\mu\sqrt{\tilde{R}}, \lambda\mu\sqrt{\tilde{R}}\left(1 - \mu\sqrt{\tilde{R}}\right)\right) = E_{3L} & \text{if } \mu \leq \sqrt{\tilde{R}}; \\ (\mu^2, \lambda\mu^2\left(1 - \mu^2\right)) = E_{3R} & \text{if } \mu > \sqrt{\tilde{R}}. \end{cases}$$

Figure 5.1 illustrates the vertical (5.5) and horizontal isoclines (5.6), and equilibria E_1, E_2 and E_3, for the chosen parameters values.

The Jacobian matrix of system (5.4) is given by

$$J = \begin{pmatrix} \lambda - 2\lambda R - \dfrac{\partial g(R)}{\partial R}\dfrac{F}{\mu} & -\dfrac{g(R)}{\mu} \\ \dfrac{\partial g(R)}{\partial R}\dfrac{F}{\mu} & -1 + \dfrac{g(R)}{\mu} \end{pmatrix}. \tag{5.7}$$

Proposition 5.3.1. *Consider the continuous piecewise differential system* (5.4), *with* $0 < \tilde{R} < 1$. *The following statements hold.*

(a) *Equilibrium point* $E_1 = (0,0)$ *is a saddle.*
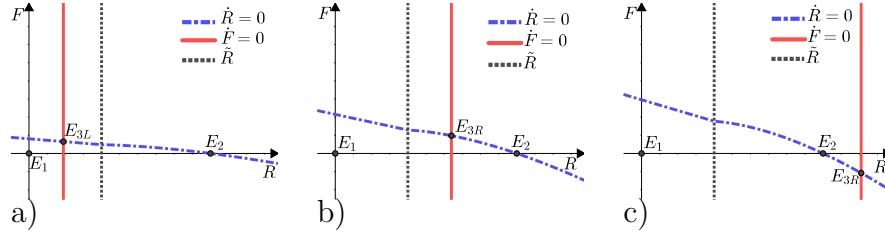
Figure 5.1: Vertical and horizontal isoclines given by equations (5.5) and (5.6). $E_1 = (0,0)$, $E_2 = (1,0)$ and E_3 are the equilibria obtained from system (5.2). Here, μ is the variation parameter and $\tilde{R} = 0.4$ and $\lambda = 8.5$. a) $\mu = 0.3$ and $E_3 = (\mu\sqrt{\tilde{R}}, F_{3L})$. b) $\mu = 0.8$ and $E_{3R} = (\mu^2, F_{3R})$. c) $\mu = 1.1$ and $E_3 = (\mu^2, F_{3R})$.

(b) *If $\mu > 1$, then equilibrium point $E_2 = (1,0)$ is a stable node, on the contrary, if $\mu < 1$, then equilibrium point $E_2 = (1,0)$ is a saddle.*

Proof.

(a) The eigenvalues of the Jacobian at E_1 are $\xi_1 = \lambda$ and $\xi_= -1$, showing that it is a saddle.

(b) At E_2 the eigenvalues are $\xi_1 = -1 + \frac{1}{\mu}$ and $\xi_2 = -\lambda$, giving the stability condition

$$\mu > 1. \tag{5.8}$$

If (5.8) is violated, then E_2 is a saddle. $\qquad\square$

Proposition 5.3.2. *Consider the continuous piecewise differential system (5.4), with $0 < \tilde{R} < 1$. Then there are five critical values $\bar{\mu}_0$, μ_1, μ_2, μ_3 and μ_4 given by*

$$\bar{\mu}_0 = \frac{2(\sqrt{1+\lambda}-1)}{\lambda\sqrt{\tilde{R}}}, \quad \mu_1 = \sqrt{\frac{-4+3\lambda-4\sqrt{1+3\lambda}}{9\lambda}},$$

$$\mu_2 = \frac{\sqrt{3}}{3}, \quad \mu_3 = \sqrt{\frac{-4+3\lambda+4\sqrt{1+3\lambda}}{9\lambda}}, \quad \mu_4 = 1,$$

such that the following statements hold.

  (a) *For $0 < \mu < \sqrt{\tilde{R}}$:*
- *if $0 < \mu \le \bar{\mu}_0$, then the equilibrium point E_{3L} is a stable focus ;*
- *if $\bar{\mu}_0 < \mu$, then the equilibrium point E_{3L} is a stable node.*

  (b) *For $\mu \ge \sqrt{\tilde{R}}$ and $\lambda > 8$:*
- *if $0 < \mu < \mu_1$, then the equilibrium point E_{3R} is a unstable node;*
- *if $\mu_1 < \mu < \mu_2$, then the equilibrium point E_{3R} is a unstable focus.*

(c) *For $\mu \geq \sqrt{\tilde{R}}$ and $\lambda \leq 8$:*
  - *if $0 < \mu < \mu_2$, then the equilibrium point E_{3R} is a unstable focus.*

(d) *For $\mu \geq \sqrt{\tilde{R}}$:*
  - *if $\mu_2 < \mu < \mu_3$, then the equilibrium point E_{3R} is a stable focus;*
  - *if $\mu_3 < \mu < \mu_4$, then the equilibrium point E_{3R} is a stable node;*
  - *if $\mu_4 < \mu$, then the equilibrium point E_{3R} is a saddle.*

Proof.

(a) For the Jacobian evaluated at equilibrium points E_{3L} and E_{3R} we find now

$$\operatorname{tr}(J_{E_{3L}}) = -\lambda\mu\sqrt{\tilde{R}} < 0, \quad \det(J_{E_{3L}}) = \lambda(1 - \mu\sqrt{\tilde{R}}) > 0,$$

$$\Delta_{E_{3L}}(\mu) = \operatorname{tr}(J_{E_{3L}})^2 - 4\det(J_{E_{3L}}) = \lambda^2\tilde{R}\mu^2 + 4\lambda\sqrt{\tilde{R}}\mu - 4\lambda.$$

To assess stability, let us consider $\Delta_{E_{3L}}$ as a function of μ. Then $\Delta_{E_{3L}}(\mu) = 0$ provides only one positive real root,

$$\bar{\mu}_0 = \frac{2(\sqrt{1 + \lambda} - 1)}{\lambda\sqrt{\tilde{R}}}.$$

For $\mu = \bar{\mu}_0$ the function $\Delta_{E_{3L}}(\mu)$ exhibits a sign change: $\Delta_{E_{3L}}(\mu) > 0$ if and only if $\mu > \bar{\mu}_0$. It follows that for $\bar{\mu}_0 \leq \mu < \sqrt{\widehat{R}}$ the point E_{3L} is a stable node, while conversely is a stable focus.

Before starting the proof of statements **(b)**–**(d)**, we present some preliminary results. For the Jacobian matrix (5.7) evaluated at E_{3R}

$$\operatorname{tr}(J_{E_{3R}}) = \frac{\lambda(1 - 3\mu^2)}{2}, \quad \det(J_{E_{3R}}) = \frac{\lambda(1 - \mu^2)}{2}$$

and $\Delta_{E_{3R}} = \operatorname{tr}(J_{E_{3R}})^2 - 4\det(J_{E_{3R}}) = \frac{\lambda}{4}(9\lambda\mu^4 + (8 - 6\lambda)\mu^2 - 8 + \lambda).$

Now making the coordinate change $s = \mu^2$ and considering $\Delta_{E_{3R}}(s) = 0$, we have

$$\frac{\lambda}{4}(9\lambda s^2 + (8 - 6\lambda)s - 8 + \lambda) = 0 \tag{5.9}$$

Solving (5.9) for s, we obtain the non-negative solutions

$$s_1 = \frac{-4 + 3\lambda - 4\sqrt{1 + 3\lambda}}{9\lambda} \quad \text{if } \lambda \geq 8; \quad s_3 = \frac{-4 + 3\lambda + 4\sqrt{1 + 3\lambda}}{9\lambda}.$$

Thus, the function

$$\Delta_{E_{3R}}(\mu) = \frac{\lambda}{4}(9\lambda\mu^4 + (8 - 6\lambda)\mu^2 - 8 + \lambda)$$

changes sign at $\mu_1 = \sqrt{s_1}$ and $\mu_3 = \sqrt{s_3}$. If $0 < \lambda < 8$ then $\Delta_{E_{3R}}$ is negative if and only if $0 < \mu < \mu_3$. For $\lambda > 8$ then $\Delta_{E_{3R}}$ is negative if and only if $\mu_1 < \mu < \mu_3$. In summary, for $\mu > 0$ we find

(i) $\det(J_{E_{3R}}) > 0$ if and only if $0 < \mu < \mu_4$.

(ii) $\mathrm{tr}(J_{E_{3R}}) < 0$ if and only if $0 < \mu < \mu_2$.

(iii) If μ_1 is feasible, i.e. $\lambda \geq 8$, then $\Delta_{E_{3R}} < 0$ if and only if $\mu_1 < \mu < \mu_3$.

(iv) If μ_1 is not feasible, i.e. $0 < \lambda < 8$, then $\Delta_{E_{3R}} < 0$ if and only if $0 < \mu < \mu_3$.

We can now to prove the statement **(b)**. Since $0 < \mu_1 < \mu_2 < \mu_3 < \mu_4$, if $0 < \mu < \mu_1$ then:

- $0 < \mu < \mu_4$, by (i) it follows that $\det(J_{E_{3R}}) > 0$;

- $0 < \mu < \mu_2$, by (ii) it follows that $\mathrm{tr}(J_{E_{3R}}) < 0$;

- $0 < \mu < \mu_3$, by (iii) it follows that $\Delta_{E_{3R}} > 0$.

Therefore, if $0 < \mu < \mu_1$ then E_{3R} is a stable node.

On the other hand, an unstable focus arises from the above first two conditions together with $\mu_1 < \mu < \mu_2 < \mu_3$; from (iii) it follows $\Delta_{E_{3R}} < 0$.

The proof of (c) and (d) are similar and therefore omitted. □

5.4 Bifurcations and numerical simulations

The equilibrium E_2 cannot give rise to oscillations, since the eigenvalues are all real. Instead, point E_{3R} goes through a supercritical Hopf bifurcation, giving rise to a stable limit cycle. To prove this we use second-order conditions, [53].

Proposition 5.4.1. *Consider the continuous piecewise differential system* (5.4), *with* $\tilde{R} \leq R$ *and* $\tilde{R} < 1$. *Taking* μ *as the variation parameter with* $\sqrt{\tilde{R}} < \mu$, *the following statements hold:*

(a) *There is a transcritical bifurcation between equilibria* E_2 *and* E_{3R} *when* μ *crosses the critical value* $\mu_4 = 1$.

(b) *A stable limit cycle arises at* $\mu_2 = \frac{\sqrt{3}}{3}$ *from a supercritical Hopf bifurcation, when* E_{3R} *becomes unstable.*

Proof.

(a) The equilibrium point E_2 coincides with the coexistence equilibrium E_{3R} at the parametric threshold $\mu_4 = 1$. The Jacobian matrix of system (5.4), evaluated at E_2 and at the parametric threshold $\mu_4 = 1$ is

$$J_{E_2}(\mu_4) = \begin{pmatrix} -\lambda & 1 \\ 0 & 0 \end{pmatrix},$$

and its right and left eigenvectors, corresponding to the zero eigenvalue, are $V = \varphi(1, -\lambda)^T$ and $Q = \psi(0, 1)^T$, where φ and ψ are arbitrary nonzero real numbers. Consider $g(R) = \sqrt{R}$ in the system (5.4) we obtain

$$
\begin{aligned}
\frac{dR}{dt} &= \lambda R(1 - R) - \frac{\sqrt{R}F}{\mu} := f_1 \\
\frac{dF}{dt} &= -F + \frac{\sqrt{R}F}{\mu} := f_2.
\end{aligned}
\tag{5.10}
$$

Differentiating partially the right hand sides of the system (5.10) with respect to μ we find

$$
f_\mu = \begin{pmatrix} \frac{\sqrt{R}F}{\mu^2} \\ -\frac{\sqrt{R}F}{\mu^2} \end{pmatrix}.
$$

Now, calculating the Jacobian matrix of (5.10) in which the elements of this matrix are differentiated with respect to μ and then evaluated at E_2 and at $\mu^\dagger$ we get

$$
Df_\mu = \begin{pmatrix} 0 & 1 \\ 0 & -1 \end{pmatrix}.
$$

In order to verify the Sotomayor's conditions for the existence of a transcritical bifurcation, [70], we consider $D^2 f((R, F); \mu)(V, V)$ defined by

$$
\begin{pmatrix}
\frac{\partial^2 f_1}{\partial R^2}\xi_1^2 + 2\frac{\partial^2 f_1}{\partial R \partial F}\xi_1\xi_2 + \frac{\partial^2 f_1}{\partial F^2}\xi_2^2 \\
\frac{\partial^2 f_2}{\partial R^2}\xi_1^2 + 2\frac{\partial^2 f_2}{\partial R \partial F}\xi_1\xi_2 + \frac{\partial^2 f_2}{\partial F^2}\xi_2^2
\end{pmatrix},
$$

where ξ_1, ξ_2 are the components of the eigenvector V. The calculation of $D^2 f$ shows then that the following three conditions for a transcritical bifurcation are satisfied

$$
\begin{aligned}
Q^T f_\mu(E_2; \mu_4) &= 0, \quad Q^T Df_\mu(E_2; \mu_4)V = \varphi\psi\lambda \neq 0, \\
Q^T D^2 f(E_2; \mu_4)(V, V) &= -\varphi^2\psi\lambda \neq 0.
\end{aligned}
$$

(b) For systems in two-dimensional spaces, a Hopf bifurcation may occur. The Jacobian matrix evaluated at E_{3R} has conjugate imaginary eigenvalues

$$
\Lambda_\pm = \frac{\tau \pm \sqrt{P(\mu)}}{4}, \quad \tau = \lambda(1 - 3\mu^2), \quad P(\mu) = \lambda^2(9\mu^4 - 6\mu^2 + 1) + \lambda(8\mu^2 - 8).
$$

Since $P(\mu)$ is continuous, $\tau(\mu_2) = 0$ and $P(\mu_2) = -\frac{16\lambda}{3} < 0$, there is an interval $T = (\mu_2 - \epsilon, \mu_2 + \epsilon)$ around μ_2, such that, $P(x) < 0$ whenever $x \in T$.

The transversality condition is satisfied: $\tau'(\mu)|\mu_2 = -3\sqrt{3} \neq 0$.

Moreover, the Hopf bifurcation at equilibrium E_{3R} is supercritical. Letting $x = R - R_{3R}$ and $y = F - F_{3R}$, the third-order Taylor series expansion for (5.10) evaluated at E_{3R} is given by

$$
\begin{aligned}
S(x,y) &= S_{R_{3R}}x + H_{F_{3R}}y + \frac{1}{2!}(S_{R_{3R}R_{3R}}x^2 + 2S_{R_{3R}F_{3R}}xy \qquad (5.11)\\
&+ S_{F_{3R}F_{3R}}y^2) + \frac{1}{3!}(S_{R_{3R}R_{3R}R_{3R}}x^3 + 3S_{R_{3R}R_{3R}F_{3R}}x^2y\\
&+ 3S_{R_{3R}F_{3R}F_{3R}}xy^2 + S_{F_{3R}F_{3R}F_{3R}}y^3)
\end{aligned}
$$

and

$$
\begin{aligned}
H(x,y) &= H_{R_{3R}}x + S_{F_{3R}}y + \frac{1}{2!}(H_{R_{3R}R_{3R}}x^2 + 2H_{R_{3R}F_{3R}}xy \qquad (5.12)\\
&+ H_{F_{3R}F_{3R}}y^2) + \frac{1}{3!}(H_{R_{3R}R_{3R}R_{3R}}x^3 + 3H_{R_{3R}R_{3R}F_{3R}}x^2y\\
&+ 3H_{R_{3R}F_{3R}F_{3R}}xy^2 + H_{F_{3R}F_{3R}F_{3R}}y^3).
\end{aligned}
$$

Thus, for R_{3R} and F_{3R} evaluated at μ_2 we obtain from (5.11) and (5.12) $S(x,y) = x' = -y + f(x,y)$, $H(x,y) = y' = \frac{1}{3}\lambda x + g(x,y)$, respectively, with

$$
\begin{aligned}
f(x,y) &= -\frac{3\lambda}{4}x^2 - \frac{3}{2}xy - \frac{3\lambda}{8}x^3 + \frac{9}{8}x^2y\\
g(x,y) &= -\frac{\lambda}{4}x^2 + \frac{3}{2}xy + \frac{3\lambda}{8}x^3 - \frac{9}{8}x^2y.
\end{aligned}
$$

In addition, x' and y; can be put into the following form by suitable changes of variables multiplying $\dot{x}$ by A^{-1} and $\dot{y}$ by B^{-1} with $A = 1$, $B = \frac{\sqrt{3\lambda}}{3}$, $u = \frac{x}{A}$ and $v = \frac{y}{B}$. Then,

$$
\dot{u} = -\omega v + f(u,v), \quad \dot{u} = \omega u + g(u,v),
$$

where the frequency of the limit cycle is given approximately by $\omega = \frac{\sqrt{3\lambda}}{3}$ and

$$
\begin{aligned}
f(u,v) &= -\frac{3\lambda}{4}u^2 - \frac{\sqrt{3\lambda}}{2}uv - \frac{3\lambda}{8}u^3 + \frac{3\sqrt{3\lambda}}{8}u^2v,\\
g(u,v) &= -\frac{\sqrt{3\lambda}}{4}u^2 + \frac{3}{2}uv + \frac{3\sqrt{3\lambda}}{8}u^3 - \frac{9}{8}u^2v.
\end{aligned}
$$

Finally, according to the analytic criterion provided by [36], we have a supercritical Hopf bifurcation because $\phi < 0$ where

$$
\begin{aligned}
\phi &= \frac{1}{16}(f_{uuu} + f_{uvv} + g_{uuv} + g_{vvv}) + \frac{1}{16\omega}[f_{uv}(f_{uu} + f_{vv}) - (g_{uv}(g_{uu} + g_{vv})\\
&- f_{uu}g_{uu} + f_{vv}g_{vv})] = -\frac{9\lambda}{64} < 0
\end{aligned}
$$

and the subscripts denote partial derivatives evaluated at $(0,0)$. $\qquad \square$
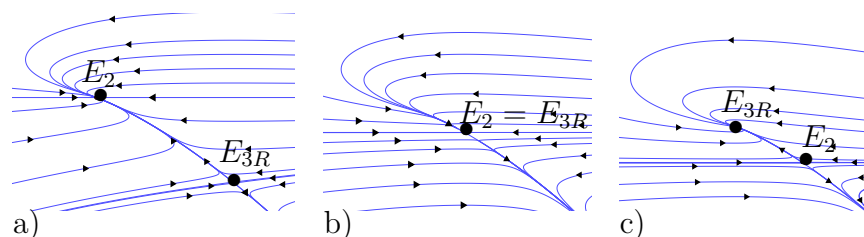
Figure 5.2: There is a transcritical bifurcation due to an exchange of stability between the equilibrium points E_2 and E_{3R} when we consider μ as a variation parameter and $\lambda = 0.258$. a) Here, E_2 is a stable node and E_{3R} is a saddle for $\mu = 1.096$. b) $E_{3R} = E_2$ is a nonhyperbolic equilibrium point for $\mu = 0.9998$. c) E_2 is a saddle and E_{3R} is a stable node for $\mu = 0.9489$. The threshold parameter value is $\tilde{R} = 0.138$.

Figure 5.2 illustrates the simulation explicitly showing the transcritical bifurcation between E_2 and E_{3R} for the chosen parameters values when the parameter μ crosses a critical value $\mu_4 = 1$.

Figure 5.3 illustrates the Hopf bifurcation of equilibrium point E_{3R} at $\mu_2 = \frac{\sqrt{3}}{3}$ for the chosen parameters values.
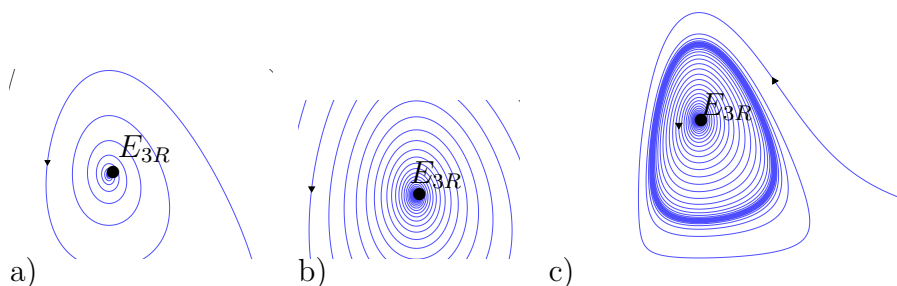
Figure 5.3: Considering μ as a variation parameter and $\lambda = 1.5981$ a limit cycle arises from equilibrium point E_{3R}, indicating a Hopf bifurcation. a) Here, E_{3R} is a stable focus and for $\mu = 0.6194$. b) E_{3R} is a stable weak focus for $\mu = 0.5769$. c) E_{3R} is a unstable focus for $\mu = 0.5628$. The threshold parameter value is $\tilde{R} = 0.04$.

Figure 5.4 illustrates the boundary equilibria bifurcations. We consider μ as a variation parameter and a limit cycle unstable arises from equilibrium point E_{3R}, due to change of stability when $\mu = \tilde{R}$.

5.5 Technical results

Now we are going to present a brief theoretical recapitulation to introduce the "half-return map" and also the results referring to $P_z(y)$.
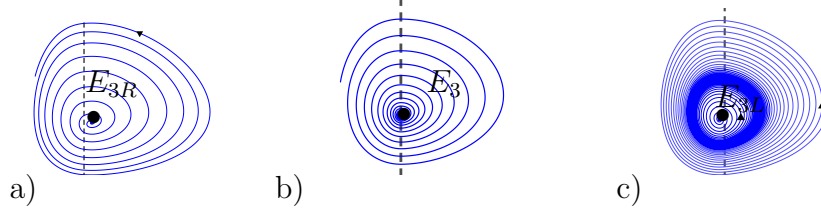
Figure 5.4: Boundary equilibrium bifurcations. Here, μ is the variation parameter, $\lambda = 1.33548$ and in this case a unstable limit cycle arises from equilibrium E_3 due to change of stability for $\mu^2 = \tilde{R}$. a) Here, $E_3 = E_{3R}$ is a unstable focus for $\mu = 0.4384$. b) There is a transition of the E_{3R} from stable to unstable for $\mu^2 = \tilde{R} = 0.4242$. In this case we have $E_{3R} = E_{3L}$. c) $E_3 = E_{3L}$ is a stable focus for $\mu = 0.4101$. The threshold parameter value is $\tilde{R} = 0.18$.

Consider a two-dimensional differential system,

$$\dot{X} = f(X), \quad X = (x, y) \in \mathbb{R}^2 \tag{5.13}$$

with smooth f, having a focus equilibrium point at the origin. By [28], the differential equation (5.13) near such equilibrium point can be written as

$$\begin{aligned} \frac{dx}{dt} &= a_{11}x + a_{12}y + R_1(x, y) \\ \frac{dy}{dt} &= a_{21}x + a_{22}y + R_2(x, y) \end{aligned} \tag{5.14}$$

with $R_1(0,0) = R_2(0,0) = DR_1(0,0) = DR_2(0,0) = 0$.

Take $\Sigma_1 = \{(0, y),\ y > 0\}$ and $\Sigma_2 = \{(0, y),\ y < 0\}$, it is easily seen that Σ_1 and Σ_2 are transverse sections to system (5.14) in a neighborhood of the origin. Thus, we can define a half-return map $P(y)$ for all points $(0, y)$ in Σ_1 with y small enough, so that the orbit starting at $(0, y)$ comes again to Σ_2 at the point $(0, P_Z(y))$. Whenever we have a focus dynamics, it is convenient to introduce a crucial parameter, namely

$$\gamma = \frac{tr(A)}{\sqrt{4\det(A) - tr(A)^2}}, \text{ where } A = \begin{pmatrix} a_{11} & a_{12} \\ a_{21} & a_{22} \end{pmatrix}. \tag{5.15}$$

Lemma 5.5.1. *Consider the system* (5.14). *Then the half-return map $P(y_0)$ has the following property*

$$\lim_{y_0 \to 0} \frac{P_Z(y_0)}{y_0} = e^{\gamma\pi}. \tag{5.16}$$

Proof. Let $\varphi(t, y_0) = (x(t, y_0), y(t, y_0))$ be the solution of system (5.14) such that $\varphi(0, y_0) = (0, y_0)$. Then, by [70], we have that

$$\varphi(t, y_0) = e^{At}(0, y_0) + \rho(t, y_0)$$

128

with

$$\lim_{y_0 \to 0} \frac{\rho(t, y_0)}{y_0} = 0.$$

Write $e^{At}(0, y_0) = (\widehat{x}(t, y_0), \widehat{y}(t, y_0))$ and $\rho(t, y_0) = (\rho_1(t, y_0), \rho_2(t, y_0))$, thus the time needed to pass from Σ_+ to Σ_- starting at $(0, y_0)$ is $\tau(y_0)$ given by less positive solution of $x(t, y_0) = 0$.

Since the origin is a focus it follows A has a pair of complex conjugate eigenvalues, namely $\alpha \pm i\beta$. Let $\widehat{\tau}(y_0)$ be the smallest positive solution of $\widehat{x}(t, y_0) = 0$; then

$$\widehat{\tau}(y_0) = \frac{\pi}{2\beta}.$$

We claim that

$$\lim_{y_0 \to 0} \tau(y_0) = \frac{\pi}{2\beta}.$$

Indeed,

$$\lim_{y_0 \to 0} \frac{\rho_1(t, y_0)}{y_0} \le \lim_{y_0 \to 0} \frac{\rho(t, y_0)}{y_0} = 0,$$

then

$$\lim_{y_0 \to 0} \frac{x_1(t, y_0)}{y_0} = \lim_{y_0 \to 0} \frac{\widehat{x}_1(t, y_0)}{y_0} = \lim_{y_0 \to 0} \widehat{x}_1(t, 1) = \widehat{x}_1(t, 1). \qquad (5.17)$$

Since $\tau(y_0)$ and $\widehat{\tau}(y_0)$ are solutions of $x_1(t, y_0) = 0$ and $\widehat{x}_1(t, 1) = 0$ respectively, by (5.17) it follows that

$$\lim_{y_0 \to 0} \tau(y_0) = \widehat{\tau}(y_0) = \frac{\pi}{2\beta}.$$

Now we will prove (5.16). Note that

$$\frac{P(y_0)}{y_0} = \frac{y(\tau(y_0), y_0)}{y_0} = \frac{\widehat{y}(\tau(y_0), y_0)}{y_0} + \frac{\rho_2(\tau(y_0), y_0)}{y_0}.$$

Then

$$\lim_{y_0 \to 0} \frac{P(y_0)}{y_0} = \widehat{y}\left(\lim_{y_0 \to 0} \tau(y_0), y_0\right) = \widehat{y}\left(\frac{\pi}{2\beta}, 1\right) = e^{\gamma\pi}.$$

$\square$

The result of the Lemma 5.5.1 allows the presentation of the following proposition dealing with the bifurcations of the equilibria at the boundary where the vector field defining the differential equation changes.

Note that the parameter $\bar{\mu}_0$ introduced in Proposition 5.3.2 depends on two other parameters, λ and $\tilde{R}$. We want to analyze $\bar{\mu}_0$ in the transition of group defense effect, that is $\bar{\mu}_0 = \sqrt{\tilde{R}}$. Thus

$$\tilde{R} = \frac{2(\sqrt{1 + \lambda} - 1)}{\lambda} := \mu_0$$

From now on, the critical value μ_0 will be used together with thresholds μ_1, μ_2, μ_3 and μ_4.

The following result shows that the critical parameter μ_0 can assume any value in the interval $(0, 1)$. In addition, the conditions for different transitions scenarios among the equilibria are presented.

Lemma 5.5.2. *Consider the four real functions*

$$s_0(x) = \frac{2(\sqrt{1+x}-1)}{x}, \quad s_1(x) = \frac{3\,x - 4\,\sqrt{3\,x+1}-4}{9x}, \quad s_2(x) = \frac{1}{3},$$

$$s_3(x) = \frac{3\,x + 4\,\sqrt{3\,x+1}-4}{9x} \ \text{ and } s_4(x) = 1.$$

The follows statements hold:

(i) *if $0 < x < -20\sqrt{2}+32$, then $s_1(x) < 0 < s_2(x) < s_3(x) < s_0(x) < s_4(x)$;*

(ii) *if $x = -20\sqrt{2}+32$, then $s_1(x) < 0 < s_2(x) < s_3(x) = s_0(x) < s_4(x)$;*

(iii) *if $-20\sqrt{2}+32 < x < 8$, then $s_1(x) < 0 < s_2(x) < s_0(x) < s_3(x) < s_4(x)$;*

(iv) *if $x = 8$, then $s_1(x) = 0 < s_2(x) < s_0(x) < s_3(x) < s_4(x)$;*

(v) *if $8 < x < 24$, then $0 < s_1(x) < s_2(x) < s_0(x) < s_3(x) < s_4(x)$;*

(vi) *if $x = 24$, then $0 < s_1(x) < s_2(x) = s_0(x) < s_3(x) < s_4(x)$;*

(vii) *if $24 < x < 20\sqrt{2}+32$, then $0 < s_1(x) < s_0(x) < s_2(x) < s_3(x) < s_4(x)$;*

(viii) *if $x = 20\sqrt{2}+32$, then $0 < s_1(x) = s_0(x) < s_2(x) < s_3(x) < s_4(x)$;*

(ix) *if $x > 20\sqrt{2}+32$, then $0 < s_0(x) < s_1(x) < s_2(x) < s_3(x) < s_4(x)$.*

Proof. Let us first prove some results that are valid for all statements. It is easy to verify that the following inequalities hold for all $x > 0$:

$$s_1(x) < s_2(x) < s_3(x) < s_4(x) \text{ and } 0 < s_0(x) < s_4(x). \tag{5.18}$$

Noting that

$$(s_1(x))' = \frac{\sqrt{3\,x+1}\,(6\,x+4) + 12\,x + 4}{27\,x^3 + 9\,x^2} > 0,$$

it follows that s_1 is increasing, and as $s_1(8) = 0$ it follows that

$$\begin{cases} s_1(x) < 0 & \text{if } x < 8; \\ s_1(x) = 0 & \text{if } x = 8; \\ s_1(x) > 0 & \text{if } x > 8. \end{cases} \tag{5.19}$$

From (5.18) and (5.19) almost all the inequalities of the lemma follow. We will consider only the nontrivial remaining cases, (i) and (vii).

(i) Solving $s_0 = s_3$ we have $x = 32 - 20\sqrt{2}$ and $x = 0^+$, i.e.,

$$\lim_{x \to 0^+} (s_0 - s_3) = 0.$$

Effectively, for $x > 0$ the equation $s_0(x) - s_3(x) = 0$ is equivalent to

$$4\sqrt{3x+1} + 3x + 14 = 18\sqrt{x+1}. \tag{5.20}$$

Now making the coordinate change $y = \sqrt{3x+1}$, we obtain

$$y^2 + 4y + 13 = 6\sqrt{3y^2 + 6},$$

that is equivalent to

$$y^4 + 8y^3 - 66y^2 + 104y - 47 = 0. \tag{5.21}$$

Solving (5.21) we obtain $y = -6\sqrt{2} - 5$, $y = 1$, double root, and $y = 6\sqrt{2} - 5$. Thus, $x = 0$ and $x = 32 - 20\sqrt{2}$ are solution of equation (5.22). Therefore, if $0 < x < 32 - 20\sqrt{2}$, then $s_3(x) < s_0(x)$.

(vii) Solving $s_0 = s_1$ we have $x = 32 + 20\sqrt{2}$. Effectively, for $x > 0$ the equation $s_0(x) - s_3(x) = 0$ is equivalent to

$$-18\sqrt{x+1} + 3x + 14 = 4\sqrt{3x+1}. \tag{5.22}$$

Now making the coordinate change $y = \sqrt{x+1}$, we obtain

$$3y^2 - 18y + 11 = 4\sqrt{3y^2 - 2}$$

that is equivalent to

$$y^4 - 12y^3 + 38y^2 - 44y + 17 = 0, \tag{5.23}$$

where
$$9 - 4\sqrt{3} \le 3y \le 9 + 4\sqrt{3}.$$

Solving (5.23) we obtain $y = -2\sqrt{2} + 5$, $y = 1$, double root, and $y = 2\sqrt{2} + 5$. Thus, $x = 32 + 20\sqrt{2}$ is the only feasible solution of equation (5.22). Therefore, if $24 < x < 20\sqrt{2} + 32$, then $0 < s_1(x) < s_0(x) < s_2(x) < s_3(x)$.

$$\square$$

Remark 5.5.3. The functions s_j with $j = 0, \ldots, 4$, were introduced in Lemma 5.5.2 for simplicity of notation. Note that $\mu_j = \sqrt{s_j(\lambda)}$ with $j = 0, \ldots, 4$, but recall that for $s_1(\lambda) < 0$, μ_1 is not feasible.

For $0 < \lambda < (20\sqrt{2}+32)$, by Lemma 5.5.2 $s_1(\lambda) < s_0(\lambda)$. Thus, considering $\max\{0, s_1(\lambda)\} < \tilde{R} < \min\{s_2(\lambda), s_0(\lambda)\}$ and $\mu = \sqrt{\tilde{R}}$ we have that E_{3L} is a stable focus and E_{3R} is an unstable focus, Proposition 5.3.2. Then, in this transition two symmetric scenarios for the boundary equilibrium bifurcation occur: subcritical and supercritical. This result is presented in the following proposition.

Proposition 5.5.4 (focus-focus). *Consider the continuous piecewise differential system* (5.4), *with* $0 < \lambda < (20\sqrt{2} + 32)$ *and* $\max\{0, s_1(\lambda)\} < \tilde{R} < \min\{s_2(\lambda), s_0(\lambda)\}$, *where* s_0, s_1 *and* s_2 *are given by Lemma 5.5.2. Taking* $s^* = \frac{1}{7}(3 - \sqrt{2})$ *as a fixed parameter and* μ *as the bifurcation parameter, the following statements hold:*

(a) *if* $\max\{0, s_1(\lambda)\} < \tilde{R} < \min\{s^*, s_0(\lambda)\}$, *then a unstable limit cycle bifurcates at* $\mu = \sqrt{\tilde{R}}$ *at a boundary equilibrium bifurcation. This bifurcation results of the transition from unstable to stable focus for the equilibrium point* E_3 *(subcritical bifurcation);*

(b) *if* $s^* < \tilde{R} < \min\{s_2(\lambda), s_0(\lambda)\}$, *then a stable limit cycle bifurcates at* $\mu = \sqrt{\tilde{R}}$ *at a boundary equilibrium bifurcation. This bifurcation results of the transition from stable to unstable focus for the equilibrium point* E_3 *(supercritical bifurcation).*

Proof. The main idea of the proof for statement (a) is to build a compact negative invariant set C_1 enclosing the stable focus E_{3L}, as it was done in [31]. By the Poincaré Bendixson's Theorem we conclude the existence of one unstable limit cycle totally contained in C_1. Following the notations from [31], we consider the half-straight lines $\Sigma^+ = \{(\tilde{R}, \lambda\tilde{R}(1 - \tilde{R}) + y), \ y > 0\}$ and $\Sigma^- = \{((\tilde{R}, \lambda\tilde{R}(1 - \tilde{R}) + y), \ y < 0\}$. Thus, we can define a left half-return map $P_L(y)$ for all points $(\tilde{R}, \lambda\tilde{R}(1 - \tilde{R}) + y)$ in Σ^+ with y small enough, so that the orbit starting at $(\tilde{R}, \lambda\tilde{R}(1 - \tilde{R}) + y)$ comes again to straight line $R = \tilde{R}$ at the point $(0, P_L(y))$ in Σ^-. On Σ^- we can define similarly a right half-return map P_R for all the points $(\tilde{R}, \lambda\tilde{R}(1 - \tilde{R}) + y)$ with $|y|$ small enough and negative. Let

$$\gamma_L = \frac{tr(J(E_{3L}))}{\sqrt{4\det(J(E_{3L})) - tr(J(E_{3L}))^2}}; \quad \gamma_R = \frac{tr(J(E_{3R}))}{\sqrt{4\det(J(E_{3R})) - tr(J(E_{3R}))^2}}$$

be the parameters given by (5.15), but now we consider the matrices $J(E_{3L})$ and $J(E_{3R})$ respectively. We claim that

$$\gamma_L + \gamma_R > 0. \tag{5.24}$$

Indeed, by [71] the inequality (5.24) is equivalent to

$$\frac{tr(J(E_{3L}))}{\sqrt{\det(J(E_{3L}))}} + \frac{tr(J(E_{3R}))}{\sqrt{\det(J(E_{3R}))}} > 0.$$

We know that $\tilde{R} < s^*$, $tr(J(E_{3L})) < 0$ and $tr(J(E_{3R})) > 0$, then by a direct computation we finally obtain

$$\left| \frac{tr(J(E_{3L}))}{\sqrt{\det(J(E_{3L}))}} \cdot \frac{\sqrt{\det(J(E_{3R}))}}{tr(J(E_{3R}))} \right| = \frac{\sqrt{2}\,\tilde{R}}{1 - 3\tilde{R}} > 1$$

Let us now consider the Poincaré map $P = P_R \circ P_L$. If $\mu = \sqrt{\tilde{R}}$ the equilibrium point E_3 is on the straight line $\Sigma^- \cup \{E_3\} \cup \Sigma^+$. Thus by Lemma 5.5.1 it follows that

$$\lim_{y \to 0} \frac{P(y)}{y} = \left(\lim_{y \to 0} \frac{P_R(P_L(y))}{P_L(y)} \right) \cdot \left(\lim_{y \to 0} \frac{P_L(y)}{y} \right) = e^{(\gamma_L + \gamma_R)\pi} > 1.$$

In this way if $y > 0$ and small enough we have

$$P(y) > y. \tag{5.25}$$

Now we can build the compact negative invariant set C_1. Let $y > 0$ be arbitrary and small so that $P(y) > y$ and denote $B_1 = (\tilde{R}, \lambda\tilde{R}(1 - \tilde{R}) + y)$ and $B_2 = (\tilde{R}, \lambda\tilde{R}(1 - \tilde{R}) + P(y))$. Thus we define the boundary of the compact negative invariant set C_1 that is the orbit from B_1 to B_2 along with segment $B_1 B_2$, see Figure 5.5.

Note that if $\mu = \sqrt{\tilde{R}}$, then $P(y) > y$, thus we can conclude that the C_1 is effectively a compact negative invariant set. Note that E_{3R} is an unstable pseudo-focus because $P(y) > y$ for all small enough, see [27].

Allowing now μ to be slightly lower than $\sqrt{\tilde{R}}$ and using the continuous dependence of solutions with respect to the parameter μ, the inequality (5.25) still holds. Thus the set C_1 remains compact and negatively invariant, but now the focus E_{3R} in its interior is stable. Therefore, by the Poincaré-Bendixson Theorem, [28]), we have the existence of one unstable limit cycle totally contained in C_1. Obviously, this set C_1 can be chosen as small as desired by taking the initial value of y sufficiently small. This shows that a limit cycle arises from equilibrium point E_{3R} through the boundary equilibrium bifurcation.

The case (b) follows a proof similar to the one of statement (a), taking into account that, in this case, we have the transition from a stable focus to an unstable one. Thus, it is necessary to build a compact positive invariant set enclosing the unstable focus E_{3R}. □

Corollary 5.5.5. *Consider the continuous piecewise differential system (5.4), with $0 < \lambda < (20\sqrt{2} + 32)$ and $\max\{0, s_1(\lambda)\} < \tilde{R} < \min\{s^*, s_0(\lambda)\}$, where s_0, s_1 and s_2 are given by Lemma 5.5.2, and $s^* = \frac{3 - \sqrt{2}}{7}$. Then the system has at least two nested limit cycles surrounding the stable focus E_{3L}. The smaller limit cycle is unstable and the larger one is stable.*
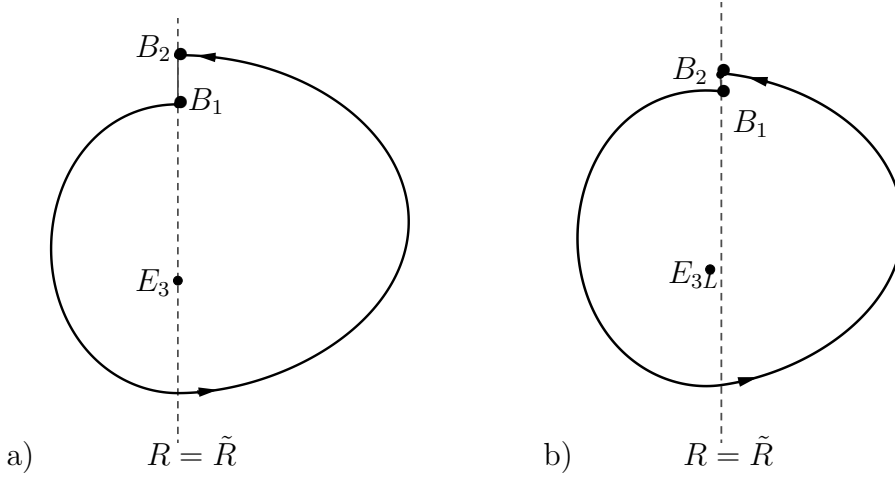
Figure 5.5: The boundary of the positive compact invariant set C_1 is composed by the orbit from B_1 to B_2 and the segment B_1B_2. $B_1 = (\tilde{R}, \lambda\tilde{R}(1 - \tilde{R}) + y)$, $B_2 = (\tilde{R}, \lambda\tilde{R}(1 - \tilde{R}) + P(y))$. a) $E_3 = E_{3L} = E_{3R}$ for $\mu = 0.4$. b) $E_3 = E_{3L}$ for $\mu = 0.39$. The parameter values are: $\tilde{R} = 0.16$, $\lambda = 1.4$ and $y = 0, 24$.

Proof. The proof is based on the following argument. The smaller unstable limit cycle from Proposition 5.5.4 is contained within a limited positive invariant set, Proposition 5.2.1. Then by Poincaré-Bendixson Theorem we have the existence of one stable limit cycle surrounding the smaller limit cycle is unstable. See Figure 5.9. □

For $\lambda > 8$, by Lemma 5.5.2 $s_0(\lambda) < s_3(\lambda)$. Thus, considering $0 < \tilde{R} < \min\{s_0(\lambda), s_1(\lambda)\}$ and $\mu = \sqrt{\tilde{R}}$ we have that E_{3L} is a stable focus and E_{3R} is an unstable node, Proposition 5.3.2. Then, in this transition a subcritical boundary equilibrium bifurcation occurs. In summary

Proposition 5.5.6 (focus-node). *Consider the continuous piecewise differential system* (5.4)*, with $\lambda > 8$ and $0 < \tilde{R} < \min\{s_0(\lambda), s_1(\lambda)\}$, where s_0 and s_1 are given by Lemma 5.5.2. Then an unstable limit cycle bifurcates at $\mu = \sqrt{\tilde{R}}$ in a boundary equilibrium bifurcation. This bifurcation results of the transition from unstable node to stable focus for the equilibrium point E_3, subcritical bifurcation.*

Proof. The proof is analogous to what was done to Proposition 5.5.4, which is the construction of a compact negative invariant set C_2 enclosing the stable focus E_{3L}. Let $H = (\tilde{R}, \lambda\mu\sqrt{\tilde{R}}(1 - \tilde{R}))$ be intersection point of the isocline $R' = 0$ with the straight line $R = \tilde{R}$. Thus, for $F > \lambda\mu\sqrt{\tilde{R}}(1 - \tilde{R})$ we have $R' < 0$ at $(\tilde{R}, F)$; conversely, for $F < \lambda\mu\sqrt{\tilde{R}}(1 - \tilde{R})$ we have $R' > 0$. Consequently, the direction of flow is determined along the $R = \tilde{R}$.

For $\mu = \sqrt{\tilde{R}}$, consider the point $A = (\tilde{R}, \lambda\tilde{R}(1 - \tilde{R}) + y)$ in the straight line $R = \tilde{R}$ with $y > 0$ and small enough. It is evident that the orbit of the point A has as α-limit the unstable node E_{3R}, see Figure 5.6. For a definition of α- and ω-limit, see for instance [70]. The orbit of the point A, but now following forward in time, hit in $R = \tilde{R}$, after a half turn around a focus E_{3L}, at point B_3. We thus obtain the boundary of the compact negative invariant set C_2 that is the orbit from B_3 to E_3, following backward in time, along with segment B_3E_3, see Figure 5.6. Although $y > 0$ and small enough, the point A is chosen arbitrarily on $R = \tilde{R}$, so for $\mu = \sqrt{\tilde{R}}$ the equilibrium point is asymptotically unstable.

Allowing now μ to be slightly lower than $\sqrt{\tilde{R}}$ and using the continuous dependence of solutions with respect to the parameter μ, the orbit starting at A goes down eventually hitting $R = \tilde{R}$ at the point $B_4 = (\tilde{R}, F)$ with $F < \lambda\mu\sqrt{\tilde{R}}(1-\tilde{R})$. Thus, the set C_2 remains compact and negatively invariant, but now the focus E_{3R} in its interior is stable. Note that now the boundary of the negative compact invariant set C_2 is composed by the orbit from B_4 to B_3, along with segment B_3B_4, where B_4 is the point obtained from orbit of A following backwards in time until it hit straight line $R = \tilde{R}$. Therefore, by Poincaré-Bendixson's Theorem we have the existence of one unstable limit cycle totally contained in C_2. Obviously, this set C_2 can be chosen as small as desired by taking the initial value of y sufficiently small. This shows that a limit cycle arises from equilibrium point E_{3R} through the boundary equilibrium bifurcation. $\square$
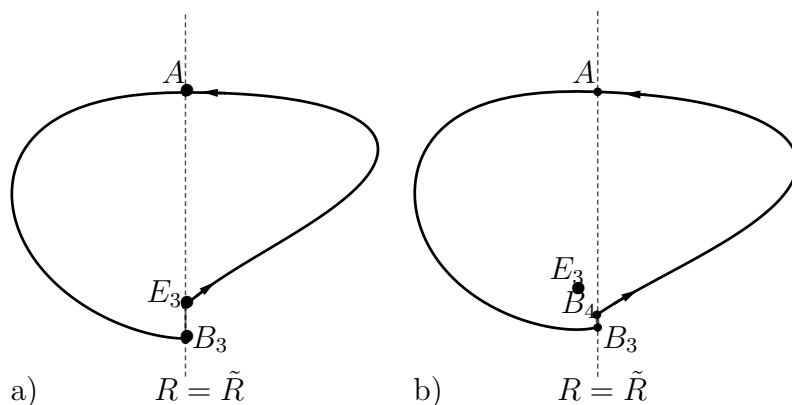
Figure 5.6: The boundary of the negative compact invariant set C_2. a) $E_3 = E_{3L} = E_{3R}$ for $\mu = 0.4$. b) $E_3 = E_{3L}$ for $\mu = 0.38$. The parameter values are: $\tilde{R} = 0.16$, $\lambda = 40$.

Corollary 5.5.7. *Consider the continuous piecewise differential system* (5.4), *with* $\lambda > 8$ *and* $0 < \tilde{R} < \min\{s_0(\lambda), s_1(\lambda)\}$, *where* s_0 *and* s_1 *are given by Lemma 5.5.2. Then the system has at least two nested limit cycles surrounding*

the stable node E_{3L}. The smaller limit cycle is unstable and the larger one is stable.

Proof. The proof follows in an analogous way to Corollary 5.5.5. □

For $\lambda > 24$, by Lemma 5.5.2 $s_0(\lambda) < s_2(\lambda)$. Thus, as $\mu = \sqrt{\tilde{R}}$ and $\max\{s_0(\lambda), s_1(\lambda)\} < \tilde{R} < s_2(\lambda)$ it follows that E_{3L} is a stable node and E_{3R} is an unstable focus, Proposition 5.3.2. Then, in this transition a supercritical boundary equilibrium bifurcation occurs. In summary

Proposition 5.5.8 (node-focus)**.** *Consider the continuous piecewise differential system (5.4), with $\lambda > 24$ and $\max\{s_0(\lambda), s_1(\lambda)\} < \tilde{R} < s_2(\lambda)$, where s_0, s_1 and s_2 are given by Lemma 5.5.2. Then a stable limit cycle bifurcates at $\mu = \sqrt{\tilde{R}}$ in a boundary equilibrium bifurcation. This bifurcation results from the transition from stable node to unstable focus for the equilibrium point E_3, supercritical bifurcation.*

Proof. We can proceed analogously to the proof of Proposition 5.5.6, but now we have the transition from unstable node to stable focus. Thus, it is necessary to build a compact negative invariant set enclosing the stable focus E_{3L}. □

Remark 5.5.9. For $\lambda > (20\sqrt{2} + 32)$, by Lemma 5.5.2 $s_0(\lambda) < s_1(\lambda)$. Thus, considering $s_0(\lambda) < \tilde{R} < s_1(\lambda)$ and $\mu = \sqrt{\tilde{R}}$ we have that E_{3L} is a stable node and E_{3R} is an unstable one, Proposition 5.3.2. In this transition, for a neighborhood of equilibrium point E_3, there is a set S constituted by a continuum of homoclinic loops around the point E_3. Effectively, consider the point $A = (\tilde{R}, \lambda\tilde{R}(1 - \tilde{R}) + y)$ at $\{R = \tilde{R}\}$ with $y > 0$ and small enough. It is evident that the orbit of the point A has as α- and ω-limit the equilibrium point E_3, see Figure 5.6.

Remark 5.5.10. If for $\mu = \sqrt{\tilde{R}}$ the exterior part of the set S is stable, then for μ slightly lower than $\sqrt{\tilde{R}}$ the continuum of homoclinic loops disappears and we conjecture that a stable limit cycle arises when the homoclinic connections break. On the other hand, if for $\mu = \sqrt{\tilde{R}}$ the exterior part of the set S is unstable, then for μ slightly lower than $\sqrt{\tilde{R}}$ the continuum of homoclinic loops disappears and we conjecture that an unstable limit cycle is born when the homoclinic connections break. Moreover, in this case the system has at least two nested limit cycles surrounding the stable node E_{3L}. The smaller limit cycle is unstable and larger one is stable, see Figure 5.7.

5.6   Discussion

In Sections 5.3, 5.4 and 5.5 we presented a mathematical analysis of the behaviour of model 5.4. In this section we present biological interpretations for the main results.
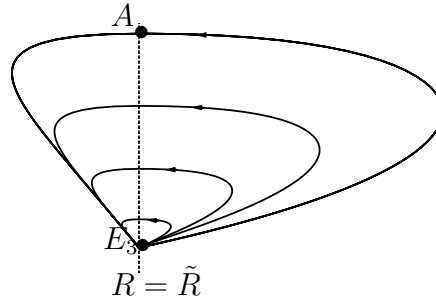
Figure 5.7: The continuum of homoclinic loops S. The parameter values are: $\tilde{R} = 0.25$, $\lambda = 110$ and $\mu = 0.5$.

The model has only three equilibria, one corresponding to total extinction (E_1), one to predator extinction (E_2) and one to coexistence (E_3). E_1 is always unstable, this effect is caused by the fact that the mortality on prey is of second-order near the origin (due to the application of the law of mass action for small groups). Of course if the theoretical trajectories of the model come too near the origin, it means that the real system is in real danger of total extinction. We should keep that in mind as we anaylize the behaviour of the model as a whole.

Points E_2 and E_3 have variation in their stability, depending on parameters $\tilde{R}$, λ and μ. Parameter $\tilde{R}$ is the threshold group size beyond wich group defense becomes effective, while $\theta = 1/\mu$ is a combination of parameters a, the predation rate with defense, e the efficiency of conversion of captures prey into new predators, K is carrying capacity of prey and m the "natural" per capita mortality rate of predators. Finally, parameter λ is the ratio between predator mortality timescale (predator average lifespan) and the prey reproduction timescale (when approximated by Malthusian dynamics, this represents the average time a prey takes to produce one descendent). All the main results can be understood from the variation of these parameters and are summed up in Figure 5.8 so we will base our discussion on this figure and its different regions.

The variation in the parameter μ depends on changes in the parameters a, e, m and K. Since $\mu = 1/\theta$, $\mu = \frac{m}{ae\sqrt{K}}$ is proportional to m and inversely proportional to both a, e and $\sqrt{K}$. Thus an increase in μ means an increase in the mortality rate or a decrease in the predation rate or conversion efficiency. Variation in $\tilde{R}$ is simply a change in the hypotheses regarding group defense, wich may vary from species to species, the only critical assumption is that it is smaller than 1 (meaning that $R^* < K$, K the carrying capacity for prey, and R^* the threshold population size for group defense). Finally, variation in λ is due to either a change in predator average lifespan or prey reproduction timescale.

Region G of Figure 5.8 represents the situation when only E_2 is stable, if μ is above the threshold $\mu_4 = 1$. Since $\mu = \frac{1/ae\sqrt{K}}{1/m}$ it can be interpreted as a ratio
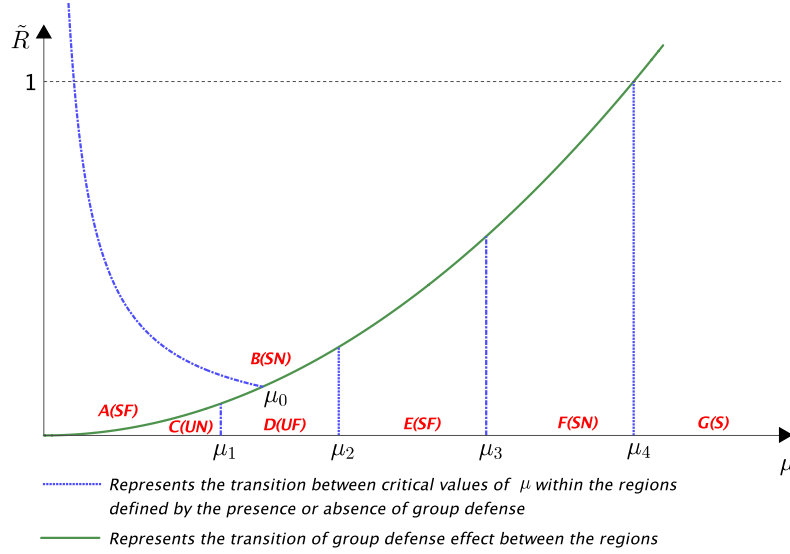
137

Figure 5.8: In this bifurcation diagrams we have a summary of behaviour of the system dynamics considering μ as a parameter of variation. We separated this diagram in seven regions. The green curve corresponds to $\tilde{R} = \mu^2$ and the blue curve corresponds to $\tilde{R} = \left(\frac{2(\sqrt{1+\lambda}-1)}{\lambda\mu}\right)$. For $\mu = \mu_4$ there is a transcritical bifurcation between E_2 and E_{3R} and for $\mu = \mu_2$ arises a Hopf bifurcation from E_{3R}. The region of parameter variation is divided in seven subregions (from A to G) for easier reference. Each region is also classified according to the topology of the trajectories in the vicinity of point E_3: S=saddle, SN=stable node, UN=unstable node, SF=stable focus, UF=unstable focus.

between two timescales. The first one is $1/ae\sqrt{K}$, which can be interpreted as the time it takes for one predator to consume enough prey to produce one descendent if prey population is kept constant at carrying capacity K. The second timescale is $1/m$ which represents predator average lifespan (how long one predator lasts in average). Thus, it is no wonder that E_2 (predator extinction) is a stable node if $\mu > 1$ (it takes longer for one predator to produce one descedennt than its average lifespan) and unstable if $\mu < 1$.

Transition from region G to F occurs at the transcritical bifurcation between E_2 and E_{3R}. In this case, in region F the only stable point is the coexistence E_{3R} and it is a node. When E_3 is a node, it means there are no oscillations in the system, but it travels directly to the equilibrium values. From region F, transition can occur to either regions A, B, or E.

Damped oscillations in the system may arise in transition from region F to either regions A or E. This can occur due to a reduction in parameter μ (meaning a more "favorable" combination of factors to the predators) or in case both $\tilde{R} > \mu_3^2$ and $\lambda < 32 - 20\sqrt{2}$. One way to interpret the rise of oscillations in the transition from F to E is to think that if the timescale of natural death

of predators $(1/m)$ is too large (m small), predators take a long time to die even if there is a low number of prey, and the dynamics of the system will have a tendency to oscillate. This can be interpreted as a delay in the effect of an adverse environment over the predators. Observe that, for, very small $\mu < \mu_1$ and $\mu < \bar{\mu}_0$ the system will definitely oscillate, either being in region A or C (even though all oscillation described so far are damped ones). Transition to region B does not change the qualitative behaviour of the system, the only critical observation is that the system evolves to an equilibrium where there is no group defense.

To observe a transition from F to A, one must have both a high value for λ (meaning that prey reproduce quickly in comparison to the timescale of the lifespan of predators) and $\tilde{R}$ (only large populations engage in group defense). If both of those conditions are present, reducing μ may give rise to oscillations.

From region E there can be transitions to either A, B or D. Transition from E to D occurs via a Hopf bifurcation, giving rise to sustained oscillations and a stable limit cycle around E_3, as in Figure 5.3. We could interpret this as an amplification of the effect mentioned earlier, that is, the delay of the impact of low prey populations on the predators. That is, predators reproduce quickly, but die slowly. This is the only transition possible if $\tilde{R} < \mu_2$.

Transition for regions A and B may occur if $\tilde{R} > \mu_2$. The transition to region A leads to no change in the qualitative behaviour of the system, both region displaying damped oscillations to an equilibrium. Finally, the transition to region B leads to no oscillations in the system and convergence to a equilibrium with no group defense. It may occur only if $8 < \lambda < 24$, meaning that the prey reproduction timescale is at least 8 times quicker than the predator mortality timescale.

Now, from region D, a most interesting bifurcation may occur in transition for region A. If $\mu_1 < \sqrt{s^*}$ ($s^* = \sqrt{(3 - \sqrt{2})/7}$), a subcritical Hopf bifurcation may occur. When the trajectories of the system are contained in the region of group defense ($R(t) < \tilde{R}$), a stable limit cycle exists, which has its origin in the Hopf bifurcation of the transition from region E to D. As the trajectories approach de boundary, the system begins to travel through both regions: with group defense and without. In the region without group defense (A), the traditional Lotka-Volterra dynamics tends to pull the trajectories to a stable focus. This tension between the two different dynamics, initially generates a boundary of attraction of the stable focus in region A, which is exactly the unstable limit cycle obtained in the bifurcation. Continuing to reduce the parameter μ, going further into region A, this region of attraction grows, eventually meeting the outer stable limit cylce and the Lotka-Volterra dynamics dominates. The outer stable limit cycle would represent a situation where the prey population presents such large fluctuations that it oscillates between group defense and individual behaviour. The inner unstable limit cycle represents the dominance of individual behaviour. This interesting bifurcation is illustrated in Figure

5.9.

If the same transition to region A is repeated but in case $\mu_1 > \sqrt{s^*}$ then the bifurcation is supercritical and the stable limit cycle that existed before the transition is destroyed. In those cases, it does not matter much if the transition occurs into region A or B, in both cases the limit cycle ceases to exist. Finally, numerical simulations indicate that transition from region C to A also results in the onset of two limit cycles if $\mu_1 < \sqrt{s^*}$ and to no-limit otherwise.
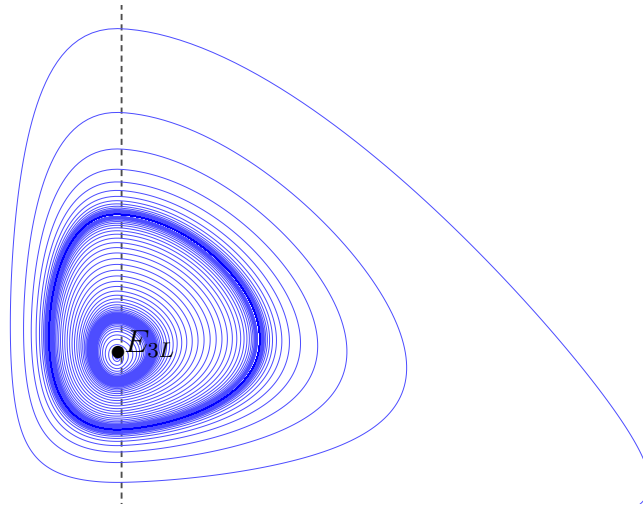
Figure 5.9: This graph illustrates two limit cycles. The phase picture containing two threshold cycles and also the equilibrium point E_{3L}, which in this case, is a stable focus. The parameter values are: $\tilde{R} = 0.21$, $\lambda = 0.81$, $\mu = 0.458$.

The effect of group defense can be understood to be favorable to the prey simply by analysing the nullclines in figure 5.1-(c). If the combination of parameters is such that the equilibrium point E_3 lies in the group defense region, then it is clear that the same population of predators lead to higher prey populations than if there were no group defense (it is easy to see that, just by extrapolating the nullcline from the region of $R < \tilde{R}$ to $R > \tilde{R}$). So the model is coherent in the sense that group defense models well the benefit for the prey population. Another simple way to recognize this is just to look at the coordinates of E_{3L} and E_{3R}, noting that the equilibrium with group defense always provides a larger prey population.

5.7 Conclusion

A alternative model to approach herd behaviour was proposed and its behaviour investigated using simulation and analytical techniques. Our results

show that the model presents novel behaviour when compared with the orignal model proposed in [3, 2]. An advantadge of this approach is that the model does not have a singularity in the Jacobian at the origin, as was the case with [3, 2]. Another fundamental difference is that the new model is coherent even for low populations of prey, where no group defense is possible, a feature that was lacking in previous approaches.

The results are interesting from the dynamical point of view, with both sub and supercritical Hopf bifurcations arising. Group defense has a positive impact for the prey population, as expected.

Part II

Evolutionary interacting population models

CHAPTER 6

MODELS FOR ALARM CALL BEHAVIOUR

The emission of alarm calls (or warning calls) is one of the many antipredator defences used by birds and mammals [19]. A considerable effort was dedicated to the study of such behaviour [76, 80, 21], because it may appear to be "altruistic", i.e. harmful to the sender and beneficial to the receiver. Alarm call signals often have acoustic characteristics that make them hard to locate [60, 14, 74], with species displaying convergent evolution of alarm call acoustic characteristics [60]. The evolution and maintenance of such properties indicate that there should be some risk in emitting alarm calls in the wild.

Various theories have been proposed to explain the evolution of alarm calls in species of birds and mammals. [76] proved, using a mathematical model, that kin selection may positively select alarm calling behaviour if individuals are full siblings. Evidence in favour of kin selection theory in alarm calling behaviour in mammals is accumulating [19, p. 195-196], creating a convincing case that it is, at least, a partial explanation for the phenomenon.

While being adequate to partially explain alarm call behaviour in some instances, kin selection theory faces difficulties in various cases when the alarm calling rate of individuals is unrelated with the kinship of benefited conspecifics [46]. Also, in many bird species, groups of non-kin individuals (and also heterospecifics) regularly display this type of behaviour [19, p. 200]. Alternative explanations for alarm call behaviour, such as reciprocal altruism, group selection or predator discouragement are not supported by field studies [19].

A simple approach to explain alarm calling behaviour is that it is beneficial to the individual. In particular, [8] presented a model where sentinel behaviour could be explained by being a strategy beneficial to the sentinel. Many of the model predictions were later confirmed by field studies [23]. Our goal in this chapter is to present models to study the selection of alarm calling behaviour

versus non-calling behaviour that depends on the costs and benefits of adopting each type of behaviour (alarmist versus non-alarmist or, equivalently, caller versus non-caller).

The theoretical framework adopted here is that of Population Ecology [29, 65] with the use of differential equations to describe the population dynamics. In this particular case, the dynamics of two populations are described: that of "alarmist" and "non-alarmist" individuals. The goal of the models is not to be a realistic representation of any particular situation, but to serve as a tool to understand the evolution of alarm calls under individual selection.

This chapter is organized as follows: in Section 6.1 we present four mathematical models of increasing complexity; Section 6.2 contains the mathematical analysis of the models behaviour, Section 6.3 summarizes the mathematical findings and discusses their biological implications. Finally, Section 6.4 gives an interpretation of the main results obtained. At first reading, Section 6.2 might be skipped. A general perspective of the models results can be obtained through Section 6.3. All proofs of mathematical propositions are deferred to the Appendix C.

6.1 Models

In this section we present four models for the selection of alarm call behaviour. The first one supposes unlimited population growth and serves as a paradigm to understand the fundamental aspects of the problem. In sequence, a model that takes into account intraspecific competition and limited population growth is proposed. Finally, the role of population size over predation rates [32, 63] is included in two further models.

6.1.1 Unlimited population growth

To describe the dynamics of selection for or against alarm call behaviour in a population, we separated the individuals into two classes: "alarmists" and "non-alarmists". Let x denote the number of "non-alarmists" and y the number of "alarmists", using a Malthusian model for population growth and accounting for mortality by predation, we can write a dynamics for the populations $x(t)$ and $y(t)$:

$$\begin{aligned}
\frac{dx}{dt} &= rx - xT_x(x,y) \\
\frac{dy}{dt} &= ry - yT_y(x,y)
\end{aligned}$$

(6.1)

where r is the net per capita growth rate (reproduction minus mortality) of the species, T_x and T_y are the per capita predation mortality rates for non-alarmists and alarmists, respectively.

Naturally, the real phenomenon of predation is very complex and is influenced by many variables that depend on the species, the environment and so on. [55] suggests a general *predatory sequence* as a scheme to analyse such processes. Here we will adopt a simplified version of such sequence.

We consider that the prey will have a constant probability of detecting the predator before a direct attack occurs and will differentiate only two scenarios. The first scenario occurs when the individual who had the chance to detect the predator was in the "non-alarmist" class. In this case, even if the individual was successful in detecting the predator, no alarm call is emitted and the population will have to face the predator under the "non-alarm" situation. The second possibility is that the individual who had the chance to spot the predator was part of the alarmist population. In this case, there is a chance that an alarm call was produced, and therefore the population faces the predator under a different condition.

Considering those two distinct scenarios, we model the per capita mortality due to predation using the following function:

$$T_x(x,y) = A\frac{x}{x+y} + B\frac{y}{x+y}. \tag{6.2}$$

Equation (6.2) is a pondered average of the mortalities rates A and B. Parameter A is the average mortality of a non-alarmist when there was no chance of an alarm call being emitted, while B is the average mortality in the case where there is a chance of emission of an alarm call.

A simple way to interpret equation (6.2) is that the average mortality of non-alarmists is the pondered average of the mortality when there is a chance of an alarm (which occurs with probability $y/(x+y)$) and when there is not (probability $x/(x+y)$). That is, when there is an attack by predators, $x/(x+y)$ of the time there will not be any alarm and $y/(x+y)$ of the time there is a chance that an alarm will be produced.

It can be shown that this form of mortality can represent the one adopted by [76]:

$$P_K = P\left(1 - a\frac{r}{n}\right) \tag{6.3}$$

where P_K is the probability of a kill in an encounter, P is the maximum kill probability, n is the total population, r the population of alarmists and $0 < a < 1$ is coefficient of alarm and detection efficiency. Equation (6.3) models a situation where the decrease in predation rate is proportional to the fraction of alarmist individuals in the population. Equation (6.2) corresponds to this case if $A > B$.

Analogously, we define the predation rate over the y population:

$$T_y(x,y) = C\frac{x}{x+y} + D\frac{y}{x+y}. \tag{6.4}$$

with obvious meanings for the parameters. The reason we adopt distinct parameters for the populations x and y is that they differ in behaviour (alarm

147

or no alarm), which may lead to distinct average mortalities in each case. For instance, giving an alarm call might increase the risk of being the target of an attack, which would translate into $D > B$.

With a change of variables $t^* = rt$ it is possible to make the time variable non-dimensional, leading to the system (dropping the asterisk for simplicity in notation):

$$
\begin{aligned}
\frac{dx}{dt} &= x \left(1 - \frac{ax}{x+y} - \frac{by}{x+y} \right) \\
\frac{dy}{dt} &= y \left(1 - \frac{cx}{x+y} - \frac{dy}{x+y} \right)
\end{aligned}
\tag{6.5}
$$

where $a = A/r$, $b = B/r$, $c = C/r$ and $d = D/r$ are the mortality rates measured in comparison with the per capita reproduction rate r.

6.1.2 Limited population growth

While the model in section (6.1.1) can provide good insight for the behaviour of a population composed of alarmists and non-alarmists, it is not realistic in the sense that most real biological systems present some degree of intraspecific competition that limits population growth. One of the simplest ways to model intraspecific competition is to include a Verhulst-type mortality in system (6.5), leading to:

$$
\begin{aligned}
\frac{dx}{dt} &= x \left(1 - \frac{x+y}{K} - a\frac{x}{x+y} - b\frac{y}{x+y} \right) \\
\frac{dy}{dt} &= y \left(1 - \frac{x+y}{K} - c\frac{x}{x+y} - d\frac{y}{x+y} \right).
\end{aligned}
\tag{6.6}
$$

Again, working with the non-dimensional variables $x^* = x/K$ and $y^* = y/K$ we obtain:

$$
\begin{aligned}
\frac{dx}{dt} &= x \left(1 - x - y - a\frac{x}{x+y} - b\frac{y}{x+y} \right) \\
\frac{dy}{dt} &= y \left(1 - x - y - c\frac{x}{x+y} - d\frac{y}{x+y} \right)
\end{aligned}
\tag{6.7}
$$

6.1.3 Group size effects

Individuals may benefit from grouping together against predators [40]. A variety of effects may contribute to the reduction of the per capita mortality rate [19] and there is some evidence that it decays as a power law with group size [32, 63].

Predation rate will be described as $T = T_P G(N)$, where T_P is the maximum per capita predation rate and $G : \mathbb{R}^+ \rightarrow (0, 1]$ is a non-dimensional

response function that describes the effects of grouping benefits in decreasing predation rates. For convenience, we will adopt an exponential decay of per capita predation mortality dependent on group size, but all conclusions remain qualitatively unaltered if the function $G(N)$ satisfies the following conditions:

1. $G(0) = 1$: predation is maximum when the population is small.

2. $G'(N) < 0$: $G(N)$ is monotonically decreasing.

3. $G''(N) > 0$: there is decreasing returns in benefits of increasing population size.

Group size effect is, then, modelled as $T = T_P \exp(-(x+y)/g)$. The parameter g (already in non-dimensional form G/K) represents the size of a group must have, in relation to the carrying capacity, for a significant decrease in mortality to be observed $(1 - 1/e)$. So, $g \approx 0$ means that grouping benefits are very effective even for small groups, while $g \gg 1$ means that the effects of group size are very weak.

We will discuss two variants of model (6.7). In the first one, all mortality rates are reduced by the group size effect. In this model, both in the case of alarm and no-alarm, all individuals benefit from the protection of being in a group.

The first variant of model (6.7) is, then:

$$
\begin{aligned}
\frac{dx}{dt} &= x \left[1 - (x+y) - e^{-(x+y)/g} \left(a \frac{x}{x+y} + b \frac{y}{x+y} \right) \right] \\
\frac{dy}{dt} &= y \left[1 - (x+y) - e^{-(x+y)/g} \left(c \frac{x}{x+y} + d \frac{y}{x+y} \right) \right]
\end{aligned}
. \tag{6.8}
$$

A second variant supposes that individuals can only profit from group protection if an alarm call was produced:

$$
\begin{aligned}
\frac{dx}{dt} &= x \left(1 - (x+y) - a \frac{x}{x+y} - e^{-(x+y)/g} b \frac{y}{x+y} \right) \\
\frac{dy}{dt} &= y \left(1 - (x+y) - c \frac{x}{x+y} - e^{-(x+y)/g} d \frac{y}{x+y} \right)
\end{aligned}
\tag{6.9}
$$

6.2   Mathematical Analysis

In this section we analyse the behaviour of the models proposed in section 6.1, but before starting, we include an important caveat for the reader. In the rest of the chapter several inequalities will arise, that have a complicated biological interpretation. For instance, $b < (>)d$ in words translates as "the average

mortality of non-callers is smaller (larger) than the mortality of callers under the alarm scenario". Similarly $a < (>)c$ is "the average mortality of non-callers is smaller (larger) than the mortality of callers under the non alarm scenario". The situations with two opposite inequalities arise most often and will be called the *mixed case*. In this situation, looking always at the non-alarm scenario, we distinguish also the population that "prevails" because of its smaller mortality. Thus e.g. the case $a < c$ and $b > d$ will be termed the *mixed case with prevailing callers*.

6.2.1 Analysis of the unlimited growth model

For model (6.5), we are interested in understanding which conditions could lead to either the survival or extinction of the populations. For biological consistency, we are supposing the right hand sides of eq. (6.5) are both zero at $(0,0)$. Thus, the dynamical system defined by Eq. (6.5) admits just $P = (0,0)$ as an equilibrium point. In the absence of alarmists, the non-alarmists goes away from zero in case of $a < 1$. Similarly, in the absence of non-alarmists the alarmist population goes away from zero in case of $d < 1$. Thus, if one of these parameters is less than 1, $P_1 = (0,0)$ is unstable.

For this model, the isoclines are lines given by equations

$$(1-a)x + (1-b)y = 0, \qquad (1-c)x + (1-d)y = 0,$$

so that $y(t) = \alpha x(t)$ for

$$\alpha = \frac{a-c}{d-b}.$$

In other words, the set S defined by line $y = \alpha x$ is invariant for the system. Clearly, this line splits up the plane in two others invariant sets: $R = \{(x,y) : y > \alpha x\}$ and $W = \{(x,y) : y < \alpha x\}$.

For this model we have the following result:

Proposition 6.2.1. *If non-callers mortalities in both scenarios exceed one, $a > 1$ and $b > 1$ then the non-callers population vanishes, $x(t) \to 0$ as $t \to \infty$. Further, if $a < 1$ and $b < 1$ then the non-callers population grows unboundedly, $x(t) \to \infty$ as $t \to \infty$.*

Geometrically, when $a, b > 1$ the isocline of x is a decreasing line through the origin and $x'(t) < 0$ for all $x, y > 0$. Thus, x-individuals go to extinction. Similarly, when $c, d > 1$ we can easily check that $y'(t) < 0$ for all $x, y > 0$. Hence, in this case, y-individuals go to extinction. In other words, when all parameters are greater than 1, both populations are going extinct.

Now, if $a < 1$ and $b < 1$ the isocline for x is a decreasing line and it is not difficult to check that $x'(t) > 0$ for all $x > 0$ and $y > 0$. In this scenario, x-individuals are going to survive. Likewise, when $c < 1$ and $d < 1$ the isocline for y is a decreasing line and $y'(t) > 0$ for all $x > 0$ and $y > 0$. Therefore,

y-individuals are going to survive. Hence, when all parameters are less than 1, both isoclines are decreasing lines crossing the origin and for all $x > 0$ and $y > 0$ we have that $x'(t) > 0$ and $y'(t) > 0$. Thus, both populations are going to survive.

In the following, we are interested in classifying the behaviour of eq. (6.5) for different settings of parameters. In order to get further information about the behaviour of the solution of eq. (6.5) let us consider the change of variables $z = x/(x+y)$ and $w = y/(x+y)$. Since $w = 1 - z$, the equation for z becomes

$$\frac{dz}{dt} = z\,(1 - z)\,[(c - a + b - d)\,z + d - b] \tag{6.10}$$

The previous equation has three equilibrium points: $\bar{z}_1 = 0$, $\bar{z}_2 = 1$ and $\bar{z}_3 = (b - d)/(c - a + b - d)$. The stability criteria for $\bar{z}_1 = 0$ and $\bar{z}_2 = 1$ of eq. (6.10) are given, respectively, by the eigenvalues:

$$\lambda_{\bar{z}_1} = d - b, \qquad \lambda_{\bar{z}_2} = a - c, \qquad \lambda_{\bar{z}_3} = \frac{(c - a)\,(b - d)}{c - a + b - d}.$$

Proposition 6.2.2. *The equilibrium point*

$$\bar{z}_3 = \frac{b - d}{c - a + b - d} \tag{6.11}$$

is feasible in the mixed case with either prevailing callers or non-callers, i.e. if and only if: (i) $c < a$ and $b < d$ or (ii) $c > a$ and $b > d$. In the first case, for prevailing callers, $\bar{z}_3$ is stable while in the second one $\bar{z}_3$ unstable.

Now, feasibility of $\bar{z}_3$ implies that the invariant set S, previously defined, lies on the first quadrant of the xy-plane. In fact, $z(t) = \bar{z}_3$ for all t means that $\bar{z}_3 = x(t)/(x(t)+y(t))$ which in turn implies that $y(t) = x(t)(1-\bar{z}_3)/\bar{z}_3 = \alpha x(t)$. The stability conditions for equilibrium $\bar{z}_3$ can also be translated in terms of asymptotic behavior of the original solution $x(t)$ and $y(t)$ as follows. If $\bar{z}_3$ is stable, then the solutions $x(t)$ and $y(t)$ are both increasing functions and, for large values of t, we have $y(t) \approx \alpha x(t)$, regardless of the initial condition. When $\bar{z}_3$ is unstable, then $\bar{z}_1$ and $\bar{z}_2$ are stable equilibrium points. Thus, the curves described by $x(t)$ and $y(t)$, on the xy-plane, are going to move away from the line $y = \alpha x$ as $t \to \infty$. For initial conditions above the line $y = \alpha x$, $y(t)$ dominates and $z(t) \to 0$ while for initial conditions below the line $y = \alpha x$, $x(t)$ dominates and $z(t) \to 1$. Whether both populations survive depends on the combination of parameters.

Proposition 6.2.3. *In the alarm scenario, if callers prevail $b > d$, then $\bar{z}_1 = 0$ is a stable equilibrium point of eq. (6.10) and considering the callers and non-callers mortalities d and b:*

  1. if $d > 1$ then $x(t) \to 0$ and $y(t) \to 0$.

    2. if $1 > b$ then then $x(t) \to \infty$ and $y(t) \to \infty$.

    3. if $b > 1 > d$ then then $x(t) \to 0$ and $y(t) \to \infty$.

Further, in the non-alarm scenario, if callers prevail $a > c$, the previous behaviors are true for all $x_o, y_o > 0$. Otherwise, items 1 - 3 are true for all $x_o, y_o > 0$ such that $x_o/(x_o + y_o) < \bar{z}_3$.

Proposition 6.2.4. *In the non-alarm scenario, if non-callers prevail $c > a$, then $\bar{z}_2 = 1$ is a stable equilibrium point of eq. (6.10) and considering the non-callers and callers mortalities a and c:*

    1. if $a > 1$ then $y(t) \to 0$ and $x(t) \to 0$.

    2. if $1 > c$ then $y(t) \to \infty$ and $x(t) \to \infty$.

    3. if $c > 1 > a$ then $y(t) \to 0$ and $x(t) \to \infty$.

Further, in the alarm scenario, if non-callers prevail $d > b$, the previous behaviors are true for all $x_o, y_o > 0$. Otherwise, items 1 - 3 are true for all $x_o, y_o > 0$ such that $x_o/(x_o + y_o) > \bar{z}_3$.

Finally, let us consider the case in which the equilibrium point $\bar{z}_3$ is stable.

Proposition 6.2.5. *In the mixed case with prevailing callers, i.e. when $a > c$ and $d > b$, solutions $x(t) \to \infty$ and $y(t) \to \infty$ if and only if*

$$a + d - (b + c) > ad - bc.$$

6.2.2 Analysis of the limited growth model

The isoclines for system (6.7) are (see also figures 6.1 and 6.2):

$$x(1 - a) + y(1 - b) - (x + y)^2 = 0, \quad x(1 - c) + y(1 - d) - (x + y)^2 = 0$$

Thus, for eq. (6.7) we have the following equilibrium points: $P_1 = (0, 0)$, $P_2 = (0, 1 - d)$, $P_3 = (1 - a, 0)$ and $P_4 = (\bar{x}, \bar{y})$ in which

$$\bar{x} = \frac{(d - b)(a - b - c + d - ad + bc)}{(a + d - b - c)^2}, \tag{6.12}$$

$$\bar{y} = \frac{(a - c)(a - b - c + d - ad + bc)}{(a - b - c + d)^2}. \tag{6.13}$$

We clearly see that equilibrium points P_2 and P_3 are feasible only if $d < 1$ and $a < 1$, respectively.

As in the previous model, in the absence of one population the other one goes away from zero depening on the size of a and d. Thus, provided that parameters a and d are less than 1, P_1 is an unstable equilibrium.
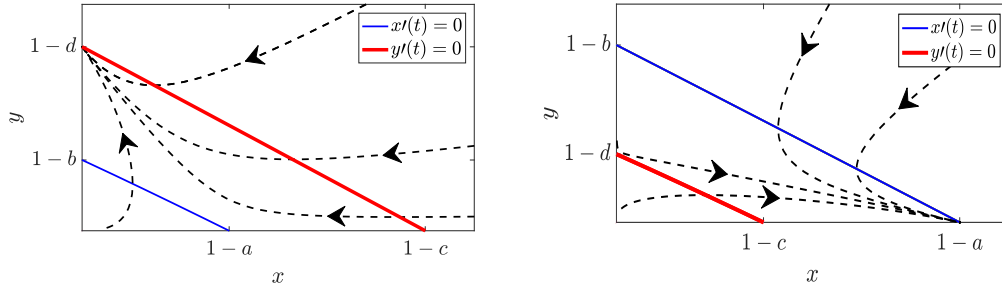
Figure 6.1: Isoclines of the limited population growth model. For this conditions, P_4 is not feasible. The red curve stands for the $x' = 0$ and and the red one for $y' = 0$. In the picture on the left, P_2 is asymptotically stable whereas P_3 is unstable. On the right, P_3 is asymptotically stable whereas P_2 is unstable.
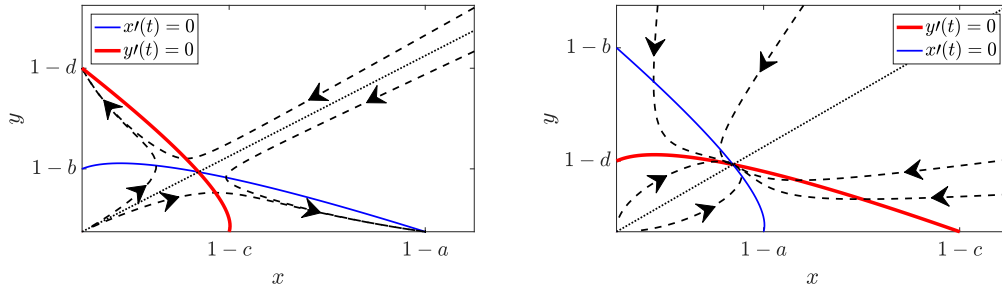
Figure 6.2: Isoclines of the limited population growth model. The existence of an equilibrium solution with nonzero coordinates. The red curve stands for the $x' = 0$ and and the red one for $y' = 0$. In the picture on the left, P_2 and P_3 are both asymptotically stable whereas P_4 is unstable. On the right, P_4 is asymptotically stable whereas P_2 and P_3 are both unstable.

For the model defined by eq. (6.7), the Jacobian matrix $J = [J_{ij}]$ at (x, y), with $x, y > 0$, is given by

$$
J = \begin{pmatrix} 1 - 2x - y - a + \dfrac{y^2\,(a - b)}{(x + y)^2} & \dfrac{x^2\,(a - b)}{(x + y)^2} - x \\[4mm] -y - \dfrac{y^2\,(c - d)}{(x + y)^2} & 1 - x - 2y - d - \dfrac{x^2\,(c - d)}{(x + y)^2} \end{pmatrix} . \quad (6.14)
$$

At the equilibrium $P_2 = (0, 1 - d)$, the eigenvalues of the Jacobian matrix are $\lambda_1 = d - b$ and $\lambda_2 = d - 1$. Thus, provided that it is feasible, P_2 is asymptotically stable when $d < b$. Further, at the equilibrium $P_3 = (1 - a, 0)$, the eigenvalues of the Jacobian matrix are $\lambda_1 = a - c$ and $\lambda_2 = a - 1$. Thus, P_3 is asymptotically stable when $a < c$.

Proposition 6.2.6. *If P_4 is feasible then one of the following are true:*
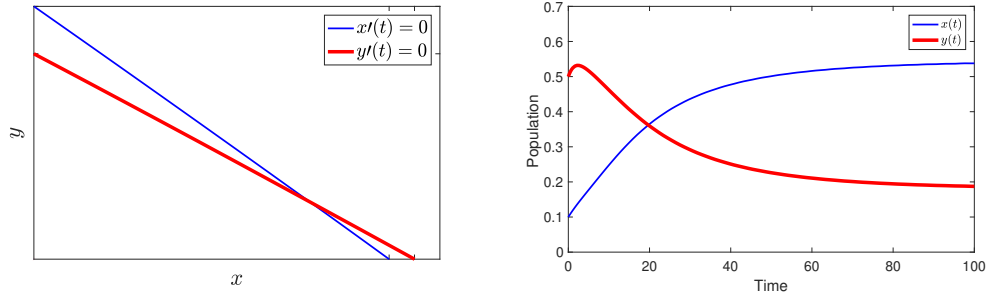
Figure 6.3: Graphical illustration for Proposition 6.2.6 with $a = 0.3$, $b = 0.2$, $c = 0.25$ and $d = 0.35$. For these parameters, the coexistence equilibrium solutions is $P_4 = (0.54, 0.18)$ that is stable, as predicted. For the initial condition $x_o = 0.1$ and $y_o = 0.5$ the solution converges to P_4 as $t \to \infty$.

1. in the mixed case with prevailing callers, i.e. $a > c$ and $d > b$. In this case, P_4 is stable.

2. In the mixed case with prevailing non-callers, i.e. $a < c$ and $d < b$. In this case, P_4 is unstable.

The last statement relies on the feasibility of P_4 (Fig. 6.3). We could easily check that

$$\frac{dx}{dt} < (1-p)x < 0$$

in which $p = \min\{a, b\} > 1$ and $x, y > 0$. Thus, when $a, b > 1$ the last inequality implies that P_4 is not feasible and $x(t) \to 0$ as $t \to \infty$. Analogously, $y(t) \to 0$ as $t \to \infty$ in case of $c, d > 1$. Thus, in order to have P_4 feasible we must have at least one parameter less than 1 in each equation of the model. Furthermore, suppose $a > c$ and $d > b$. When all parameters are less than 1, the first part of items 1 and 2 are sufficient conditions for the feasibility of P_4. In fact, assuming that $1 > a > c$ and $d > b$ we have that

$$a - c + d - b - ad + bc = a - c + d(1-a) + b(c-1) > (a-c)(1-b)$$

and since $b < 1$, it follows that $a - c + d - b - ad + bc$ is positive. Therefore, by eq. (6.12) and eq. (6.13) we have that P_4 is feasible. On the other hand, assuming that $a < c$ and $d < b < 1$ we have that

$$a - c + d - b - ad + bc = d - b + c(b-1) + a(1-c) < (d-b)(1-c).$$

In this case, provided that $c < 1$, the expression $a - c + d - b - ad + bc$ is negative and hence eq. (6.12) and eq. (6.13) imply that P_4 is feasible. Now, let us analyse the behaviour of the solution of eq. (6.7) when P_4 is not feasible.

154

Proposition 6.2.7. *If callers prevail in both scenarios, i.e. $a > c$ and $b > d$, the coexistence point P_4 is not feasible and P_2 is stable when the callers mortality in the alarm case does not exceed one, i.e. $d < 1$. Otherwise, P_1 is stable.*

Similarly, we have the following result.

Proposition 6.2.8. *If non-callers prevail in both scenarios, i.e. $a < c$ and $b < d$, the coexistence point P_4 is not feasible and P_3 is stable when the non-callers mortality in the non-alarm case does not exceed one, i.e. $a < 1$. Otherwise, P_1 is stable.*

From the previous discussion, we must point out that in the case where all equilibrium points are feasible, the asymptotic stability of P_2 and P_3 imply the instability of P_4. On the other hand, when P_4 is unstable, P_2 and P_3 are both asymptotically stable.

When $a = c$ the equilibrium point P_4 is no longer feasible, and the equilibrium $P_3 = (1 - a, 0)$ undergoes a bifurcation and its stability relies on whether $b > d$ or $b < d$. In fact, the set $[0, 1] \times [0, 1]$ is invariant for the dynamical system defined by eq. (6.7). Thus, when $d > b$ the equilibrium points P_2 and P_1 are unstable and the solution converges to P_3.

6.2.3 Analysis of group size effects - variant 1

Clearly, $P_1 = (0, 0)$ is an stable equilibrium point for eq. (6.8) if and only if $a > 1$ and $d > 1$.

When $y = 0$, the equilibrium points of eq. (6.8) are defined by the equation

$$f(x) = 1 - x - ae^{-x/g} = 0. \tag{6.15}$$

The Jacobian matrix for points satisfying eq. (6.15) is given by

$$J = \begin{pmatrix} (ax/g)\mathrm{e}^{-x/g} - x & 0 \\ a\mathrm{e}^{-x/g} - x - b\mathrm{e}^{-x/g} + (ax/g)\mathrm{e}^{-x/g} & 1 - c\mathrm{e}^{-x/g} - x \end{pmatrix}$$

whose eigenvalues are

$$\lambda_1 = 1 - x - ce^{-x/g} \qquad \lambda_2 = x\left(a/ge^{-x/g} - 1\right). \tag{6.16}$$

Thus, we can state the following results:

Proposition 6.2.9. *If the non-callers mortality in the non-alarm case does not exceed one, i.e. $a < 1$ then there is only an equilibrium point on the x-axis, say $P_1 = (\bar{x}, 0)$. This equilibrium point is stable if non-callers prevail in the non-alarm scenario, i.e. $c > a$ and unstable if they do not.*

Proposition 6.2.10. *When the non-callers mortality in the non-alarm scenario exceeds both one and the threshold group size, i.e. $a \geq \max\{1, g\}$ on the x-axis we can have:*

1. *No equilibrium point when $g\left[\ln(ag^{-1}) + 1\right] > 1$.*

2. *One equilibrium point when $g\left[\ln(ag^{-1}) + 1\right] = 1$.*

3. *Two equilibrium points, say $P_1 = (\bar{x}_1, 0)$ and $P_2 = (\bar{x}_2, 0)$ with $\bar{x}_1 < \bar{x}_2$, when $g\left[\ln(ag^{-1}) + 1\right] < 1$. In this case, when non-callers prevail in the non-alarm scenario, i.e. $c > a$, P_1 is unstable and P_2 is stable. Conversely, both are unstable.*

In the case where $a \leq g$, the function $f(x)$ in eq. (6.15) is a decreasing function and so there is only one equilibrium point on the x-axis. The stability of such an equilibrium relies on having $a > c$ or $a < c$.

We can state similar results for equilibrium points on the y-axis.

Proposition 6.2.11. *If $d < 1$ then there is only an equilibrium point on the y-axis, say $P_1 = (0, \bar{y})$. This equilibrium point is stable if callers prevail in the alarm scenario, i.e. $b > d$ and unstable conversely.*

Proposition 6.2.12. *When the callers mortality in the alarm scenario exceeds both one and the threshold group size, i.e. $d \geq \max\{1, g\}$ on the y-axis we can have:*

1. *No equilibrium point when $g\left[\ln(dg^{-1}) + 1\right] > 1$.*

2. *One equilibrium point when $g\left[\ln(dg^{-1}) + 1\right] = 1$.*

3. *Two equilibrium points, say $P_1 = (0, \bar{y}_1)$ and $P_2 = (0, \bar{y}_2)$ with $\bar{y}_1 < \bar{y}_2$, when $g\left[\ln(dg^{-1}) + 1\right] < 1$. In this case, when callers prevail in the alarm scenario, i.e. $b > d$, P_1 is unstable and P_2 is stable. Conversely both are unstable.*

Now, let us turn our attention to the existence of the equilibrium point in which both species survive. For $x, y > 0$ the isoclines of eq. (6.8) are defined by the following implicit equations:

$$
\begin{aligned}
1 - (x + y) - e^{-(x+y)/g}\left(a\frac{x}{x+y} + b\frac{y}{x+y}\right) &= 0 \\
1 - (x + y) - e^{-(x+y)/g}\left(c\frac{x}{x+y} + d\frac{y}{x+y}\right) &= 0.
\end{aligned}
\tag{6.17}
$$

From the previous equation such an equilibrium point $P = (\bar{x}, \bar{y})$ must satisfy the relation

$$
\bar{y} = \frac{a - c}{d - b}\bar{x}
\tag{6.18}
$$

and thus, in order for $P = (\bar{x}, \bar{y})$ to be feasible, the parameters must satisfy: *(i)* $a > c$ and $d > b$ or *(ii)* $a < c$ and $d < b$. Now, replacing y by $(a-c)x/(d-b)$, $\bar{x}$ must satisfy

$$1 - (1 + \alpha)x - \beta e^{-(1+\alpha)x/g} = 0 \tag{6.19}$$

in which

$$\alpha = \frac{a - c}{d - b}, \qquad \beta = \left(\frac{a + \alpha b}{1 + \alpha}\right). \tag{6.20}$$

The eigenvalues of the Jacobian matrix for points on the line $y = \alpha x$ are given by:

$$\lambda_1 = 1 - (1 + \alpha)\, x - \left(\frac{a + \alpha d}{1 + \alpha}\right) e^{-(1+\alpha)x/g} \tag{6.21}$$

$$\lambda_2 = 1 - 2(1 + \alpha)x - \beta e^{-(1+\alpha)x/g} + \frac{a + \alpha b}{g} x e^{-(1+\alpha)x/g}. \tag{6.22}$$

Using the previous equations we can state the following result:

Proposition 6.2.13. *If $\beta < 1$ then there is an equilibrium point $P = (\bar{x}, \bar{y})$ in which $\bar{x} > 0$ and $\bar{y} > 0$. This equilibrium point is stable in the mixed case when callers prevail, i.e. $a > c$ and $d > b$ and unstable in the mixed case when non-callers prevail, i.e. $a < c$ and $d < b$.*

Proposition 6.2.14. *If $\beta > 1$ then eq. (6.8) has:*

1. *No nonzero equilibrium point when $g\left[\ln\left(\beta g^{-1}\right) + 1\right] > 1$.*

2. *One nonzero equilibrium point when $g\left[\ln\left(\beta g^{-1}\right) + 1\right] = 1$.*

3. *Two nonzero equilibrium points, say $P_1 = (\bar{x}_1, \bar{y}_1)$ and $P_2 = (\bar{x}_2, \bar{y}_2)$, in which $\bar{x}_1 < \bar{x}_2$ and $\bar{y}_1 < \bar{y}_2$, in case of having $g\left[\ln\left(\beta g^{-1}\right) + 1\right] < 1$. Furthermore, if callers prevail in the mixed case, i.e. $a > c$ and $d > b$, P_1 is unstable and P_2 is stable. Both are unstable in the mixed case when non-callers prevail, i.e. $a < c$ and $d < b$.*

The line $y = \alpha x$ is an invariant set, say S, for the dynamical system defined by Eq. (6.8). In fact, defining $z(t) = -\alpha x(t) + y(t)$ we have that $z'(t) = -\alpha x'(t) + y'(t)$. Now, using Eq. (6.14) for all $(x, y) \in S$ we have that $z'(t) = 0$. Thus, for every initial condition on S we have that $z(t) = 0$ for all $t > 0$. That is, if $y_o = \alpha x_o$ then $y(t) = \alpha x(t)$ for all $t > 0$, which proves that S is invariant. In this way, when the equilibrium points on the line S are unstable, solutions generated by initial conditions above the line S are going to converge to equilibrium points on the y-axis. On the other hand, solutions generated by initial conditions below the line S are going to converge to equilibrium points on the x-axis.

By the previous results we can conclude that the surviving of species relies not only on the combination of the parameters values but it relies also on the
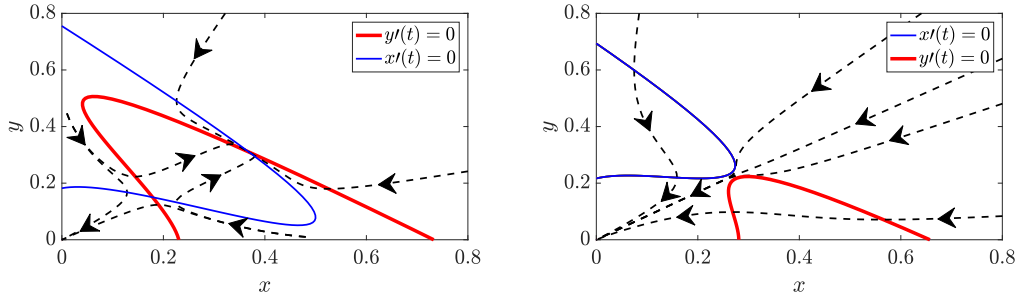
Figure 6.4: Graphical illustration for Proposition 6.2.15 with $a = 1.46$, $b = 1.20$, $c = 1.25$ and $d = 1.45$. On the left, we set $g = 0.3$ and thus we have two coexistence equilibrium solution: one unstable and the other one asymptotically stable. For these parameters, the origin is also asymptotically stable. On the right, we set $g = 0.51$ and thus there is no coexistence equilibrium solution. All solutions converge to zero.

initial conditions. That is, depending on the combinations of parameters the system defined by Eq. (6.8) can present an Allee effect. For instance, if $a, d > 1$ then the origin is a stable equilibrium point. Further, if the third condition of Proposition 6.2.14 is satisfied then there are two stable equilibrium points: $P_1 = (0,0)$ and $P_2 = (\bar{x}, \bar{y})$ in which $\bar{x}, \bar{y} > 0$. Of course, the convergence to each one of these equilibrium points depends on the initial condition.

To clarify this behaviour, let us analyse the following case.

Proposition 6.2.15. *Suppose all mortalities exceed one, i.e. $a, b, c, d > 1$ and consider the mixed case with prevailing callers, i.e. $a > c$ and $d > b$. There is a $\bar{g}$ such that for each $g < \bar{g}$ there are two critical values $n_1 \leq n_2$ such that:*

1. *both solutions converge to $P = (\bar{x}, \bar{y})$, $\bar{x} > 0$ and $\bar{y} > 0$ when the initial condition (x_o, y_o) satisfies $x_o + y_o > n_2$.*

2. *both solutions converge to $P = (0,0)$ when the initial condition (x_o, y_o) satisfies $x_o + y_o < n_1$.*

6.2.4 Analysis of group size effects - variant 2

As the previous models, the origin $P_1 = (0,0)$ is an stable equilibrium point of Eq. (6.9) if and only if $a > 1$ and $d > 1$.

Now, on the x-axis the equilibrium points can be found by setting $y = 0$ in Eq. (6.9) and so, $(1 - a, 0)$ is also an equilibrium point. Setting $x = 0$ in Eq. (6.9), the equilibrium points on the y-axis are defined by the solutions of

$$1 - y - de^{-y/g} = 0.$$

Further, we can state the following result:

Proposition 6.2.16. *For Eq. (6.9) it turns out that:*

1. *If $a < 1$ then $P = (1-a, 0)$ is an equilibrium, stable if non-callers prevail in the non-alarm scenario, i.e. $c > a$ and unstable conversely.*

2. *If $d < 1$ then there is only an equilibrium $P = (0, \bar{y})$ on the y-axis. This equilibrium is stable if callers prevail in the alarm scenario, i.e. $b > d$ and unstable conversely.*

Furthermore, assuming $d > 1$ and $\gamma = g\left[\ln\left(dg^{-1}\right) + 1\right]$ then:

3. *There is no equilibrium on the y-axis when $\gamma > 1$.*

4. *There is an equilibrium on the y-axis when $\gamma = 1$.*

5. *There are two equilibria on the y-axis, say $P_1 = (0, \bar{y}_1)$ and $P_2 = (0, \bar{y}_2)$, $\bar{y}_1 < \bar{y}_2$, in case of having $\gamma < 1$. Further, if $b > d$ then P_1 is unstable and P_2 is stable. Both are unstable if $b < d$.*

Besides the x axis and y axis, the isoclines of Eq. (6.9) are given by

$$1 - (x + y) - \left(a\frac{x}{x+y} + b\frac{ye^{-(x+y)/g}}{x+y}\right) = 0$$

$$1 - (x + y) - \left(c\frac{x}{x+y} + d\frac{ye^{-(x+y)/g}}{x+y}\right) = 0. \tag{6.23}$$

By comparing these two equations, we can conclude that at the equilibrium $P = (\bar{x}, \bar{y})$ we must have:

$$(\bar{x} + \bar{y}) - (\bar{x} + \bar{y})^2 - \alpha\bar{x} = 0, \qquad \bar{y} = \alpha\bar{x}e^{-(\bar{x}+\bar{y})/g} \tag{6.24}$$

in which $\alpha = (a - c)/(d - b)$. Thus, as necessary condition to existence of $P = (\bar{x}, \bar{y})$ the parameters must satisfy: *(i)* $a > c$ and $d > b$ or *(ii)* $a < c$ and $d < b$.

The previous equalities allow us to state the following

Proposition 6.2.17. *If $a + \alpha b > 1 + \alpha$ then there are $\bar{g}$ and $\hat{g}$ such that Eq. (6.9) has:*

1. *No nonzero equilibrium point when $g \geq \bar{g}$.*

2. *Two nonzero equilibrium points, say $P_1 = (\bar{x}_1, \bar{y}_1)$ and $P_2 = (\bar{x}_2, \bar{y}_2)$, in which $\bar{x}_1 + \bar{y}_1 < \bar{x}_2 + \bar{y}_2$, in case of having $g \leq \hat{g}$. Furthermore, if in the mixed case callers prevail, i.e. $a > c$ and $d > b$ then P_1 is unstable and P_2 is stable. Both are unstable if instead in the mixed case non-callers prevail, i.e. $a < c$ and $d < b$.*

The next result follows directly from the previous proof.

Proposition 6.2.18. *If $a + \alpha b < 1 + \alpha$ Eq. (6.9) has an equilibrium point $P = (\bar{x}, \bar{y})$. Further, P is stable when in the mixed case callers prevail, i.e. $a > c$ and $d > b$ and unstable conversely.*

159

Figure 6.5: Graphical illustration for Proposition 6.2.17 with $a = 1.3$, $b = 1.2$, $c = 1.25$, $d = 1.35$, $g = 0.23$ (left) and $g = 0.30$ (right). On the left, for these parameters, the coexistence equilibrium solutions are $P_1 = (0.14, 0.24)$ and $P_2 = (0.05, 0.86)$. As predicted P_1 is unstable whereas P_2 is stable. On the right, there is no coexistence equilibrium solutions.
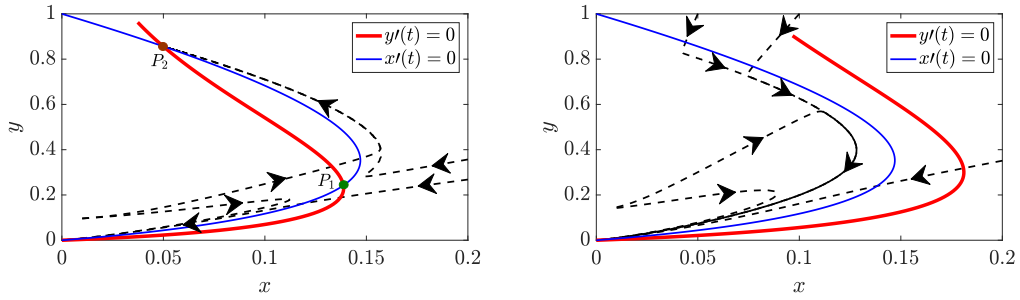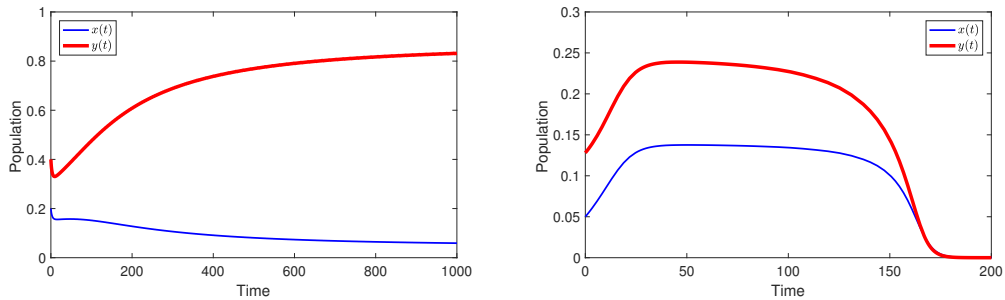

Figure 6.6: Graphical illustration for Proposition 6.2.17 with $a = 1.3$, $b = 1.2$, $c = 1.25$, $d = 1.35$ and $g = 0.23$. As predicted the convergence to the coexistence equilibrium depends on the initial condition. On the left we set $(0.2, 0.4)$ as initial condition whereas on the right we set $(0.05, 0.128)$.

6.3 Discussion

We begin the discussion section by making a summary and a biological interpretation of the results of section 6.2.

6.3.1 Summary of analysis and biological interpretation of the models

Model 1 - Unlimited growth

In model 1 we have just two components in the dynamics of the population: Malthusian growth and death by predation. Since both ingredients may be unlimited, cases in which the populations tend to infinity can be observed. Even if extremely simple and unrealistic in the dynamics aspect, the model can provide the basic insight as to which type of individual will prevail (in terms of frequency) in the population, depending on the values of parameters a, b, c and d.

Equation (6.10) is the the dynamics of the frequency of non-alarmists in the population ($z(t)$) and captures the essence of our discussion, it is a form of replicator equation [68]. For such equation of the frequency, three equilibria may exist: alarmists dominate the population ($\bar{z}_1 = 0$), non-alarmists dominate the population ($\bar{z}_2 = 1$) and a mixed equilibrium where there is a balance in the frequency of the populations ($\bar{z}_3 = \alpha = (a-c)/(d-b)$). Given these three equilibria, we have only four distinct qualitative behaviours for the dynamics: non-alarmists dominate, alarmists dominate, both behaviours are evolutionarily stable and, finally, both are unstable. In table 6.1 we present the relations between the parameters, the result of the evolutionary dynamics and some biological interpretation.

Naturally, the mortality rates also define if each population of the types ($x(t)$ and $y(t)$) is going to survive, and that depends on their relations with the population growth rate (in non-dimensional form, they are compared to 1). Propositions 6.2.1 to 6.2.5 give the rigorous proofs of those relations. They state respectively the conditions for unlimited growth or disappearance for the "non-alarmist" population, the conditions under which both "non-alarmist" and "alarmist" thrive coexisting, when each one survives alone, and when both these populations grow without bounds. The coefficient $\alpha = (a-c)/(d-b)$ is also important, because it represents the ratio of alarmists per non-alarmists in case of a mixed equilibrium or the slope of the separatrix in case of bistability.

Model 2 - limited growth

Model (6.7) incorporates the limiting effects of population growth through intraspecific competition. Propositions 6.2.6-6.2.8 illustrate the mutual relationships between feasibility of the coexistence equilibrium and stability of the

161

Table 6.1: Qualitative behaviour of model (6.1) and biological interpretation.

Conditions	Which type of individual does better in case of:		Evolutionary outcome
	Alarm	No-alarm	
$a < c$ and $b < d$	Non-alarmists	Non-alarmists	Non-alarmists dominate
$a > c$ and $b > d$	Alarmists	Alarmists	Alarmists dominate
$a < c$ and $b > d$	Alarmists	Non-alarmists	Both strategies are stable, mixed equilibrium unstable
$a > c$ and $b < d$	Non-alarmists	Alarmists	Both strategies are unstable, mixed equilibrium stable

points in which only "non-alarmists" or "alarmists" thrive. What propositions 6.2.6-6.2.8 show is that the basic relations depicted in table 6.1 still hold in the new model. In the model without competition, when one strategy dominates the other, individuals of the inferior strategy can still survive in the population, even though they represent a decreasing fraction of the total population as the time advances. In the model with competition, this possibility is excluded by the introduction of intraspecific competition.

Some care has to be taken, again, with the relation of the parameters in comparison with unity, when they are greater, the whole population may go extinct.

Model 3 - Group size effects - variant 1

The suggestion that individuals might benefit from the retention of conspecifics (see also section 6.3.3) due, for example, to Trafalgar, confusion [19][p. 274] or dilution effects, led us to propose a model to incorporate this factor in the reduction of the predation rate. In this variant, those effects take place independently if an alarm call was produced or not. The results indicate that, under certain assumptions in the functional response, these benefits of grouping are not enough to change the qualitative results presented in table 6.1.

The results do not change qualitatively, basically because the benefit that one individual enjoys by the retention of another conspecific is, of course, shared by every other individual of the population. Therefore, just this factor is not enough to generate *differential fitness* (comparison between gains), which is very important in the competition of the two strategies. A simple way to understand this is to write the equation for the frequencies of non-alarmists in

the population for this model, which we denote by $u(t)$:

$$\frac{du}{dt} = u\,(1-u)\,e^{-(x+y)/g}\,[(c-a+b-d)\,z+d-b]\,. \qquad (6.25)$$

Equation (6.25), above, is almost identical to equation the replicator equation (6.11). Since the exponential term $e^{-(x+y)/g}$ is always positive, we can deduce that the qualitative behaviour of both equations is identical. So, again, this means that the qualitative relations between the strategies do not change in terms of the frequencies. The major change is with respect to the survival of the species.

In the previous models, usually one or two single parameters would define if the populations would survive. Now, since we have group size effects, results are more complex and may depend on the initial conditions. Just as a way of understanding this, we can decompose the behaviour of the model into two ingredients: frequencies and population size. In terms of frequencies the behaviour is exactly analogous to previous models. When it comes to population size, now there may be an effect analogous to an "Alee effect", meaning that if the initial population size is too small, benefits of grouping are inefficient and populations may go extinct.

The exact conditions over the parameters for the existence of such effects with respect to equilibrium frequencies $u = 0$ (non-alarmists dominate), $u = 1$ (alarmists dominate) and $u^* = \alpha$ (mixed equilibrium) are worked out and proved in propositions 6.2.9 to 6.2.15. It is also worth to note that the value of the mixed equilibrium ratio between alarmists and non-alarmists is not changed by the inclusion of benefits of grouping (which work for both alarm and non-alarm scenarios - such as the dilution effect).

Propositions 6.2.9 to 6.2.12 illustrate respectively the situations in which no, one or two equilibria with only "non-alarmists" may arise, and the corresponding situation involving instead only the "alarmist" population. For the two populations coexisting together, the possible alternatives are stated in Propositions 6.2.13 and 6.2.14, while Proposition 6.2.15 discusses the bistability between coexistence and the system disappearance.

Model 4 - Group size effects - variant 2

This model also may present a behavior analogous to an "Alee effect". The conditions for survival of just one of the "non-alarmists" or "alarmists" populations are given in Proposition 6.2.16. Propositions 6.2.17 and 6.2.18 instead discuss respectively the feasibility and multiplicity of the coexistence equilibrium and its stability. As proved in proposition 6.2.17, for small values of g this model may have a coexistence equilibrium that is asymptotically stable besides the origin. In this case, the convergence of the solution to one or another depends on the initial condition. We can see this effect illustrated in the simulations in the figures 6.5 and 6.6. However, here the frequencies of the

coexistence equilibrium depends not only on the parameters a, b, c and d but also it depends on the threshold group size g.

6.3.2   Selfish, mutualistic and altruistic alarm calls

In sections 6.1, 6.2 and 6.3.1 we discussed four distinct models for the selection of alarmist or non-alarmist behaviour in a population composed of both types of individuals. The analysis showed that the average mortality rates due to predation, represented by parameters a, b, c and d are the key elements to define which behaviour can evolve by individual selection. In this section we discuss some biological theories and observations and its relations with the results of the models.

In view of the summary of the behaviour of the models (section 6.3.1), the first three models have almost identical behaviour in relation to those four fundamental parameters. Only the model that includes benefits of grouping just in the case of an alarm has some significant difference in behaviour. Our discussion will be focused one the relations between a, b, c and d, with some commentaries on the case of the second variant of group size effects.

In first place, we must make an observation on the reasons of why parameters a, b, c and d may differ from one another. Differences between a and b, or between c and d are simpler to account for, since they are related with two distinct situations: the chance of existence or non-existence of an alarm call prior to the attack of the predator. On the other hand, differences between a and d or between c and d (which are the ones that really matter for the behaviour of the models) are subtler.

For instance, if there is a "cost" (in terms of increasing risk) of giving an alarm call, we can suppose that $b < d$. If all other factors remain equal, non-alarmist individuals never increase their chance of being attacked by issuing alarm calls, so their average mortality is the same in all cases where an alarm call was produced. On the other hand, alarmists will sometimes be the ones who produced the alarm call, thus, the increased mortality in those specific situations increase the average mortality of the class. There is mixed evidence if this is the case for all alarms calls [19, p. 187-189]. In particular, [75] registered increased mortality for alarm callers in relation to one predator species (terrestrial) but decreased mortality in relation to another (aerial). In fact, even in the case where alarm calling has no intrinsic "cost", if the caller is consistently the one closest to the predator, still we would have $b < d$ because the average mortality of non-callers would be smaller than that of callers under the alarm scenario.

Differences between a and c might occur due to the differential behaviour when spotting a predator. The individual who is the first to spot the predator might consistently be the closest to it and, if proximity leads to increased risk, we would have $a > c$, simply because the average mortality of non-callers would

be greater than those of callers when the alarm is not given. Therefore, we can interpret different biological scenarios by changing the relations between the parameters.

It must be observed, though, that the inference of the impact of more complex scenarios on the average mortalities of each class, is not straightforward. For a rigorous analysis it is necessary to think of a more complete predatory sequence and calculate the impact on the average mortalities explicitly. The fact that the average mortalities may depend on the actual size of the classes is one possible direction of model improvement.

[19] (p. 190) presents a classification of alarm calls directed at conspecifics that consists of three categories: selfish (benefit the caller but harm the receiver), mutualistic (benefit both caller and receiver) and altruistic (harming the caller and benefiting the receiver). Such type of terminology, introduced by Hamilton [38, 39, 88], is based in four possible combinations of two qualities. Given a certain action, the individuals involved in it may be classified as actors or recipients. The results of the action upon an individual may be classified as a "benefit" if they increase fitness or "harm" if they decrease it. Therefore, given the results for actor/recipient, we obtain four distinct categories: "selfishness" $(+/-)$, "altruism" $(-/+)$, "mutualism" $(+/+)$ and "spitefulness" $(-/-)$. Even though spite is rare in nature, it is included here for a complete theoretical treatment.

Recalling the meaning of the parameters a (average mortality of non-caller under no alarm), b (average mortality of non-callers under alarm), c (average mortality of caller under no alarm) and d (average mortality of callers under alarm), one possible interpretation of the relations between the parameters based on the four interaction types $(+/-)$, $(-/+)$, $(+/+)$ and $(-/-)$, is given in table 6.2.

Table 6.2: Relations between parameters given the four distinct types of interaction.

Type	Parameter relations
Selfish $(+/-)$	$a < b$ and $c > d$
Mutualistic $(+/+)$	$a > b$ and $c > d$
Altruistic $(-/+)$	$a > b$ and $c < d$
Spiteful $(-/-)$	$a < b$ and $c < d$

We acknowledge that there may be other possible interpretations, but we remark that the mathematical analysis is not affected by such conflicts. Once the relations between the parameters is well-established, the evolutionary outcomes are well-defined.

Selfish alarm calls

If we interpret a "selfish" alarm call as one that decreases the mortality rate of callers and increases the mortality rate of non-callers, both in relation to the non-alarm scenario, in terms of the parameters of the model, we would have $a < b$ (mortality rate of non-callers are increased in the case of an alarm), and $d < c$ (mortality rates of callers is decreased in case of alarm). Under such conditions, three of the four evolutionary outcomes of table 6.1, are possible, depending on the exact values of the parameters. The only unfeasible outcome is the total dominance of the non-callers, but the strategy could still be stable if non-callers did better in the non-alarm scenario.

In terms of the parameters of the models, it does not matter much the comparisons between a and b or between c and d, which would measure the efficiency of the alarm in preventing the predator to achieve a successful attack. What really matters are the relations between the a and c or b and d. If we suppose that callers and non-callers do equally well under the non-alarm scenario ($a = c$), then we can infer from $a < b$ and $d < c$ that $d < b$. That is, the mortality rate of callers is smaller than those non-callers under the alarm scenario. In this case, callers dominate and the behaviour is evolutionarily stable. The same occurs if callers do better even in the non-alarm scenario ($a > c$).

If, for any reason, the non-callers do a little better under the non-alarm scenario ($a < c$) then both strategies are stable and the evolutionary outcome depends on the initial condition. Now, the separatrix is given by the line $y = \alpha x$, if the advantage of alarmists in the alarm scenario ($b - d$) is much greater than the advantage of non-alarmists in the non-alarm scenario, we obtain a separatrix very close to the x-axis. That means that small perturbations in the frequencies of behaviours could lead to the total establishment of alarmist behaviour. Such initial variation of frequencies could be initiated through kin-selection, for instance, and then take-off and spread to the whole population.

If we include the benefits of grouping when there is an alarm (model (6.9)), meaning that although non-callers would do better in the non-alarm situation without these benefits ($a < b$), with the inclusion of the effect they could do better in the alarm scenario ($a > e^{-(x+y)/g}b$), depending on the size of the population and the efficiency of the benefits of grouping. The complete behaviour of the model is more complicated, and the separatrix for the establishment of the strategies is no longer a straight line. But it can be observed, as expected, that as the efficiency of grouping benefits increases, the region of attraction of the non-caller strategy increases. This means that the effect of the "selfish" alarm may get diluted due to the benefits of grouping and the "take-off" of the alarmist population becomes more difficult.

One can imagine a hypothetical scenario where calling behaviour serves as an extreme signal of pursuit deterrence (for a definition of pursuit deterrence see [19], p. 244) to the point that predators choose to attack preferably non-

callers (which are not displaying that they are alert). Under such conditons the mortality rate of non-callers under the alarm scenario might be greater than in the case of no alarm. Finally, one must also observe that such type of alarm, if ever observed in nature, would have a very distinct aspect when compared to beneficial alarm calls. For instance, there should be no pressure in lowering localizability, since now the alarm itself is a sign of unprofitability.

Mutualistic alarm calls

The case where both caller and receiver are benefited by the emission of alarm calls can be related to the models by choosing the parameters so that $a > b$ and $c > d$. Thus, the alarm is beneficial to both callers and non-callers. In this case, which type of individual benefits *more*, whether caller or non-caller, is not explicitly defined. So, no clear relation between d and b or a and c can be deduced using only this information.

That individuals can reap benefits from group protection when an alarm call is emitted does not help, [69, 24], what matters most is which type is benefited the most. When costs and benefits are approximately equal, they provide a perfect scenario for the evolution of nepotism, where kin selection should play a crucial role. No wonder there is good evidence for kin selection in many instances of alarm calling behaviour.

When alarm calls are mutualistic, the selection of alarmist and non-alarmist behaviour will depend on the relative benefits that each type of individual obtains. If alarmists and non-alarmists are equally preyed upon under the "non-alarm" scenario ($a = c$), and there is a increased risk in emitting an alarm call that provides equal protection for all individuals ($d > b$), then alarmist behaviour will not be selected for (by individual selection alone). We shall refer to the case of $d > b$ as "mildly altruistic".

If non-callers suffer higher average mortality rates under the non-alarm scenario ($a > c$), frequency-dependent selection dominates and both behaviours can survive in the population, the exact proportions depending on the particular model adopted (dependent on $a - c$, $d - b$ and groupsize effects). This should be the case when the one closest to the predator has both a higher probability of spotting the predator and of being the target of an attack. Under the non-call scenario, non-caller individuals have a higher probability of being the one closest to the predator, so their average mortality under this scenario, when compared to callers, should be a little higher.

Group size effects (those of model (6.9)) can significantly shift the equilibrium population fraction of each strategy. When grouping benefits are very effective even for low population numbers (low when compared to the carrying capacity, $g < 1$) the fraction of alarmists increases. If grouping is not very effective, the proportion of alarmists decreases.

It is worth to note that while the steady state in which there is a non-zero fraction of both alarmists and non-alarmists may represent a population that

is composed of individuals that adopt either one or other strategy 100% of the time, it can also be understood as a population of individuals adopting a "mixed strategy" [77]. That is, individuals may or may not give the alarm, having a probability of adopting one or the other strategy. In the case of the unlimited growth model (eq. (6.5)) the probability of adopting one strategy or the other is given by $\bar{z}_3$ and $1 - \bar{z}_3$ ($\bar{z}_3$ is the proportion of non-alarmists in the steady state where both populations are nonzero).

The conclusion is that "mildly altruistic" alarm calls can evolve to a mixed equilibrium in situations where the individual that spots the predator is subject to an increased risk ($d > b$ but $c < a$). Grouping benefits may help the establishment of alarmist behaviour. We recall that we are not modelling kin selection in these models.

Altruistic alarm calls

If we interpret altruistic alarm calls as in table 6.2, we have that the average mortality of the alarmist class increases in case of alarm while the mortality of non-alarmists decrease, that is $a > b$ and $c > d$. If one suppose that non-callers do equally well or better than callers ($a \leq c$) under the non-alarm scenario, then it we can infer that $b < d$, which leads to the dominance of non-alarmist behavior.

If $a > c$, the resulting behaviour will depend on the relation between b and d. The most likely is that we still have $b < d$, so that the resulting evolutionary equilibrium is a mixed equilibrium. If we had $b > d > c$, that would mean that callers in the non-alarm scenario do better than non-callers warned by an alarm, which looks unlikely. So, if callers do a little better under the non-alarm scenario, that would result in a stable mixed equilibrium.

Recalling that the ratio between of callers and non-callers is given by $\alpha = (a-c)/(d-b)$, in the case of altruistic scenario, a low ratio works against the spread of alarmist behaviour. That is because the proportion of the population (or frequency with which an individual chooses to emit an alarm) is low if $a \approx c$ and $d \gg b$. So, in this case there is only the establishment of a very low frequency of alarmists, and it may represent cases in which alarm is more restricted to help kin-related individuals. Here the effects of benefits of grouping change the equilibrium ratio in favor of alarmists ($(a-b)/e^{(-(x+y)/g}(d-b))$) reducing the effects of the altruistic alarm and increasing the frequency of alarmists in the population.

Spiteful alarm calls

Interpreting a spiteful alarm call as one which increases the mortality of both classes, we would have $a < b$ and $c < d$. Theoretically, any of the four resulting outcomes of table 6.1 is possible, since the relations between a and c (who does

better with no alarm) and b and d (which class is harmed more by the alarm) are undefined.

Harmful alarm calls would imply in a very different evolutionary relationship between callers and receivers. While receivers should evolve to detect well and respond quickly to beneficial calls, under the existence of harmful calls, receivers would be selected to resist the call (and act as if there was no alarm). In this sense, the relation between callers and receivers could only be evolutionarily stable if not responding to the alarm led to even worse results.

In the discussion of selfish alarm, we created a scenario of extreme pursuit deterrence in which the mortality of non-callers would be increased when compared to the non-alarm scenario. A spiteful alarm would be one in which also the mortality of callers would be increased. For instance, they might draw the attention of the predator, otherwise unaware of the presence of prey to the group. If the mortality of non-callers is increased more than that of callers ($b > d$) such behaviour could evolve through individual selection. To the best of our knowledge, we know no evidence of such types of "alarm behaviour".

6.3.3 Benefits of retaining group members and similar scenarios

[78] proposed an approach to explain alarm call behaviour:

> If it is beneficial for some animals to live in groups with conspecifics (see Bertram 1978; Pulliam and Caraco 1984), or even in groups including other species, then the loss of individuals from the group may reduce the overall benefit of the group to each survivor. If this loss of benefit is greater than the risk incurred by delivering a warning signal, then animals that warn group members of impending predator attack may have a selective advantage over those that do not. The selective advantage would not derive from kinship and it would not require specific acts of reciprocity (or distinction between cheaters and alarm senders).

The inclusion of benefits of grouping in models (6.8) and (6.9) has two important effects:

1. It creates an effect similar to an "Alee effect". Depending on the combination of parameters, very low populations may not benefit enough from grouping to scape extinction.

2. In variant 2 (benefits of grouping only under alarm), the proportion under equilibrium may shift towards the alarmist population.

Both effects do not change the fundamental relations between parameters a versus b and c versus d, that define the selection of alarmist or non-alarmist behaviour.

Thus, under the light of individual selection and the models proposed, such theory alone would not be enough to explain the selection of alarmist behaviour. What matters really is which class benefits most from the alarm call (b versus d) or is harmed by not issuing an alarm (a versus c). Even under the assumption of no-intraspecific competition, as in model (6.5), if the benefit is greater for the non-alarmists, the fraction of the population composed by non-alarmists would increase in time, approaching one as time increases. Therefore, under the framework of individual selection, we conclude that the hypothesis of benefits of retaining group members is not a sufficient explanation for the maintenance of alarmist behaviour in a population.

On the other hand, we have shown that grouping benefits, model (6.9), favours the selection of a majority of alarmists in the co-existence scenario. This is not the exact mechanism suggested by [78] but it is related to it in the sense that, by retaining group members, alarmists diminish the weight of the cost of issuing alarm calls in proportion to the costs of not-issuing alarm calls ($\bar{x}/\bar{y} = G^*(d-b)/(a-c)$, $G^* = e^{-(\bar{x}+\bar{y})/g}$, $0 < G^* < 1$).

Analogous to Smith's reasoning, is the suggestion by [25]: under particular conditions, it might be in the interest of the individual to emit an alarm call, lowering the chance of the group of prey being detected and thus his own chance of being attacked. Another analogous reasoning is arguing that ensuring any group member is not taken may reduce probability of predator returning to that area for another meal. This type of situation, again, does not guarantee selection of alarmist behaviour, because it impacts the mortalities of both classes. It may benefit the individual, but it may benefit equally, or more, the individuals of the other class.

6.3.4 Anecdoctal evidence for the evolution of alarm calls

[24] presents a study about the functions of alarm call in redshanks. The data collected and the conclusions of the biologist are coherent with the relations presented with the expected relation between parameters a, b, d and d [24] (text in bold inserted by us):

> There did not appear to be a cost associated with alarm calling in flight as sparrowhawks **(one of the predators of redshanks)** rarely switched birds during an attack (0.6% of $N = 535$ attacks on redshank flocks; unpublished data), and the individuals initially attacked were late or non-callers rather than callers (Cresswell 1993a). Callers would benefit because the number of birds in the air would be increased, adding to the "confusion" (see Cresswell 1993a). Those birds that were approached most closely, and consequently with the most to gain by encouraging other birds to

join the flying flock, called most frequently. A call by the bird be-
ing chased might still result in recruiting other redshanks to join it
because a redshank on the ground was much more vulnerable than
any flying bird on attack by a sparrowhawk (Cresswell 1993b).

All elements necessary for the evolution of alarm call behaviour by individual
selection are present in the biologist's description: low cost of alarm calls
($b \approx d$), strong penalty for either not responding to a call or not emitting
it ($a > c$) and grouping benefits . It is also interesting to observe that this
particular case is also an example of alarm calling behaviour that cannot be
directly explained by kin selection.

6.4   Conclusions

The results obtained by the analyses of the models indicate that alarm calls
can evolve through individual selection under particular assumptions relating
the average mortalities of each class of behaviour. Using a framework of Popu-
lation Ecology, it was possible to study some of the main explanations for the
emergence of alarm call behaviour under individual selection.

We derived conditions over the average mortalities for the evolution of
selfish, mutualistic, altruistic and spiteful alarm calls. In many particular
cases, where both strategies could survive or be stable, kin selection could
play a important role for the selection of alarm call behaviour.

The models suggest at least one main mechanism for the establishment of
alarm call behaviour without resort to kin selection. The average mortalities
of non-callers would be a little higher than callers in the non-alarm scenario,
simply because the individual who had the chance to spot the predator might
be a little more exposed to danger than the others ($a > c$). Naturally, such
argument is symmetric and the average mortalities of callers in the alarm
scenario should be also a little higher than those of non-callers ($d > b$).

If calling behaviour increases a little the chance of being attacked (which
should be the case at least for some species, given the evidence of the evolution
of non-localizability characteristics of alarm calls), then the difference $a - b$
should be smaller than $d - b$. Since the equilibrium fraction is $y/x = (a -
b)/(d - b)$, selection does not work much in favor of alarmists. If group effects
are included, the balance may shift in favor of callers, because the equilibrium
fraction is now $y/x = (a - b)/G^*(d - b)$, $G = e^{-(x+y)/g}$. If grouping benefits
are efficient ($g \ll 1$), we can have a strong selection for alarmist behaviour.
We believe this is the most realistic representation presented by the models
studied for the evolution of alarm calls through individual selection.

In this manner, we suggest that the theory that the benefits of retaining
group members could lead to the evolution of alarm call behaviour is not
sufficient for the evolution of alarm calling, but works as a complement in

the framework used in the models. Finally, it is important to notice that the inclusion of group size effects in the models, depending on the rates of mortality, may lead to the creation of an effect similar to an "Alee effect". In such cases, small populations may be led to extinction due to the lack of enough individuals for the efficiency of grouping benefits. So, depending on the predation rates, there might be a critical minimum population size for this mechanism to work.

Appendix B

In this appendix we present proofs of propositions presented in this chapter.

Proof. (**Proposition 6.2.1**): For the first case, it turns out that

$$\frac{dx}{dt} = \frac{x}{x+y}\left[(1-a)x + (1-b)y\right] < (1-p)x < 0$$

in which $p = \min\{a, b\} > 1$. On the other hand, if both parameters are greater than 1 then we have then

$$\frac{dx}{dt} = \frac{x}{x+y}\left[(1-a)x + (1-b)y\right] > (1-p)x > 0$$

in which $p = \max\{a, b\} < 1$. □

Proof. (**Proposition 6.2.2**): In fact, since $z(t) \in [0,1]$ for all $t \geq 0$, the following inequality must be true

$$0 < \frac{b-d}{c-a+b-d} < 1.$$

Thus, clearly, we must have $b - d > 0$ and $c - a + b - d > 0$ or $b - d < 0$ and $c - a + b - d < 0$. In the first case, it turns out that $b - d < c - a + b - d$ which implies that $c > a$. In the second, we have that $b - d > c - a + b - d$. Hence $a > c$ and the conclusion follows directly from this inequality.

The eigenvalues for this point are given by

$$\lambda_{\bar{z}_3} = \frac{(c-a)\,(b-d)}{c-a+b-d}.$$

Thus, in the first case the, the numerator of $\lambda_{\bar{z}_3}$ is positive whereas the denominator is negative. Therefore, the equilibrium point $\bar{z}_3$ is feasible and stable only when condition (i) is satisfied. □

Proof. (**Proposition 6.2.3**): As we saw previously, $b > d$ implies that $\bar{z}_1$ is an asymptotically stable equilibrium point. Thus, if $a > c$ then $\bar{z}_3$ is no longer feasible and $z(t)$ decreases to zero as $t \to \infty$ for all $z_o \in (0,1)$. On the other

hand, when $a < c$ then $\bar{z}_3$ is unstable and $z(t)$ decreases to zero as $t \to \infty$ for all $z_o \in (0, \bar{z}_3)$. Writing $x'(t)$ and $y'(t)$ in terms of $z(t)$ we have:

$$\frac{dx}{dt} = x\left[1 - az(t) - b(1 - z(t))\right]$$

$$\frac{dy}{dt} = y\left[1 - cz(t) - d(1 - z(t))\right].$$

Since $1 - z(t) < 1$ and $z(t)$ is a monotonic function,

$$\frac{dx}{dt} > x\left[1 - az(T) - b\right] \qquad \frac{dy}{dt} > y\left[1 - cz(T) - d\right]$$

for every fixed $T > 0$. If $d < b < 1$ then there is $T > 0$ such that $[1 - az(T) - b] = \alpha_1 > 0$ and $[1 - cz(T) - d] = \alpha_2 > 0$ for all $t > T$ and therefore $x(t), y(t) \to \infty$ as $t \to \infty$.

On the other hand,

$$\frac{dx}{dt} < x\left[1 - b(1 - z(T))\right] \qquad \frac{dy}{dt} < y\left[1 - (1 - d)z(T)\right]$$

for every fixed $T > 0$. If $1 < d < b$ then there is $T > 0$ such that $[1 - az(T) - b] = \alpha_1 < 0$ and $[1 - cz(T) - d] = \alpha_2 < 0$ for all $t > T$ and therefore $x(t), y(t) \to 0$ as $t \to \infty$.

Finally, when $b > 1 > d$, using the previous inequalities for $x'(t)$ and $y'(t)$, there are $\alpha_1 < 0$ and $\alpha_2 > 0$ such that $x'(t) < \alpha_1 x$ and $y'(t) > \alpha_2 y$ for all $t > T$ for some $T > 0$. Thus, $x(t) \to 0$ and $x(t) \to \infty$ as $t \to \infty$ and the proposition is proved. $\qquad\square$

(Proposition 6.2.4) can be proved using an analogous reasoning.

Proof. **(Proposition 6.2.5)**: First, since $a > c$ and $d > b$, $\bar{z}_3$ is asymptotically stable and $z(t) \to \bar{z}_3$ as $t \to \infty$ for all $z_o \in (0, 1)$. As a consequence, $x(t) \to \infty$ if and only if $y(t) \to \infty$ as $t \to \infty$. Further, $x(t) \to 0$ if and only if $y(t) \to 0$ as $t \to \infty$. As we stated before, the line $y = \alpha x$, $\alpha = (a - c)/(d - b)$, defines an invariant set S and an initial condition (x_o, y_o) belongs to S if and only if $z_o = x_o/(x_o + y_o) = \bar{z}_3$. In order to prove the statement it is enough to analyse the signal of $x'(t)$ for initial conditions on the set S. Now, for every $(x, y) \in S$ we have
$$\frac{dx}{dt} = \frac{1}{1 + \alpha} \frac{a - c + b - d + bc - ad}{d - b}.$$
Therefore, since $d - b > 0$, it turns out that $x'(t) > 0$ if and only if $a - c + b - d > ad - bc$ and the statement is proved. $\qquad\square$

Proof. **(Proposition 6.2.6)**: By eq. (6.12) and eq. (6.13), $\bar{y} = (a - c)/(d - b)\bar{x}$. Assuming P_4 feasible we must have $(a - c)/(d - b) > 0$. That is, if $a > c$ then

173

$d > d$ and when $a < c$ we must have $d < b$. This proves the first part in both items. At P_4, the eigenvalues of the Jacobian matrix are given by

$$\lambda_1 = -\frac{(a-c)\,(d-b)}{a-c+d-b} \quad \lambda_2 = a - 1 - \frac{(a-b)\,(a-c)}{a-c+d-b}.$$

Further, we have that

$$\lambda_1\lambda_2 = \frac{(a-c)\,(d-b)\,(a-c+d-b-ad+bc)}{(a-c+d-b)^2}.$$

Since P_4 is feasible we have that λ_1 is always negative. Furthermore, when $a > c$ and $d > b$ eq. (6.12) and eq. (6.13) imply that $a - c + d - b - ad + bc$ must be positive. Therefore, in this case we have that $\lambda_1\lambda_2 > 0$ which implies that λ_2 is also negative and this proves the first item of the statement. In a similar way, we can also prove the second claim. $\square$

Proof. (**Proposition 6.2.7**): According to Proposition 6.2.6, P_4 is not feasible for this configuration of parameters. The stability of P_2 follows directly from the expression of the eigenvalues of the Jacobian matrix at P_2, which are $\lambda_1 = d - b$ and $\lambda_2 = d - 1$. $\square$

(**Proposition 6.2.8**) is proved in an analogous way.

Proof. (**Proposition 6.2.9**): Since $f'(x) = -1 + (a/g)e^{-x/g}$ and $f''(x) = -(a/g^2)\,e^{-x/g}$ it turns out that $f(x)$ has a maximum at $x_m = g\ln(a/g)$. Now, assuming $a < 1$, since f is concave, $f(0) > 0$ and $f(1) < 0$, there is only one $\bar{x}$ such that $f(\bar{x}) = 0$. Hence, in this case, there is only an equilibrium point on the x-axis. It is not difficult to check that $\bar{x} > x_m$.

Now, if $c > a$ then eq. (6.15) and eq. (6.16) imply that $\lambda_1 < 1 - x - ae^{-x/g} = 0$. On the other hand, we have that $\lambda_2 = xf'(x)$ and since $f'(\bar{x}) < f'(x_m) = 0$ it follows that λ_2 is also negative at the equilibrium point. Therefore, P_1 is stable. In case of $c < a$, we have that $\lambda_1 > 0$ which means that P_1 is unstable. $\square$

Proof. (**Proposition 6.2.10**): As before, the maximum value of $f(x)$ is given by $f(g\ln(a/g)) = 1 - g\ln(a/g) - g$. Thus, since f is concave, $f(0) < 0$ and $f(1) < 0$, the conclusion about the existence of equilibrium points depends on whether the maximum value of $f(x)$ is negative, zero or positive.

Let us assume that $P_1 = (x_1, 0)$ and $P_2 = (x_2, 0)$ are feasible. By eq. (6.16), λ_1 is positive when $a > c$ which implies that both equilibrium points are unstable. Assuming $c > a$ we have that $\lambda_1 < 0$. Now, we can easily check that $x_1 < x_m < x_2$ in which x_m is the maximum point of $f(x)$. Since $f'(x)$ is a decreasing function it turns out that $f'(x_2) < 0 < f'(x_1)$. Thus, $\lambda_2 = xf'(x)$ is negative at x_2 and positive at x_1. Therefore, if $c > a$ then P_1 is unstable and P_2 is stable. $\square$

Propositions 6.2.11 and 6.2.12 are also proved in a similar fashion.

Proof. (**Proposition 6.2.13**): Defining the function $f(x)$ by

$$f(x) = 1 - (1 + \alpha)x - \beta e^{-(1+\alpha)x/g} \tag{6.26}$$

it turns out that $f'(x) = -(1+\alpha) + (a + \alpha b)\, g^{-1} e^{-(1+\alpha)x/g}$ and $f''(x) = -(1 + \alpha)\,(a + \alpha b)\, g^{-1} e^{-(1+\alpha)x/g}$ and thus $f(x)$ is a concave function. Assuming $a - 1 < \alpha(1 - b)$, we have that $f(0) > 0$ and $f(1) < 0$. Thus, since $f(x)$ is concave, there is only one point $\bar{x}$ such that $f(\bar{x}) = 0$ and, therefore $P = (\bar{x}, \alpha\bar{x})$ is an equilibrium point for eq. (6.8).

Now, comparing eq. (6.18) and eq. (6.21) we can conclude that $\lambda_1 < 0$ if and only if $d > b$. On the other hand, using eq. (6.18) again, we have that $\lambda_2 = \bar{x} f'(\bar{x})$. Since $\bar{x}$ must be greater than the point x_m where $f(x)$ reaches its maximum value, we have that $f'(\bar{x}) < 0$ and so $\lambda_2 < 0$. Now, by the feasibility condition, $P = (\bar{x}, \bar{y})$ is stable when $a > c$ and $d > b$ and unstable when $a < c$ and $d < b$. $\qquad\square$

Proof. (**Proposition 6.2.14**): Defining $f(x)$ as in eq. (6.26), the function f reaches its maximum value at

$$x_m = \frac{g}{1 + \alpha} \ln\left(\beta g^{-1}\right) \tag{6.27}$$

which is $f(x_m) = 1 - g \ln\left(\beta g^{-1}\right) - g$. Since $f(0) < 0$, $f(1) < 0$ and $f(x)$ is concave, the existence of equilibrium points relies on having $f(x_m) < 0$, $f(x_m) = 0$ or $f(x_m) > 0$. Thus, when $f(x_m) > 0$ there are points $\bar{x}_1 < x_m < \bar{x}_2$ such that $f(\bar{x}_1) = f(\bar{x}_2) = 0$ and, therefore, $P_1 = (\bar{x}_1, \alpha\bar{x}_1)$ and $P_2 = (\bar{x}_2, \alpha\bar{x}_2)$ are equilibria.

By the concavity of $f(x)$ we have $f'(\bar{x}_1) > 0$ and $f'(\bar{x}_2) < 0$. Using the same argument as in the last proposition, we have that $\lambda_2 = \bar{x}_1 f'(\bar{x}_1) > 0$ and $\lambda_2 = \bar{x}_2 f'(\bar{x}_2) < 0$. This implies P_1 is unstable. On the other hand, at both equilibria we have $\lambda_1 < 0$ when $d > b$ and $\lambda_1 > 0$ when $d < b$. Now, using the feasibility conditions for points on the line $y = \alpha x$ we can conclude that P_2 is stable when $a > c$ and $d > b$ and unstable when $a < c$ and $d < b$. $\qquad\square$

Proof. (**Proposition 6.2.15**): As $a, b > 1$, $a + \alpha b > 1 + \alpha$ which in turn implies that $\beta > 1$. The expression $g\left[\ln(pg^{-1}) + 1\right]$, $p = \max\{a, d, \beta\}$, converges monotonically to zero as $g \to 0$. We also have that $g\left[\ln(pg^{-1}) + 1\right] > 1$ when $g = p$. So, there is a $\bar{g}$ such that $g\left[\ln(pg^{-1}) + 1\right] < 1$ for each $g < \bar{g}$. Therefore, for a g satisfying $g < \bar{g}$, the hypotheses of the third item in propositions 6.2.10, 6.2.12 and 6.2.14 are satisfied and Eq. (6.8) has seven equilibrium points: $P_1 = (0,0)$; $P_2 = (x_1, 0)$ and $P_3 = (x_2, 0)$, $x_1 < x_2$; $P_4 = (0, y_1)$ and $P_5 = (0, y_2)$, $y_1 < y_2$; $P_6 = (w_1, \alpha w_1)$ and $P_7 = (w_2, \alpha w_2)$, $0 < w_1 < w_2$. By the hypotheses, P_1 and P_7 are asymptotically stable.

We are going to prove that there is a heteroclinic orbit connecting P_2 and P_6. In order to prove it, let (x_o, y_o) be a initial condition on the (1-dimensional) stable manifold of P_6, below the line $y = \alpha x$. Since it is bounded, the solution

generated by this initial condition must converge to the equilibrium point as $t \to -\infty$. In this case, this solution cannot converge neither to P_1 nor to P_7 since these equilibrium points have empty unstable manifolds. Thus, the solution must converge either to P_2 or P_3 as $t \to -\infty$.

Suppose that it converges to P_3, that is, there is an heteroclinic orbit connecting P_6 to P_3. Now, consider the set U enclosed by the line $y = \alpha x$, $x \geq w_1$, the x-axis from $x \geq$ and the heteroclinic orbit connecting P_2 to P_6. All solutions with initial condition on the interior of U must converge to P_7 as $t \to \infty$ because the stable manifolds of P_6 and P_3 are not in the interior of U. The unstable manifold of P_6 is the line segment connecting P_6 to P_7 and, therefore, it does not belong to the interior of U. Thus, solutions starting on U cannot converge to P_6 as $t \to -\infty$. In this way, since all solutions are bounded, they would have to converge to P_3 as $t \to -\infty$ and, therefore, the unstable manifold of P_3 would have dimension 2. But this is a contradiction that comes from considering an heteroclinic orbit connecting P_3 to P_6. Therefore, the solution through a initial condition (x_o, y_o) on the stable manifold of P_6 must converge to P_2 as $t \to -\infty$ which implies that there is a heteroclinic orbit connecting P_2 to P_6. Similarly, we can conclude that there is a heteroclinic orbit connecting P_4 to P_6.

Now, consider the set Q bounded by the line segments connecting P_1 to P_2 and P_1 to P_4 as well as the heteroclinic orbits connecting P_2 to P_6 and P_4 to P_6. Of course this set is invariant and contains only the stable equilibrium P_1. Thus, all solutions starting on Q converge to P_1 as $t \to \infty$. Likewise, all solutions starting on the interior of the complement of A converge to P_7 as $t \to \infty$. Finally, to prove the statement it is enough to define n_1 and n_2 as the minimum and maximum value of $x + y$, respectively, on the orbits connecting P_2 to P_6 and P_4 to P_6. □

(**Proposition 6.2.16**) is proved in a way analogous to (**Proposition 6.2.14**).

Proof. (**Proposition 6.2.17**): The existence of nonzero equilibria relies on the existence of solutions for Eq. (6.24). Now, defining $u = x + y$ and $v = x - y$ we can rewrite it as

$$v = \frac{2u}{\gamma}\left(1 - \frac{\gamma}{2} - u\right), \qquad v = u\left(\frac{e^{-u/g} - \alpha}{e^{-u/g} + \alpha}\right) \tag{6.28}$$

where $\gamma = a + \alpha b$. Since we are looking for positive solutions, comparing these two equations it turns out that u must satisfy:

$$s(u) = \gamma - (1 - u) - \alpha(1 - u)e^{u/g} = 0 \tag{6.29}$$

and by hypothesis we have that $s(0) = \gamma - (1 + \alpha) > 0$ and $s(1) = \gamma > 0$. Now, define $f(u) = \gamma - 1 + u$ and $h(u) = \alpha(1 - u)e^{u/g}$ so that $s(u) = f(u) - h(u)$. Thus the equilibrium solution is given by $f(u) = h(u)$. Taking $g \geq 1$ we can

easily check that $s'(u) > 0$ for all $u \in [0,1]$ so that Eq.(6.29) has no solution. On the other hand, we have that $h'(u) = (\alpha/g)(1 - g + u)e^{u/g}$ which implies that $h(u)$ is an increasing function on the interval $(0, 1 - g)$ and decreasing on the interval $(1 - g, 1)$. Furthermore, we can verify that $h(\sqrt{g}) \to \infty$ as $g \to 0$ so that $s(\sqrt{g}) < 0$ for a fixed $g \leq g_1$, with g_1 arbitrarily small. Since $s(u)$ is continuous there must exist a $u_1 \in (0, \sqrt{g})$, depending on g, such that $s(u_1) = 0$. Since $s(u) > s(u_1)$ for $0 < u < u_1$ and $s(u) < s(u_1)$ for $u \in (u_1, g)$ it turns out that $s'(u_1) < 0$. Similarly, $h(1 - g) \to \infty$ as $g \to 0$ and so, for a fixed $g \geq g_2$, with g_2 small, there must be a $u_2 \in (1 - g, 1)$, depending on g, such that $s(u_2) = 0$ and at this point $s'(u_2) > 0$. This proves the existence of equilibrium points as stated in the proposition.

Now, let $F(x, y)$ and $G(x, y)$ be the right hand sides of Eq.(6.9). Since $x = 0.5(u + v)$ and $y = 0.5(u - v)$, using the first equality of Eq.(6.28), the partial derivatives of F and G can be written in terms of u. At the equilibrium points u_i we have $e^{u_i/g} = (ad - bc - (b - d)(u_i - 1))/((a - c)(1 - u_i)) = S$. Using these variables, the determinant of the Jacobian matrix J at $P_i = (x_i, y_i)$ is given by

$$\det(J_{P_i})(u_i) = \frac{(a - c)u_i(u_i - 1)^2 s'(u_i)}{g(ad - bc)^2} \tag{6.30}$$

whereas the trace of J at $P_i = (x_i, y_i)$ is given by

$$\text{tr}(J_{P_i})(u_i) = \frac{-g(ad - bc)p(u_i) - (a - c)u_i(u_i - 1)q(u_i)}{g(ad - bc)^2} \tag{6.31}$$

with

$$p(u) = (a - c)(d - b) + u\left[b(a - c) + c(d - b)\right],$$

$$q(u) = (u - 1)(b - d)^2 + d(ad - bc).$$

Assuming $a > c$, and thus $d > b$, we find $\det(J_{P_1}) < 0$ which implies that P_1 is an unstable equilibrium point. In this case $\det(J_{P_2}) > 0$, so that for the stability of P_2 we consider the value of $\text{tr}(J_{P_2})$. As we have shown, $u_2 > 1 - g$, i.e. $u_2 - 1 > -g$. Since $ad - bc$ and $p(u)$ are positive, we have

$$\text{tr}(J_{P_2})(u_2) < \frac{(u_2 - 1)(ad - bc)p(u_2) - (a - c)u_2(u_2 - 1)q(u_2)}{g(ad - bc)^2}.$$

Rewriting the right hand side of last inequality we come up with

$$\text{tr}(J_{P_2})(u_2) < \frac{(1 - u_2)(d - b)Q(u_2)}{g(ad - bc)^2}$$

in which

$$Q(u) = \eta u^2 + \left[(ad - bc)(a - 2c) - \eta\right] u - (a - c)(ad - bc)$$

177

and $\eta = (a - c)(d - b) > 0$. Thus, the function $Q(u)$ is convex, $Q(0) = -(a - c)(ad - bc) < 0$ and $Q(1) = -c(ad - bc) < 0$ and so $Q(u) < 0$ for all $u \in [0, 1]$. Therefore $\text{tr}(J_{P_2})(u_2) < 0$ which implies that P_2 is stable.

Now, assuming $a < c$, and thus $d < b$, it follows that $\det(J_{P_2}) < 0$ which implies that P_2 is unstable. In this case, $\det(J_{P_1}) > 0$ and we want to prove the instability of P_1. Since $u_1 < \sqrt{g}$ it turns out that $1 - u_1 > 1 - \sqrt{g}$. For this parameter configuration $-q(u_1) > -q(\sqrt{q}) > 0$ and therefore $-q(u_1)(c - a)u_1(1 - u_1) > -q(\sqrt{g})(c - a)u_1(1 - \sqrt{g})$ which in turns implies

$$\text{tr}(J_{P_1})(u_1) > \frac{g(bc - ad)p(u_1) - q(\sqrt{g})(c - a)(1 - \sqrt{g})u_1}{g(ad - bc)^2}.$$

The right hand side of last inequality is a linear function of u, say $l(u) = mu + n$, whose coefficients are given by

$$m(g) = \frac{(1 - \sqrt{g})\left[(1 - \sqrt{g})\eta_2^2 + d(bc - ad)\right]\eta_1}{g(bc - ad)^2} - \frac{b\eta_1 + c\eta_2}{bc - ad}$$

$$n = \frac{\eta_1\eta_2}{bc - ad}$$

in which $\eta_1 = c - a > 0$ and $\eta_2 = b - d > 0$. Since $l(0) > 0$ and $m(g) \to \infty$ as $g \to 0$ it turns out that there exists a $g_3 > 0$ such that $l(u) \geq 0$ for all $u \in [0, \sqrt{g}]$ and therefore $\text{tr}(J_{P_1})(u_1) > 0$ for all $g \leq g_3$. Thus, taking $\bar{g} = 1$ and $\hat{g} = \min\{g_1, g_2, g_3\}$ the statement is proved. $\qquad \square$

(**Proposition 6.2.18**) can be obtained as a consequence of (**Proposition 6.2.17**).

CHAPTER 7

GENERAL CONCLUSIONS

In this thesis we introduced several nonlinear mathematical models applied to ecopidemiology and evolution. They were built taking into account the biological hypothesis of the real life problems.

In the first part of this thesis, we investigated the interaction between population dynamics through ecological models.

In Chapter 1 we investigated the differences in the dynamics between two predator-prey models with a generalist predator in the first model and specialist in two preys in the second one. The predator has an alternative food source that is implicit in the first model, but in the second one we have considered it explicitly. The most significant difference between the two models lies in the fact that the grazing pressure on the preferred prey and carrying capacity of the predator determine the stable coexistence of prey and predator when the alternative resource is implicit. It is interesting to note that for predator-prey models with specialist predator and logistic growth for the prey population, we cannot find any scenario of extinction of the prey species due to overexploitation.

In Chapter 2 we compared the dynamics between two predator-prey models where a transmissible disease spreads among the prey species: the predator is generalist in the first model and specialist for two prey species in the second one. The alternative food resource for the predator is implicit in the first model, but in the second one we have considered it explicit. In the first model the infection rate on the prey population determines the stable coexistence of healthy prey, infected prey and predator when the predator has an alternative resource. However, in the second model, when we consider the explicit resource for the predator species, in addition to the infection rate, also the grazing pressure on the alternative prey determines the stable coexistence for all ecosystem populations.

In Chapter 3 we have compared the dynamics between two predator-prey

models where a transmissible disease spreads among the predators.The alternative prey for the predator is implicit in the first model, but in the second one we have made it explicit. The most important parameters determining the type of possible changes in the system behaviour, leading to transcritical bifurcations, are the growth rate r of the prey population X and the mortality of the infected predator ν. In the case where the mortality rate ν of the infected predator exceeds the infection rate β of healthy predator Z, the environment becomes infection-free due to the extinction of the infected predators W. There is no possibility of a scenario where in the ecoepidemic model (3.2), the infected predators thrive without the presence of the main and of the alternative prey because $P_5^{[ep\_ep]}$ is unstable. However, healthy and infected predators survive without the presence of the main prey in both systems (3.1) and (3.2). In this case, the alternative prey provides the food for predators in both models. The environment in which only the healthy predator Z survives in the absence of the main prey is possible in both scenarios. The disease-free equilibrium points clearly can represent the coexistence between X and Z populations. The coexistence also has the same behaviour in both environments, i.e. with and without a transmissible disease among the predator population Z.

In Chapters 1, 2, and 3, we investigated and compared prey-predator population dynamics in which two distinct situations were considered: an alternative food resource for the predator in addition to its main prey and a dynamic in which this hidden resource becomes explicit so that the predator is a specialist in two species of distinct prey.

Overall, considering the results of the Chapters 1, 2, and 3, where models were compared for which the prey is at one time hidden, with a generalist predator, or explicit, with a specialist one, we can identify some general findings for such dynamics. We note that for the disease free systems (Chapter 1) and systems in which the main prey is infected by some type of disease (Chapter 2), the stability of equilibria that represent the system composed by main-prey-free ($P_3^{[p\_hp]}$, $P_5^{[p\_ep]}$, $P_5^{[p\_ehp]}$, $P_{10}^{[p\_eep]}$) depends mainly on three parameters in both cases: r, a, L. However, when considering the dynamics in which the predator population is susceptible to an infection (Chapter 3), in addition to these parameters, the parameters ν and β that mean disease horizontal transmission between predator individuals and the mortality of infected predator W, respectively, are also important when we have the same biological situation represented by equilibria $P_3^{[ep\_hp]}$ and $P_7^{[ep\_ep]}$.

Similarly, the parameters r, a, L, s, b are essential to ensure the stability of coexistence ($P_4^{[p\_hp]}$, $P_7^{[p\_ep]}$) in a disease-free system (chapter 1) and of the equilibrium that represents the disease-free system ($P_6^{[p\_ehp]}$, $P_{11}^{[p\_eep]}$) in a dynamic where it is considered a transmissible disease in the main prey population X (Chapter 2). Recall that r and s represent growth rates, a and b t hunting rates and L the carriyng capacity of the healthy predador.

In the dynamics in which a transmissible disease is considered in the predators population (Chapter 3), in addition to these parameters, the parameters β (disease horizontal transmission between predator individuals) and b (mortality of alternative prey by healthy predator) become essential for the stability of the equilibria that represent the same biological situations ($P_4^{[p\_ehp]}$, $P_8^{[p\_eep]}$), i.e., a disease-free environment regardless of whether or not there is a possibility of the transmissible disease in individuals of the predators population.

Finally, considering the species coexistence ($P_7^{[ep\_hp]}$, $P_{13}^{[ep\_ep]}$) in the dynamics presented in Chapter 2 and the species coexistence ($P_6^{[p\_ehp]}$, $P_{11}^{[p\_eep]}$) presented in Chapter 3, the essential parameters for all species coexist even with a transmissible disease are β (disease horizontal transmission between predator individuals), b (mortality of alternative prey by healthy predator) and λ (disease horizontal transmission between main prey individuals).

The investigation performed in Chapters 1, 2 and 3 was essential to provide the understanding needed to deal with models of predator-prey type, in which the possibility of a transmissible disease affecting prey and predator populations is considered. It was possible to explore different mathematical ways to understand how the interaction between individuals of the same species and different species occurs. Such studies were essential in helping us to investigate more specific problems, such as Chapter 4.

In Chapter 4 we presented a model for the study of prey-predator dynamics with the presence of disease and herd behaviour. The theoretical analysis and the numerical simulations suggest that, in the majority of the parameter combinations studied, the behaviour of the model can be predicted by the analysis of just four fundamental quantities in the system represented by mortality rate of predators, which is crucial to define the survival of the predator species and the basic reproduction number calculated in the two disease-free equilibria of the system. Some parameters of the system are related to the vertical and horizontal transmission rates and the model shows that the intraspecific competition between healthy and diseased prey on the infected prey population has a negative effect on the spread of the disease. Therefore, it is clear that a species with the behaviour of marginalizing or being hostile to the diseased individuals reduces the chance of permanence of an epidemics in the population.

In Chapter 5 we investigated an alternative way to approach herd behaviour. The model behaviour was investigated using simulation and analytical techniques. Our results show that the model presents novel behaviour when compared with the original model proposed in [3, 2]. An advantadge of this approach is that the model does not have a singularity in the Jacobian at the origin, as was the case with [3, 2]. Another fundamental difference is that the new model is coherent even for low populations of prey, where no group defense is possible, a feature that was lacking in previous approaches.

The results are interesting from the dynamical point of view, with both

sub and supercritical Hopf bifurcations arising. Group defense has a positive impact for the prey population, as expected.

In the second part of the thesis are presented dynamical systems that consider some evolution models where we discussed four distinct models for the selection of alarmist or non-alarmist behaviour in a population composed of both types of individuals. The analysis showed that the average mortality rates due to predation are the key elements to define which behaviour can evolve by individual selection.

Research in other areas involving transmissible diseases in wildlife species [9, 20, 61] and also evolutionary behaviours of bird and mammalian species [19, 24, 76, 21], provide data, in specific and general cases, that serve as tools to investigate in detail the spread of certain diseases, the dynamics and interaction among populations of wild animals and also, to estimate the survival of species through studies related to the evolutionary behaviour.

Thus, adapting our present theoretical studies in this thesis, as a perspective of future researches, we can try to get data that are present in situations of real wildlife as a form to validation of our research and also to do some contribution to other areas of knowledge.

BIBLIOGRAPHY

[1] P. A. Abrams, R. D. Holt, and J. D. Roth, *Apparent competition or apparent mutualism? shared predation when populations cycle*, Ecology (1998), 201–212.

[2] V. Ajraldi, M. Pittavino, and E. Venturino, *Modelling herd behavior in population systems*, Nonlinear Analysis Real World Applications **12** (2011), 2319–2338.

[3] V. Ajraldi and E. Venturino, *Mimicking spatial effects in predator-prey models with group defenses*, Proceedings of the 2009 International Conference on Computational and Mathematical Methods in Science and Engineering, J. Vigo Aguiar, P. Alonso, et al. (Editors), Gijón, Asturias, Spain, June 30th - July 3rd (2009), 57–66.

[4] R. M. Anderson and R. M. May, *The invasion, persistence and spread of infectious diseases within animal and plant communities*, Philos. Trans. R. Soc. London B **314** (1986), 533–577.

[5] L. M. E. Assis, M. Banerjee, and E. Venturino, *Comparing predator-prey models with hidden and explicit resources*, Annali dell' Università di Ferrara (2018), 1–25.

[6] M. Banerjee and S. Banerjee, *Turing instabilities and spatio-temporal chaos in ratio-dependent holling-tanner model*, Mathematical Biosciences **236(1)** (2012), 64–76.

[7] M. Banerjee, B. W. Kooi, and E. Venturino, *An ecoepidemic model with prey herd behavior and predator feeding saturation response on both healthy and diseased prey*, Mathematical Models in Natural Phenomena, https://doi.org/10.1051/mmnp/201712208 **12** (2017), 133–161.

183

[8] P. A. Bednekoff, *Mutualism among safe, selfish sentinels: a dynamic game*, The American Naturalis **150** (2005), 373–392.

[9] R. G. Bengis, N. P. J. Kriek, D. F. Keet, J. P. Raath, V. De Vos, and H. F. A. K. Huchezermeyer, *An outbreak of bovine tuberculosis in a free-ranging buffalo in the kruger national park*, Journal of Veterinary Research **63** (1996), 15–18.

[10] S. Bertolino, P. Lurz, and R. Sanderson, *Predicting the spread of the american grey squirrel (sciurus carolinensis) in europe: a call for a co-ordinated european approach*, Biological Conservation **141(10)** (2008), 2564–2575.

[11] M. J. Brandt and X. Lambin, *Movement patterns of a specialist predator, the weasel mustela nivalis exploiting asynchronous cyclic field vole microtus agrestis populations*, Acta Theriologica **52(1)** (2007), 2865–2874.

[12] F. Brauer, P. Van den Driessche, and J. Wu, *Mathematical epidemiology*, Springer, New York, 2008.

[13] G. Bravo and L. Tamburino, *Are two resources really better than one? : Some unexpected results of the availability of substitutes*, Journal of Environmental Management **92** (2011), 2865–2874.

[14] C. H. Brown, *Ventroloquial and locatable vocalization in birds*, Z. Tierpsychol **65** (1986), 273–288.

[15] I. M. Bulai and E. Venturino, *Shape effects on herd behavior in ecological interacting population models*, Mathematics and Computers in Simulation **141** (2017), 40–55.

[16] C. A. Buzzi, T. Carvalho, and R. D. Euzébio, *On Poincaré-Bendixson theorem and non-trivial minimal sets in planar nonsmooth vector fields*, Publ. Mat. **62** (2018), 113–131.

[17] S. Das Sankha C. Kunal, *Biological conservation of a preypredator system incorporating constant prey refuge through provision of alternative food to predators: A theoretical study*, Acta Biotheor **62(1)** (1914), 183–205.

[18] E. Cagliero and E. Venturino, *Ecoepidemics with infected prey in herd defence: the harmless and toxic cases*, International Journal of Computer Mathematics **93(1)** (2016), 108–127.

[19] T. Caro, *Antipredator defenses in birds and mammals*, University of Chicago Press, Chicago, 2005.

[20] A. Caron, P. C. Cross, and J. T. Du Toit, *Ecological implications of bovine tuberculosis in african buffalo herds*, Ecol. Appl. **13** (2003), 1338–1345.

[21] E. L. Charnov and J. R. Krebs, *The evolution of alarm calls: altruism or manipulation?*, The American Naturalist **109** (1975), 107–112.

[22] C. W. Clark, *Mathematical bioeconomics: the optimal management of renewable resources*, Wiley Series, New York, 1990.

[23] T. H. Clutton-Brock, M. J. O'Riain, P. N. M. Brotherton, D. Gaynor, R. Kansky, A. S. Griffin, and M. Manser, *Selfish sentinels in cooperative mammals*, Science **284** (1999), 1640–1644.

[24] W. Cresswell, *The function of alarm calls in redshanks, Tringa totanus*, Animal Behaviour **47** (1994), 736–738.

[25] R. Dawkins, *The selfish gene*, Oxford University Press, Oxford, 1976.

[26] P. Van den Driessche and J. Watmough, *Reproduction numbers and sub-threshold endemic equilibria for compartmental models of disease transmission*, Mathematical Biosciences **180** (2002), 29–48.

[27] M. di Bernardo, C. J. Budd, A. R. Champneys, and P. Kowalczyk, *Piecewise-smooth dynamical systems*, Springer-Verlag, London, 2008.

[28] F. Dumortier, J. Llibre, and J. C. Artès, *Qualitative theory of planar differential systems*, Springer, Berlin, 2006.

[29] L. Edelstein-Keshet, *Mathematical models in biology*, McGraw-Hill Inc., New York, 1988.

[30] M. M. A. El-Sheikh and S. A. A. El-Marouf, *On stability and bifurcation of solutions of an seir epidemic model with vertical transmission*, International Journal of Mathematics and Mathematical Sciences **56** (2004), 2971–2987.

[31] R. Euzébio, R. Pazim, and E. Ponce, *Jump bifurcations in some degenerate planar piecewise linear differential systems with three zones*, Physica D: Nonlinear Phenomena **325** (2016), 75–85.

[32] W. A. Foster and J. E. Treherne, *Evidence for the dilution effect in the selfish herd from fish predation on a marine insect*, Nature **293** (1981), 466–467.

[33] H. I. Freedman, *Deterministic mathematical models in population ecology*, HIFR Consulting Ltd, Edmontonr, Alberta, Canada, 1980.

[34] G. Gimmelli, B. W. Kooi, and E. Venturino, *Ecoepidemic models with prey group defense and feeding saturation*, Ecological Complexity **22** (2015), 50–58.

[35] A. Gosso, V. La Morgia, P. Marchisio, O. Telve, and E. Venturino, *Does a larger carrying capacity for an exotic species allow environment invasion? some considerations on the competition of red and grey squirrels*, J. of Biol. Systems **20(3)** (2012), 221–234.

[36] J. Guckenheimer and J. H. Philip, *Nonlinear oscillations, dynamical systems, and bifurcations of vector fields*, Springer Science and Business Media **42** (2013).

[37] P. K. Hadeler and H. I. Freedman, *Predator-prey population with parasitic infection*, J. Math. Biol. **27** (1989), 609–631.

[38] W. D. Hamilton, *The genetical evolution of social behavior*, Journal of Theoretical Biology **7** (1964), 1–16.

[39] _____ , *Selfish and spiteful behaviour in an evolutionary model*, Nature **288(5277)** (1970), 1218–1220.

[40] _____ , *Geometry for the selfish herd*, Journal of Theoretical Biology **31** (1971), 295–311.

[41] M. Haque, B. L. Li, S. Rahman, and E. Venturino, *Effect of a functional response-dependent prey refuge in a predatorprey model*, Ecological Complexity **20** (2014), 248–256.

[42] M. Haque, S. Rahman, and E. Venturino, *Comparing functional responses in predator-infected eco-epidemics models*, BioSystems **114** (2013), 98–117.

[43] M. Haque and E. Venturino, *The role of transmissible diseases in the holling-tanner predator-prey model*, Theoretical Population Biology **70(1)** (2006), 273–1288.

[44] M. A. Hixon, *Species diversity: prey refuges modify the interactive effects of predation and competition*, Theor Popul Biol. **39(2)** (1991), 178–200.

[45] C. C. Holling, *The components of predation as revealed by a study of small-mammal predation of the european pine sawfly*, Canadian Entomologist **9** (1959), 293–320.

[46] J. L. Hoogland, *Why do gunnisons prairie dogs give anti-predator calls?*, Animal Behaviour **51** (1996), 871–880.

[47] J. M. Jeschke, M. Kopp, and R. Tollrian, *Predator functional response:discriminating between handling and digesting prey*, Ecological Monographs **72** (2002), 95–112.

[48] J. Jiang and L. Niu, *On the equivalent classification of three-dimensional competitive leslie/gower models via the boundary dynamics on the carrying simplex*, J. Math Biol **74(5)** (2017), 1223–1261.

[49] W. Kermack and A. McKendrick, *Contributions to the mathematical theory of epidemics*, Proc. Roy. Soc A 115 (1927).

[50] Q. J. A. Khan, E. Balakrishnan, and G. C. Wake, *Analysis of a predator-prey system with predator switching*, Bull. Math. Biol. **66** (2004), 109–123.

[51] Q. J. A. Khan, B. S. Bhatt, and R. P. Jaju, *Switching model with two habitats and a predator involving group defence*, J. of Nonlinear Mathematical Physics **5** (1998), 212–223.

[52] B. W. Kooi and E. Venturino, *Ecoepidemic predator-prey model with feeding satiation prey herd behavior and abandoned infected prey*, Math. Biosc. **274** (2016), 58–72.

[53] Y. Kuznetsov, *Elements of applied bifurcation theory*, Springer, 1998.

[54] E. Venturino L. M. E. de Assis, M. Banerjee, *Comparison of hidden and explicit resources in ecoepidemic models of predator-prey type*, Computational and Applied Mathematics **preprint accepted** (2018).

[55] S. L. Llima and L. M. Dill, *Behavioral decisions made under the risk of predation: a review and prospectus*, Canadian Journal of Zoology **68** (1990), 619–640.

[56] A. J. Lotka, *Contribution to the theory of periodic reaction*, J. Phys. Chem. **14(3)** (1910), 271–274.

[57] _____ , *Analytical note on certain rhythmic relations in organic systems*, PNAS-doi:10.1073/pnas.6.7.410 **6(7)** (1920), 410–415.

[58] P. Marc, A. Canard, and Y. Frederic, *Spiders(araneae) useful for pest limitation and bioindication*, Agriculture, Ecosys. Environ. **74(1-3)** (1999), 229–273.

[59] P. Marchesi, N. Lachat, R. Lienhard, Ph. Debieve, and C. Mermod, *Comparaison des régimes alimentaires de la fouine (martes foina erxl.) et de la martre (martes martes l.) dans une region du jura suisse*, Revue Suisse Zool. **96** (1989), 281–296.

[60] P. Marler, *Characteristics of some animal calls*, Nature **176** (1955), 6–8.

[61] A. L. Michel, R. G. Bengis, D. F. Keet, M. Hofmeyr, L. M. De Klerk, P. C. Cross, A. E. Jolles, D. Cooper, I. J. Whyte, P. Buss, and J. Godfroid, *Wildlife tuberculosis in south african conservation areas: Implications and challenges*, Veterinary Microbiology **112** (2006), 91–100.

[62] M. A. Miller, P. C. White, and R. G. Bengis, *Tuberculosis in south african wildlife: Why is it important?*, SU Language Centre SUN Media **ISBN:978-0-7972-1552-8** (2015).

[63] M. J. Morgan and J. J. Godin, *Antipredator benefits of schooling behaviour in a cyprinodontid fish, the banded killifish (Fundulus diaphanus)*, Zeitschrift fr Tierpsychologie **70** (1985), 236–246.

[64] V. La Morgia and E. Venturino, *Understanding hybridization and competition processes between hare species: implications for conservation and management on the basis of a mathematical model*, Ecological Modeling **364** (2017), 13–24.

[65] J. D. Murray, *Mathematical biology*, Springer, New York, 1989.

[66] E. W. Montroll N. S. Goel, C. Maitra Samaresh, *On the volterra and other nonlinear models of interacting populations*, Rev. Mod. Phys., American Physical Society **43(2)** (1971), 231–276.

[67] R. K. Naji and R. M. Hussien, *The dynamics of epidemic model with two types of infectious diseases and vertical transmission*, Journal of Applied Mathematics (2016), 16 pages, ID 4907964, http://dx.doi.org/10.1155/2016/4907964.

[68] M. A. Nowak, *Evolutionary dynamics: exploring the equations of life*, Harvard University Press, Cambridge, 2006.

[69] N. W. Owens and J. D. Goss-Custard, *The adaptive significance of alarm calls given by shore birds on their winter feeding grounds*, Evolution **30** (1976), 397–398.

[70] L. Perko, *Differential equations and dynamical systems*, Springer, New York, 2001.

[71] E. Ponce, J. Ros, and E. Vela, *Limit cycle and boundary equilibrium bifurcations in continuous planar piecewise linear systems*, International Journal of Bifurcation and Chaos **25(3)** (2015), 18 pages.

[72] A. F. Renwick, P. C. White, and R. G. Bengis, *Bovine tuberculosis in southern african wildlife: a multi-species pathogen system*, Epidemiol. Infect **135** (2007), 529–540.

[73] S. E. Riechert, *The hows and whys of successful pest suppression by spiders: insights from case studies*, J. Arachnol. **27** (1999), 387–396.

[74] W. A. Searcy and K. Yasukawa, *Eavesdropping and cue denial in avian acoustic signals*, Animal Behaviour **124** (2017), 273–282.

[75] P. W. Sherman, *Alarm calls of belding's ground squirrels to aerial predators: nepotism or self-preservation?*, Behavioral Ecology and Sociobiology **17** (1985), 313–323.

[76] J. M. Smith, *The evolution of alarm calls*, The American Naturalist **99** (1965), 59–63.

[77] _____, *Evolution and the theory of games*, Cambridge University Press, Cambridge, 1982.

[78] R. J. F. Smith, *Evolution of alarm signals: Role of benefits of retaining group members or territorial neighbors*, The American Naturalist **128** (1986), 604–610.

[79] W. Spencer, H. Rustigian-Romsos, J. Strittholt, R. Scheller, W. Zielinski, and R. Truex, *Using occupancy and population models to assess habitat conservation opportunities for an isolated carnivore population*, Biological Conservation **144** (2011), 788–803.

[80] R. L. Trivers, *The evolution of reciprocal altruism*, The Quarterly Review of Biology **46(1)** (1971), 35–57.

[81] P. Turchin, *Complex population dynamics: A theoretical/empirical synthesis*, Princeton University Press, Princeton, 2003.

[82] E. Venturino, *The influence of diseases on lotka-volterra systems*, Rocky Mountain J. of Mathematics **24** (1994), 381–402.

[83] _____, *A minimal model for ecoepidemics with group defense*, Biological Systems **19** (2011), 763–781.

[84] _____, *Ecoepidemiology: a more comprehensive view of population interactions.*, Math. Model. Nat. Phenom. **11(1)** (2016), 49–90.

[85] E. Venturino and S. Petrovskii, *Spatiotemporal behavior of a prey-predator system with a group defense for prey*, Ecological Complexity **14** (2013), 37–47, http://dx.doi.org/10.1016/j.ecocom.2013.01.004.

[86] V. Volterra, *Variazioni e fluttuazioni del numero dindividui in specie animali conviventi*, Mem. Acad. Lincei Roma **2** (1926), 31–113.

[87] _____, *Variations and fluctuations of the number of individuals in animal species living together*, ICES Journal of Marine Science **3(1)** (1928), 3–5.

[88] S. A. West, A. S. Griffen, and A. Gardner, *Social semantics: altruism, cooperation, mutualism, strong reciprocity and group selection*, Journal of evolutionary biology **20(2)** (2007), 415–432.

[89] X. Zhou and J. Cui, *Analysis of stability and bifurcation for an seiv epidemic model with vaccination and nonlinear incidence rate*, Nonlinear Dynamics **63(4)** (2011), 639–653.